An investigation into the role of Small Ubiquitin-like MOdifier (SUMO) in plant response to phosphate deficiency

VAISHNAVI MUKKAWAR

An investigation into the role of Small Ubiquitin-like MOdifier (SUMO) in plant response to phosphate deficiency

Vaishnavi Mukkawar

A thesis submitted for Doctor of Philosophy

Department of Biosciences

Durham University

April 2023

Under the supervision of

Prof. Ari Sadanandom

Abstract

Rice (*Oryza sativa*) is a staple food crop for more than half of the world's population and provides 20% of dietary energy all over the world. Although it is the main source of calories, nearly 60% of rice is grown in soils which are low in phosphorus especially in Asia and Africa.

Inorganic Phosphate (Pi) is a non-renewable and indispensable macroelement for plant growth. Pi levels in soil are modulated by interaction with other elements such as aluminium and iron. This interaction between other elements regulates the availability of Pi to plants even after the application of fertilizers. Given the limitations of bioavailable Pi in soils, it is important to develop crops tolerant to low phosphate. This would be helpful to resource-poor farmers.

Due to their immobile nature plants have developed complex molecular signalling pathways that allows them to discern changes in the environment and adapt their growth and development. Post Translation Modifications (PTMs) play an important role in plants in providing a conduit to detect the changing environment and influence molecular signalling pathways to adapt growth and development. In recent years the PTM SUMOylation has been shown to be critical for plant growth and development. It is known that plants experience hyperSUMOylation of target proteins during stresses such as heat, salinity, drought and phosphate starvation. We provide new evidence for the role of SUMO in plant responses to Pi starvation. Here we demonstrate that PSTOL1 is SUMOylated *in planta*, and this affects its autophosphorylation activity. Moreover, we have investigated the targets of PSTOL1 using yeast two hybrid and coimmunoprecipitation techniques. Further, we also provide new evidence for the role of SUMO in plant responses to Pi starvation in rice and *Arabidopsis*. Our data demonstrated that overexpression of non – SUMOylatable version of OsPSTOL1 negatively affects the root parameters of rice grown under low Pi. Interestingly, our data also showed that overexpression of PSTOL1 in a heterologous system, *Arabidopsis* positively impacts overall plant growth under high and low Pi by modulating root system architecture.

Therefore, unraveling the role of SUMOylation to improve plants' ability to survive in phosphorus-deficient soil will open-up new ways to enhance the productivity of rice varieties.

Abbreviations

- AD – Activation domain
- ALMT1 - ALUMINIUM-ACTIVATED MALATE TRANSPORTER
- AMF - arbuscular mycorrhiza fungi
- APS - ammonium persulphate
- Arabidopsis
- ATP – Adenosine triphosphate
- BILs - backcross inbred lines
- CAPS - Cleaved Amplified Polymorphic Sequences
- CDPKs - CALCIUM-DEPENDENT KINASES
- CO-IP- Complex-Immunoprecipitation
- Col-0 - Columbia-0
- CR - crown roots
- CSM – Complete Supplement Mixture
- DBD – DNA-binding domain
- DeSI - DeSUMOylating isopeptidases
- DOS - DELAY OF ONSET OF SENESCENCE
- DRGs - differentially regulated genes
- EDTA – Ethylenediaminetetraacetic acid
- EGTA – Ethylene glycol-bis (β-aminoethyl ether)-N,N,N`N`-tetraacetic acid
- ER - Endoplasmic reticulum
- GFP - Green fluorescent protein
- GlyGly - Diglycine
- HA - Hemagglutinin
- HATs - High-affinity transporters
- Hpt^R - Hygromycin gene
- HRP - Horseradish peroxidase
- INDEL - insertion/deletion
- INDEL - transposon-rich insertion-deletion
- InsP - inositol polyphosphates
- IPTG – Isopropyl β-D-1-thiogalactopyronoside
- kDa – kilodalton

- KOH – Potassium Hydroxide
- LATs - Low-affinity transporters
- LB media – Luria-Bertani media
- LiAc – Lithium acetate
- LPR1/2 - Low phosphate root 1/2
- MBP - maltose-binding protein
- MCS - Multiple Cloning Site
- MeOH – Methanol
- $MnCl_2$ – Manganese (II) chloride
- MS – Murashige and Skoog media
- MyBP – Myelin basic protein
- NaCl – Sodium Chloride
- NaH_2PO_4 – Monosodium phosphate
- NEM – N-Ethylmaleimide
- NERICA - New Rice for Africa
- NILs - near-isogenic lines
- NLA – NITROGEN LIMITATION ADAPTATION
- NPR1 - NONEXPRESSER OF PR GENES 1
- OAs - Organic acid
- OTS1OTS2 – OVERLY-TOLERANT-TO-SALT 1/2
- PAGE – Polyacrylamide gel electrophoresis
- PAPs - Purple Acid phosphates
- PCR – Polymerase chain reaction
- PDR2 - Phosphate Deficiency Response 2
- PHF1 - PHOSPHATE TRANSPORTER TRAFFIC FACILITATOR
- PHL1 - Phosphate starvation response-like 1
- PHR1 - Phosphate starvation response
- Pi - Inorganic phosphate
- PIBS - PHR1-binding sites
- PKs - Protein Kinases
- PR - Primary root
- PSR - Phosphate Starvation Response

- PSTOL1 - Phosphorus-starvation tolerance 1
- PTMs - Post-translational modifications
- PTs - Phosphate transporters
- Pup1 - Phosphate uptake 1
- QTL - Quantitative trait locus mapping
- RAB-DB - Rice Annotation Project Database
- RGAP (formally known as MSU) – Rice Genome Annotation Project
- RMD1 - RICE MORPHOLOGY DETERMINANT 1
- RNases - Ribonucleases
- ROS - Reactive oxygen species
- RR library – Regia + Regulators library
- RSA - Root system architecture
- RT - room temperature
- RT-PCR - reverse transcriptase-polymerase chain reaction
- SAE1/2 - SUMO-activating enzyme1/2
- SCE1 - SUMO conjugating enzyme
- SD/-L selective media without leucine
- SDS - Sodium dodecyl sulfate
- SHR - SHORT ROOT
- SPS - Sucrose Phosphate Synthase
- SPX-MFS2 - SYG1, PHO81 and XPR1- major facilitator superfamily
- SPXs - SYG1, PHO81 and XPR1
- SQD2 - Sulfoquonovosyldiacylglycerol 2
- STOP1 - SENSITIVE TO PROTON RHIZOTOXICITY
- SUMO - Small ubiquitin-like modifier
- TBST – Tris-buffered saline with 0.1% Tween® 20
- TE – Tris-EDTA
- TEMED - Tetramethylethylenediamine
- TFs – Transcription factors
- ULPs - Ubiquitin-like proteases
- WRKY-transcription factors
- Y2H – Yeast-two-hybrid

- YPDA – Yeast extract peptone dextrose

Declaration

This thesis is submitted to the University of Durham in support of my application for the degree of Doctor of Philosophy. It has been composed of myself and has not been submitted in any previous application for any degree. The work (including data generated and data analysis) was carried out by the author except where explicitly states otherwise.

Vaishnavi Mukkawar (Navi)

Statement of copyright

Acknowledgments

A very big thank you to my supervisor Professor Ari Sadanandom for his guidance, driving ambition, endless support, and patience. Without him, this project would have not been completed thank you again for being a true inspiration for me. I will always be thankful for building up my confidence to pursue my career as a plant biologist and for giving me useful life lessons over these four years. I see myself in a better position professionally and personally. I am very grateful to him for giving me this opportunity to work under his tutelage and I hope I can work with him again in the future!

I would also like to express my gratitude to my co-supervisor, Dr. Elaine Fitches for her kind advice and support throughout my Ph.D. Additionally, this endeavor would not have been possible without the generous support from GCRF-CDT, especially Professor Douglas Halliday and Mrs. Abir van Hunen.

Also, I would like to express my deepest appreciation to Dr. Cunjin Zhang for undertaking rice transformation for me and helping me by providing valuable advice during the whole course of my Ph.D. Words cannot express my gratitude to Luke Cartlidge for making it possible for me to come to work during covid times. Thank you for providing me with the car rides!! To postdocs: Dr. Dipan Roy, Dr. Prakash Kumar Bhagat, Dr. Sumesh Kakkunnath and Dr. Srayan Ghosh for encouraging me to think outside the box and for advice throughout. Thank you to Dr. Dipan Roy and Dr. Sumesh Kakkunnath for proofreading my thesis chapter. Also, working with Dr. Dipan Roy on the upcoming paper was a great pleasure. Special thanks to Dr. Mansi, Dr. Mahsa Mohavedi and Dr. Alberto Campanaro for helping me learn more about the project. A big thanks to Dr. Rebecca Morrell and Catherine Gough for helping me settle into the lab when I first arrived in the lab. I really appreciate Lisa Clark for preparing brownies for me, listening to my non-stop chit-chat without getting annoyed and proofreading my chapter, Xian Long for making authentic Chinese noodles, Katie for going with me for Starbucks coffee and my partner in crime, Pimmy who accompanied me to every crazy idea I ever had, and of course, thank you for teaching me bioinformatic lessons. I hope I will have again an impromptu trip with you. Pimmy is especially acknowledged for being a friend to be held dear always.

Big thank you to my thesis committee members – Professor Adam Benham and Dr. Gary Sharples for providing me with motivation and help whenever I needed it.

A very special thank you to Dr. Alok Sinha and Dr. Meetu Gupta for their support and helped me realize my true potential. Thank you for putting your trust in me for this project. I loved the discussion about the books with Dr. Sumaira Tayyebba and I still practice the valuable suggestions from you during my experiments. I hope I can work with you again!

Special thank you to my friends - Dr. Atreyee Mishra, Hirunika Perera, Divya Jain and Piyush Goyal for making plans and filling these four years in Durham with amazing memories. Hirunika, I will miss our Friday movie nights with pizza. I am very grateful to have you as a friend.

I also want to thank the other staff in the department that have kept everything running and helped me with my research including the microscopy facility staff and the technicians that grow all the plants! Thanks so much for helping my research run more smoothly. Special thanks to Emma Robinson for sorting issues for me so smoothly.

Special thanks to Stephen Seymour and Lesley Seymour for their help and for making us feel home-like. It was a great pleasure to meet and get to know you both.

Thank you to my friends from India – Tani, Harsh, Niti, Dr. Sonu, Vinti and Shireen for the long telephonic conversations and for giving me life philosophy lessons. Thank you all for being a constant support for the past 11 years!! Also, I would like to mention my friends from school – Dr. Nikita, Vipin, Mohit Dr. Priya, Feli and Prafful for being wonderful and amazing people in my life for the last 15 years. Thank you all for your friendship. I am also very grateful to my teachers – Dr. Rohit Bhatia, Dr. Taruna Arora, Dr. Bhupender Kumar, Dr. Meenakshi Vacher, Dr. Sandeep Yadav and Dr. Archana Burman for motivating me to pursue my career in science.

Ultimately, I would like to thank my parents – Mrs. Anita Mukkawar, Mr. Arvind Mukkawar and my little brother Sahil Mukkawar for not giving up on me and supporting me through thick and thin. I owe my Ph.D. degree to my family and thank you for making it possible for me to achieve my dreams.

Contents

List of publications

1. Clark, L., Sue-Ob, K., Mukkawar, V., Jones, A.R. and Sadanandom, A., 2022. Understanding SUMO-mediated adaptive responses in plants to improve crop productivity. *Essays in biochemistry*, *66*(2), pp.155-168.

List of Tables

List of figures

Chapter 1

Introduction

1.1 Oryza sativa- a necessary food crop

Rice (*Oryza sativa*) has been considered an essential food crop for more than half of the world's population and the most cultivated staple crop worldwide. China, India, Indonesia, Bangladesh, Vietnam and Thailand are the largest rice producing countries for whom cultivating rice is considered a main source of income. Apart from being a major income source, rice also provides dietary energy (20%) which is more than wheat (19%) and maize (5%). The latest projections have shown that as the world's population continues to increase to an estimated 9 billion by 2050, food production will be required to increase by 70% from 2005/07 – 2050 in order to meet the ever-growing demand (FAO, 2009). Therefore, to meet this demand, rice production must also be increased by at least 25% by 2030 (Li et al., 2014). As this demand continues to put pressure onto an already vulnerable agricultural system, this can lead to a global issue involving food insecurity as the demand becomes even more difficult to achieve due to the drastic effects of climate change on soil quality leading to low nutrient availability and water accessibility as well as many more issues (Giri et al., 2018).

1.1.1 Low Phosphorus in soil

Abiotic stresses such as nutrient deficiency in soil is a major threat to food security. The three most important macronutrients are Nitrogen, Potassium and Phosphorus and are required for plant production, however, their deficiencies continue to escalate with exhaustive crop production. Nitrogen can be manufactured by chemical reactions or produced by symbiotic associations such as legume-*Rhizobium*. For potassium, natural reserves are sufficient, therefore, deficiency of potassium is not an issue like phosphorus and nitrogen deficiency. The importance of phosphorus is receiving widespread attention because it is an essential nutrient that comes from a non-renewable resource (Hasanuzzaman Agronomic Crops. Volume 3, Springer, 2020 and Lott et al., 2011). Phosphorus is an indispensable element for all living organisms as it is the main component of biomolecules - nucleic acids, ATP and lipids. The demand for phosphorus increases in order to support the healthy and robust growth of living organisms. Plants acquire phosphorus from the soil, but the accessibility of phosphorus is limited primarily because naturally, loss of phosphorus is either compensated by soil-plant cycling system and this cycle is restored by the slow and steady process of rock weathering or supplemented via fertilizers, however, only 10-20% of phosphorus supplied by fertilizers is free for plants to use and the rest is bound to the ions present in soil (Crombez et al., 2019). Moreover, fertilizers are mostly derived from phosphate rock which unfortunately is a non-renewable resource. Recent projections estimated that “peak phosphorus” production will be reached in 30 years which will resultantly lead to a decrease in fertilizers production and an increase in the price of fertilizers, which ultimately will lead to a rise in food prices as low phosphorus results in reduced crop yield. However, other reports suggested that some phosphorus reserves are overlooked and can last for 600 years but these reserves are restricted to Morocco and Western Sahara. The main concern regarding these reserves can be technical and under economic constraints or these reserves may be impossible to reach physically (Alewell et al., 2020). The insufficiency of phosphorus fertilizers and the unavailability of natural resources are some issues that will affect poor farmers, especially in countries where rice is cultivated as a major income source. Therefore, a long-term strategy is needed to address the global threat of phosphorus limitation. Exploring the genetic determinants that can be associated with the high productivity of rice under low phosphorus is a valid approach and this

approach can be useful for breeding programs (Mickelbart et al., 2015 and Gamuyao et al., 2012).

1.2 Understanding of phosphate sensing and signaling in plants

Levels of Pi can limit crop yield; therefore, it is important to investigate the regulatory mechanisms underpinning adaptive response in plants to cope with low phosphate (Pi) in soil. The understanding of the mechanism is an important step for boosting the P uptake or P use efficiency in crops. Plants maintain Pi-level homeostasis by applying various approaches – if a plant experiences low external Pi, local signals are induced such as signals to change root system architecture (RSA). RSA adaptions include primary root (PR) growth cessation, lateral root development and root-microbiome interaction enhancements. On the other hand, long-distance or systemic signals are produced in response to changes in internal Pi. Systemic signals include initiation of Phosphate Starvation Response (PSR) cascade and phloem-mediated traffic signals to improve Pi remobilization, redistribution and acquisition (Ham et al., 2018).

1.2.1 Local signals responsive to change in external Pi

a) Adaptations of Root system architecture (RSA) in low Pi

Fluctuations in external Pi, enable plants to adapt their root architecture to increase topsoil foraging under low phosphate conditions. These responses can vary between monocots and dicots. Monocots plants such as rice, wheat and maize respond to low Pi by elongating primary root length, developing more crown roots, changing in the angle of crown roots and increasing the length of root hair. Unlike monocots, dicots plants such as *Arabidopsis thaliana* develop a shallower root system in low Pi by cessation of primary root length, enhancing lateral root/root hair density/length under low Pi (Huang and Zhang ., 2020) (**Figure 1.1**).

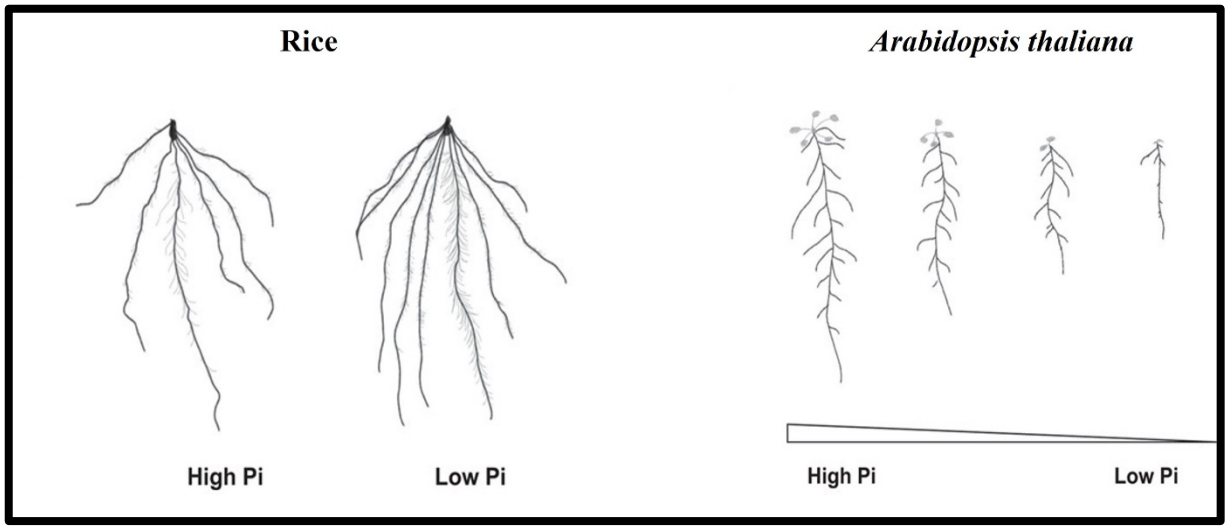

Figure 1.1: Root developmental responses under high and low Pi in rice and Arabidopsis. Image adapted from Liu., 2021.

The underlying mechanism PR growth response depends upon a few key genes studied in *Arabidopsis*. Interaction between PHOSPHATE DEFICIENCY RESPONSE 2 (PDR2); encoding a P-type 5 ATPase and ferroxidases LOW PHOSPHATE ROOT1/2 (LPR1/2) is an essential step to maintain stem cell niche by changing meristem activity in an ER-dependent pathway. Parallelly, a transcription factor SENSITIVE TO PROTON RHIZOTOXICITY (STOP1) activates a transporter known as ALUMINIUM ACTIVATED MALATE TRANSPORTER (ALMT1), which is incorporated into plasma membrane where it regulates malate secretion into apoplasm. Oxidation of Fe^{+2} to Fe^{+3} by LPR1 leads to the accumulation of Fe^{+3} in the apoplasm where it makes a complex with malate. This complex activates the production of reactive oxygen species (ROS) that initiate the callose deposition in the stem cell niche of the primary root. Deposition of callose hinders trafficking via a transcription factor such as SHORT ROOT (SHR) which results in the loss of stem cell function, therefore, the inactivation of primary root growth (Chiou and Lin ., 2011; Satheesh et al., 2022). Homologs of AtLPR1/2 and AtPDR2 are OsLPR5 in rice which maintains ferroxidase activity suggesting that it is involved in the regulation of Pi homeostasis. Although the root growth response is different in rice and *Arabidopsis* under low Pi, the PDR-LPR pathway model is conserved in dicots and monocots. Besides the PDR-LPR pathway, RICE MORPHOLOGY DETERMINANT 1 (RMD1) modulates the angle of crown roots (CR), making CR distribution shallower under Pi-deficient soil conditions (Lu et al., 2022). In rice, *OsPHR2*, (the homolog

of AtPHR1), *OsMYB2P-1* and *ltn1* (the homolog of *Arabidopsis* PHO2) are some important genes to enhance the elongation of primary root and lateral roots to increase Pi uptake (Zhou et al., 2008, Dai et al., 2012 and Hu et al., 2011). Under low Pi, the auxin gradient is important to trigger LR proliferation by enhancing auxin sensitivity through increasing the expression of the receptor of auxin, TIR1 in the pericycle cells. Also, strigolactone participates in the modulation of RSA by induction of synthesis of strigolactone when the root experiences low Pi. Increasing SL secretion into the rhizosphere will favour colonization by arbuscular mycorrhiza fungi (AMF) and it is well-known that AMF plays a critical role in the acquisition of Pi in plants. Finally, the interaction between lateral roots and AMP regulates RSA to prevailing soil conditions (Ham et al., 2018).

1.2.2 Systemic Pi Starvation pathway

In *Arabidopsis*, a significant part of Pi homeostasis is centered around key transcription factors, PHOSPHATE STARVATION RESPONSE 1 (PHR1) and PHOSPHATE STARVATION RESPONSE-LIKE 1 (PHL1). These transcription factors control responses to Pi starvation signals by regulating and modulating membrane lipids, increasing the ratio of root-shoot growth, initiating Pi scavenging and transport activities, anthocyanin biosynthesis and suppressing photorespiration and photosynthesis (Puga et al., 2017). PHR1 and other PHL transcription factors regulate via binding to a DNA motif of GNATATNC (also known as PHR1-binding sites (PIBS)) in the promoter region of nearly 2000 genes (Chiou and Lin .,2011 and Crombez et al., 2019) encoding genes like SPXs (SYG1, PHO81 and XPR1), signal molecules such as IPS1/At4, miRNAs, Phosphate transporters (PTs), biosynthetic genes of galactolipids, sulfolipids and purple acid phosphatases (PAPs) (Wu et al., 2013).

SPX domain proteins are relatively conserved in eukaryotes, and they act as a sensor of Pi in form of inositol polyphosphates (InsP). Biochemical and genetic assay data showed that InsP promotes the binding of SPX proteins with PHR to suppress Pi starvation responses under sufficient Pi conditions in both *Arabidopsis* and rice (Lu et al., 2022). In Pi-deficient conditions, the association between SPX proteins and PHR1 is disrupted and PHR1 is released, to induce the expression of genes involved in phosphate starvation signalling. PHR1 induce their expression via binding to the PIBS motif in the promoter region of these genes. In rice, OsPHR1 and OsPHR2 proteins are homologs of AtPHR1. Eventually, reports have also shown

that OsPHR3 and OsPHR4 are also involved in Pi homeostasis and Pi signalling along with OsPHR1 and OsPHR2 (Ruan et al., 2017 and Guo et al.,2015). The regulatory mechanisms mediated by PHR proteins in rice and Arabidopsis are comparable.

In Pi deficient condition, PHR1 also induces expression of Pi transporters (PHT1) and PHOSPHATE TRANSPORTER TRAFFIC FACILITATOR (PHF1), an endoplasmic reticulum (ER) exit cofactor that allows PHT1 to migrate to the plasma membrane to improve the Pi acquisition and remobilization (Puga et al., 2017 and González et al., 2005). Moreover, PHT1 is negatively controled by ALIX and CK2α2β3 kinase with both of these proteins affecting the accumulation of PHT1 in the plasma membrane via distinct mechanisms under phosphate-deficient conditions (Puga et al., 2017)

Additionally, mobile mRNAs are potential candidates involved in systemic signals. The miRNAs such as miR399, miR827, miR156, miR2111 and miR778 are produced by Pi deficiency. Under the low Pi conditions, PHR1 induces expression of shoot-derived miR399 movement into the root through the phloem by releasing post-transcription negative control on PHT1 transporters. It is here where miR399 mediates cleavage of the PHO2 and NLA transcripts resulting in the enhancement of the uptake of Pi in roots which then leads to an increase in the translocation of Pi from root-to-shoot. Rice homolog, OsPHO2 is the target of miR399, suggesting the miR399-PHO2 pathway is conserved in both rice and *Arabidopsis*. Another well-studied miRNA in rice is miR827, this miRNA is upregulated in Pi deficiency and targets OsSPX-MFS1 and OsSPX-MFS2 (SYG1, PHO81 and XPR1- major facilitator superfamily) and negatively regulates these two genes to respond to external phosphate conditions because the SPX domain in proteins aid in Pi sensing and Pi transport whereas, the MFS domain is found in membrane proteins which are important for the transport of small solutes. (Lu et al., 2022 and Lin et al., 2010).

Biosynthetic genes such as PAPs catalyse the hydrolysis of Pi from phosphomonoesters. Low Pi induce specific PAPs, for instance, AtPAP12 and AtPAP26 are secreted by root that search Pi from extracellular Pi-esters, whereas AtPAP26 have a dual role that functions in Pi recycling of vacuole (Tran et al., 2010). The rice ortholog of AtPAP26 is OsPAP26 which also plays a dual role in plants during Pi starvation: remobilization of Pi from senescing to non-senescing leaves and utilization of organic Pi (Gao et al., 2017). In rice, Sulfolipids, sulfoquonovosyldiacylglycerol 2 (SQD2) recycles Pi from membrane phospholipids (Wu et

al., 2013) whereas in Arabidopsis, expression of *AtSQD1* and *AtSQD2* is upregulated in both root and leaf of the thylakoid membrane. On the other hand, galactolipids are increased in the extraplastidic membrane and thylakoid membrane in Pi-starved *Arabidopsis* seedlings. The induction of galactolipids results in lipid alteration mediated by auxin and cytokinin.

Pi starvation also induces some phosphate transporters (PTs) for Pi uptake, translocation, Pi distribution and uploading, vacuolar import and export. For instance, in *Arabidopsis*, the *Pht1* family consists of high-affinity Pi transporters. *AtPT1* and *AtPT4* are two important Pi transporter for Pi uptake (Fang et al., 2009) this is evident where double mutants exhibited a 75% reduction in efficiency to uptake Pi compared to wild-type seedlings (Shin et al., 2004). In rice, OsPT2 and OsPT6 were primarily expressed in the roots under low Pi conditions. Knockdown of *OsPT6* affects both Pi uptake and Pi translocation from roots to shoots. Another major high-affinity PT in rice is OsPT8.The expression of OsPT8 is increased especially in roots while its expression in shoots is not affected in Pi starvation. Knockdown of *OsPT8* results in a decrease in total Pi uptake, root and shoot biomass (Wu et al., 2013).

Although the latest progress in understanding both molecular and physiological mechanisms to improve nutrient acquisition is impressive, significant work is still going on to uncover much more before being able to transfer these discoveries into crops to enhance their nutrient efficiency. Another way is the identification of molecular markers that is of particular value for the development of phosphorus-efficient rice varieties.

1.3 Discovery of genetic determinant to improve phosphate tolerance in rice based on natural variation

A lack of phosphorus can severely limit rice yield and the rising cost of fertilizers is a taxing issue for farmers. Therefore, exploring rice varieties that show yield above average on P-deficient soil can be used for investigating genetic determinants (generally identified using Quantitative trait locus mapping, QTL). The effect of that locus can be studied and evaluated after back-crossing in other rice varieties.

To develop improved cultivars, breeders were focusing on the cultivars under low P conditions. Tolerance to low P was measured as grain yield, dry weight, tiller number or relative tiller number and the most important parameters are - P-use efficiency (internal efficiency) and P-uptake efficiency (external efficiency). Wissuwa et al., 1998 used molecular linkage maps in rice which allowed the examination of quantitatively expressed traits into Mendelian factors, also known as Quantitative trait locus mapping (QTL). Their objective was to identify and map QTL associated with indicators of tolerance to low Pi - dry weight, tiller numbers, P-uptake efficiency (external efficiency) and P-use efficiency (internal efficiency). In recent years, a particular group of rice, known as *aus*-type varieties were identified which can grow in poor soil in some region in India. These *aus*-type varieties have been identified as an important source of tolerance genes. For example, the *SUB1A* gene was discovered in *aus*-type rice and rice plants with this gene can survive in flooded fields for 2 weeks. Another *aus*-type rice, Kasalath, was identified to be tolerant of Pi deficiency. To find the potential QTLs for P-deficiency tolerance in rice, *Japonica* was crossed with *indica* (Nipponbare X Kasalath) where *Japonica* represents intolerant variety to low Pi. 98 backcross inbred lines (BILs) were generated, and phenotypic responses were recorded. Four potential QTLs were identified regarding P uptake on chromosomes 2,6,10 and 12. Among 98 BILs, major QTL linked to marker C443 on chromosome 12 explains major variation in dry weight (26.5%) and P-uptake (27.9%). Apart from the C443 marker, QTLs on chromosomes 2 and 6 (minor QTLs) also have a positive effect on P-deficiency and these positive alleles come from 'Kasalath'. Breeders can transfer the improved P-uptake ability from a variety like Kasalath into breeding material which will have a higher harvest index to improve the productivity of rice under low Pi. Wissuwa and Ae et al., 2001 developed near-isogenic lines (NILs) for major QTL linked to marker C443 on chromosome 12 and minor QTL linked to C498 on chromosome 6 and using these NILs their phenotypic responses are recorded in low Pi. P uptake was improved by a factor of 3-4 times in NIL-C443 than in Nipponbare whereas the improvement was seen in the range of 60-90% in NIL-C498. The data also showed that both QTLs improved specifically the uptake of phosphorus in low Pi soil because the effects of these QTLs are linked to root surface area. Further investigation also revealed that Nipponbare had reduced surface area in P deficiency whereas NILs - C443 could retain half of its non-stress condition root-surface area. Therefore, they decided to map this major QTL on the long arm of chromosome 12 and named as *Pup1* (*Phosphorus uptake 1*) (Wissuwa et al., 2002). It was obvious that the presence of *Pup1* in Kasalath (tolerant donor parent) showed three times higher grain yield and phosphorus uptake in low-phosphorus soil than in Nipponbare (intolerant parent). It was reported after fine

mapping the population derived from Kasalath X Nipponbare that the Nipponbare reference genome sequence did not display any potential genes associated with phosphorus metabolism. Therefore, the corresponding region in Kasalath was sequenced and it revealed transposons- and retrotransposons-related elements. 68 potential genes in the Kasalath *Pup1* region were identified and some of these genes were present in this region which was exclusively known as the insertion/deletion (INDEL) region, and it explained the difference in the size of the region between Nipponbare and Kasalath. It was unclear if this represents the deletion in Nipponbare or insertion in Kasalath, hence named INDEL region. 14 putative genes were chosen for reverse transcriptase-polymerase chain reaction (RT-PCR) to confirm gene models (Heuer et al., 2009).

1.4 Discovery of PSTOL1 gene

From previous reports, it was identified the INDEL region in Kasalath was absent from Nipponbare and other intolerant rice varieties. Finally, five candidate genes (*OsPupK04-1, OsPupK05-1, OsPupK20-2, OsPupK29-1* and *OsPupK46-2*) were shortlisted from 68 *Pup1* gene model and their gene expression was examined using RT-PCR. The data showed expression of *OsPupK46-2* was different in low and high phosphorus conditions, and it was later assumed that this protein might have a role in P homeostasis signalling and sensing. Thereafter, the candidate was named phosphorus-starvation tolerance 1 (*PSTOL1*). To gain insight into *PSTOL1* gene function, the protein sequence showed similarity with serine/threonine receptor-like kinases of the LRK10L-2 subfamily. PSTOL1 kinase lacks amino-terminal extension hence it was classified as a receptor-like cytoplasmic kinase. Furthermore, phylogenetic analyses confirm that OsPSTOL1 kinase is truncated to a single kinase domain compared to genes present in members of the Gramineae family which usually have kinase domains, a transmembrane domain and a N-terminal domain important for interaction with microbes (Kettenburg et al., 2022). Overexpression of PSTOL1 coding region in IR64 and Nipponbare (representing *indica* and *japonica* respectively) showed that 60% increase in grain yield when transgenic lines were grown in P-deficient soil. Superior performance was observed when the PSTOL1 gene was overexpressed in IR64 plants. Parallelly, experimental results conducted in hydroponic solution showed that IR64 PSTOL1

overexpressing lines have enhanced root surface area and total root length under both high (100µM) and low (10µM) P concentrations. Further experiments also showed that PSTOL1 expression was detected in stem nodes from where the formation of crown roots initiates. Taken together, data showed that PSTOL1 is a key regulator for root growth and crown root development, as a result, root growth is enhanced in low P conditions. Increasing root surface area and root length will help plants uptake more P from topsoil (Gamuyao et al., 2012). To understand the molecular function of OsPSTOL1 in rice, analysis from Affymetrix gene-array and Agilent microarray showed that P-starvation genes did not change in overexpressing PSTOL1 rice transgenic lines. Alternatively, authors identified other 23 genes related to root growth and stress response that showed lower and higher expression in the transgenic lines irrespective of the Pi supply and developmental stage. Among these 23 genes, *HOX1* is well associated with the role played by OsPSTOL1 in root development because *HOX1* is a positive regulator of root cell differentiation whereas, *DOS* (*DELAY OF ONSET OF SENESCENCE)* gene expression has been shown to delay leaf senescence. *DOS* gene and gene encoding WRKY-transcription factors are located on chromosome 1 and these genes were shown to associate with *OsPSTOL1* in association studies. Intriguingly, among the constitutively upregulated genes, a potential peptide transporter was also upregulated probably to uptake more P. However, further investigation needs to be done as to how OsPSTOL1 overexpression regulates their expression to increase root surface area to maximize Pi uptake.

Additional investigation revealed that allelic variation was investigated across more than sequenced 3000 rice accessions. J and K- functional alleles were identified in two different sub-groups of rice. The authors showed that K-allele in genotypes has more transcript abundance in both deep and shallow roots. Interestingly, 64% of the landraces showed the presence of *OsPSTOL1*: 17% have J-alleles in *Japonica* and aromatic rice landraces and 43% have K-allele dominant in *indica* and *aus* landraces which agrees with *OsPSTOL1* role in enhancing root growth in Kasalath. The absence of *OsPSTOL1* in the rice haplotype was seen in East Asia. To investigate further, the J-allele of *OsPSTOL1* is prominent in the *Japonica* landrace from an area having depleted irrigation and rice grown in rainfed upland. K-allele is diminished in *indica* irrigated lowland landraces; however, it has a comparable frequency in the rainfed uplands and lowlands. (Kettenburg et al., 2022).

Following the work from Gamuyao et al., 2012, reports showed NERICA (New Rice for Africa) varieties have high yield ability but are intolerant to phosphorus deficiency, therefore,

work was started to identify the PSTOL1 allelic diversity among NERICA rice varieties such as CG14 which is one of *O.glaberrima* accessions and is a founder parent for NERICAs (Pariasca-Tanaka et al., 2014). Subsequently, Vigueira et al., 2016 findings suggested the presence of non-functional and functional allele of PSTOL1 in Asian rice varieties which includes wild, domesticated and weedy varieties of rice. The balance between these functional and non-functional alleles can be considered as an adaptation with a geographical variation. Consequently, the presence of a superior allele of PSTOL1 in all accessions of *O.rufipogon* was also assessed and these three accessions (IRGC 106506, IRGC 81989 and IRGC 104639) revealed they harbour a superior allele of PSTOL1, although the marker-assisted transfer of these alleles is already initiated (Neelam et al., 2017) to characterize the superior allele of PSTOL1. Haplotypes of PSTOL1 were not only investigated in phosphorus-deficient soil but novel allelic combinations were also reported in rice genotypes grown in acidic soil (Yumnam et al., 2017). Although extensive work has been done to identify a superior allele of PSTOL1 in other rice accessions to generate phosphorus-efficient rice varieties, considerable work has to be done to identify downstream targets of PSTOL1 and later elucidate the underlying mechanism of PSTOL1. Recent studies by Kumar et al., 2021 revealed the role of the important genes expressed during P-starvation conditions and one of them could be a target of OsPSTOL1. The study presented the significant role of jasmonate/auxin induced proteins acting as signalling molecules (LOC_Os04g22900, LOC_Os01g36580), transporters (OsPHT1;6. OsPHT1;10), glycerophosphoryl diester phosphodiesterase family protein (LOC_Os03g40670), auxin-responsive protein (LOC_Os05g48270), LTPL-protease inhibitor (LOC_Os10g40430, LOC_Os10g40480), transcription factors (LOC_Os03g51690), phosphatases (LOC_Os01g52230, LOC_Os08g17784, LOC_Os11g38050, LOC_Os07g01540, LOC_Os05g02310), AP2 domain containing proteins (LOC_Os08g36920, LOC_Os10g11580), MYB family TFs (LOC_Os03g62100, LOC_Os02g22020), glycine-rich cell wall structural proteins (LOC_Os10g31530, LOC_Os10g31540) and core histone domain-containing protein (LOC_Os10g28230), in conferring tolerance in rice under low Pi (Kumar et al., 2021).

Interestingly, *PSTOL1* orthologs in other crops such as wheat, sorghum and maize were identified, and targeting their expression will pave the way to develop crops that can grow in phosphorus-deficient soil without loss of yield and biomass. But the characterization of these *PSTOL1* orthologs in other crops is yet to be investigated. Some research groups demonstrated the identification of PSTOL1 homolog in sorghum genome, *Sb03g00676, Sb03g031690*

(alleles of *SbPSTOL1*) and PSTOL1-like gene *Sb07g02840* exhibited improved P uptake by increasing root surface area, modulating root diameter and subsequently increasing grain weight (Bernardino et al., 2019, Hufnagel et al., 2014, Li et al., 2015). Another study in maize by Mukherjee et al., 2014 and Azevedo et al., 2015 identified four potential homologs of PSTOL1 that primarily expressed in roots and interestingly, QTL mapping showed these homologs co-localise with QTL for root biomass, root morphology and other P-uptake related characters. However, it is unclear if these PSTOL1 homologs in maize are a better option for molecular breeding. In wheat, twenty-two *TaPSTOL1* gene family members were identified and characterized. *TraesCS1A02G018000*, *TraesCS1A02G018600*, *Traes3A02G012900*, *Traes3A02G018200, Traes3A02G018500* and *TraesCS2B02G558600* were co-localized with the phosphorus related QTLs in the wheat genome. *TraesCS3A02G018500* showed upregulation under low Pi, but it does not co-localize with the phosphorus related QTLs. However, it co-localizes with QTL of dry weight which demonstrated the different role of PSTOL1 genes in various other stress conditions in wheat (Abbas et al., 2022). Recent reports also showed that heterologous expression of OsPSTOL1 in wheat enhanced shoot and root growth when compared to null segregant. More P and N content accumulated in shoots because transcriptomic analysis of root and crown roots demonstrated that the transcript level of the genes associated with P recycling and remobilization was upregulated under low Pi. As shown by Gamuyao et al., 2012, 23 differentially regulated genes (DRGs) were identified in IR64 overexpressing OsPSTOL1 rice transgenic lines. Similarly, in wheat, 11 DRGs which are orthologs in rice were identified especially *OsDOS* and S-adenosyl methionine decarboxylase (SAMDC2) which is an important component in polyamine biosynthesis. Moreover, OsPSTOL1 regulates the transcript level of transcription factors managing reproductive development, sugar homeostasis and nutrient assimilation. Collectively, authors showed that expression of OsPSTOL1 is beneficial in wheat for changing root architecture and increasing grain yield (Kettenburg et al., 2022). Taken together, *OsPSTOL1* might act in the conserved pathway, and the expression of this gene might affect developmental and environmental responses in all the other monocot crops.

1.5 Role of post-translational modification in various biotic and abiotic stress conditions

Plants are sessile in nature and therefore, they depend on elaborate molecular mechanisms that allow them to respond and comprehend the variations in the environment to mount an adaptive response (Roy and Sadanandom ., 2021 and Verma et al., 2017). Among these intricate molecular mechanisms, post-translational modifications (PTMs) are important elements of how plants will mount an adaptive response during stress conditions (Clark et al., 2022). PTMs expand proteome activity to mediate responses under biotic and abiotic stress (Miura and Hasegawa., 2010).

Phosphorylation, ubiquitination and acetylation are the most studied PTMs according to the dbPTM database (Clark et al., 2022). Protein phosphorylation is a reversible regulatory mechanism that play important role in enzymes and membrane channel activity. This modification occurs mainly on Tyr, Thr and Ser and His residues. Amongst other PTMs, ubiquitination is considered another important PTM because of its reversible and versatile nature as ubiquitination can occur on all 20 amino acids. Moreover, ubiquitylation plays a vital role in the degradation of intracellular proteins through 26S proteasome (Ramazi and Zahiri., 2021). Parallel to ubiquitination, SUMOylation is another influential PTM system and had gained widespread attention because of its reversible nature and dynamic role in protein modification in plants during stress survival (Clark et al., 2022). SUMOylation is able to regulate various biological processes such as growth and development, light signalling, flowering, responses to abiotic stresses and biotic stresses like pathogen infection (Verma et al., 2017) and in contrast to ubiquitination, SUMOylation of target proteins has many downstream effects such as prevention of protein degradation, regulating the subcellular localization of the protein, preventing lysing residues prone to any other PTMs and regulating the interaction of proteins with their targets to alleviate the damage caused by stress (Clark et al., 2022). Apart from studying a single regulatory PTM, recent studies also highlighted the importance of PTM crosstalk to mount an adaptive response to the smallest changes in the environment (Dai Vu et al., 2018). For instance, the first ever SUMOylation-phosphorylation cross-talk was identified in the BR response pathway. A transcription factor, CESTA (CES) was SUMOylated by SUMO1 and SUMO2 at lysine 72 and as a result, SUMOylated-CES relocalised to nuclear bodies upon BR treatment. Relocalization of SUMOylated-CES is an

important step for its transcriptional activation. But phosphorylation of CES at serine 55 and 77 by CALCIUM-DEPENDENT KINASES (CDPKs) weakens its SUMOylation and thereby impairs nuclear body formation. Another example of phosphorylation-SUMOylation interplay was found in a salicylic acid receptor, NONEXPRESSER OF PR GENES 1 (NPR1) essential for the induction of immune responses. Phosphorylation of serines 55 and 59 blocks the SUMOylation of NPR1. This step is necessary because protein can be in a latent state under no stressful conditions. However, upon exposure to pathogens, induction of salicylic acid will facilitate the phosphorylation of NPR1 at serine 589 and threonine 373 by SnrK2.8 to mediate the transport of NPR1 from the cytoplasm to the nucleus. In the nucleus, NPR1 is SUMOylated and probably alters its affinity towards transcriptional repressors for defense genes. Moreover, SUMOylation is also important for further phosphorylation at serines 11 and 15, which results in enhanced SUMOylation of NPR1. This enhanced SUMOylated form of NPR1 has an affinity to bind to the transcriptional activator and induce the expression of downstream genes related to pathogenesis. Therefore, an interconnection between these modifications can coordinate input from two different signalling mechanisms to modulate stress responses in plants.

1.5.1 SUMOylation and its role in maintaining homeostasis under stress

SUMO (small ubiquitin-like modifier) proteins are present in single-celled eukaryotes such as *Saccharomyces* cerevisiae, plants and mammals. In plants, SUMOylation is important for light regulation, hormone signalling, development, flowering time, and abiotic and biotic stress responses (Rosa ., 2018). The critical role of SUMO was highlighted when deletion of only SUMO isoform, also known as SMT3, in yeast cells leads to loss of cell viability and in *Arabidopsis thaliana* s*umo1sumo2* knockout mutants are embryonic lethal (Morrell and Sadanandom., 2019 and Roy and Sadanandom., 2021). SUMO protein is an 11kDa protein and its structure is like ubiquitin containing a signature fold known as the β-grasp fold (Roy and Sadanandom., 2021). Through, computer analysis only one isoform in yeast was identified, eight isoforms of SUMO in *Arabidopsis* and six isoforms of SUMO in rice. In *Arabidopsis*, *AtSUMO1/2* are highly expressed, and functionally conserved and their expression is regulated under stress conditions like human SUMO2/3, although other SUMO proteins such as *AtSUMO 3* and *5* are also expressed, they do not maintain their capacity to interact with SUMO conjugating enzymes, E2 (AtSCE1) (Castaño-Miquel et al., 2011). In rice, transcript analysis of *OsSUMO1/2* showed high-level expression irrespective of genotype and tissues whereas

here the authors first time observed *OsSUMO3* transcript, however, its expression is tissue and genotype dependent in their studies (Rosa et al., 2018). On the other hand, Teramura et al., 2021 reported transcript levels of *OsSUMO1*, *OsSUMO2, OsSUMO3* and *OsSUMO5* were seen in all tissues which suggest their expression is constitutive. The transcript level of *OsSUMO4* was detected in tissue except developing seeds and spikelets and the transcript level of *OsSUMO6* was detected in tissue except for seeds and developing roots. Taken together, *OsSUMO1*, *OsSUMO2, OsSUMO3* and *OsSUMO5* are expressed in all tissue except the expression of *OsSUMO4* and *OsSUMO6* which shows tissue specificity. Moreover, the *in-vivo* analysis demonstrated that all SUMO from rice is involved in SUMOylation. But only OsSUMO1/2 are functionally characterized under salt and drought stress (Srivastava et al., 2016 and Srivastava et al., 2017) and no functional analysis has been reported yet for other SUMOs. Phylogenetic tree analysis also revealed OsSUMO3,4,5 and 6 evolved after monocotyledons had evolved suggesting their importance, particularly for the Gramineae family. Recent studies showed the identification of *OsSUMO7* in the rice genome, and it is constitutively expressed in all plant organs (Ibrahim et al., 2021).

Likened to ubiquitination, SUMOylation also occurs through a series of biochemical steps which includes activation, conjugation and ligation of SUMO to the target protein. To begin with, SUMO proteases – Ubiquitin-like proteases (ULPs) having SUMO peptidase activity will recognize a carboxy-terminal diglycine (GlyGly) motif in SUMO proteins and via its peptidase activity will remove 10 amino acids after GlyGly motif to generate mature SUMO. As a result, the diglycine motif on the SUMO protein is exposed and is ready for conjugation with the target protein. The next step is the activation of SUMO protein catalyzed by E1 - SUMO-activating enzyme1/2 (*SAE1/2*). *SAE1/2* is a heterodimer of a regulatory subunit *SAE1a/SAE1b,* and the other subunit is known as the catalytic subunit, SAE2. The activation involves the ATP molecule hydrolysis, forming a high-energy thioester bond between the carboxyl group of glycine (Gly) in SUMO and the sulfhydryl group of a cysteine residue in SAE2. The activated SUMO protein is transferred from SAE2 to a cysteine residue of E2 - SUMO conjugating enzyme (SCE1) to form the SUMO-SCE1 thioester complex. The last step involves the SUMO-SCE1 complex that catalyzes the process of conjugation of SUMO protein on lysine residue in the target protein via an isopeptide bond between the ε-amino group of lysine (K) and glycine residue of SUMO carboxyl-terminal. Typically, the lysine residue belongs to SUMOylation consensus motif Ψ KXE/D where Ψ represents a hydrophobic residue, K is the lysine residue conjugate with SUMO, X is any amino acid and E/D is the presence of either glutamate or

aspartate. Though the process of conjugation of SUMO to target protein can be directly catalyzed by E2, however, the interaction between SUMO-SCE1 complex and the target protein is not sufficient sometimes, therefore, SUMO ligases, E3 are necessary to assist in the transfer. E3 facilitates the precise positioning between the SCE1-SUMO complex and substrate. The presence of the SP-RING domain in E3 ligase aid the interaction between SCE and substrate (**Figure 1.2**).

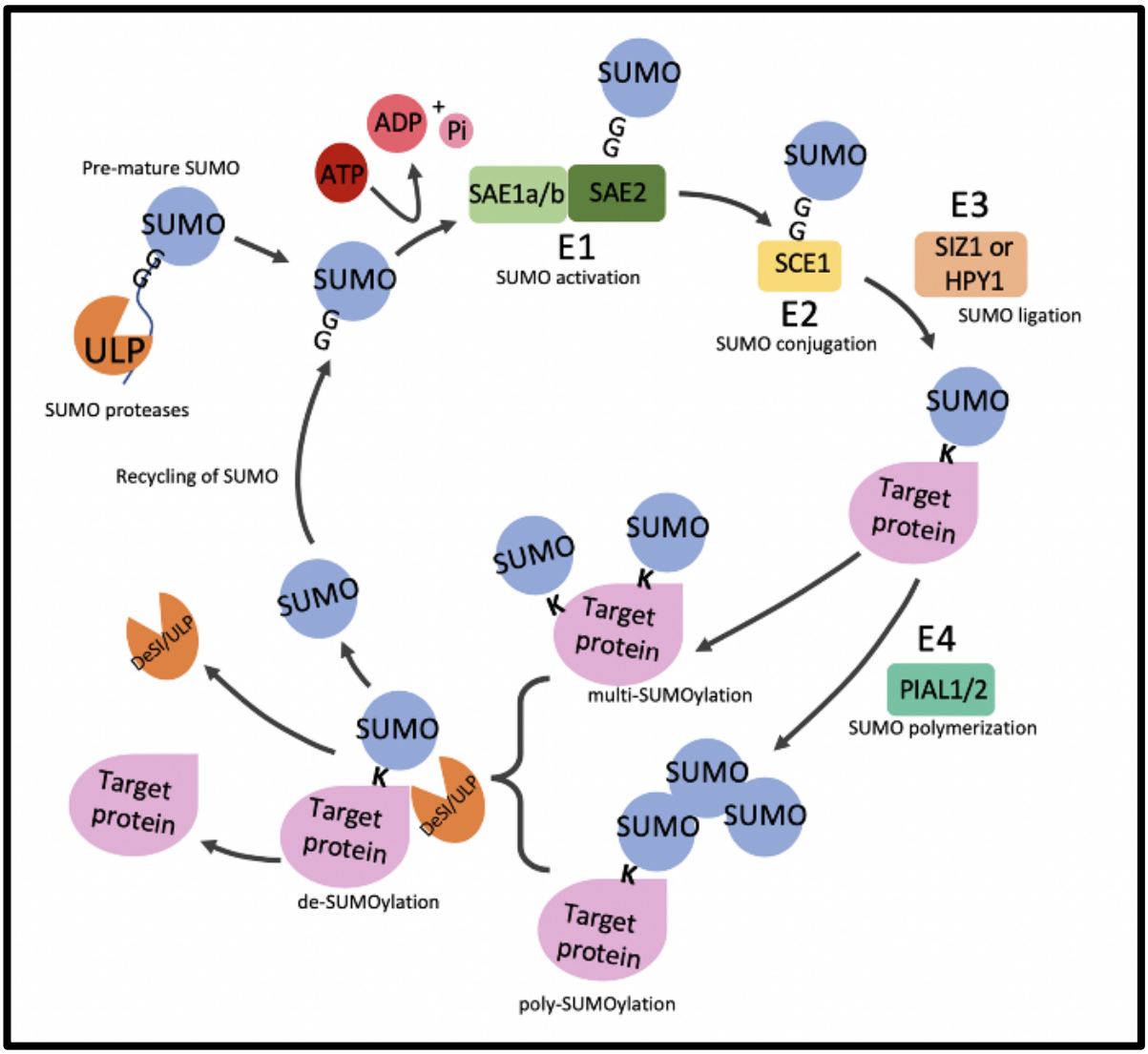

Figure 1.2: The SUMO cycle – a brief overview.

The SUMO cycle begins with the maturation of SUMO from precursor SUMO via a SUMO ULP protease. Peptidase activity of ULPs results in cleaving 10 amino acids after the diglycine motif in SUMO. Mature SUMO is activated by the E1 enzyme which aids ATP hydrolysis and facilitates the complex formation between SAE2 and SUMO. The complex is transferred from SAE2 to SCE1, E2. SUMO-SCE1 catalyzes the process of SUMOylation onto a lysine residue of the target protein. However, SUMO E3 ligase precisely transfers the SUMO from SCE1 onto target proteins. SUMO E4

is a further step in the SUMO cycle and promotes the formation of SUMO chains. Finally, SUMO proteases – ULPs or DeSIs will cleave the SUMO from the target protein via a process known as deSUMOylation to make pools of free SUMO, thereby, making the process of SUMOylation reversible. Image adapted from Clark, L., Sue-Ob, K., Mukkawar, V., Jones, A.R. and Sadanandom, A., 2022. Understanding SUMO-mediated adaptive responses in plants to improve crop productivity. Essays in biochemistry, 66(2), pp.155-168.

a. E1-SUMO-activating enzyme

In *Arabidopsis* and rice, the E1-SUMO activating enzyme consists of three subunits- *SAE1a*, *SAE1b* and *SAE2*. E1 activating enzyme catalyze the first step in the SUMO conjugation pathway, therefore, E1 plays very essential roles in a eukaryotic system. Especially, catalytic subunit-*SAE2* catalysis majority of function and mutation of *SAE* in Arabidopsis, *Atsae2*, affect the early development of plants as *Atsae2* mutant plants are embryo lethal. Therefore, limited data is available on the role of *AtSAE2* in response to stress conditions, but probably it is because *Atsae2* mutants are embryo lethal. Conversely, *Atsae1a* mutants are viable and its role in abiotic stress has been proposed. *Atsae1a* mutants when subjected to heat and drought treatment exhibited defects in phenotype and subsequently reduced SUMO-conjugation accumulation. Currently, information about *Atsae1b* null mutants under stress conditions is still unknown. The role of OsSAE1a is well established for maintaining nutrient homeostasis (specifically P and N) in rice, however, the role of OsSAE1b and OsSAE2 in stress conditions is still unknown (Vivek et al., 2017, Morrell and Sadanandom., 2019 and Clark et al., 2022).

b. E2-SUMO Conjugating enzyme

The SUMO-conjugating enzyme, *AtSCE1* is a critical enzyme within the SUMO cycle because it can aid the SUMO conjugation directly to the target protein. Interestingly, *AtSCE1* mutants are embryonic lethal i.e., embryo development is arrested at an early stage. *AtSCE1* mutants being embryonic lethal, the information about its role in stress is limited. However, crops have several genes encoding SCE1 (**Figure 1.3**). In rice, three SCEs genes were discovered- *OsSCE1*, *OsSCE2* and *OsSCE3* and their responses under abiotic stresses have been observed. *OsSCE1* expression was greatly induced by polyethylene glycol 6000 (PEG6000), which ultimately suggests that OsSCE1 protein might involve in mounting adaptive response during drought conditions (Nurdiani et al., 2018). Moreover, reports from Nigam et al.,2008 showed

that *OsSCE1* and *OsSCE2* transcript levels were changed by high temperatures. Interestingly, *OsSCE3* has been shown to improve tolerance to drought conditions in rice and growth recovery was 90-96% observed after 2 days of drought stress when compared with WT with a recovery rate of 40-64% (Clark et al., 2022).

c. E3- SUMO ligase

Unlike *Arabidopsis* E1 and E2 knockouts, SUMO E3 ligase mutants are viable but were phenotypically dwarf and surprisingly, the mutant has shown effective responses in various stress conditions. AtSIZ1 ligase regulates responses to abiotic stresses such as high salt, heat, drought, phosphorus deficiency and low temperature. Yoo et al., 2006 showed that the *siz1* mutant shows thermal hypersensitivity, and on other hand, Catala et al., 2007 demonstrated that the *siz1* mutant has a lower tolerance to drought stress. Reports from Miura et al., 2007 showed that SUMOylation of ICE1 by SIZ1 dependent pathway will activate the expression of *CBF3/DREB1A* and downregulation of *MYB15* expression results in conferring tolerance to low temperature. AtSIZ1 is a positive regulator of basal thermotolerance, drought tolerance, and conferring tolerance under low temperature, whereas AtSIZ1 mediated SUMOylation can control mechanism that acts both positively and negatively under phosphate deficient conditions (Miura et al., 2005), while mutations in *SIZ1* enhance tolerance to salt stress (Miura et al., 2011). The data clearly suggest the important role of AtSIZ1 in plant growth and development under stress conditions. The SUMO E3 ligase OsSIZ1 of rice also exhibited conserved functions like AtSIZ1. Overexpressing OsSIZ1 in *Arabidopsis*, improve thermotolerance and enhance tolerance to both salinity and drought stress (Mishra et al., 2018). In *ossiz1* mutants, total phosphorus (P) and phosphate (Pi) was increased than WT type irrespective of Pi supply (Wang et al., 2015). Heterologous expression of OsSIZ1 in cotton plants has also been shown to increase drought tolerance, improve growth, and increase fibre yield (Clark et al., 2022). Overexpression of OsSIZ1 in creeping bentgrass significantly improves performance under water and heat stress by modulating root growth, enhancing water retention and cell membrane integrity when compared to WT controls (Li et al., 2012).

In *Arabidopsis*, another E3 ligase *AtMMS21/AtHPY2* has been shown to negatively regulate drought tolerance. Knockout of the *AtMMS21/AtHPY2* is viable and beneficial in response to drought stress but it is accompanied by undesirable severe defects that are not worth the trade-off. OsMMS21, a SUMO ligase is a homolog of AtMMS21 where OsMMS21 rice T-DNA

mutant exhibits a dwarfism phenotype that indicates the involvement in rice development. The author also showed OsMMS21 is probably involved in responses mediated by auxin. However, the characterization of OsMMS21 is yet to be done (Jiang et al., 2021). Conversely, OsHPY2.2 expression was decreased in shoot tissues under drought stress (Margarida PhD thesis, 2019).

d. E4 Ligases

E4 SUMO ligases function by promoting SCE1-dependent SUMO chain formation and are currently not as vastly identified in crops in comparison with *Arabidopsis* as observed in other SUMO components (**Figure 1.3**). *Atpial1* and *Atpial2* mutants demonstrated improved growth performance when seedlings are subjected to salinity and osmotic stress. The literature is again limited regarding the role of crop E4 ligases in stress responses (Clark et al., 2022).

e. SUMO proteases

SUMO proteases are an important component within the SUMO cycle because SUMO proteases carry out two key functions in the SUMO system. First, immature SUMO undergoes maturation by cleaving 10 amino acids after the diglycine motif via SUMO proteases' hydrolase/peptidase activity. Secondly, SUMO proteases cleave SUMO from the target protein via isopeptidase activity resulting in a pool of free SUMO. This process makes SUMOylation a reversible modification.

In the ubiquitin system, E3 ligases are assumed to provide specificity in ubiquitination due to an enormous number of E3 ligases. In contrast to the ubiquitin system, only a few E3 ligases are identified in the SUMO system. On the other hand, a significant number of SUMO proteases have been identified which probably suggests that SUMO proteases provide specificity in the SUMO system in *Arabidopsis* and other crop plants (**Figure 1.3**).

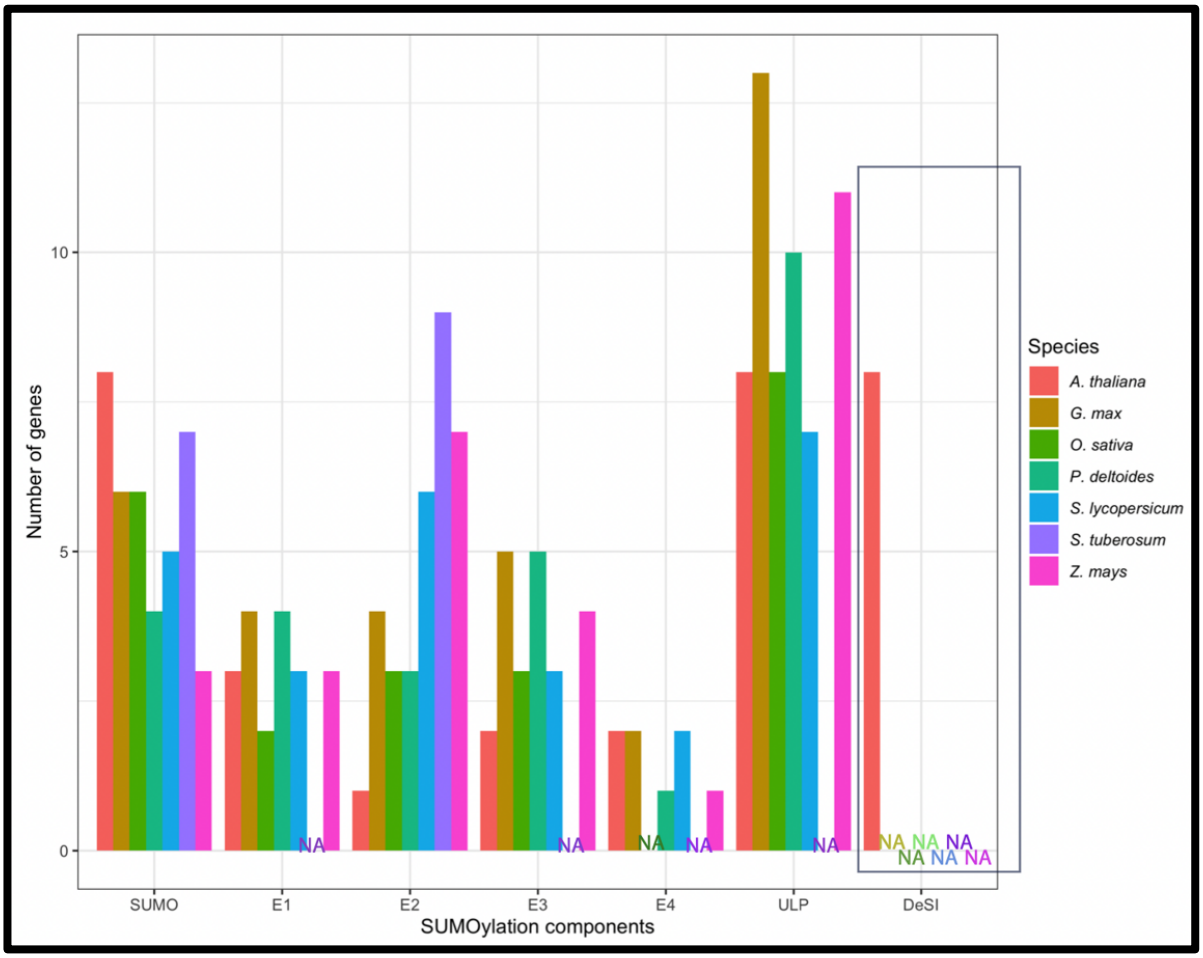

Figure 1.3: Collective summary of the SUMO components involved in the SUMO cycle of *Arabidopsis thalinan*, soybean (*G.max*), rice (*O. sativa*), tomato (*S.lycopersicum*), potato (*S. tuberosum*), and maize (*Z.mays*). Image adapted from Clark, L., Sue-Ob, K., Mukkawar, V., Jones, A.R. and Sadanandom, A., 2022. Understanding SUMO-mediated adaptive responses in plants to improve crop productivity. Essays in biochemistry, 66(2), pp.155-168.

Currently, all the SUMO proteases identified are cysteine proteases because they have cysteine residue in their active site which is critical for proteolytic cleavage. SUMO proteases identified are either the ULPs (Ubiquitin-like proteases) or DeSI (DeSUMOylating isopeptidases). Cysteine proteases are characterized by proteolytic mechanisms and therefore, ULPs belong to the CE clan and DeSI belongs to the CP clan. Presently, in *Arabidopsis*, eight ULPs have been identified and six of them are characterized as SUMO proteases. *AtOTS1* and *AtOTS2* were identified in response to salinity stress where it was observed that during high-salt growth conditions, *AtOTS1/OTS2* were degraded to regulate salt stress response, on the other hand, *Atots1ots2* double mutants exhibited extreme sensitivity to salt stress. Likewise, *AtOTS1/2 is*

also responsible for the deSUMOylation of *auxin response factor 7* (*ARF7*) to provide roots with hydropatterning during wet environments by forming lateral roots in the direction of water-regulating osmotic stress. Bailey et al., 2016 reported *Atots1ots2* double mutants displayed increased resistance to virulent *P.syringae* and increased levels of SUMO conjugation and salicylic acid. Thereby, *AtOTS1/OTS2 has* also have shown to play a role in immunity. Other ULPs such as *AtSPF1* and *AtSPF2* have been shown to play role in immunity by facilitating the SUMOylation of WRKY33 during infection from *Botrytis cinerea* and flg22 treatment. Phosphorylation of WRKY33 is mediated by SUMOylation which facilitates the interaction of mitogen-activated protein kinases (MAPKs), MAPK3 and MAPK6. Other than ULPs, there is inadequate literature regarding the role of DeSI proteases in the *Arabidopsis*, but Orosa et al., 2018 have shown that AtDesi3a protease plays important role in FLS2-mediated immunity. Induction of flagellin caused degradation of AtDesi3a which promotes the SUMOylation of FLS2. As a result, BIK1 is dissociated from the FLS2 complex and thereby activates PTI intracellular immune signaling.

When it comes to the role of SUMO proteases in the response to stress in crops very little is known; however, recent reports have shown eight ULPs are identified, and some reports also showed twelve ULPs in rice (Yates et al., 2016). Though, the role of only two ULPs - OsOTS1 and OsOTS2 has been reported in salt and drought stress in rice. Rice transgenic lines overexpressing *OsOTS1* have been shown to degrade under increasing levels of salinity, indicating that SUMO conjugation in rice plants is important for enhancing salt tolerance by downregulating the activity of OsOTS1/2 protease activity. Moreover, *OsOTS1* has also been shown to mediate drought tolerance in rice plants. The promoter of the *OsOTS3* gene has light-regulation cis-acting regulatory elements (CREs), however, Rosa et al., 2018 also showed the basal expression levels of *OsOTS3* were low in both LC and Nipponbare rice varieties. Knockout of *OsFUG1* exhibits defects in seed fertility, seed weight and panicle architecture whereas knockout of *OsELS1* rice plants will show reduced plant height and defects in flowering time (Rosa and Abreu., 2019). In current literature, there is no identification of DeSI proteases in any crops due to their recent characterization in *Arabidopsis*. DeSI proteases from *Arabidopsis* have a PPPDE domain (catalytic domain, HxNCN) and by using the domain to search in the rice genome (kindly helped received by Miss Kawinnat Sue-ob), 10 OsDeSIs were identified (**Figure 1.4**). But further validation of these OsDeSI is required in the future.

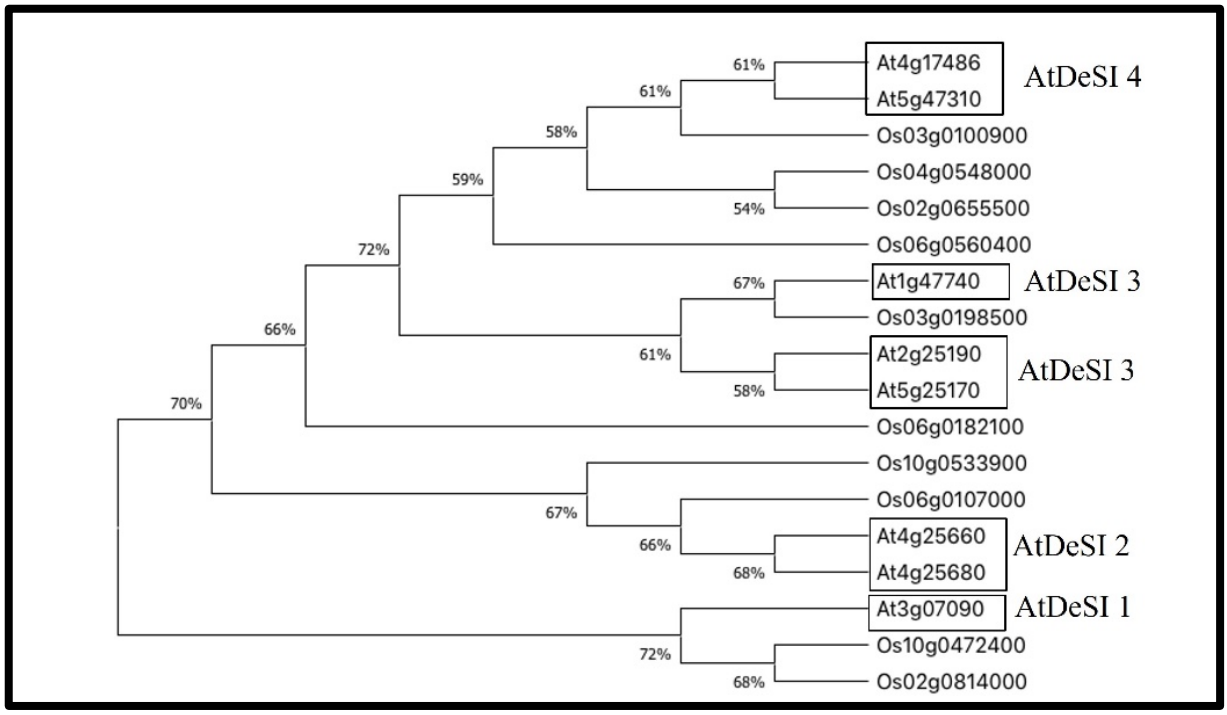

Figure 1.4: Phylogenetic analysis of the DeSI genes of rice and *Arabidopsis*. The protein sequences were aligned by MEGA X and constructed a phylogenetic tree by the maximum likelihood method with 1000 bootstraps.

1.6 Emerging role of SUMOylation in regulating Pi starvation responses

Post-translational modification such as SUMOylation has emerging importance in abiotic and biotic stress responses. A unique characteristic of SUMO is that there will be a strong increase in SUMO conjugates under stress conditions; this pattern of SUMO conjugation under stress conditions has been seen to be conserved in all eukaryotic systems. The role of SUMOylation is well studied, especially in Arabidopsis, under various abiotic stress responses, including water availability, salinity, extreme temperatures, oxidative stress, and nutrient imbalance. Previous literature had showed the critical role of *AtSIZ1* in controlling Pi-starvation responses. *siz1* seedlings display the exaggerated response that is correlated with Pi deficiency which includes cessation of primary root length while increasing root hair number and length and lateral root number, anthocyanin accumulation and shoot/root ratio is decreased. The data indicate that AtSIZ1 is a negative regulator of signalling under Pi deficiency that regulate root system architecture and anthocyanin accumulation. Under low Pi, mRNA levels of Pi

starvation-responsive genes – *AtPS3*, *AtPT2* and *AtPS2* were increased in *siz1* seedlings. Increase expression of these genes results in a change of root architecture and anthocyanin accumulation thereby indicating the critical role of involvement of AtSIZ1 in the Pi starvation sensing mechanism. Interestingly, AtSIZ1 can also act as a positive regulator in the P-starvation response pathway. Transcript accumulation of *AtIPS1* and *AtRNS1* is reduced in *siz1* seedlings as compared to the wild type. Activation of these genes will promote the interaction of AtPHR1 with the PIBS motif in the promoter of these genes. The authors also showed *AtSIZ1* involved in the SUMOylation of AtPHR1. The hypothesis is that SUMOylation of AtPHR1 will activate the transcription of *AtIPS1* and *AtRNS1* genes in Pi deprivation. This paper confirms that AtSIZ1 mediated SUMOylation of AtPHR1 positively controls the transcription activation of *AtIPS1* and *AtRNS1*, however, SUMOylated-AtPHR1 do not show significant phenotypic change or on the expression of *AtPS3*, *AtPT2* and *AtPS2*, thereby negatively controlled by AtSIZ1 (Miura et al., 2005). Fujii et al., 2005 also demonstrated that ubiquitin-conjugating enzyme (UBC) is the target of miR399 and it downregulates the accumulation of UBC transcript to control the plant responses to Pi deficiency. Authors hypothesized that since AtSIZ1 is involved in regulating Pi starvation responses, it may be possible that UBC functions together with E3 ligase from the SUMOylation pathway. Another MYB transcription factor, *MYB62*, is activated in response to low Pi which can be dependent on translational regulation by SUMOylation (Yang et al., 2010). LPR2 regulates the response in roots when local Pi changes and was also identified as a SUMOylated protein. But whether SIZ1 or MMS21 specifically recognizes LPR2 is still unknown. Two purple acid phosphates (PAP10 and PAP26) respond to Pi starvation by controlling internal Pi recycling or Pi release from organophosphates for plants to uptake and have also been found as being SUMOylated (Pan et al., 2019).

Following work on the characterization of AtSIZ1, OsSIZ1 was also characterized to investigate the role of Pi starvation responses in rice. The transcript level of *OsSIZ1* does not change in response to changes in Pi supply. This could be because SUMOylation might affect the protein that functions downstream of SIZ1. *ossiz1* mutants have increased total P and Pi concentrations in both shoots and roots under high and low Pi supply therefore, expression of phosphate transporter (PT) genes involved in Pi response were evaluated. The transcript level of *OsPT8* and *OsPT1* was increased in *ossiz1* mutants, especially under Pi starvation, thereby it is likely to increase Pi acquisition. On the other hand, the expression of another PTs such as PT2 and PT6 are negatively regulated by OsSIZ1. Homolog of Arabidopsis miR399 in rice,

OsmiR399a expression is suppressed in *ossiz1* mutants. The data suggest that OsSIZ1 can act both positively and negatively to regulate the genes involved in the Pi starvation mechanism in rice, which agrees with the literature in Arabidopsis. Potential SUMO sites are found in *OsPHR2,* and its expression is a change under Pi-replete conditions in *ossiz1* mutants (Wang et al., 2015). Pei et al., 2017 showed that like OsSIZ1, OsSIZ2 have similar effects on the expression of transcription factors- *OsPHR1* and *OsPHR2*, Pi transporter – OsPT1 and OsPT8 and ossiz2 mutants have increased levels of Pi and total P in different tissues. Taken together, the author showed that OsSIZ2 acts positively and negatively to govern Pi homeostasis, but OsSIZ1 will have a pronounced effect in regulating Pi starvation responses in rice.

The functional role of other SUMO components was also investigated such as *OsSAE1a*. Mutation in *OsSAE1a* effect shoot and root length i.e., there is a reduction in both parameters in high and low Pi when compared to WT plants. Further investigation suggested that higher uptake of Pi in +P and -P in roots of RNAi lines of OsSAE1a, indicating its negative role in Pi acquisition. In the contrast, there is a similar distribution of Pi in shoot and roots between WT and RNAi lines regardless of Pi supply suggesting the role of OsSAE1a is not involved in the mobilization of Pi. Overall, mutation of OsSAE1a has a differential effect on total P concentration in a tissue-specific manner under low and high Pi conditions (Pei et al., 2020).

The recent findings on the role of SUMO components in regulating Pi homeostasis in both *Arabidopsis* and rice are exciting. Given the reversible and dynamic nature of SUMO in stress conditions, it governs the physiology, morphology, biochemistry and molecular level of proteins in response to phosphate starvation. Even though work has been done to elucidate the role of SUMO in Pi regulon, many intriguing questions remain to be answered.

1.7 The implication of SUMO in future-proofing crops against climate change

There is limited literature about the role of SUMO in crops therefore, it is important to study SUMO components in *Arabidopsis* and how these SUMO components provide a mechanism of defense against abiotic and biotic stresses. The studies in *Arabidopsis* will provide an outline of SUMOylation machinery in crops. **Figure 1.3** showed that number of SUMO components,

particularly E2, E3, and ULPs genes have expanded in crops - soybean (*G.max*), rice (*O. sativa*), tomato (*S.lycopersicum*), potato (*S. tuberosum*), and maize (*Z.mays*) when compared with *Arabidopsis*. This increase is likely ascribed to an evolutionary advantage in crops to enable their survival and the requirement of extra SUMO genes in crop species to provide an extra layer of regulation that is not needed in *Arabidopsis*. Thus, SUMO reveals a conserved core stress response pathway in model plants and crops. Identification of SUMOylated targets regulating adaptive responses could pave the way to generating stress-tolerant crops.

The aim of this PhD project was to investigate the role of SUMOylation in regulating OsPSTOL1 mechanism to confer tolerance to plants under Pi-starved conditions. We examine effect of SUMOylation on the PSTOL1 kinase activity and target selectivity, localization and PSRs in rice and *Arabidopsis*.

1.8 Study objectives

The main objectives of this work are as follows:

a. Investigating the SUMOylation status of PSTOL1 and the non-SUMOylatable version of PSTOL1 and furthermore, determine the role of SUMO sites in regulating the autophosphorylation activity of PSTOL1.

b. Investigating the targets of PSTOL1 by employing Yeast two-hybrid and Co-immunoprecipitation techniques.

c. Characterization of PSTOL1 and the non-SUMOylatable version in a heterologous system, *Arabidopsis* through phenotypic analysis of PSTOL1 transgenic lines under different Pi regimes.

d. Characterization of PSTOL1 and the non-SUMOylatable version through phenotypic analysis of overexpressing PSTOL1 rice transgenic lines under high and low Pi.

Chapter 2

Materials and methods

2.1 Materials

The *Nicotiana benthamiana* leaves, rice and *Arabidopsis* seedlings were used as plant material for experimental work in this thesis.

The chemicals used for the experimental work in this thesis were bought from Sigma-Aldrich, Fisher Scientific, VWR, New England Biolands or Melford.

2.1.1 Vectors

Table 2.1 Vector size and antibiotic resistance used

Vector	Size (bp)	Promoter	Resistance	Purpose
pENTR D-TOPO	2580	N/A	Kanamycin	Gateway entry vector
pENTR4 dual	3757	N/A	Kanamycin	Gateway entry vector
pJET 1.2	2974	T7 promoter	Ampicillin	Cloning vector
pEarlygate 104	12,505	35S promoter	Kanamycin	N-terminal YFP tag plant expression
pEarlygate 201	11,779	35S promoter	Kanamycin	N-terminal HA tag destination vector
pEarlygate 100	11,648	35S promoter	Kanamycin	Destination vector with no tag
pMAL c5X	5677	lacIq promoter	Ampicillin	Expression and purifying of recombinant MBP fused protein in *E.coli*
pDEST 32	12266	ADH1 promoter	Gentamicin	Yeast two hybrid screening
pDEST 22	8930	ADH1 promoter	Ampicillin	Yeast two hybrid screening

2.1.2 Bacterial Strains

Table 2.2 List of bacteria used in this study

Organism	Strain	Resistance	Purpose
Agrobacterium tumefaciens	GV3101	Rifampicin and Gentamicin	Arabidopsis transformation and N.benthamiana transient transformation
Escherichia coli	DH5alpha	n/a	For maintaining and propagation of plasmid
Escherichia coli	BL21 (DE3)	Chloramphenicol, Streptomycin, Kanamycin	For expressing protein
Escherichia coli	CCDB+		For propagation of empty plasmid

2.1.3 Yeast strains

Table 2.3 List of yeast strain used in this study

Yeast species	Strain	Genotype	Use
Saccharomyces cerevisiae	Pj69-4a	MATalpha trp1-901 leu2-3 ura3-52 his3-200 gal4gal80v LYS::GAL1-HIS3 GAL2-ADE2 met::GAL7-lacz	Yeast two hybid
	YM4271	MATa, ura3-52,his3-200,ade-101,ade5, lys2-801,leu 2-3,112, trp1-901,tyr-501,gal4D,gal8D,ade::hisG	Yeast two hybid

2.1.4 Antibodies

Table 2.4.1 List of primary antibodies

Antibody	Host	Working Concentration (TBST)	Supplier
Anti-FLAG	Mouse	1:8000	Sigma Aldrich
Anti-GFP	Rabbit	1:10000	Abcam

Anti-SUMO1	Rabbit	1:2500	Manufactured inhouse
Anti-HA	Rat	1:2500	Sigma Aldrich
Anti-MBP	Mouse	1:10000	NEB

Table 2.4.2 List of secondary antibodies

Antibody	Host	Working Concentration (TBST)	Supplier
Anti-Rat-HRP	Goat	1:20000	Sigma Aldrich
Anti-rabbit-HRP	Donkey	1:20000	Abcam
Anti-mouse-HRP	Rabbit	1:20000	Sigma Aldrich

2.1.5 Enzymes

Table 2.5 List of enzymes used in this thesis

Enzymes	Supplier
Polymerases MyTaqTM Red Mix	Bioline
Q5® Hot Start High-Fidelity DNA Polymerase	New England BioLabs
Brilliant III Ultra-Fast SYBR® Green	Agilent technologies

Gateway Life Technologies pENTR D-TOPO	Thermo Fisher
Life Technologies Gateway cassette LR clonase II	Thermo Fisher
Reverse Transcription Invitrogen SuperScript® II Reverse Transcriptase	Thermo Fisher
Invitrogen RNaseOUT™ Recombinant Ribonuclease Inhibitor	Thermo Fisher
T4 DNA ligase	New England BioLabs
DNaseI	Promega
Restriction Enzymes- PvuI HF, SalI, PstI, BglII	New England BioLabs

2.1.6 Antibiotics

Table 2.6 Working and stock concentration of antibiotics used in the study.

Antibiotic	Stock Solution (mg/ml)	Working Concentration (µg/ml)	Supplier
Kanamycin	50	50	Melford
Hygromycin	40	40	Melford
Basta (Glufosinate ammonium)	20	20	Flurochem
Rifampicin	25	50	Duchefa Biochemie

Gentamicin	25	25	Melford
Streptomycin	100	50	Melford
Carbenicillin	50	50	Melford
Chloramphenicol	34	34	Duchefa Biochemie

2.1.7 Ladders

Table 2.7 List of ladders

Ladder	Supplier
DNA hyperladder^{TM} 1Kb plus	Bioline
50bp DNA ladder	NEB
Page Ruler^{TM} Plus Prestained Protein Ladder	Thermo fisher

2.1.8 Kits

Table 2.8 List of kits used in this thesis

Kits	Supplier
ZR Plasmid Miniprep^{TM} isolation kit	Zymo

Zymoprep yeast Plasmid Miniprep II	Zymo
Gel DNA recovery kit	Monarch®
pENTR/D-TOPO cloning kit	Thermo Fisher
MACS®microbead system	Miltenyi Biotech
DNeasy®Plant Mini kit	Qiagen
NEBExpress®MBP Fusion and Purification system	NEB
ProQuest™ Two-Hybrid System with Gateway™Technology	Thermofisher

2.1.9 Buffers

Ultrapure deionized water was used to make all buffers.

TE Buffer:

0.01% Tris-HCl pH 7.5

0.001% EDTA

SOC:

2% tryptone

0.5% yeast extract

0.05% Nacl

0.019% KCl

after autoclaving add 0.036% glucose and

0.001% $Mgcl_2$

TAE buffer:

2M Tris-HCl

5.71% Glacial acetic acid

0.06M disodium EDTA

Genomic DNA extraction buffer from Arabidopsis seedlings:

0.2% Tris-HCl (pH 7.5)

0.25% NaCl

0.025% EDTA

0.5% sodium dodecyl sulphate (SDS)

Genomic DNA extraction buffer from rice seedlings:

0.5N NaOH

Tris HCl pH 8

For yeast

PEG 3350	8ml of 50% PEG 3350
1M Lithium Acetate (LiAc)	10.2g lithium acetate was dissolved in 100ml deionized water
0.9% NaCl	0.9g of NaCl in 100ml deionized water and autoclave
1.1X TE/LiAc	1.1ml of 10X TE buffer was combined with of 1M LiAc (10X). The volume was made upto 10ml

For protein expression and analysis

SDS-PAGE running gel:

0.38 M Tris-HCl (pH 8.8 at 25˚C)

0.1% Sodium dodecyl sulphate(SDS)

8-15% (w/v) 29:1 Acrylamide:Bis-acrylamide

0.05% (w/v) Ammonium persulphate (APS)

0.07% (v/v) Tetramethylethylene-diamine

(TEMED)

SDS-PAGE stacking gel:

132 mM Tris-HCl (pH 6.8 at 25˚C)

0.1% SDS

4% (w/v) 29:1 Acrylamide:Bis-acrylamide

0.05% (w/v) APS

0.15% (v/v) TEMED

4x SDS Loading Buffer:

200mM Tris-HCl (pH 6.8 at 25°C)

8% (w/v) SDS

50mM EDTA

20mg Bromophenol blue

4% w/v β-mercaptoethanol

40% (v/v) glycerol

10x SDS-PAGE Running Buffer:

250mM Tris-HCl (pH 8.3 at 25°C)

1.9M glycine

1% (w/v) SDS

1x SDS-PAGE Running buffer:

25mM Tris-HCl (pH 8.3 at 25°C)

190mM glycine

0.1% (w/v) SDS

Coomassie Stain:

0.25% (w/v) Coomassie Brilliant Blue R-250

10% (v/v) MeOH

10% (v/v) glacial acetic acid

Coomassie Destain:

10% (v/v) MeOH

10% (v/v) glacial acetic acid

10x Transfer Buffer:

250mM Tris

1.9M glycine

1x Transfer Buffer:

25mM Tris

190mM glycine

20% (v/v) MeOH

10x TBS:

500mM Tris (pH 7.4 at 25°C)

9% (w/v) NaCl

1x TBST:

50mM Tris (pH 7.4 at 25°C)

0.9% (w/v) NaCl

0.1% (v/v) Tween20

Blocking Solution: 5% (w/v) non-fat milk powder in 1xTBST

ECL Solution 1:

2.5mM luminol

0.4 mM p-coumaric acid

100mM Tris pH 8.5

ECL Solution 2:

0.02% hydrogen peroxide

100mM Tris pH 8.5

SUMO Extraction Buffer:

(For Arabidopsis)

1mM EDTA

1% (v/v) NP-40

0.5% (w/v) Sodium deoxycholate

0.2% (w/v) SDS

20mM NEM

50mM Tris-HCl (pH 8.5 at 25°C)

150mM NaCl

1 protease inhibitor cocktail tablet

SUMO Extraction Buffer

(For Rice)

25mM Tris-HCl (pH 8)

150mM NaCl

1mM EDTA

0.7% (v/v) NP-40

0.25% (w/v) Sodium deoxycholate

70mM NEM

2% Glycerol

0.1% Triton X-100

20mM $MgCl_2$

50mM KCl

1 protease inhibitor cocktail tablet

CO-IP Buffer:

150mM NaCl

50mM Tris-HCl (pH 8 at 25°C)

5mM EDTA

10% (v/v) glycerol

0.1% (v/v) Triton-X

10mM DTT

1 protease inhibitor cocktail tablet

Ponceau S Stain:

0.5% (w/v) Ponceau S

1% (v/v) glacial acetic acid

Elution buffer:

50mM Tris base

20mM Reduced glutathione, pH 8.0

1M IPTG: 238.31mg IPTG in 1ml MQ water; filter sterile

Column buffer:

20Mm Tris HCl pH=7.4

200mM Nacl

1mM EDTA

0.5M Maltose: 3.603g maltose in 20ml MQ water.

Kinase reaction buffer (10x):

25mMTris HCl pH=7.4

	5mM $MgCl_2$
	20mM ATP
	2.5mM EDTA
	1mM DTT
	25mM ATP
	5mM BGP
	20mM Na_3VO_3
	2.5mM EGTA
	50mM $MnCl_2$
Phostag	5mM Phos-tag

2.2 Media

2.2.1 For Bacteria

Luria Bertani broth:

2% LB broth (lennox)

1% microagar (if required)

After autoclave, add appropriate antibiotic

Rich medium+glucose+carbenicillin:

2% LB broth (lennox)

2g glucose per liter, autoclave

sterile carbenicillin was added to media

2.2.2 For Yeast

YPDA:

1% yeast extract

2% peptone

2% glucose

0.01% adenine hemisulfate

1.2% microagar

Synthetic defined (SD) medium:

2.67% DOB

0.079% CSM

2% agar

1M 3-amino-1,2,4-triazole (3-AT): 0.84g 3-AT dissolved in MQ water

2.2.3 For Arabidopsis

½ MS (Melford) for growing Arabidopsis seedlings:

0.22% Murashige & Skoog Basal Salt Mixture

0.8% phytoagar (if required)

1% sucrose (if required)

pH 5.7 with KOH

Murashige & Skoog Modified Basal Salt Mixture (phytotech lab):

0.61% Murashige & Skoog Basal Salt Mixture

0.8% phytoagar (if required)

pH 5.7 with KOH

2.2.4 For Rice (Oryza sativa)

½ MS (Melford) for growing Rice seedlings:

0.22% Murashige & Skoog Basal Salt Mixture

0.4% Gerlite (if required)

1% sucrose

pH 5.7 with KOH

Murashige & Skoog Modified Basal Salt Mixture (phytotech lab):

0.61% Murashige & Skoog Basal Salt

Mixture

0.35% phytoagar (if required)

pH 5.7 with KOH

Yoshida Growth media for growing rice seedlings

Table 2.9 Preparation of stock solutions

Element	Reagent	Preparation g/1L of distilled water
N	NH_4NO_3	91.4
P	$NaH_2PO4.2H_2O$	40.3
K	$K_2 SO_4$	71.4
Ca	$CaCl_2$	88.6
Mg	$MgSO_4 \cdot 7H_2O$	324
After dissolving macronutrients, pH was adjusted to 4.5 with concentrated HNO_3. Make up to 1 litre volume with distilled water.		

Mn	$MnCl_2 \cdot 4H_2O$	15
Mo	$(NH_4)_6 \cdot MO_7O_{24} \cdot 4H_4O$	0.74
B	H_3BO_3	9.34
Zn	$ZnSO_4 \cdot 7H_2O$	0.35
Cu	$CuSO_4 \cdot 5H_2O$	0.31
Fe	FeEDTA	
Citric acid (monohydrate)		119

The nutrient media was prepared according to concentration of each component mentioned in Table 2.9 expect the final concertation of phosphorus ($NaH_2PO4.2H_2O$) was modified to 100μM (high Pi) and 3μM (low Pi) respectively.

Modified Phosphate media

For preparing modified phosphate media to examine the *Arabidopsis* seedlings under different phosphate condition, MS media (Duchefa) lacking nitrogen, potassium and phosphorus was used. Nitrogen (NH_4NO_3) and potassium (KNO_3) were supplemented according to concentration mentioned for full strength MS. Later, final concentration of phosphorus (KH_2PO_4) was added to media to prepare for high (1.25mM) and low Pi (3μM) media respectively.

2.3 Plant Growth and treatment

2.3.1 *Nicotiana benthamiana* growth

N.benthamiana seeds were sown onto moist Levington F2 plus sand compost in a tray. To maintain the humidity for seedlings the tray was covered with a lid. The seedlings were grown in a growth room with temperature of 21°C and a 16/8-hour light/dark programme. 1-week seedlings were transferred into individual 10cm pots where they were allowed to grow under same conditions until the plants had produced 5-7 leaves.

2.3.2 For *Arabidopsis thaliana*

*Arabidopsis thaliana*tissue culture

All Arabidopsis seedlings were grown on ½ MS medium (Melford) or full-strength MS (phytotech) with 0.8% agar. Media was allowed to cool down to 50°C before adding selective agents.

Arabidopsis thaliana sterilization for tissue culture

Arabidopsis seeds were sterilized using chlorine gas generated from the reaction between 3ml concentrated hydrochloric acid and 97ml of 12% hypochlorite solution. The sterilization was set up in a closed box in a fume hood. The seeds were allowed to sterilize for 10-12 hours before being ventilated in laminar hood to remove chlorine gas. The seeds were placed on ½ MS or full MS plates, and the plates were sealed with micropore tape (3M). The sealed plated

were transferred for stratification at 4°C for 3 days. After 3 days, the plates were then placed vertically at 21°C temperature in 16/8-hour light/dark programme in a Sanyo growth cabinet.

***Arabidopsis thaliana* growth**

Arabidopsis seeds were sown in most Levington F2 plus sand compose treated with Calpyso SC 480 insecticide (Bayer). The seeds were then stratified for 3 days at 4°C before being transferred to growth room. The plants were grown under long day conditions: 16light hours at 22°C and 8 dark hours at 20°C with a constant relative humidity of 70%.

2.3.3 For Rice *(Oryza sativa)*

Rice tissue culture

Rice seedlings were grown on ½ MS medium, 1% sucrose and 0.4% gerlite. Media was allowed to cool down to 50°C before adding selective agents.

Rice seeds sterilization for tissue culture

The mature rice seeds were dehusked with a rice husker and seeds were collected into a sterile 50-ml tube. The seeds were surface sterilized in 20ml of 70% ethanol for 10seconds and then in 25ml of 2% sodium hypochlorite for 22-25minutes with shaking. The seeds were rinsed with sterile water for 5 times. Extra water was removed, and the seeds were placed on ½ MS plates. The seeds were stratified at 28°C for 3 days before transferring them to light at 28°C.

Rice growth

The 7-10 days old seedlings were transferred to John Innes number 2 soil in 60cm pots . The pots were kept in growth room with a temperature 28°C. The plants were raised in 16/8 hours photoperiod with approximately 70% relative humidity.

2.4 Raising and selection of PSTOL1 transgenic lines in *Arabidopsis thaliana* and Rice

2.4.1 Floral dipping of *Arabidopsis thaliana*

The floral dip method was followed as described by Clough and Bent 1998. Protein expression vectors with gene of interest cloned is transformed into *Agrobacterium tumefaciens* strain GV3101 (pMP90). Positive colonies are streaked on plates with Rifamycin, gentamycin and kanamycin (specific to vector transformed into *Agrobacterium* strain). 10ml of liquid LB with same selection was inoculated from freshly streaked plates and grown overnight at 28°C with shaking at 200rpm. 1% of starter culture was inoculated into 500ml of liquid LB with appropriate selection and grown at 28°C with shaking at 200rpm for 24hours. The cells were centrifuged at 4500rpm (3170g) for 10minutes, and supernatant disposed. The cells were resuspended in 400ml 5% (w/v) of sucrose in sterile water. 0.02% of Silwett-L77® was added to the culture. The stage of Arabidopsis plants is very important for the floral dipping. 4–5-week-old grown under long-day condition with unopened inflorescence is the best stage for having maximum positive transformants. The bolts were dipped for 30 seconds with agitation. Once dipping was over, the plants were laid down in trays and covered with plastic dome for 24 hours for maintaining humidity. The plastic dome was removed after 24 hours, and plants were allowed to stand upright. The plants were allowed to grow in 16/8-hour light/dark programme in a growth room until they set seeds.

Selection of transgenic *Arabidopsis thaliana*

T1 (primary transformants) were selected by spreading seed on soil soaked with 0.1% Glufosinate (marketed as Basta, Bayer). The seeds were stratified for 2 days at 4°C. The resistant seedlings were selected after 3 weeks and transferred to fresh soil with no selection. The seedlings were grown under long day conditions until plants set seeds. T2 (second generation) seeds were collected and sterilised as described above. The seeds were spread on ½ MS plates supplemented with 20mg/ml final glufosinate-ammonium (BASTA) and the plates sealed with micropore tape (3M). The seeds were stratified at 4˚C for 3 days. The plates were then moved to growth cabinets and grown for 10-12 days. At this stage, the seedlings were screened for resistance at a ratio of 3:1 (resistance : susceptible) to select for transgenics containing a single transformation insert. Few seedlings were picked out from selected lines and were transferred to soil with no selection. Plants were allowed to set seed and T3 (third generation) seeds were collected for screening again. T3 seeds were sterilised and spread on ½ MS plates supplemented with 20mg/ml final glufosinate-ammonium and the plates sealed with micropore tape (3M). The seeds were stratified at 4˚C for 3 days. The plates were then moved to Sanyo growth cabinets and grown for 10-12 days. The plants were then screened for complete resistance indicating the homozygous state of plants. Again, seedlings from selected lines were then transferred to soil without selection. The individual plants were allowed to grow in long-day conditions to set seeds.

2.4.2 Generation of PSTOL1 transgenic lines in rice (kindly done by Dr.Cunjin Zhang)

The full length CDS sequence of OsPSTOL1 was amplified from Kasalath genomic DNA and cloned into pDTOPO vector. The gene was subcloned into binary vector pIPKb002 which has ubiquitin promoter. The construct was introduced into Agrobacterium tumefaciens strains EHA105 and then transformed into rice (O.sativa cv Nipponbare).

Selection of transgenic rice by evaluating the transgene copy number

At T0 stage, the pure genomic DNA from rice seedlings was isolated using the DNeasy®Plant Mini kit (Qiagen). SYBR Green qPCR (Quantitative polymerase chain reaction) was carried out in thermal cycler Rotorgene Q. To calculate the PSTOL1 copy number, a relative quantification method was used. In this approach, the absolute value was used : one for the endogenous reference gene (Sucrose phosphate synthase, SPS) and one for the target specific gene from transgenic plants (Hygromycin gene). The relative values are then compared to positive control which on previous investigation had shown single copy SPS gene in GM (genetically modified) rice. The quantitative RT-PCR result of the SPS gene amplification was to represent total rice genome copy number, which was designed to normalize the reaction and thereby enabling estimation of the transgene copy number.

The transgenic rice plants that showed the single-copy insertion in T0 stage were allowed to grow and set seeds for further analysis. The T1 seeds were collected and sterilised as described above and were placed on ½ MS plates supplemented with 40mg/ml hygromycin for 3:1 segregation ratio. The seeds were placed in dark at 28°C for 3 days before transferring them to light for analysis. The seedlings from selected lines were transferred to soil and allowed them to set seeds. T2 seeds are collected and sterilised and placed on ½ MS plates supplemented with 40mg/ml hygromycin for screening homozygous transgenics.

2.5 Microbiological Procedures

2.5.1 Generation of chemically competent *E.coli*

The selected *E.coli* strain (e.g.DH5a) was streaked out onto a fresh LB agar plate with no selection and incubated at 37˚C for 24 hours. A single colony was selected using a sterile loop

and used to inoculate 10ml of LB media. The culture was grown for 16 hours at 37˚C. 1ml of the culture was then used to inoculate 200ml of LB media, with shaking at 220rpm, at 37˚C for further 6 hours. The bacterial culture was transferred to chilled centrifuge tubes and centrifuged at 4000rpm for 15minutes at 4˚C. The supernatant was removed, and the cells were resuspended in 10ml of ice-cold TE buffer. The culture was re-centrifuged under same conditions, the supernatant removed, and the cells resuspended in 10ml of ice-cold liquid LB. The cells were the stored at -80˚C in 100µl aliquots.

2.5.2 Generation of chemically competent *Agrobacterium tumefaciens*

The selected *Agrobacterium tumefaciens* (e.g. GV3101) was streaked out onto a fresh LB agar plate with rifamycin and gentamicin selection and incubated at 28 ˚C for 48 hours. A single was selected using a sterile loop and used to inoculate 10ml of LB media with rifamycin and gentamicin. The culture was grown for 24 hours at 28˚C. 1ml of the culture was then used to inoculate 200ml of LB media with rifamycin and gentamicin and incubated , with shaking at 220rpm at 28˚C for further 18 hours. The culture was transferred to chilled centrifuge tubes and centrifuged at 4000rpm for 15minutes at 4˚C. The supernatant was removed, and the cells resuspended in 10ml of ice-cold TE buffer. The culture was re-centrifuged under same conditions, the supernatant removed, and the cells resuspended in 20ml of ice-cold liquid LB. The cells were the stored at -80˚C in 100µl aliquots.

2.5.3 Preparation of yeast competent cells

Fresh yeast strain (PJ69-4α) was streaked on YPDA plate and incubated at 30˚C for approximately 3 days. Single colony was inoculated in 10ml YPDA medium and incubated for 8-12 hours at 30˚C with shaking at 250rpm. 50ml of YPDA was prepared in 250ml flask and

5µl culture was transferred to 50ml YPDA. The media was incubated at 30˚C with shaking at 250rpm until the OD reached 0.15-0.3. Once the desired O.D. had been reached, cells were centrifuged at 700g for 5minutes at room temperature (RT). Supernatant was discarded and the

pellet was resuspended in 100ml of fresh YPDA. The culture was again incubated at 30˚C until O.D. was reached 0.4-0.5 (3-5 hours) with shaking at 250rpm. 100ml YPDA culture was divided into two 50ml sterile falcon conical tubes and again centrifuged at 700g at 5minutes. The supernatant was discarded, and pellet was dissolved with 30ml deionized water. The culture was again centrifuged at 700g at 5minutes, and supernatant was discarded. The pellet was dissolved in 1.5ml 1.1Xte/LiAC. The cell suspension was transferred into 1.ml microcentrifuge tubes and centrifuged at high speed for 15seconds. After centrifugation step, the supernatant was discarded, and pellet was resuspended in 600µl 1.1Xte/LiAC. 50µl from above culture was aliquoted into 1.5ml microcentrifuge tubes.

2.6 DNA/RNA analysis

2.6.1 Primer designing

For Arabidopsis

Arabidopsis thaliana gene coding DNA sequences were retrieved from The *Arabidopsis* Information Resource (TAIR).

For Rice

Rice Genome Annotation Project (previously also known as MSU) or Rice annotation Project Database (RAB-DB) programs were used to retrieve *Oryza sativa* gene coding DNA sequences.

2.6.2 Polymerase chain reaction (PCR)

Colony PCR

Individual bacterial/agrobacterial colonies were dissolved in 10µl water or LB and 2µl was used as DNA template for PCR reaction. The PCR as carried out using different set of primers- vector specific primers, vector-gene specific primers and gene specific primers. The different combination of primers will ensure the recombinant gene insert after bacterial transformation.

Table 2.10 Colony PCR set up:

Component	10µl reaction
2X Bioline My Taq Red Mix	5
Forward primer (10pm/µl)	0.5
Reverse primer (10pm/µl)	0.5
DNA template	2
Sterile water	To 10

Table 2.11 Cycling programme used during colony PCR

Temperature	Time	Number of cycles
95˚C	3min	-
95˚C	30sec	x30
58˚C	30sec	
72˚C	1min per kb	
72˚C	5 min	-
10˚C	µ	-

Once PCR is over, the reactions were run on an agarose gel to check the size of gene insert and gene plus vector size.

Cloning PCR

- Q5™ (NEB) cloning polymerase was used amplify the different genes using the primers with CACC added to the 5' end of forward primer and reverse primer designed to amplify with or without stop codon for cloning using pDTOPO cloning kit.

- Primers with correct restriction sites added were used for cloning in pENTR4/pMAL vector system. The template DNA used for cloning were either amplified from cDNA, genomic DNA or plasmid.

Table 2.12 PCR set up for cloning by Q5 polymerase

Component	50µl reaction
5x Q5™ reaction buffer	10µl
10mM dNTPs	1µl
Forward primer (10pm/µl)	0.5µl
Reverse primer (10pm/µl)	0.5µl
DNA template	100-200ng
Q5™ High fidelity polymerase	0.5µl
5x Q5 High GC Enhancer (optional)	10µl
Sterile water	To 50

Table 2.13 Cycling programme used for cloning by Q5 polymerase

Temperature	Time	Number of cycles
95˚C	3min	-
95˚C	30sec	x25
58˚C	30sec	
72˚C	30sec per kb	
72˚C	5 min	-
10˚C	µ	-

The PCR reaction was analyzed for correct size on agarose gel. The PCR product from agarose gel was cut using sharp scapel and DNA purified using Gel extraction kit (Qiagen kit).

Genotype analysis by PCR

The primers were developed for CAPS (Cleaved Amplified Polymorphic Sequences) markers.

The primers for CAPS can be based on single nucleotide change.

Table 2.14 PCR set up for genotyping analysis

Component	10µl reaction
2X Bioline My Taq Red Mix	5
Forward primer (10pm/µl)	0.5
Reverse primer (10pm/µl)	0.5
DNA template (rice or Arabidopsis gDNA)	2
Sterile water	To 10

Table 2.15 Cycling programme used for genotyping analysis

Temperature	Time	Number of cycles
95˚C	3min	-

95˚C	30sec	X30
58˚C	30sec	
72˚C	30sec per kb	
72˚C	5 min	-
10˚C	µ	-

PCR product was analyzed for correct size on agarose gel. The PCR product from agarose gel was cut using sharp scalpel and DNA purified using Gel extraction kit (Qiagen kit). The purified PCR product was subjected to restriction digestion by endonuclease.

Real-Time PCR (Quantitative PCR, qPCR)

Primers for qPCR were designed to target genes using NCBI BLAST (Geer et al., 2010). This was to ensure the specificity of primers to target gene. The cDNA quality and primer annealing temperature was tested using gradient PCR. The components for reaction are listed below in table 2.16 were run in Qiagen Rotogene®Q under the programme conditions in table

Relative expression was compared between genotypes and treatments using target primers and primers to the housekeeping gene ACTIN2 (At3g18780) from Arabidopsis and OsACTIN 1 (LOC_Os03g50885) from Oryza sativa for normalisation (the in-house standard housekeeping gene). Technical repeats were conducted in triplicate for each sample and comparisons were performed using the comparative quantification using $2^{\wedge(-\text{delta } C_T)}$ using the software provided by Qiagen. Melting curve analysis for eachreaction was conducted using the software provided by Qiagen.

Table 2.16 qPCR set up

Component	10µl reaction
SYBR green	5
Forward primer (10pm/µl)	0.5
Reverse primer (10pm/µl)	0.5
Template cDNA	1
Sterile water	To 10

Table 2.17 Programme for qPCR using Rotogene Q machine

Temperature	Time	Number of cycles
95˚C	3min	-
95˚C	10sec	X40
58˚C	30sec	
72˚C	2minute	

2.6.3 Agarose gel electrophoresis

To visualize the different fragments of DNA, different percentage (between 0.8-1.2%) agarose gels were made. The higher percentage gels were used to visualize small fragments of DNA whereas lower percentage gels were used to visualize large fragments of DNA. Agarose was

added to the 1x TAE buffer to make a 0.8-1.2% solution was then heated in a microwave until the agarose had dissolved. The solution was allowed to cool down before ethidium bromide was added to a final concentration of 0.0001%. The solution was then poured into an appropriately sized gel mold, a 8/20 well comb added and the solution allowed to set. The gel was then placed into gel tank contained 1x TAE buffer. 5µl of appropriate hyperladder (either 50bp, 100bp or 1Kb depending on size fragment) (Bioline) was pipetted into the first well. The gel tank was run from 80-120V. The DNA fragments were visualized in BioRed Gel Doc 2000.

- The procedure can be followed to analyze the RNA on the agarose gel.
- For PCR reaction using Q5, 10x loading dye was added to final concentration of 1x to PCR reaction before loading into the wells.

2.6.4 Gel Extraction

The fragment to be extracted was first run on agarose gel. The gel was placed on a UV light box and the expected DNA fragment was cut using a sharp scalpel and put into a pre weighed 1.5ml tube. The tube was then reweighed to get the weight of the gel. The gel extraction was done following the instructions in the Qiagen Gel extraction kit. 12µl of sterile water was used as final elution.

2.6.5 DNA Extraction:

From bacteria:

Positive bacterial colonies (confirmed by colony PCR) were inoculated in 10ml LB culture supplemented with appropriate antibiotics incubated overnight at 37˚C. Recombinant plasmids

were purified using a ZR Plasmid Miniprep kit-Classic (Zymo research). The amount of DNA was quantified using a NanoDrop™One (Thermo Scientific).

- If plasmid was isolated from Agrobacterium tumefaciens, same procedure was followed. The quantity of DNA was low whenever plasmid was isolated from Agrobacterium tumefaciens.

DNA extraction from Yeast

The yeast colony was dispensed into 1.5ml SD/-LWH in 2ml microcentrifuge tube was allowed to incubate at 28˚C overnight. The plasmid was isolated from yeast colony using Zymoprep™ Yeast Plasmid Miniprep II kit.

Genomic DNA extraction from *Arabidopsis thaliana*

A single leaf disc was cut using the end of a P10 pipette tip. The disc was ground briefly in a 1.5ml microcentrifuge tube using a mini-pestle. 150µl of extraction buffer was added and the mix ground again until homogenous. The sample was centrifuged at 13,000 rpm for 5minutes. 100µl of the supernatant was transferred to a fresh tube and 100µl of neat isopropanol was added and mixed via inversion. The mixture was incubated at room temperature for 5minutes. Samples were centrifuged at 13,000 rpm for 10 minutes and the supernatant was discarded. The pellet was mixed gently with 500µl of 70% EtOH and centrifuged at 13,000 rpm for 5 minutes. The supernatant was discarded, and the pellet left to air-dry for 15 minutes. The dry pellet was then dissolved in 50µl of 10mM Tris (pH 8.5 at 25˚C). The quality of the gDNA extraction was then checked via PCR using Actin primers.

Crude Genomic DNA extraction from rice seedlings

The fresh leaf was cut and ground briefly in a 1.5ml microcentrifuge tube using a mini pestle. 50µl of 0.5N NaOH was added to ground tissue. 5µl of crushed tissue was added to 245µl of 100mM Tris HCl pH 8 and boiled for 2-3 minutes. 5µl was used as a DNA template for 25µl PCR reaction.

Pure Genomic DNA extraction from rice seedlings

The fresh leaf was cut and ground by liquid N_2 briefly in a 1.5ml pre-chilled microcentrifuge tube using a mini pestle. The procedure to extract pure genomic DNA was followed as per the instruction on DNeasyPlant Mini Kit.

2.6.6 RNA Extraction

RNA extraction from *Arabidopsis thaliana*

The plant tissue was flash freeze in liquid N_2 and was ground into a fine powder using a precooled microcentrifuge and micropestle. The RNA was extracted using the ZR zymo RNA extraction kit (ZYMO). All extractions were performed following the instructions provided in the supplied kit. RNA was eluted in DEPC water and quantified by measuring absorbance at l260nm and l280nm using a NanoDrop™ One (Thermo Scientific).

RNA extraction from rice seedlings

7-10 days rice seedlings were used to extract the RNA. The tissue was ground into fine powder using a prechilled mortar and pestle. The ground tissue was transferred to prechilled 2ml microcentrifuge tube. TRIzol reagent was added to ground tissue in microcentrifuge and was vortex for 2-3 minutes. 200µl chloroform was added to per ml of TRIzol reagent and shake vigorously for 15 seconds. The mixture was centrifuged at 4˚C at 18000g for 15 minutes. After centrifugation, the mixture was separated into 3 phases- a red organic phase (containing protein), an interphase (containing DNA) and a colorless upper aqueous phase (containing RNA). The aqueous phase was transferred to fresh tube and 0.5ml of isopropanol was added. The sample was again centrifuged at 4˚C at 18000g for 15 minutes. RNA will be precipitated as a white pellet at the bottom of tube. The supernatant was removed, and the RNA pellet was washed with 1ml of 75% ethanol (in DEPC). The sample was centrifuged again at 4˚C at 18000g for 10 minutes. The ethanol was removed, and the pellet was allowed to dry. The pellet was dissolved in 30µl DEPC water.The RNA sample was stored in -80˚C.

RNA purification by Sodium Acetate precipitation

One volume of chloroform was added to RNA in microcentrifuge tube and was vortexed for 5 minutes. The mixture was centrifuged at 18,000g for 5minutes at 4˚C. Upper phase was transferred to fresh microcentrifuge tube. 3 volumes of ice-cold ethanol and 1/10 volume of 3M Sodium acetate pH 4.8 was added to and incubate at -20˚C overnight. The mixture was centrifuged at 4˚C for 1hour at 18,000g. The supernatant was discarded and 1ml of 75% ethanol (in DEPC) was added and again centrifuged at 4˚C for 30 minutes at 18,000g. Supernatant was discarded again, and the pellet was allowed to dry and resuspended in 30µl DEPC water.

2.6.7 cDNA synthesis

From *Arabidopsis* seedlings

RNA was extracted using ZR zymo RNA extraction kit (ZYMO) as per instruction from the whole Arabidopsis plants to be used as a substrate for cDNA synthesis. 1µl of each oligo dT (500µg/ml) and dNTP mix (10µM each) was added to the reaction and incubated at 65˚C for a further 5 minutes. The reaction was then chilled briefly on ice and spun down. 4µl 5X First strand buffer, 2µl 0.1M DTT,1µl RNaseOUT and 1µl Superscript^{Ò}II Reverse Transcriptase was added to the reaction and was allowed to incubate at 42˚C for 50 minutes. Finally, the reaction was heated to 70˚C for 15 minutes to terminate the reaction. The final cDNA was made up to 100µl by adding 80µl ultra-pure water (1:5 ratio). The quality of the resultant cDNA was tested by PCR with actin primers.

From Rice seedlings

RNA was extracted and was subjected to DNase treatment. 2µg of RNA, 1µl 10x DNase buffer, 1µl DNase was added together, and final volume was made up to 10µl by DEPC water. The reaction was incubated at 37˚C for 30 minutes. 1µl of STOP solution was added to solution to cease the reaction. The reaction was then incubated at 65˚C for 5minutes. After incubation, reaction was chilled briefly on ice and spun down. The same protocol was followed as described above. The quality of the resultant cDNA was tested by PCR with actin primers designed according to OsACTIN gene.

2.6.8 pENTR4 Cloning

The target gene were amplified using primers flacking relevant restriction sites. The PCR products were run on agarose gel and the desired product was cut out of the gel using sharp scalpel. The DNA fragment was purified using Qiagen Gel DNA recovery kit. The purified DNA fragment and pENTR4 vector was then digested with the relevant restriction sites for overnight at 37˚C. The digested product was run on a 0.8% agarose gel and again correct sized fragment and pENTR4 backbone was cut from the gel using a sharp scalpel. The fragments were purified using Qiagen Gel DNA recovery kit. The digested products were then ligated in 10µl reaction together using T4 DNA ligase overnight at 4˚C. The ligation reaction was then transformed into *E.coli* DH5a.

- For cloning in pMAL c5X vector, the same protocol was followed as described above.

2.6.9 pENTR4/D-TOPO Cloning

For pENTR4/D-TOPO cloning, it is important to add CACC at the 5'end of the forward primer and gene was amplified and purified as described above. The purified DNA and vector were ligated as per instruction provided in the Invitrogen kit. The reaction contents were then transformed into *E.coli* DH5a.

2.6.10 Restriction Digestion

Standard restriction digestion

A standard restriction digestion was followed for digesting the insert and vector for pENTR4 or pMAL c5X cloning. The restriction digestion reactions were incubated 37˚C overnight. The digested products were then run on an agarose gel.

Table 2.18 showing restriction digestion setup components in standard restriction digest with NEB enzymes

Component	50µl reaction
10x compatible NEB buffer	5
DNA	1µg
Restriction endonuclease (NEB)	5 U per µg DNA
Sterile water	Up to 50µl

Table 2.19 showing Restriction digestion setup components for genotyping the transgenic lines

Component	20µl reaction
10x compatible NEB buffer	2µl
PCR purified product	6µl
BglII	1
Sterile water	Up to 20µl

2.6.11 T4 DNA Ligase reaction

T4 DNA ligase reactions were carried out to anneal two DNA fragments after restriction digestion containing corresponding restriction sites. For a standard ligase reaction, the ratio of vector to insert was 1:3 however the ratio can be varied depending on the size (in kb) of each

fragment. The reaction was incubated overnight at 4˚C. The reaction was transformed into *E.coli* DH5a.

Table 2.20 showing Ligase reaction setup components for T4 DNA ligase

Component	20µl reaction
10x T4 DNA Ligase Buffer	2µl
Vector	50ng
Insert	37.5ng
T4 DNA ligase	1µl
Sterile water	Upto to 20µl

2.6.12 LR Reaction into Gateway® Destination Vectors

Few Gateway destination and pENTR4/D-TOPO vectors sometimes have same antibiotic resistant gene, so it is important to digest the recombinant gene with NruI or PvuI (NEB) in entry vector, ensuring the gene of interest was not also digested. This step is important to ensure that entry vector is not replicated in *E.coli* DH5a after transformation and only LR recombinant plasmid (destination vector with insert) can grow. The LR reaction was performed as described in table below:

Table 2.21 showing LR reaction setup components

Component	10µl reaction
TE buffer pH 8	2µl
Entry vector	50ng
Destination vector	150ng
LR	0.5
Sterile water	Upto to 10µl

2.7 Protein Expression

2.7.1 Protein expression and purification from *E.coli*

E.coli strain BL21 was transformed with MBP fused with PSTOL1 in pMAL vector. Transformed colony was confirmed by PCR using PSTOL1 gene specific primers. The positive colony for PSTOL1 WT and PSTOL1$^{2K/R}$ was inoculated in 10ml LB cultures containing the appropriate antibiotic (50µg/ml carbenicillin) for 16 hours at 37˚C. The optimum conditions for expressing fusion protein were achieved by testing the different conditions using following method.

100µl of overnight culture was added to a 10ml LB culture with appropriate antibiotic (50µg/ml carbenicillin). Two 10ml culture was grown at 37˚C on shaker until optical density (O.D.) at 600nm of the culture was between 0.6-0.8. 1ml culture was taken as uninduced sample and spun down. 3ml culture was separated in six different 15ml falcons. Two different IPTG concentrations was used to induce the cultures- 0.5mM and 1mM. Both IPTG concentration

was used for induction respectively and culture were grown on three different temperatures - 37˚C, 28˚C and 18˚C. 3 hours after IPTG induction, further samples were taken. All samples were then spun down at 10000rpm for 5minutes. For total protein extract, the pellet was mixed in 200µl 1x SDS-PAGE loading buffer. For insoluble and soluble fractions, pellet was mixed with bugbuster (Novogen, Billerica, USA) volume according to the weight of pellet. 1 tablet of complete^{TM} mini EDTA-Free Protease Inhibitor Tablets (Roche, Indianapolis, USA) was mixed with 10ml the bugbuster before adding to pellet. Cell suspension was incubated on rotating mixer at slow setting for 20minutes. The cell suspension was centrifuged at 13000rpm (16,200g) for 30minutes at 4˚C. The supernatant was transferred into new microcentrifuge tube. The pellet after centrifugation was dissolved in 200µl 1x SDS-PAGE loading dye and 4x SDS-PAGE loading dye was added to volume of supernatant collected. 20µl of all samples- Uninduced, Total protein, soluble and insoluble fraction was loaded onto SDS-PAGE to analyse the protein content. The protein was then visualized by immune blotting. The conditions were recorded once the optimal condition was known for MBP-PSTOL1 fusion protein expression

Purification of tagged proteins

250ml of rich broth + glucose and carbenicillin was inoculated with 2.5ml (1%) of an overnight culture of cells containing the MBP-PSTOL1 WT, MBP-PSTOL1$^{2K/R}$ fusion plasmid and vector control (empty c5X vector). The procedure of inducing protein expression was followed as above. The cells suspension was centrifuged at 13000rpm (16,200g) for 30minutes at 4˚C after incubating with bugbuster. The supernatant was transferred into new microcentrifuge tube. 200µl of supernatant was separated as an Input sample. The equal volume of bugbuster and column buffer was mixed together.

Before starting the purification steps, amylose resins were equilibrated. 150µl of amylose resin was added to 1.5ml microcentrifuge. 500µl bugbuster + column buffer was added to amylose resins, incubated at rotating mixer for 10minutes at 4˚C and spun down at 1000rpm for 1minute. This step was repeated two times.

The cell lysate (Supernatant + Bugbuster + column buffer) was incubated with equilibrated beads on an end-to-end rotator at slow speed setting for 2-3hours at 4˚C. After the incubation was over, the cell lysate is spun down at 1000rpm for 1minute. The supernatant was discarded and 1ml of 1x column buffer was added and incubated at rotator for 5minute. Repeat the same step five times.

The fusion proteins were eluted with four different maltose concentrations- 0.5mM, 1mM,3mM and 10Mm. These different concentrations of maltose were prepared in 1x column buffer. The fusion protein was eluted with 200µl column buffer + maltose. Eight fractions (two elution by each concentration of maltose) were collected. The eluted fractions were loaded on SDS-PAGE and analyzed with Coomassie blue staining.

in-vitro phosphorylation assay study of purified PSTOL1 protein from *E.Coli*

To perform the in-vitro phosphorylation assay – MBP tagged PSTOL1 WT and PSTOL1$^{2K/R}$ and empty vector was transformed into *E.Coli* BL21 strain. Protein was purified as described in the method above. The purified proteins were incubated in the kinase reaction buffer for 1hour at 30˚C. The reaction was stopped by addition of 4x loading dye and denatured at 95˚C for 5minutes. Samples were loaded on both 10% SDS-PAGE and Phos-tag SDS-PAGE.

In vivo reconstituted SUMOylation assay in *E.coli*

To perform in-vivo SUMOylation assay, open reading frame (ORFs) of AtSCE1a and AtSUMO1 (AA or GG) were cloned in two different Multiple Cloning Site (MCS) respectively in pCDFDuet vector. While ORF of AtSAE1a/b-AtSAE2 were cloned in pACYCDuet vector using same strategy. *E.coli* BL21 was transformed with pCDFDuet-AtSUMO1 (AA or GG)-

AtSCE1a and pACYCDuet-AtSAE1a/b-AtSAE2 plasmids (Okada et al., 2009). After transformation, the cells with these two plasmids were used for preparation of competent cells. The competent cells with SUMO1-AA will act as negative control of in vivo SUMOylation assay because SUMO1-AA cannot ligate to other proteins.

	+SS Competent cells	-SS Competent cells
pCDFDuet-AtSUMO1-AtSCE1a	SUMO1-GG	SUMO1-AA
pACYCDuet-AtSAE1a/b-AtSAE2		

Using this reconstituted SUMOylation system, difference in SUMOylation status of PSTOL1 WT and PSTOL1$^{2K/R}$ was investigated.

Analysis on Phostag SDS-PAGE

To detect phosphorylation of substrate and autophosphorylation of kinase itself, Phos-tag SDS-PAGE was used for analysis. 5µM Phos-tag and 10µM $MnCl_2$ was added while preparing the resolving gel and allow it to polymerize. Preparation of stacking gel is same as described below. The samples were loaded, and the gel was run at very slow speed with low constant voltage of 50mV at 4˚C.

The gel was equilibrated with transfer buffer supplemented with 1mM EDTA for 30minutes. The buffer was changed after every 10minutes. To remove the EDTA, the gel was then equilibrated with transfer buffer without EDTA for 30minutes. The transfer was changed after every 10minutes.

The standard western blot procedure was followed.

SDS-PAGE

Sodium dodecyl sulphate polyacrylamide gel electrophoresis (SDS-PAGE) was used analyse and separate the proteins according to molecular weight. SDS is anionic detergent which bounds to the proteins giving the protein overall negative charge, hence denaturing the tertiary structure of proteins. This allows the separation of proteins on the basis of size.

SDS-PAGE is also called discontinuous gel because this method is composed of two type of gel preparation- Stacking and Resolving Gel.

The protein is loaded in stacking gel and in resolving gel, proteins bands are resolved.

These gels can cast as follows:

Stacking gel: 5% acrylamide, 0.125M Tris pH 6.8, 0.1% SDS, 0.1% ammonium persulphate and 0.01% TEMED.

Resolving gel: ranged from 10-15% acrylamide, 0.375M Tris pH 8.8, 0.1% SDS, 0.1% ammonium persulphate and 0.04% TEMED.

2x or 4x SDS PAGE loading buffer was used added to the samples to final concentration of 1x in order to denature the sample. The sample with SDS PAGE loading dye was heated at 95˚C for 5minutes and then loaded on the stacking gel.

The separation of proteins as discrete bands can be visualized by Coomassie staining or transferred to a PVDF membrane for western blotting.

Western Blotting

The gel (without stacking gel) was submersed in transfer buffer for equilibration. Meanwhile, a PVDF membrane was submersed in 100% methanol for 1minute. The membrane was then soaked in transfer buffer for 5minutes. Within a clamp ready cassette was prepared with blotting paper and sponges. The gel and PVDF membrane were sandwiched between blotting paper and sponges in blotting cassette. The proteins were allowed to transfer overnight at 25V at 4˚C from SDS-PAGE onto membrane.

The membrane was removed and was incubated in 5% semi-skimmed milk (blocking solution) for 2hours at room temperature. After 2 hours, the membrane was washed with 1x TBST and incubated with primary antibody in 1x TBST. The incubation with primary antibody can vary from 3hours at room temperature to overnight incubation at 4˚C. After primary antibody incubation, the membrane was rinse with 1x TBST for 5minute. This step was repeated for 5 times. Once this wash cycle was completed the membrane was incubated with secondary antibodies (HRP) for 1 hour at room temperature. Wash cycle was repeated as mentioned above. The ECL solution1 and solution 2 were mixed in 1:1 ratio and membrane was incubated with ECL solution mix for 1minute and sealed in a light-proof cassette. In a dark room, X-ray film was placed on membrane and removed after various time periods. The reaction between ECL and HRP antibody caused light and the exposed film was developed using Xograph Compact 4x Automated Processor (Xograph Imaging Systems).

Coomassie Blue Staining

Coomassie blue staining is another way to visualize the discrete band separation of protein. The resolving gel was stained for 30minutes with slow shaking in Coomassie Blue stain. After 30minutes, gel was soaked in Coomassie-destain. The destain solution was changed after every 1 hour until proteins bands were clearly visible.

2.7.2 Protein extraction from *N.benthamina* leaves

Infiltration of *N.benthamina*

The recombinant plasmid was transformed into *Agrobacterium* and single colony was inoculated into 10ml LB with relevant antibiotics (rifamycin and gentamicin were added to LB media which are specific to *Agrobacterium* strain and antibiotic resistance for recombinant plasmid to grow was also added). The cultures were incubated overnight in an orbital shaker at 28˚C at 220rpm. The cells were pelleted at 20˚C at 5000rpm for 10minutes and resuspended in 10ml 10mM sterile $MgCl_2$. The culture was again centrifuged at 20˚C at 5000rpm for 10minutes. The pellet was again resuspended in 10ml 10mM sterile $MgCl_2$. The cultures were diluted to the OD600 0.2 in total volume of cultures. The cultures were infiltrated into a 5-7 N.benthamina leaves using 1ml sterile syringe. The plant was kept at 20˚C on a long day cycle for 3 days.

Transient assay in *N.benthamina*

For SUMO:

PSTOL1 WT and PSTOL1$^{2K/R}$ was transformed into *Agrobacterium* strain GV3101 and were coinfiltrated along with 35:HA-SUMO and P19 into *N.benthamiana*. The infiltrated samples were collected after 3 days and freeze in liquid nitrogen. Samples were grinded into fine powder by liquid nitrogen in mortal and pestle. To fine powder PVPP and SUMO extraction buffer was added. The samples were defrosted and was spun in a centrifuge at 8500rpm for 15minutes. The supernatant was transferred to a new microcentrifuge tube and spun again at 14000rpm for

5minutes. The supernatant was again transferred into new microcentrifuge tube. Supernatant collected was incubated with MACS® microbeads (Miltenyi Biotech) for 30 minutes, supernatant was run down a magnetic column and column was washed five times by 200µl extraction buffer. The protein was eluted using 4x SDS loading dye heated for 5 minutes at 98˚C. The eluted protein was loaded onto a SDS-PAGE gel for protein separation.

For CO-IP:

For CO-IP, the same protocol was followed as described above. The buffer composition was different for CO-IP.

in vitro* phosphorylation assay of PSTOL1 immunoprecipitated from *N.benthamiana

PSTOL1 WT and PSTOL1$^{2K/R}$ was transformed into *Agrobacterium* strain GV3101 and were coinfiltrated along with 35:HA-SUMO and P19 into *N.benthamiana*. The infiltrated samples were collected after 3 days and freeze in liquid nitrogen. Samples were grinded into fine powder by liquid nitrogen in mortal and pestle.To fine powder PVPP and extraction buffer (SUMO extraction buffer without NEM) was added. The samples were defrosted and was spun in a centrifuge at 8500rpm for 15 minutes. The supernatant was transferred to a new microcentrifuge tube and spun again at 14000rpm for 5 minutes. The supernatant from each sample was again transferred and divided into two different microcentrifuge tube. Supernatant collected was incubated with MACS® microbeads (Miltenyi Biotech) for 30 minutes, supernatant was run down a magnetic column and column was washed five times by 200µl extraction buffer.

For in vitro phosphorylation assay, 50µl of 1x kinase buffer was added to the column and allowed to run through column. The column was taken out from magnetic stand and again 50µl of 1x kinase buffer was added to the column and allowed to run through column. The supernatant (protein bound to GFP beads) was collected in 1.5ml microcentrifuge tube. The

sample was incubated at 30˚C for 1 hour. The sample was again run through the column and washed five times by 200µl extraction buffer. The protein was eluted using 4x SDS loading dye heated for 5 minutes at 98˚C. The eluted protein was loaded onto a SDS-PAGE gel and Phos-tag SDS PAGE for protein separation.

2.7.3 Protein extraction from *Arabidopsis*

Total protein:

7-10 old Arabidopsis seedlings were frozen and frozen tissue was ground to fine powder with chilled pestle and mortar. The 1x SDS buffer was used as extraction buffer in ratio of 1:1 (weight/volume). The mixture was centrifuged at 8500 rpm for 15 minutes and supernatant was transferred to 2ml microcentrifuge tube. The mixture was again centrifuged at 14000 rpm for 5 minutes and supernatant was again transferred to new 2ml microcentrifuge tubes. To 900µl of supernatant, 300µl of 4x SDS loading dye was added and heated for 5 minutes at 98˚C. The samples were loaded to SDS-PAGE gel for western blotting.

Immunoprecipitation for demonstrating SUMOylated PSTOL1 from *Arabidopsis* transgenic lines expressing PSTOL1

Frozen leaf tissue was ground to a fine powder with chilled pestle and mortar. The ice-cold SUMO buffer was added. Upon defrosting the tissue (now liquid paste) was then transferred to a pre-cooled microcentrifuge tube. The tubes were centrifuge at 4˚C at 8500 rpm for 15 minutes. The supernatant was transferred to new pre-cooled microcentrifuge tube and again the supernatant was centrifuged at 4˚C at 14000 rpm for 10 minutes. Supernatant was again transferred to new 2ml microcentrifuge tubes. 20-25µl MACS^{Ò} microbeads (Miltenyi Biotech) were added to 2ml supernatant incubated for 30 minutes. Supernatant was run down a magnetic column and column was washed five times by 200µl extraction buffer. The protein was eluted

using 4x SDS loading dye heated for 5 minutes at 98˚C. The eluted protein was loaded onto a SDS-PAGE gel for protein separation.

2.7.4 Protein extraction from Rice seedlings

Total protein

Protocol for protein extraction from rice seedlings was followed as described above except the difference is of additional centrifugation step at 14000 rpm for 10 minutes.

Immunoprecipitation for demonstrating SUMOylated PSTOL1 from rice transgenic lines expressing PSTOL1

Protocol for immunoprecipitation from rice seedlings was followed as described above except the difference is of buffer composition and additional centrifugation step at 14000 rpm for 10 minutes.

***in vitro* phosphorylation assay of PSTOL1 immunoprecipitated from rice seedlings**

Rice seedlings were ground into fine powder by liquid nitrogen in mortal and pestle.To fine powder PVPP and extraction buffer for protein isolation from rice was added. The samples were defrosted and was spun in a centrifuge at 8500rpm for 15 minutes. The supernatant was transferred to a new microcentrifuge tube and spun again at 14000rpm for 5 minutes. The supernatant from each sample was again transferred and divided into two different microcentrifuge tube. Supernatant collected was incubated with MACS$^{\dot{O}}$ microbeads (Miltenyi

Biotech) for 30 minutes, supernatant was run down a magnetic column and column was washed five times by 200µl extraction buffer.

For in vitro phosphorylation assay, 50µl of 1x kinase buffer was added to the column and allowed to run through column. The column was taken out from magnetic stand and again 50µl of 1x kinase buffer was added to the column and allowed to run through column. The supernatant (protein bound to GFP beads) was collected in 1.5ml microcentrifuge tube. The sample was incubated at 30˚C for 1 hour. The sample was again run through the column and washed five times by 200µl extraction buffer. The protein was eluted using 4x SDS loading dye heated for 5 minutes at 98˚C. The eluted protein was loaded onto a SDS-PAGE gel and Phos-tag SDS PAGE for protein separation.

2.8 Yeast two hybrid

Yeast transformation

The plasmid DNA was added to competent cells and gently mixed. 500µl of PEG/LiAc was added to and incubated at 30˚C for 30minutes. 20µl DMSO was added and incubated at 42˚C in water bath for 15minutes. After incubation, yeast cells were centrifuged at high speed for 15 seconds, and supernatant was removed. The pellet was dissolved into 1ml YPDA media and incubated at 30˚C with shaking at 250rpm. Culture was centrifuged again at high speed for 15seconds. Supernatant was discarded and pellet was dissolved in 1ml 0.9% NaCl solution. 100µl of solution was spread on selective media (SD/-L). The plate was incubated ta 30˚C for 3-5 days.

Yeast Mating

The ORFs of TFs are amplified and combined into donor plasmid which has att sites. Once the donor plasmids were ready, TF ORFs were recombined into yeast compatible plasmid pDEST^{TM} 22. After confirming the clones, the plasmids were transformed into yeast strain YM4271. The library was purchased from Nottingham Arabidopsis Stock Centre (NASC) as glycerol stocks. The first step was to revive the frozen library (as glycerol stock) on SD/-W. Other way to revive the frozen library was to reviving on YPDA media (less stringent media) and then transferring to SD/-W (more stringent media). The plates were allowed to incubated for 3days at 28˚C. 96-pin replicator was used in this experiment. The preys were transferred from SD/-W to 200µl YPDA media using 96-pin replicator and allowed to grow on shaking for 1day at 28˚C. Meanwhile, bait was grown in 200ml YPDA media in Erlenmeyer flask alongside the preys. 100µl Bait was added to 100µl RR library preys using 96-pin replicator and incubated for 2days at 28˚C with shaking. This step allowed for mating to take place. The next step was to inoculate the mated culture into 96-well plates with selection media i.e. SD minimal base media without leucine and tryptophan (SD/-LW) for 1day at 28˚C with shaking . This selection media allowed diploid cells to grow. To confirm that mating has happened and subsequently to investigate the positive interactions, diploid cultures were spotted on the plates with agar containing SD/-LW for scoring diploids and SD/-LWH for checking positive bait-prey interactions.

2.9 Imaging

Confocal Microscopy

For *N.benthamiana* or Arabidopsis leaves/Arabidopsis or rice roots

For in vivo plant leaf imaging, leaf sections were cut (approximately 0.5cm^2) and placed on a microscopy slide (Fischer Scientific), a droplet of perfluoroperhydrophenanthrene (PP11) was added before covering the leaf section with a 22x22mm cover slip (Menzel-Glaser, Waltham, USA). The slide was placed on the stage of a Zeiss LSM 880 Airyscan confocal microscope (Zeiss, Oberkochen, Germany). A 64x objective oil lens was used for viewing and an Argon-Ion gas laser was used to excite YFP at 514nm and GFP at 488nm.

2.10 Software packages

Sequence analysis and primer design

Snap Gene viewer version 5.2.4 Ó 2004-2021 GSL biotech

Figure preparation

FIJI-Version 2.9.0

Mega X Version 11.0.6 1993-2021 (Kumar et al., 2018)

Clustal X Version 2.1 (Larkin et al., 2007)

Phylogenetic tree construction

Rice Genome Annotation Project (https://www.rice.uga.edu.org/) and TAIR (https://www.arabiopdis.org/) were used to retrieve protein. Alignments were made using ClustaIX (https://www.ebi.ac.uk/Tools/msa/clustalo/) and visualized using Jalview (https://www.jalview.org/). Bootstrap Neighbor-Joining trees were made using ClustaIX and visualized using MEGAX (https://www.megasoftware.net/).

Software for determining SUMO sites

SUMO site predictions were carried out using in-house experimental software developed using similar algorithms to GPS-SUMO (https://sumosp.biocuckoo.org/online.php.). The software was developed by Stuart Neils (PhD thesis 2014).

2.11 Data analysis

Data were expressed as mean ± SEM. Statistical differences were tested with ANOVA Turkey test post hoc or Dunnett's multiple comparison test. Turkey test post hoc was used to compare the mean between three or more groups while Dunnett's multiple comparison test was used to compare the mean of all the group with the control. The value $P<0.05$ were considered statistically significant. Statistical analysis was done using software Prism-GraphPad.

Chapter 3

Protein Biochemistry of PSTOL1 in *E.coli* and *Nicotiana benthamiana*

3.1 Introduction

Protein phosphorylation by protein kinases is an important covalent Post-Translational Modification (PTMs) that modulates their functions such as subcellular localization, stability, the binding specificity of target proteins and enzymatic activity (Kinoshita et al., 2006 and Sugiyama and Uezato., 2022). Recent studies by Nishioka et al., 2020 showed that the regulation of photosynthetic activities is under the control of the phosphorylation status of the photosystem II (PS II) core and the light-harvesting complex of PSII (LHC II). Therefore, to anticipate the activation and downstream mechanism of protein kinases, it is important to determine the activity of these kinases (Sugiyama and Uezato., 2022)

An important feature of Protein Kinases (PKs) is their autophosphorylation activity. This feature of PKs regulates the protein conformation to maximize substrate recognition which directly affects the functional properties of the protein. An example of regulating functional mechanism by autophosphorylation activity is hetero-oligomerization of BR receptor-like

kinase, BR1 and BAK1. Autophosphorylation of various Tyr and Thr residues commence BR signal transduction after BR binding. Thus, it is important to investigate the autophosphorylation activity of PKs to understand its mechanism (Nemoto et al., 2011) and hence we decided to examine the autophosphorylation activity of PSTOL1 kinase.

Over the years, to study the phosphorylation state of the protein phosphoproteomic methods such as mainstream Mass Spectrometry (MS) or the classic and still widely used method of isotope labeling of the phosphate group focused on interpreting protein phosphorylation status. However, each approach has its strengths and limitations. The latter approach requires proper reference samples for the quantification of protein phosphorylation or multi-site phosphorylation. An obvious problem linked with this approach is exposure to radiation while handling radioactive isotopes. The former approach needs proteolytic digestion of the protein which leads to difficulty to trace the information about the protein. Moreover, determining time-dependent changes and abundance ratio for proteins with varying phosphorylation statuses is also difficult with MS. (Kinoshita et al.,2015, Donoghue and Smolenski., 2022). Forset Resonance energy transfer (FRET) provides insight into microdomain formation and compartmentation of kinase signaling; however, the approach is restricted by the need to overexpress the protein marker which leads to misleading endogenous signaling events (Donoghue and Smolenski., 2022).

In 2003, Phos-tag SDS PAGE was described as an electrophoretic technique that uses a novel phosphate-binding tag or Phos-tag (1,3-bis[bis(pyridine-2-ylmethyl)-amino] propan-2-olato) and a dinuclear metal (Zn^{+2} and Mn^{+2}) complex polymerized into resolving gel. The principle of Phos-tag SDS PAGE is based on the interaction between the Phos-tag and phospho-group on protein in separating gel. The separation of the protein (based on molecular weight), an operating procedure, protein sample preparation, and the reagents used for Phos-tag SDS-PAGE are like the conventional SDS-PAGE technique. The only exception is simply the addition of an acrylamide pendant Phos-tag in separating gel. Immobilized Phos-tag in resolving gel, traps the phosphorylated protein and as a result, phosphorylated protein will migrate slowly when compared to non-phosphorylated protein. Gel-shifted bands of protein can be seen on Phos-tag SDS-PAGE (**Figure 3.1**).

It is also used for deciphering if the protein has multiple phosphorylation sites which can result in the multiple phosphorylation states of the protein. The multiple phosphorylation of the protein results in the differences in electrophoretic mobilities of several phosphorylated forms of the same protein. Phos-tag SDS-PAGE is also sensitive and highly accurate for distinguishing the nearly related or alike proteins with a similar number of phosphorylated amino acid residues because the different phosphorylation sites display different mobility observed as a separate band (Kinoshita et al., 2015). This difference in mobility is due to the amino acid residues nearby the phospho-site (Donoghue and Smolenski., 2022).

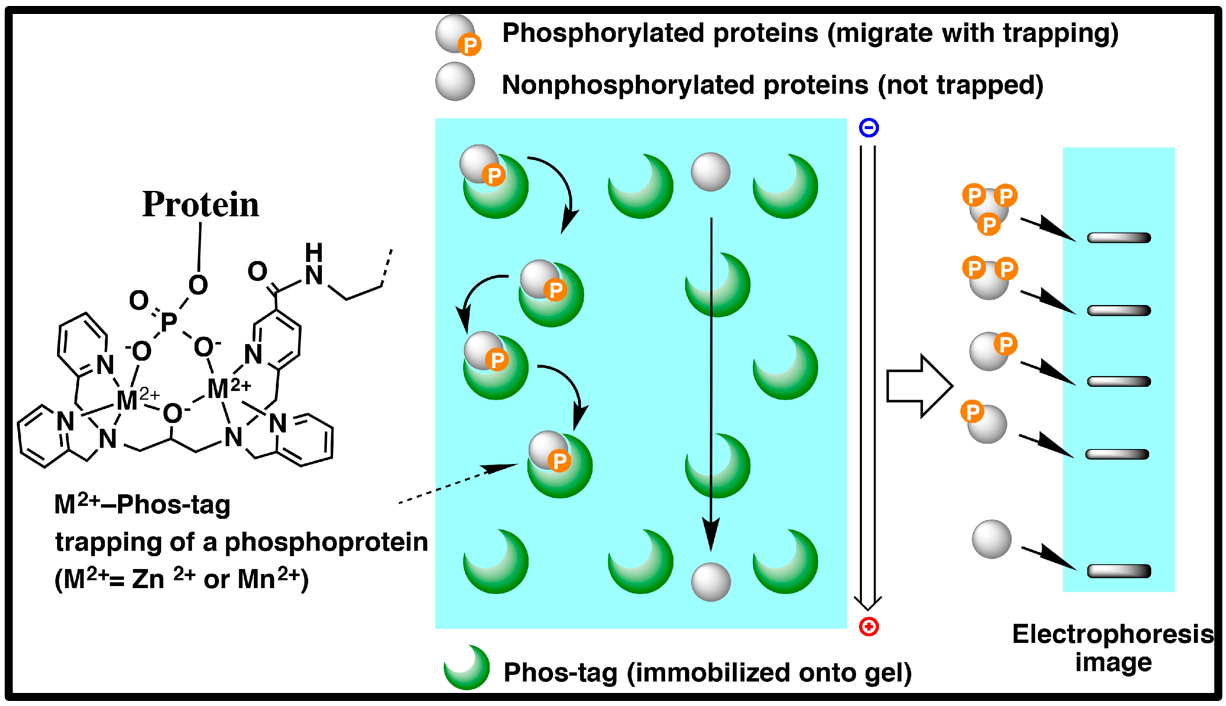

Figure 3.1: Schematic representation of working principle of Phos-tag SDS-PAGE.

This allows the separation of multiple phosphorylated states of protein as different bands in presence of divalent cations Mn^{+2} or $Zn^{+2.}$

There are two methods to visualize the phosphorylated and dephosphorylated protein on SDS-PAGE- Mn^{+2}- Phos-tag SDS-PAGE using the Laemmli's Buffer System and Zn^{+2} – Phos-tag SDS-PAGE using a neutral -pH buffer system. Mn^{+2}- Phos-tag SDS-PAGE followed by

western blot analysis is most widely used since this method can be performed with conventional SDS-PAGE and western blotting reagents and equipment. This method is based on a buffer system used in the resolving gel that has an alkaline pH (Laemmli's buffer system) which has a valuable feature because phosphoproteins such as histidine and aspartate are liable to hydrolysis under acidic conditions thereby contributing to the progress in bacterial two-component transduction system. While this method offers some advantages, it has some disadvantages also. Because this method uses alkaline pH as a basis, it is difficult to store the gel for a longer period as it leads to hydrolysis of polyacrylamide (Kinoshita et al.,2015 and Kinoshita et al.,2022)

3.2 Crosstalk between phosphorylation and other post-translational modifications

Gamuyo et al., 2012 showed that PSTOL1 is a functional kinase using *in vitro* phosphorylation assay however, it is still unknown how PSTOL1 kinase regulates the molecular mechanism. In recent years, it well reported that protein activity is regulated by multiple PTMs which generally serve as molecular switches for numerous pathways (Zhang and Zeng., 2020) and sometimes these PTMs act in a coordinated manner to regulate the responses. We were particularly interested in studying the role of SUMOylation and how it plays a vital role in regulating PSTOL1 protein. The important reason to choose SUMOylation as our main interest is because SUMOylation is dynamic in nature, and it is considered an important way to facilitate cellular changes essential in plants to adapt to environmental abiotic and biotic stresses (Clark et al., 2022). Interestingly, the PSTOL1 protein sequence was scanned for potential SUMO binding sites using in-house bioinformatic software, HyperSUMO (Nelis, PhD thesis 2014). We found that PSTOL1 has two predicted SUMO sites – lysines at the 20th and 225th position. Therefore, we hypothesized that – First, PSTOL1 is subjected to both modifications (SUMOylation and Phosphorylation). Secondly, SUMOylation is possibly a key PTM regulating the kinase activity of PSTOL1. Thirdly, identification of PSTOL1 targets using a yeast-two-hybrid screening system and Co-Immunoprecipitation techniques will allow us to

understand the relationship between SUMOylation and phosphorylation in PSTOL1 Kinase function.

Therefore, to study the crosstalk between SUMOylation and phosphorylation, we mutated these two SUMO sites from lysine to arginine. From hereafter, the non-mutated version will be addressed as PSTOL1 WT and the SUMO site mutated version will be addressed as PSTOL1$^{2K/R}$. This will allow us to investigate the role of these two post-translational modifications in regulating the PSTOL1 mechanism.

3.3 Cloning of PSTOL1 gene in the pMAL system

PSTOL1 WT and PSTOL1$^{2K/R}$ gene was cloned in the pMAL-5 vectors system. These vectors have a *malE* gene of *E.coli*, which translates maltose-binding protein (MBP). As a result, MBP fusion protein can be expressed in these systems. The *malE* gene is followed by a multiple cloning site that allows for cloning the CDS of interest in frame with the malE gene to allow high-level expression of the cloned gene as these vectors have robust "tac" promoter and malE translational initiation signals. pMAL system has two vectors- pMAL-c5X and pMAL-p5X. In the latter, the fusion protein is effectively exported to the periplasm of *E.coli* whereas the pMAL-c5X vector expressed the MBP fusion in the cytoplasm. In this study, we used the pMAL-c5X vector for our experimental set up.

The open reading frame of PSTOL1 WT and PSTOL1$^{2K/R}$ was cloned in pMAL-c5X. The genes were amplified from entry clone pDTOPO-PSTOL1 WT and pDTOPO-PSTOL1$^{2K/R}$ respectively (kindly donated by Dr. Cunjin Zhang), by gene specific primers flanking the restriction sites SalI and PstI sites. The gene was cloned into the SalI and PstI restriction sites in pMAL-c5X vector. PCR amplification product was analyzed on an agarose gel by size

separation electrophoresis for confirmation of the predicted size of the amplicon (**Figure 3.2 A** and **B**). Once the size of the amplicon was confirmed, the PCR amplified product and pMAL-c5X vector was digested by SalI and PstI enzymes. A ligation reaction was set up between the digested amplified product and the pMAL-c5X vector. The ligation mixture was transformed into DH5α competent *E.coli* cells. Positive colonies were checked by PCR using gene specific primers (**Figure 3.2 C**). Plasmids were isolated from colony PCR positive clones and were subject to restriction digestion by SalI and PstI for further confirmation of the clones (**Figure 3.2 D**).

The clones were further verified by sequencing to ensure that the gene was in-frame with the tag and the vector is mutation free. The constructs were transformed into BL21 cells and grown on media containing carbenicillin. The presence of the construct was confirmed by PCR again.

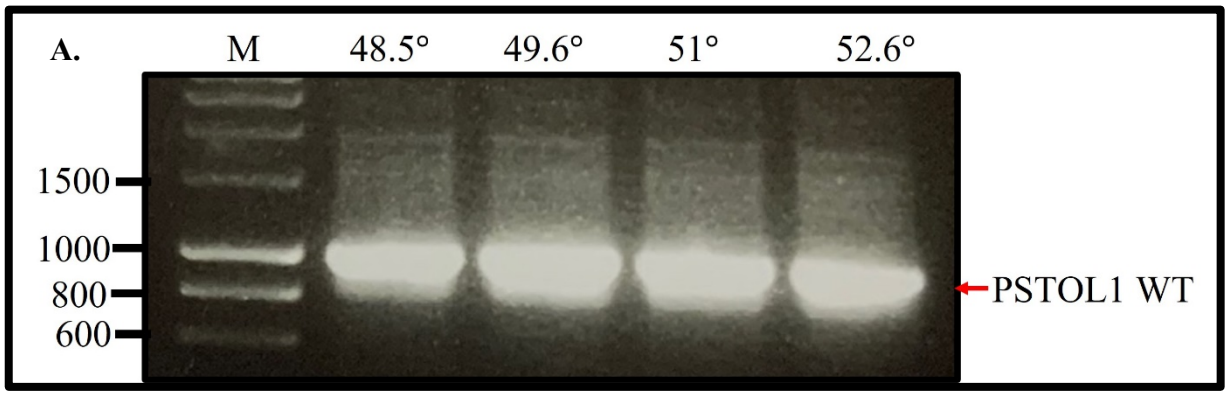

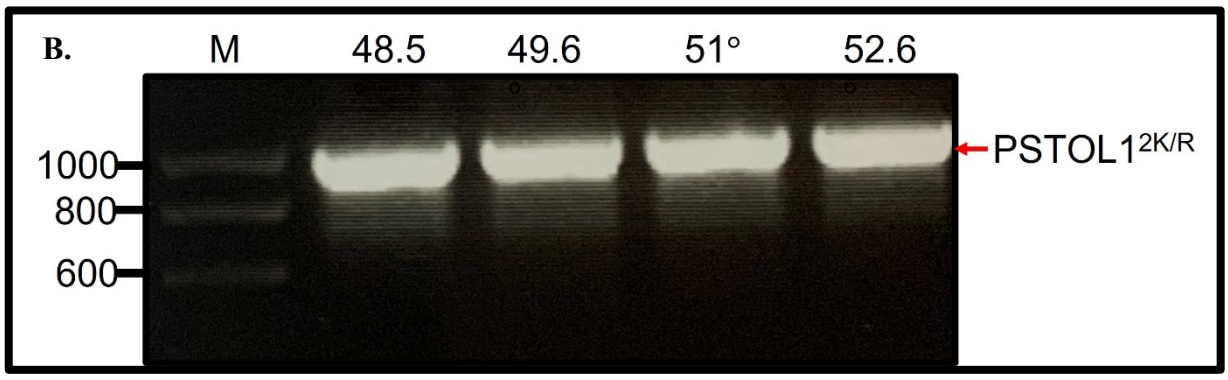

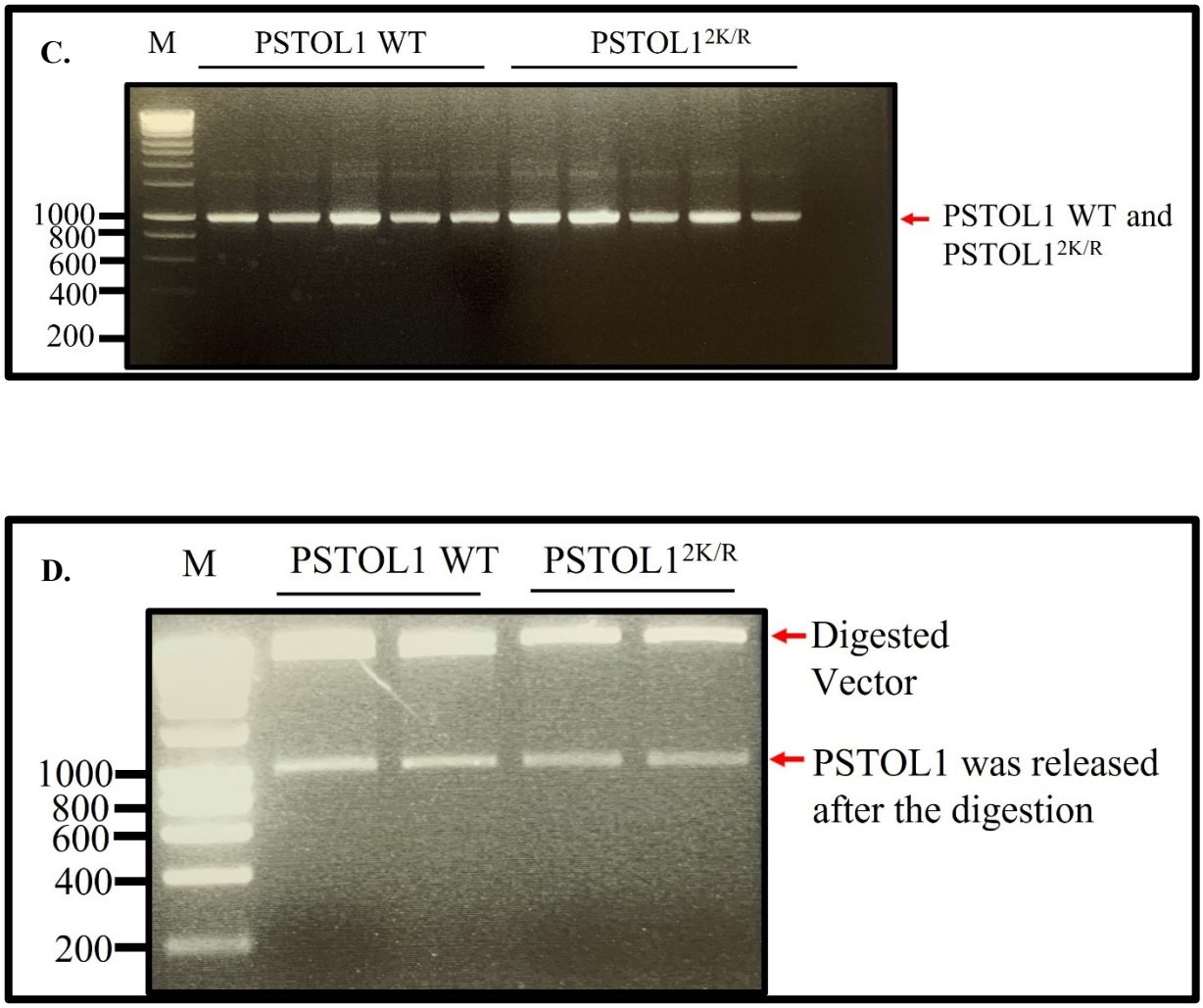

Figure 3.2: Cloning of *Oryza sativa* PSTOL1 WT and PSTOL1$^{2K/R}$ in MBP tagged c5X vector.

The open reading frame of PSTOL1 WT and PSTOL1$^{2K/R}$ was amplified by proofreading DNA polymerase Q5 (NEB) at different temperatures (48.5°, 49.6°, 51°, and 52.6°) from entry clones-PSTOL1 WT and PSTOL1$^{2K/R}$ using gene specific primers having SalI and PstI restrictions site sequences flanking the primers. (A.) shows the resulting amplicon of PSTOL1 WT (B.) shows the resulting amplicon of PSTOL1$^{2K/R}$ analyzed on a 1% agarose gel by electrophoresis size separation. (C.) The positive clones were analyzed by PCR using gene specific primers. (D.) Plasmids were isolated from positive clones. Plasmids were digested at 37° for 2 hours using SalI and PstI. The digested product was analyzed on 1% agarose gel by electrophoresis size separation. Bands corresponding to the vector and PSTOL1 gene were observed on the gel ensuring that the gene was ligated in the right orientation in between appropriate restriction sites SalI and PstI.

A pilot experiment for checking recombinant protein induction was set up. The confirmed construct - PSTOL1 WT was grown in 10ml LB culture supplemented with carbenicillin at 37° until O.D.600 reached a reading of 0.6. 1ml samples were taken and processed as uninduced (UI) controls. IPTG was added to a final concentration of 1mM to the remaining culture. The remaining culture was divided into three different 15ml falcons and was allowed to grow at three different temperatures - 18°, 28° and 37°. 1ml samples were taken after 3 hours. The samples were then processed into 3 categories- total protein (TP), soluble extract (S), and insoluble extract (P). The recombinant protein expression was seen at both 28° and 37° temperatures although, recombinant protein expression was best seen in the supernatant (or soluble) fraction at 28° at the expected size of MBP-PSTOL1 WT at 80kDa (**Figure 3.3**). However, no expression of recombinant protein was seen at 18°. The condition under which the PSTOL1 protein expressed was recorded for further optimization.

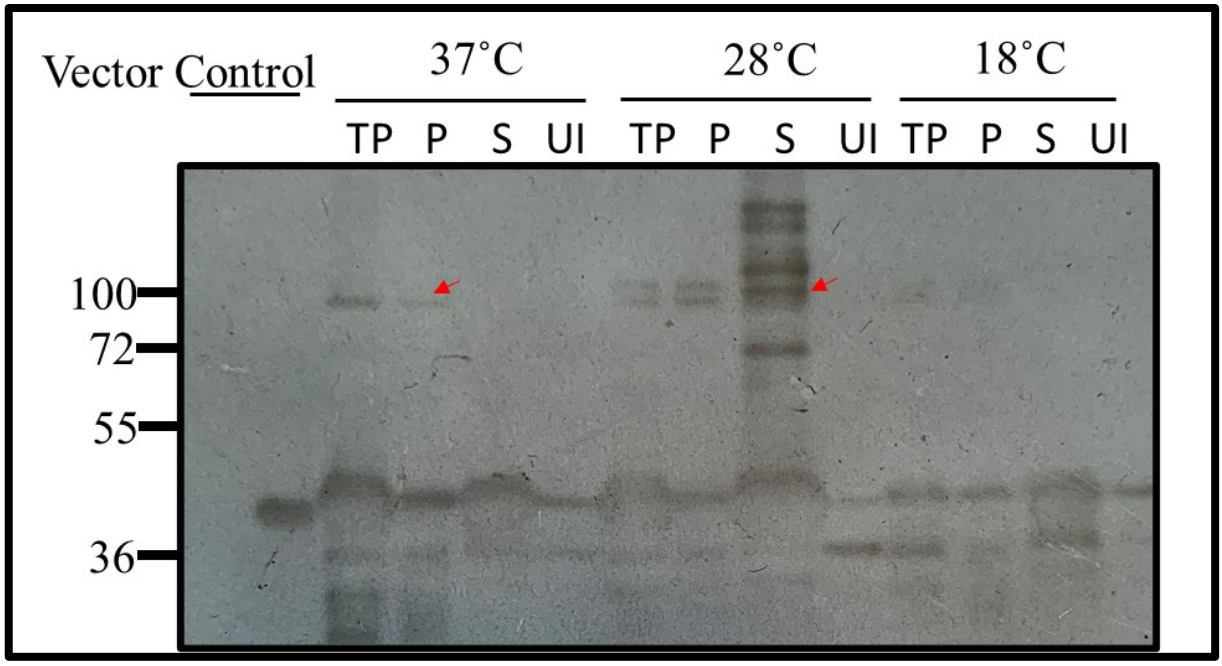

Figure 3.3: Optimization of expression of MBP-tagged PSTOL1 WT protein in *E.coli*

A single colony of transformed BL21 cells with recombinant plasmid- PSTOL1 WT was inoculated in 10ml culture and grown overnight at 37°. 1% inoculation of primary culture was added to new LB media supplemented with carbenicillin until O.D.600 reached 0.6. 1ml samples were taken and processed as pre-induced controls and 1mM IPTG was added to the rest of the culture, and it was grown at three different temperatures- 18°, 28° and 37° for 3hours. The 1ml samples were taken to check protein induction. The samples were processed by Bugbuster into 2 categories- soluble (supernatant) and insoluble (pellet) extract. Uninduced (UI), Soluble (S), insoluble (P), and total extract (TP) were

analyzed on SDS-PAGE followed by western blotting of gels to confirm PSTOL1 protein expression (red arrows indicate MBP-PSTOL1 WT).

The protocol for recombinant protein expression was further optimized. The protocol was exactly followed as above, however, after adding IPTG the culture was allowed to grow at 28°C overnight. **Figure 3.4** shows that the expression of recombinant protein was seen in the soluble fraction at 28° and no expression was seen in the uninduced sample suggesting that the band corresponding in the soluble fraction is PSTOL1 protein (**Figure 3.4**).

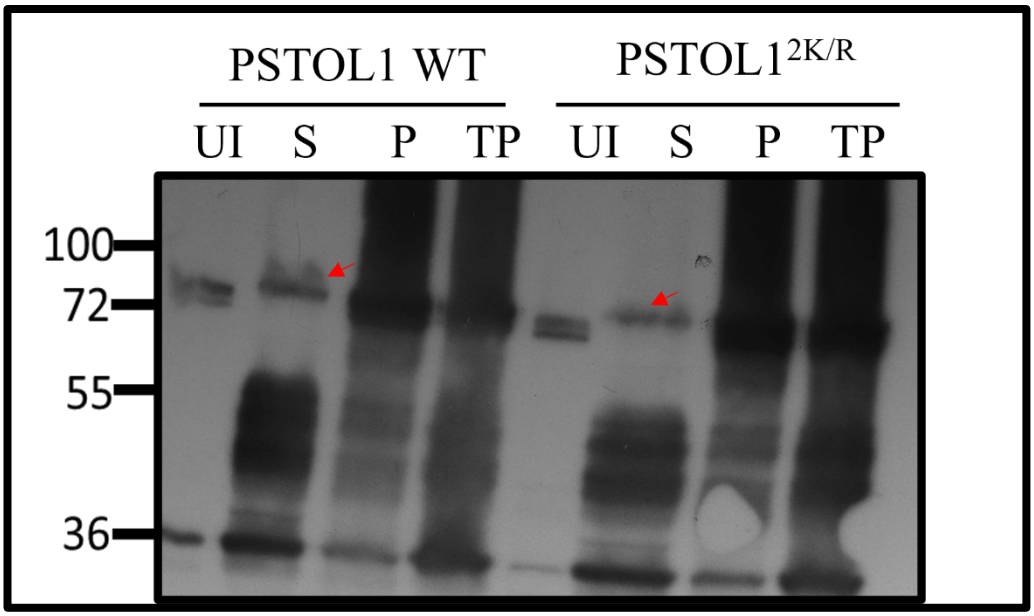

Figure 3.4: Expression of recombinant PSTOL1 WT and PSTOL1$^{2K/R}$ in *E.coli*.

E.coli cells with pMAL-c5X PSTOL1 WT and PSTOL1$^{2K/R}$ constructs were grown until an OD600 reach 0.6. Samples were processed as total protein (TP), supernatant (S), and pellet (P) fractions. The samples were taken before IPTG induction and was used as uninduced (UI) control. 1mM IPTG was added to the bacterial culture and the culture was grown at 28° overnight. The samples were analyzed on SDS-PAGE gel. Protein was indicated by a red arrow in supernatant fraction whereas no expression of protein was not seen in uninduced fraction.

3.4 Purification of *E.coli* expressed recombinant PSTOL1 protein

Protocol for PSTOL1 protein expression was optimized as described above. The purification of PSTOL1 protein was achieved by resuspending in Bugbuster reagent/ protease inhibitor mix. This mix was prepared for disruption of the cell wall of *E.coli* resulting in the release of soluble protein. The supernatant was used as starting material for the purification. 200µl supernatant was taken as input control for further purification steps.

The amylose resin was added to the supernatant in a 1.5ml microcentrifuge and was incubated for 3 hours on a rotator mixer at a slow setting. After the incubation, resins were settled down by centrifugation at 1000rpm for 1 minute. The fusion protein was eluted with column buffer + 10mM maltose. The protein fractions were collected and analyzed on SDS-PAGE. The proteins were visualized by Coomassie staining (**Figure 3.5 A** and **B**) and immunoblotting for confirming the expression of the purified protein (**Figure 3.5 C**).

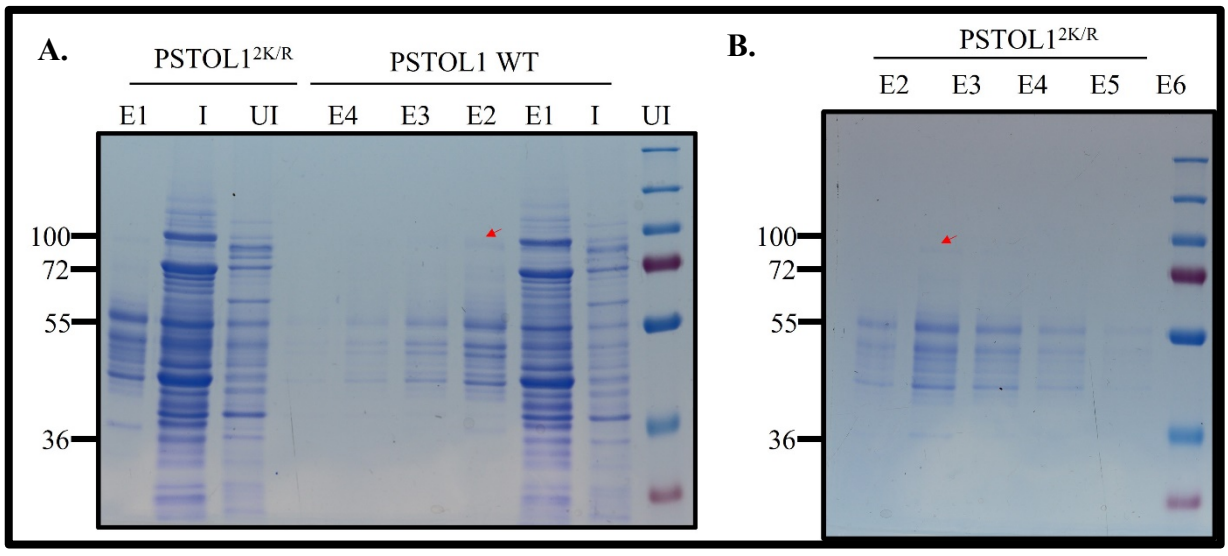

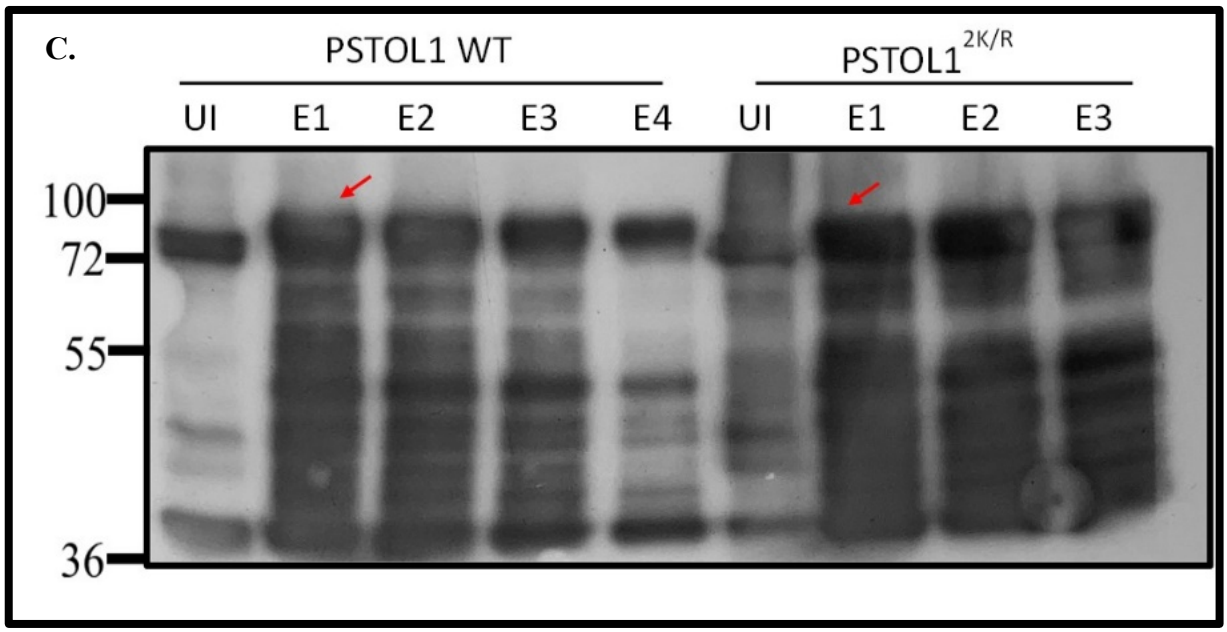

Figure 3.5: Purification of MBP tagged-PSTOL1 WT and PSTOL1$^{2K/R}$ protein.

BL21 cells having c5X-PSTOL1 WT and c5X-PSTOL1$^{2K/R}$ plasmids were grown at optimal conditions as described above for protein expression and later the cells were harvested. The pellet was dissolved in Bugbuster/protein inhibitor mix for lysis and the supernatant was collected and incubated with amylose resin. Column buffer + 10mM Maltose was used to elute the MBP tagged. All the fractions collected were added to 4x SDS loading buffer and protein fractions were analyzed on SDS-PAGE (A.) MBP-PSTOL1 WT and (B.) MBP-PSTOL1$^{2K/R}$ were visualized by coomassie staining respectively. (C.) Proteins were separated on SDS-PAGE and were transferred to a PVDF membrane. Proteins were visualized by probing the membrane with αMBP antibody. Uninduced (UI), Input (I), and Fractions (E) were loaded onto SDS-PAGE to analyze the expected size at 80kDa. The red arrow indicates the expected size of the protein.

3.5 *in-vivo* reconstituted SUMOylation assay

To investigate the SUMOylation status of PSTOL1, MBP tagged PSTOL1 WT and PSTOL1$^{2K/R}$ clones were transformed to the reconstituted SUMOylation system and grown on media containing carbenicillin, chloramphenicol and streptomycin as previously described by Okada et al., 2009. The positive colonies containing PSTOL1 CDS (975bp) were checked by PCR, using gene specific primers (**Figure 3.6**).

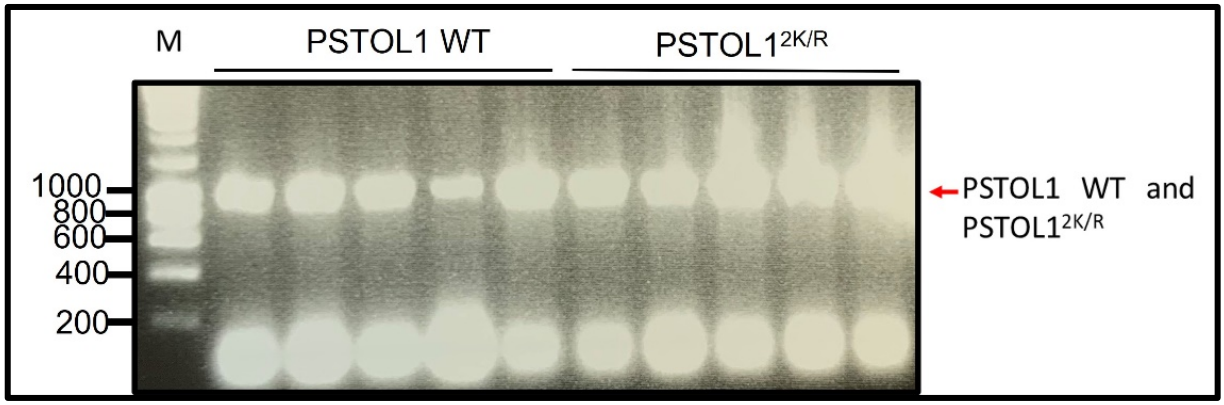

Figure 3.6: MBP-tagged PSTOL1 WT and PSTOL1$^{2K/R}$ plasmids were transformed into *E.coli* reconstituted SUMOylation system.

The figure shows the amplification of PSTOL1 WT and PSTOL1$^{2K/R}$ from *E.coli* colonies that grow on selection media.

The protocol to express and purify PSTOL1 from bacteria was described above and the same method was used. From the **Figure 3.5** above, we can observe that it is difficult to visualize the protein using coomassie staining. This time the protein was visualized directly using immunoblotting. The protein was transferred from SDS-PAGE to PVDF membrane. The membrane was probed with αMBP antibody to visualize the expression of recombinant protein. (**Figure 3.7**).

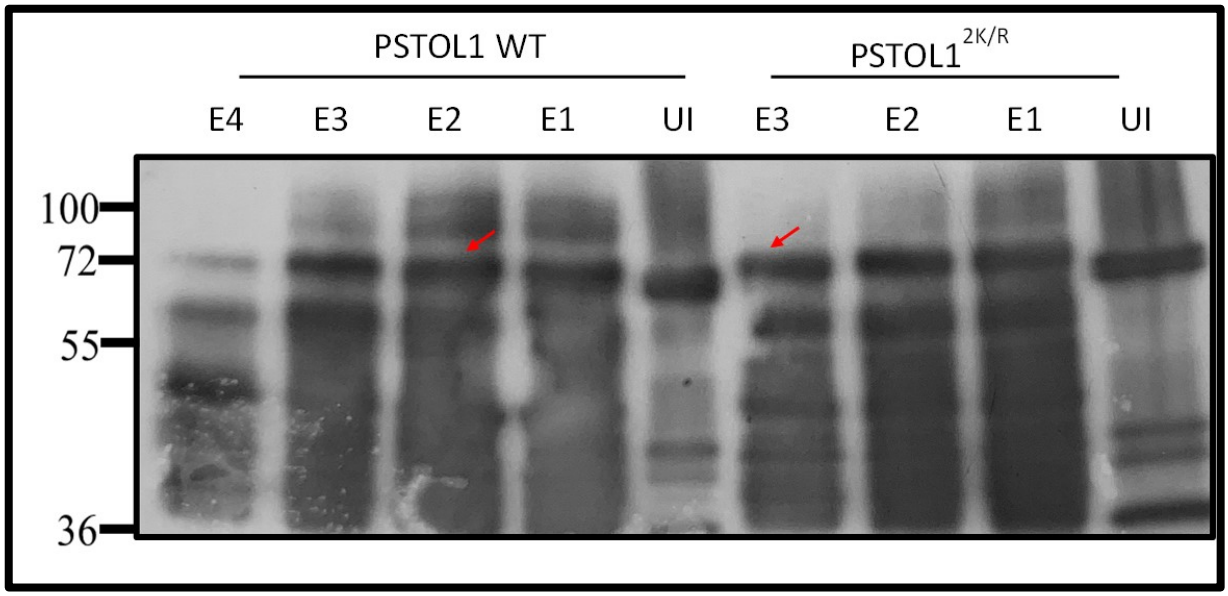

Figure 3.7 : Purification of recombinant PSTOL1 WT and PSTOL1$^{2K/R}$ from reconstituted SUMOylation system.

BL21 cells containing PSTOL1 WT and PSTOL1$^{2K/R}$ were grown at optimal conditions for protein expression and the cells were harvested. The pellet was dissolved in Bugbuster/protein inhibitor mix for lysis and the supernatant was collected and incubated with amylose resin. Column buffer + 10mM Maltose was used to elute the MBP tagged. All the fractions collected were added to 4x SDS loading buffer and protein fractions were analyzed on SDS-PAGE. Proteins were separated on SDS-PAGE and were transferred to a PVDF membrane. Proteins were visualized by probing the membrane by αMBP antibody. Uninduced (UI), Input (I), and Fractions (E) were loaded onto SDS-PAGE to analyze the expected size. Red arrow indicates the expected size of protein at 80kDa.

Purified MBP tagged-PSTOL1 WT and PSTOL1$^{2K/R}$ proteins were loaded on SDS-PAGE along with uninduced and input samples. Immunoblot analysis by αSUMO1 antibody showed that two bands for MBP-PSTOL1 WT purified protein (in **Figure 3.8 A** indicated by two white arrows), indicating that SUMO moieties were conjugated to MBP-PSTOL1 WT protein. However, the bands were not observed for MBP-PSTOL1$^{2K/R}$ purified protein suggesting the loss of SUMOylation as predicted. Hence, the data showed that lysine 20 and 225 are potential sites of SUMOylation in vitro (**Figure 3.8 A**). When proteins were probed with αMBP antibody, the higher bands corresponding to polySUMOylation was not observed. This confirms that the αSUMO1 antibody specifically binds to SUMO1/2 conjugates of protein (**Figure 3.8 B**).

However, immunoblot analysis by αMBP also showed that PSTOL1$^{2K/R}$ purified protein is less when compared with PSTOL1 WT protein expression. We also observed partial SUMOylation in vector alone expressing MBP. Therefore, it is important to investigate the PSTOL1 SUMOylation status *in-planta* in combination with reconstituted SUMOylation system for better understanding of SUMOylation status of PSTOL1.

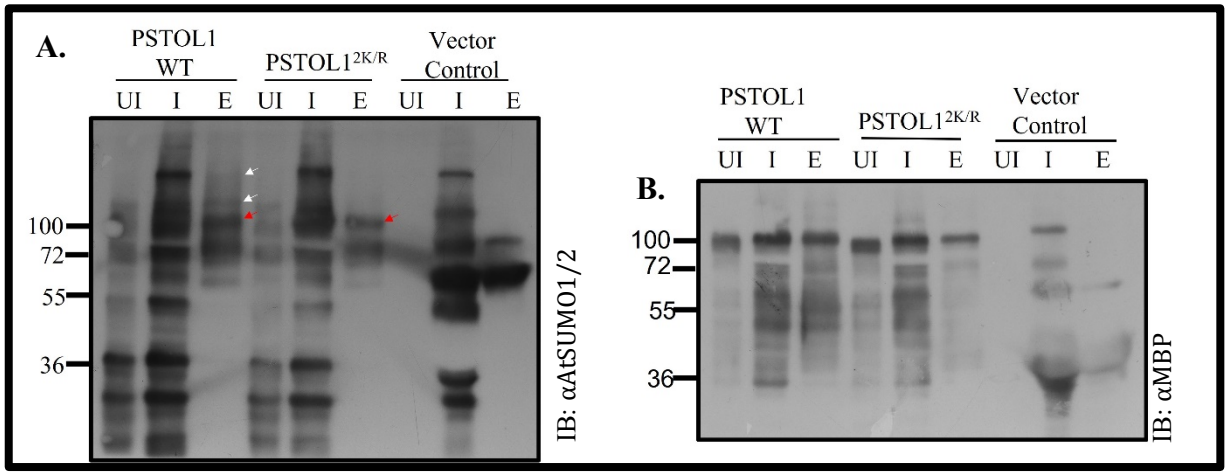

Figure 3.8 : Reconstituted SUMOylation assay.

N-terminal MBP tagged PSTOL1 WT and PSTOL1$^{2K/R}$ proteins were purified from *E.coli* BL21 cells. The uninduced, input and purified protein samples were added to 1x SDS-PAGE loading buffer and heated at 98°C for 5minutes. The samples were loaded on SDS-PAGE and proteins were transferred to a bloating membrane and probed with αSUMO1 (A.) and (B.) αMBP .(A.) Immunoblot analysis by αSUMO1 antibody indicates that PSTOL1 WT is SUMOylates while PSTOL1$^{2K/R}$ is not, indicating that lysine 20 and 225 can be potential sites of SUMOylation *in vivo*. Red arrows indicate molecular weight of MBP-tagged PSTOL1, and white arrows indicate bands corresponding to poly-SUMOylation (B) protein was probed with αMBP. Uninduced (UI), Input (I), and Eluted Fraction (E)

3.6 *in-vitro* phosphorylation assay

in-vitro phosphorylation assays are used to determine the activity of specific kinases from cells. In this assay, purified recombinant protein kinase (expressed in *E.coli* BL21 cells) transfer the gamma (γ-P) phosphate group from ATP to the target substrate, known as a cross-phosphorylation reaction. However, sometimes kinases add phosphate groups to itself, a process known as autophosphorylation.

An *in-vitro* phosphorylation assay was performed to investigate the PSTOL1 kinase autophosphorylation activity. In this study, ATP acts as a donor for kinase to transfer gamma phosphate either to substrate (cross-phosphorylation reaction) or add them to itself (autophosphorylation reaction). We used commercially available substrate Myelin basic protein (MyBP). It is widely used as a substrate in various *in vitro* phosphorylation assays because MyBP has multiple sites for protein phosphorylation.

Three different phosphoryl reactions were set up using bacterial purified MBP-PSTOL1 WT and MBP-PSTOL1$^{2K/R}$ proteins in microcentrifuge tubes (**Figure 3.9**). The first reaction includes purified protein incubated with sterile water. This reaction was a negative control for the *in-vitro* phosphorylation reaction. In the second reaction, purified proteins were incubated with 1x kinase buffer including ATP but without Myelin Basic Protein (MyBP). This reaction was set up to determine the autophosphorylation activity of PSTOL1 WT and PSTOL1$^{2K/R}$. Third reaction included 1x kinase buffer (which includes ATP), MyBP (substrate), and purified bacterial proteins.

The summary of all three reactions is given below:

a. Protein – ATP - MyBP: Control reaction
b. Protein + ATP - MyBP: To study the autophosphorylation activity of protein
c. Protein + ATP + MyBP: To study the cross-phosphorylation activity of protein

Phos-tag analysis was done to detect the phosphorylation state of PSTOL1 WT and PSTOL1$^{2K/R}$. Specifically, 5µM of Phos-tag acrylamide and 10µM $MnCl_2$ were added to resolving gel mix during preparation.

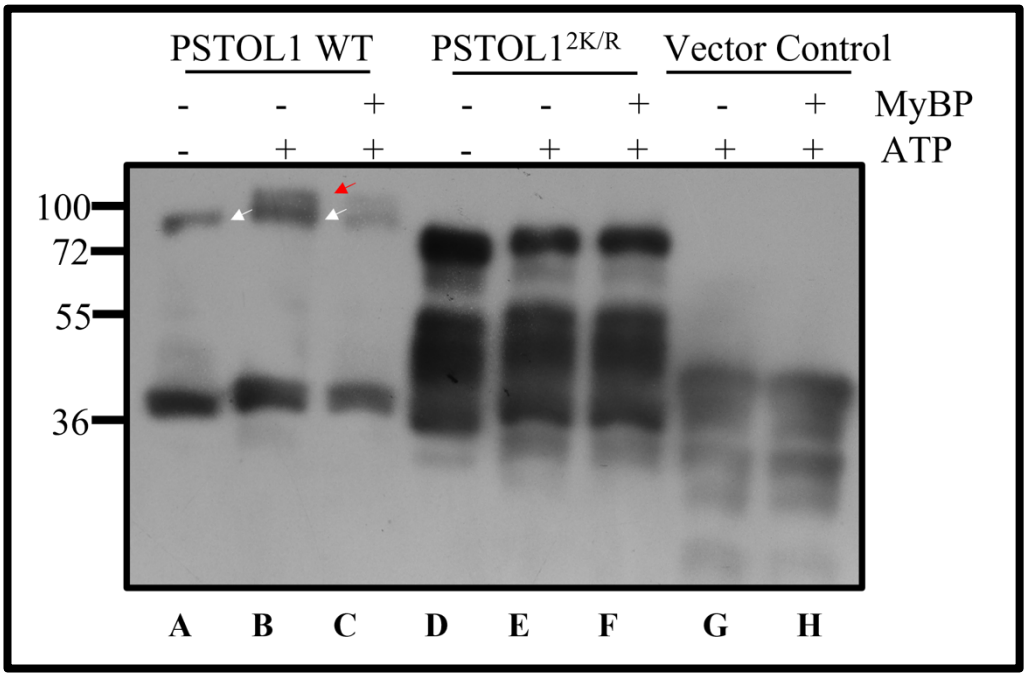

Figure 3.9 : Immunoblots of *in-vitro* phosphorylation assays resolved on a SDS PAGE phos-tag gels.

Purified MBP tagged bacterial proteins MBP- PSTOL1 WT and PSTOL1$^{2K/R}$ incubated with and without MyBP in kinase reaction mixture (including ATP) to determine cross-phosphorylation and autophosphorylation activity respectively. In vector control, autophosphorylation and cross-phosphorylation activity was not detected. The western blot represents samples run on Mn^{+2} Phos-tag gels with 5µM of Phos-tag acrylamide and 10µM $MnCl_2$. The red arrow indicates the phosphorylated form of the protein above 80kDa, and white arrow indicates the dephosphorylated form of protein at expected size of 80kDa.

The Phos-tag gel analysis of MBP-tagged PSTOL1 WT and PSTOL1$^{2K/R}$ protein purified from *E.coli*, showed that in lane B and C of **Figure 3.9**, PSTOL1 WT protein was separated into two different forms because of altered mobility of phosphorylated (indicated by red arrow) and non-phosphorylated (indicated by white arrow) form. When PSTOL1 WT protein was incubated without kinase buffer, it ran as a single band at 80kDa (**Figure 3.9 lane A**)

confirming that the shift in the band is phosphorylated form of PSTOL1 WT (**Figure 3.9 Lane B** and **C**). Western blot also showed that the autophosphorylation activity of PSTOL1 WT when the purified PSTOL1 WT protein was incubated with kinase buffer including ATP (**Figure 3.9 Lane B**). We also observed higher amount of both forms of PSTOL1 WT protein when it was only incubated with ATP (**Figure 3.9 lane B**). Incubation of PSTOL1 WT protein with both ATP and MyBP showed less intensity of both phosphorylated and dephosphorylated form of PSTOL1 WT (**Figure 3.9 lane C**). We speculate cross-phosphorylation of MyBP by PSTOL1 WT kinase. However, further experiments must be done to confirm the cross-phosphorylation activity of PSTOL1 WT kinase on substrates. On the other hand, we cannot detect any phosphorylated form of PSTOL1$^{2K/R}$ protein when incubated with ATP or MyBP (in **Figure 3.9 lane E** and **F**). Therefore, the data showed that there is no detectable autophosphorylation or cross-phosphorylation activity of PSTOL1$^{2K/R}$ kinase protein (**Figure 3.9 lane E** and **F**). We also included vector alone as a negative control in this experiment to eliminate any non-specific phosphorylation activity by MBP tag.

We wanted to further study, autophosphorylation activity of SUMOylated PSTOL1 WT and non-SUMOylated version of PSTOL1. *in-vitro* phosphorylation assay was set up using purified SUMOylated PSTOL1 proteins and non-SUMOylated version of PSTOL1 as described above.

The figure highlights that PSTOL1 WT is autophosphorylated (**Figure 3.10 lane B**) and probably MyBP was phosphorylated by PSTOL1 WT kinase (**Figure 3.10 lane C**). Clearly, mutating SUMO sites in PSTOL1 impacts on both autophosphorylation and cross-phosphorylation activity which can be seen in Lane E and F. This substantiated our earlier results shown in **Figure 3.9**.

Collectively, the data suggested that PSTOL1 WT kinase can autophosphorylate itself whereas mutating SUMO sites completely abolish the autophosphorylation activity of PSTOL1$^{2K/R}$. We propose that probably SUMOylation might have an essential role in orientating the substrate precisely for PSTOL1 kinase activity facilitating the transfer of γ-phosphate to substrate

efficiently. Thereby, SUMOylation is possibly regulating the kinase activity of PSTOL1 kinase. Further investigation in this work would be highly insightful.

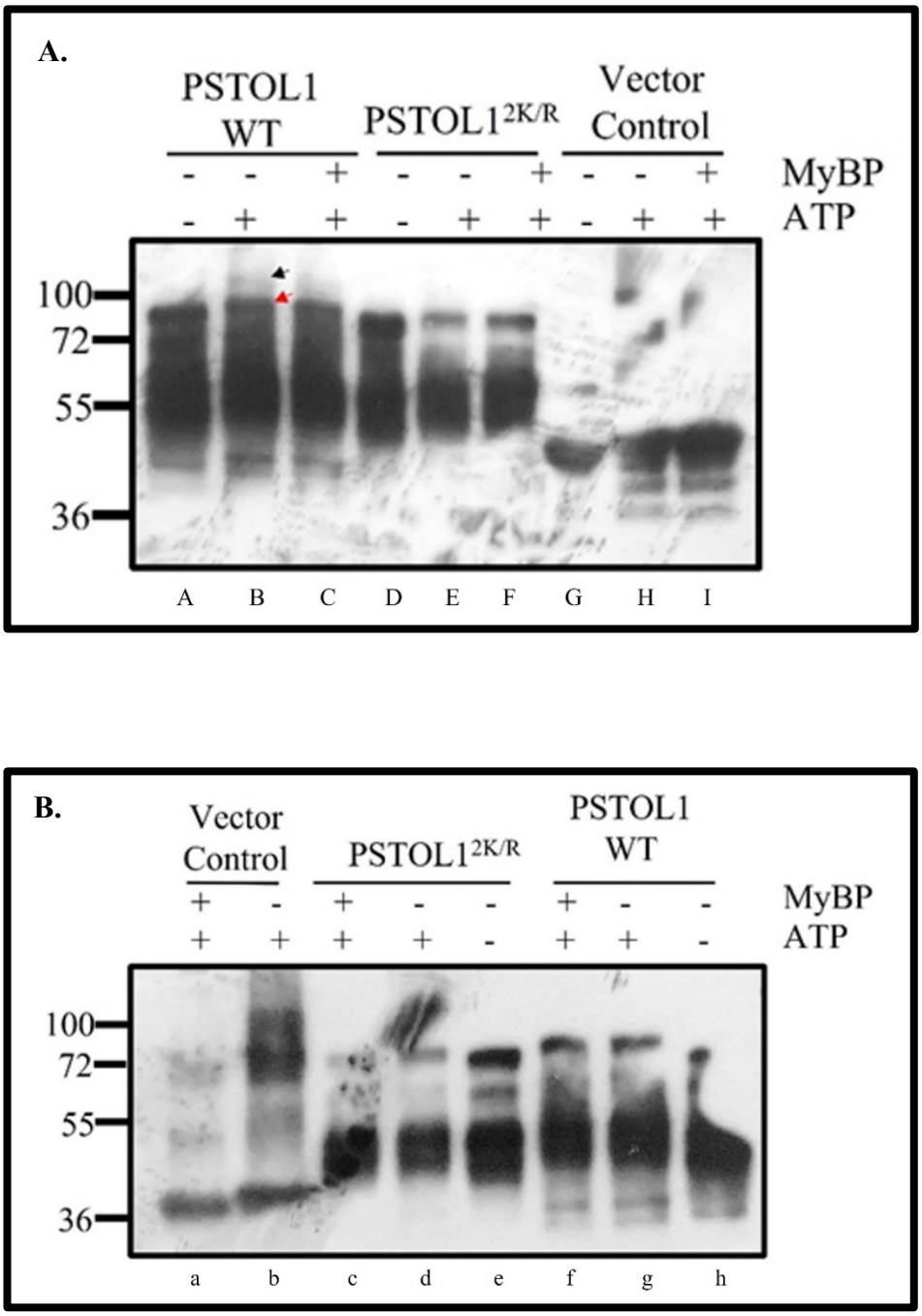

Figure 3.10: *in-vitro* phosphorylation assay conducted using N-terminal MBP tagged SUMOylated form and non-SUMOylated form of PSTOL1.

SUMOylated PSTOL1 (PSTOL1 WT) and non-SUMOylated version of PSTOL1 ($PSTOL1^{2K/R}$) were purified from *E.coli*. The purified proteins were incubated with and without MyBP in kinase reaction mixture (including ATP) to determine cross-phosphorylation and autophosphorylation activity

respectively. (A.) The western blot probed with αMBP represents samples run on Mn^{+2} Phos-tag gels with 5µM of Phos-tag acrylamide and 10µM $MnCl_2$. (B.) The parallel samples were run on the standard SDS-PAGE and probed with αMBP. Black arrow indicates the phosphorylated form of the protein and red arrow indicates the dephosphorylated form of protein.

Taken together, *in vivo* reconstituted SUMOylation assays and *in-vitro* phosphorylation assays provided evidence that presence of potential SUMO sites in PSTOL1 may regulate its kinase activity. We wanted to ascertain the role of SUMOylation of PSTOL1 on its phosphorylation activity *in planta*. To investigate this, a transient assay in *N.benthamiana* using 35::GFP:PSTOL1 WT and 35::GFP:PSTOL1$^{2K/R}$ was performed. GFP-PSTOL1 WT or GFP-PSTOL1$^{2K/R}$ was co-expressed with SUMO in *N.benthamiana* leaves. GFP was used as a negative control. Recombinant GFP-PSTOL1 WT and GFP-PSTOL1$^{2K/R}$ transient expression was confirmed by western blotting with αGFP monoclonal antibodies (Clonetech) (**Figure 3.11 A**). The SUMOylation status of GFP-PSTOL1 WT when compared to GFP-PSTOL1$^{2K/R}$ was confirmed via western blotting with αAtSUMO1/2 antibodies. From **Figure 3.11 B** we can also see that in vivo SUMO immunoprecipitation assays showed that there is considerable reduction in SUMOylation status of PSTOL1$^{2K/R}$ when compared to PSTOL1 WT (**Figure 3.11 B**) because band corresponding to GFP-PSTOL1 was observed in the lane GFP-PSTOL1 WT. A faint band was observed in the lane corresponding to the GFP-PSTOL1$^{2K/R}$. Therefore, confirming the mutation of predicted SUMO sites from lysine to arginine would abolish the PSTOL1 SUMOylation. This validated the earlier data of immunoblots from SUMO reconstituted system, though, in **Figure 3.8 A** showed that PSTOL1 WT was poly-SUMOylated whereas *in-planta* PSTOL1 WT exhibits a single band at around 65 kDa.

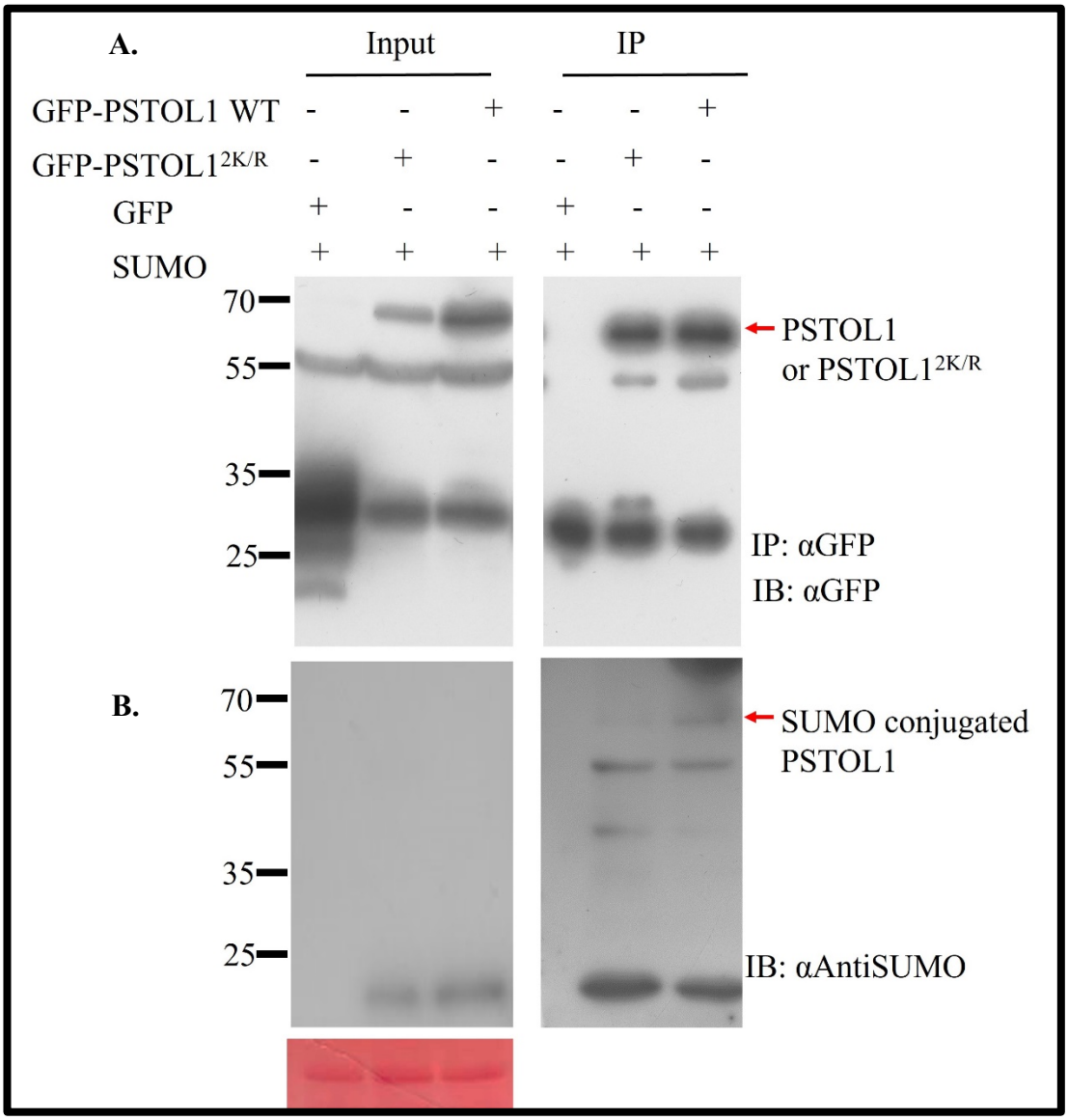

Figure 3.11: The GFP-PSTOL1$^{2K/R}$ is potentially not SUMOylated in transient assay.

A. Western blot showing α-GFP IP and α-GFP IB of recombinant GFP-PSTOL1 WT, GFP-PSTOL1$^{2K/R}$ and a GFP control infiltrated with P19 suppressor protein and SUMO in 1:1:1 ratio. Bands corresponding to GFP-PSTOL1 WT, GFP-PSTOL1$^{2K/R}$ and the YFP control can be seen in all lanes. 10µl of IP was loaded on SDS-PAGE.

B. Western blot showing α-GFP IP and α-AtSUMO1/2 IB of recombinant GFP-PSTOL1 WT, GFP-PSTOL1$^{2K/R}$ and a GFP control infiltrated with P19 suppressor protein and SUMO in 1:1:1 ratio. A band corresponding to GFP-PSTOL1 WT can be seen in the IP lane indicating mono-SUMOylation of GFP-PSTOL1 WT. A faint band can be seen in the IP lane of GFP-PSTOL1$^{2K/R}$, indicating that mutation of SUMO sites will significantly abolish the SUMOylation. 100µl of IP was loaded on SDS-PAGE.

3.7 Immunokinase assay/ *in vitro* kinase assay

To investigate the autophosphorylation activity of PSTOL1 protein kinase *in-planta*, the GFP-PSTOL1 WT and GFP-PSTOL1$^{2K/R}$ protein kinase was immunoprecipitated using GFP beads. The purified proteins were incubated with 1x kinase buffer including ATP for 1 hour at 30°C. Samples were subjected to Phos-tag analysis and blots were probed by αGFP antibody. SDS-PAGE without the addition of Phos-tag acrylamide was run alongside Phos-tag gel.

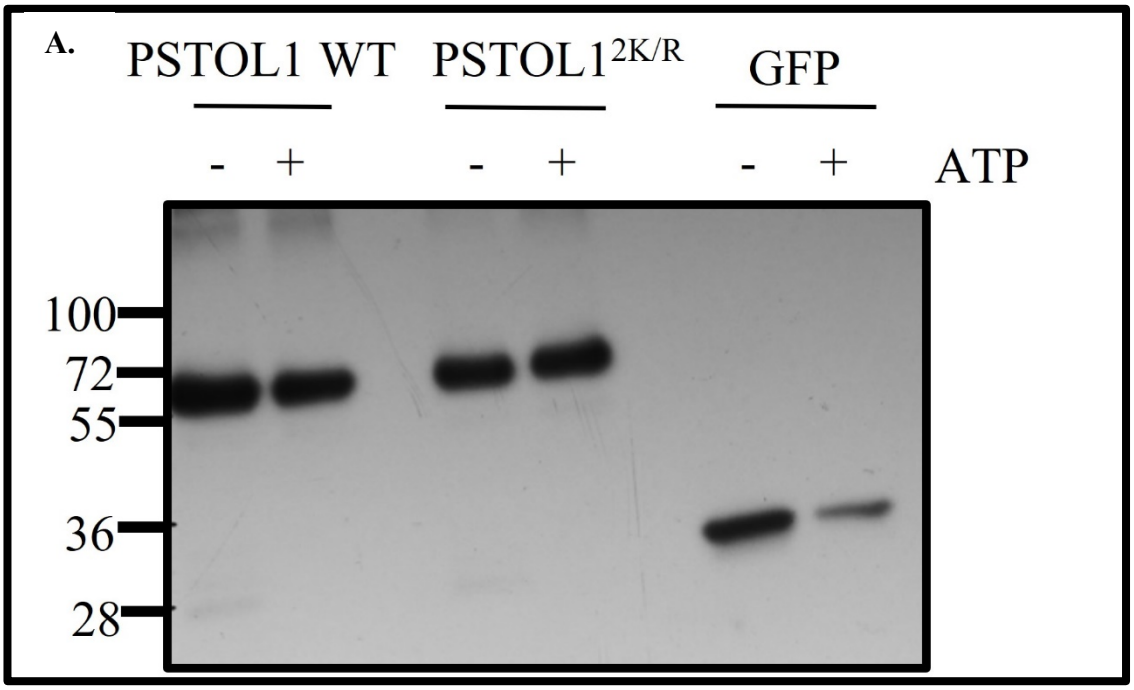

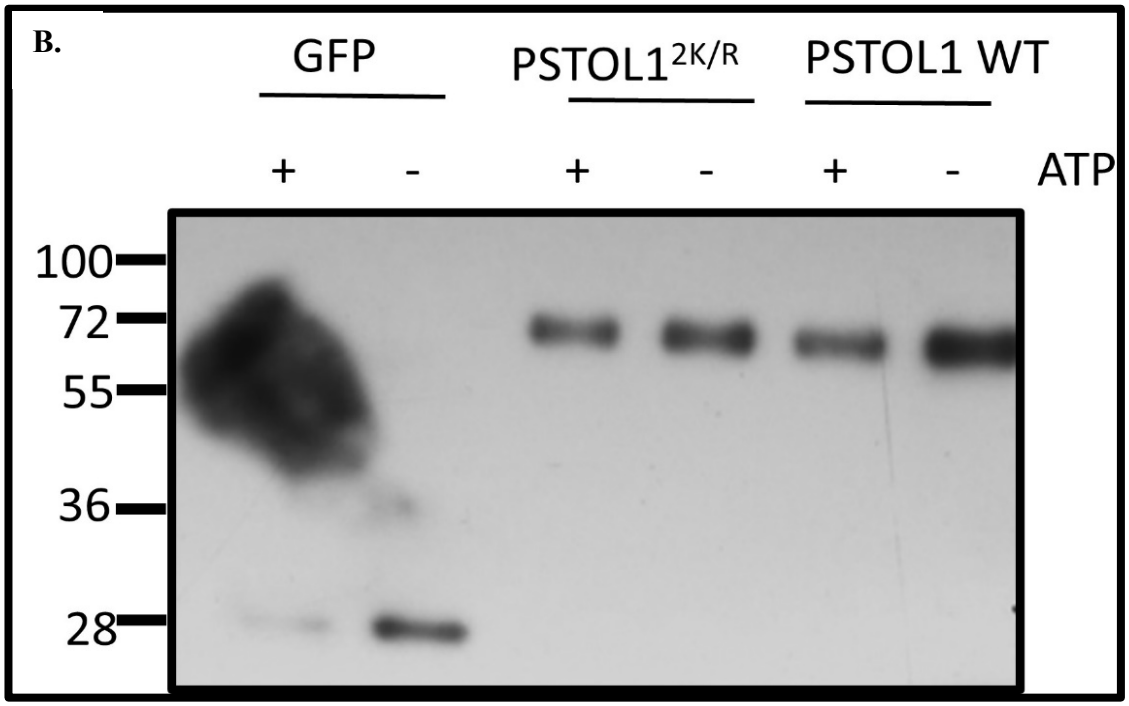

Figure 3.12: Immunokinase assay/*In vitro* phosphorylation assay.

Protein was extracted using extraction buffer and immunoprecipitated using GFP beads. Immunoprecipitated GFP-PSTOL1 WT, GFP-PSTOL1$^{2K/R}$ and GFP were used as sample for in-solution kinase assay. (A.) The western blot probed with αGFP represents samples run on Mn^{+2} Phos-tag gels with 5μM of Phos-tag acrylamide and 10μM $MnCl_2$. (B.) The samples were also run on the standard SDS-PAGE and probed with αGFP antibody.

In contrast to *in-vitro* phosphorylation assay (**Figure 3.9** and **3.10 A**), there was no significant difference observed *in-planta* in autophosphorylation activity of PSTOL1 WT and PSTOL1$^{2K/R}$. Two separate forms of PSTOL1 WT were not observed and instead PSTOL1 WT and PSTOL1$^{2K/R}$ both run as a single band at 65kDa when subjected to Phos-tag gel analysis. There are several factors to optimize the strategy for employing Phos-Tag acrylamide pendant used for separation of phosphorylated and non-phosphorylated forms of protein from plants. Bekešovà et al., 2015 showed that it is important to establish appropriate extraction buffer conditions to maintain the phosphorylation status of protein. Besides optimizing buffer conditions, it is also crucial to optimize the metal cation (Mn^{+2} or Zn^{+2}) used to separate the phosphorylated and non-phosphorylated forms of protein. Some research by Kumar G., 2018, Ban et al., 2013 and Smékalová et al., 2014 showed that Zn^{+2} Phos-tag SDS PAGE with neutral gel buffer system was an improved method for separating the two forms of proteins. The

original procedure for post-electrophoretic treatment of the Phos-Tag gel demonstrated by Kinoshita et al., 2006 recommended 10minute incubation time in transfer buffer supplemented with 1mM EDTA, however, this step is inadequate to transfer the forms of protein since certain form of protein can occur as a minute fraction. To overcome this issue, EDTA concentration can be increased 10mM whilst also increasing the time of incubation to 1 hour. The buffer was also changed frequently. Also, it is critical to remove methanol from washing steps because it may hinder the transfer of protein from gel to PVDF membrane.

Other than these technical issues, we also speculate another reason to differences between in -vitro and in planta data. Some protein kinases are activated when exposed to various biotic and abiotic stresses. Studies in rice showed that OsMSRMK2 (a mitogen -activated protein kinase) will show activation only by abiotic stresses such as ROS burst, drought, or salinity (Agrawal et al., 2002). Calcium dependent protein kinases (CDPKs or CPKs) also show activation or repression due to abiotic stresses in plants (Atif et al., 2019). Therefore, we hypothesized that PSTOL1 may exist in different forms when a plant is exposed to stress related to phosphorus. Unfortunately, due to lack of time, this study could not be further investigated.

3.8 PSTOL1 cellular localization in leaves of *Nicotiana benthamiana*

The CDS of PSTOL1 gene was cloned into YFP tagged plant expression vector series pEARLYGATE (pEG) (Earley et al., 2006). These vectors were used to transform the bacterium *Agrobacterium tumefaciens* GV3103 cells; this strain of bacteria is used to transiently express protein of interest when infiltrated into *N.benthamiana* leaves (Vijn and Govers 2003). 3 days after syringe infiltration, 1cm squared sections of the leaf were carefully cut and placed under a microscope slide for viewing in a confocal microscope Zeiss LSM 880.

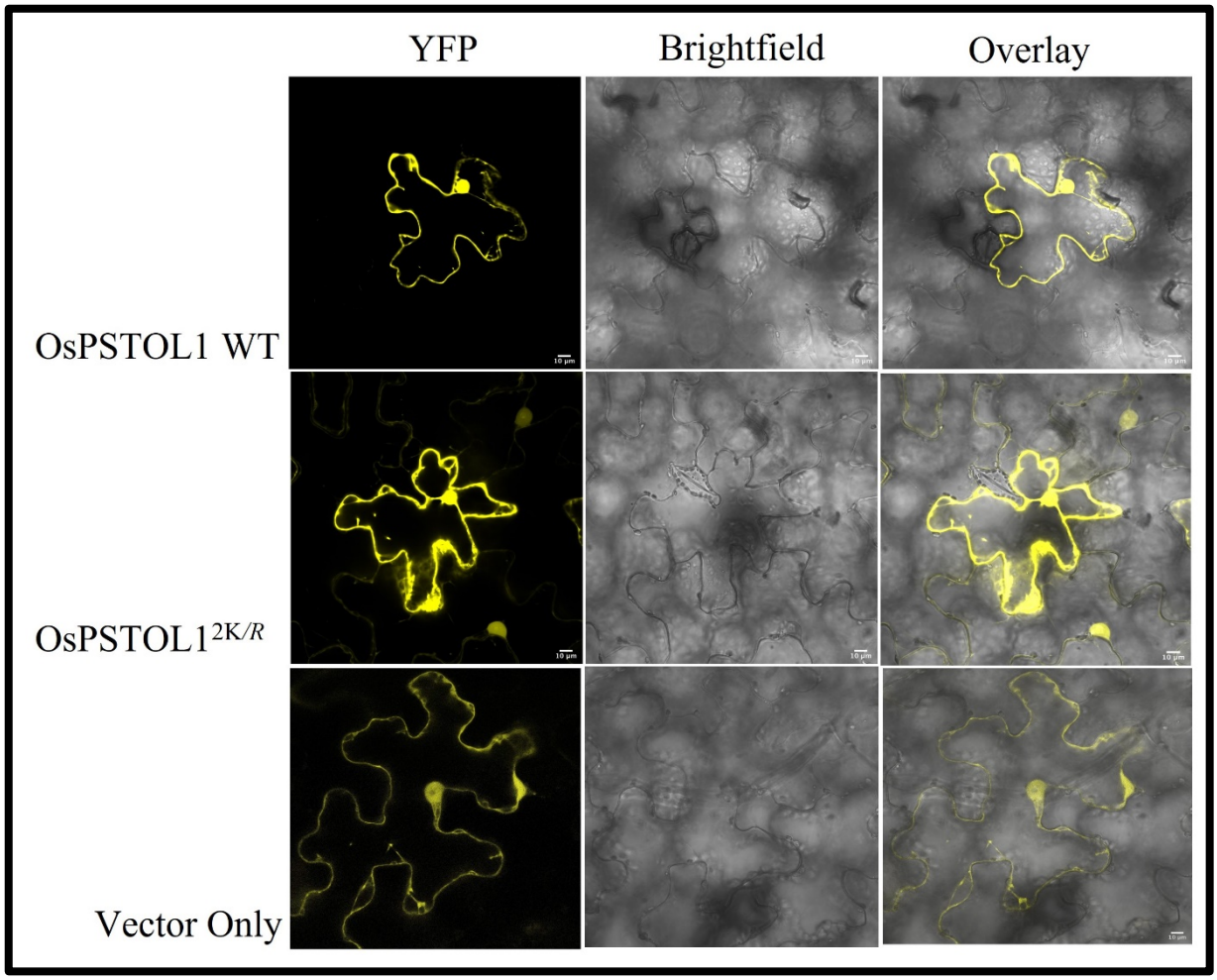

Figure 3.13: YFP tagged PSTOL1 WT and PSTOL1$^{2K/R}$ localizes in nucleus and cell membrane/cytoplasm when expressed in *N.benthamiana* leaves.

N.benthamiana leaves were infiltrated with *Agrobacterium tumefaciens* expressing PSTOL1 constructs, YFP, SUMO and P19 respectively. The *Agrobacterium* culture expressing all constructs were diluted in 10mM $MgCl_2$ to an O.D. 600 of 0.2 each. The infiltrated plants were allowed to grow for 3 days. The Zeiss 880 microscope was used to visualize PSTOL1 WT, PSTOL1$^{2K/R}$ and YFP in the leaf. The 'Vector only' panel shows the localization of the YFP protein from pEG104 vector. YFP-PSTOL1 WT and YFP-PSTOL1$^{2K/R}$ are observed to be present in nucleus and cell membrane in *N. Benthamiana* plant cells. The localization was analysed by Zeiss LSM 880 confocal laser scanning microscope using a 60 × 1.4NA lens using laser excitation at 514 nm and emission filters 524-580 nm.

Figure 3.13 showed that YFP-PSTOL1 WT and YFP-PSTOL1$^{2K/R}$ localize to the nucleus and cell membrane/nucleus like vector only controls. Fusion proteins of YFP-PSTOL1 WT and YFP-PSTOL1$^{2K/R}$ in the transient expression system was confirmed by western blotting with αGFP monoclonal antibodies (Clonetech) (**Figure 3.11 A**). We also investigate the localization

of PSTOL1 WT and PSTOL1$^{2K/R}$ in *Arabidopsis* and rice which is discussed in chapter 4 and chapter 5 respectively.

3.8 Investigating the target of PSTOL1 kinase

The next step was to identify the target substrates of PSTOL1 kinase. Gamuyo et al., 2012 showed that PSTOL1 overexpressing lines has more P content when compared to null transformants. However, the underlying mechanism of PSTOL1 remained elusive until today. Therefore, identification of PSTOL1 targets is necessary to unveil the mechanism which can be absent from other rice varieties which are intolerant to phosphorus deficiency.

We primarily used two methodologies to identify the targets of PSTOL1- Yeast two hybrid (Y2H) and Complex-immunoprecipitation (CO-IP).

3.8.1 Yeast two Hybrid

3.8.1a Introduction

A practical method to predict the function of a protein is by identifying its interacting partner (Keskin, et al., 2008). A vast number of biological processes are reliant on protein-protein interactions (Wong et al., 2017). Various techniques by means of biochemical approaches- affinity chromatography, co-immunoprecipitation and while molecular approaches include-

yeast two hybrid are employed to map the interaction between proteins (Causier and Davies et al., 2001).

Yeast two hybrid based on the observation that transcription factors from eukaryotic system have distinct and separable domains- DNA binding domain (DBD) and Activation domain (AD). The promoter region of gene is recognized and bound by DNA binding domain leading to activation domain to recruit other proteins from transcription machinery to activate the transcription of the gene (**Figure 3.14**) (Causier and Davies et al., 2001 and Ferro and Trabalzini et al., 2013).

We have used ProQuest™ Two Hybrid System, which includes yeast expression vectors- pDEST™ 22 has GAL4 activation domain (GAL4 AD; Prey) with tryptophan as a selection marker whereas pDEST™32 has DNA Binding domain (GAL4 DBD; Bait) with leucine as a selection marker. Along with these two expression vectors, the kit also provides the control vectors to include them as positive controls for yeast two hybrid experiments. These controls plasmids are based on interaction between RalGDS and KrevI. Mutations in RalGDS will affect the interaction with KrevI.

Bait or protein of interest was cloned into pDEST™32 vector that contains a leucine selection marker and the vector was transformed into PJ69-4α yeast strain. Transformed yeast cells are selected by growing on minimal Synthetic Defined (SD) base media without leucine (SD/-L). This SD base media has all amino acids except leucine. Likewise, Prey are cloned in to pDEST™ 22 and transformed into YM4271 yeast strain and the yeast colonies are selected on minimal Synthetic Defined (SD) base media without tryptophan (SD/-W). These yeast strains are genetically engineered to contain LacZ and HIS3 as reporter genes. These reporter genes encode the functional protein that provides a simple readout of interaction between two proteins. If the two proteins i.e., bait and prey interact in yeast cell, DBD and AD will come together to re-form transcription factor and later will activate the expression of reporter genes. Positive interaction can be confirmed by two ways: 1. Interaction between bait and prey can be detected by selecting on plates lacking histidine. Positive interaction between two proteins in

yeast cells will enable yeast cells to grow in media lacking histidine. 2. Another way to check the interaction is by β-galactosidase activity. If there is no interaction between two proteins, yeast cells harboring both plasmids will grow white in color on plates of SD base media with X-α-GAL. The yeast colonies will look blue in color if two proteins interact with each other. To increase the stringency of yeast two hybrid screens sometimes more than one reporter genes are evaluated parallelly.

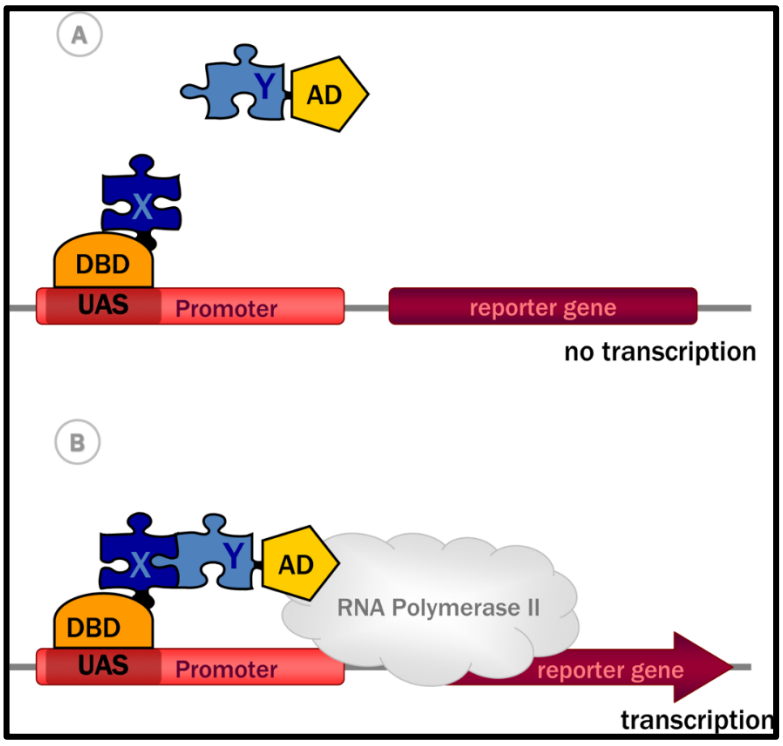

Figure 3.14: Schematic representation of classic yeast-two hybrid system.

(A) shows a negative interaction which ultimately results in no transcription activation of reporter gene. (B) The interaction between X and Y reconstituted the transcription factor, leading to recruitment of RNA polymerase II for transcription activation of downstream reporter gene. Adapted from Brückner et al., 2009.

3.8.1b Checking the autoactivation

A common restraint in yeast two hybrid experiment is that when a gene fragment subcloned in the vector is transformed into yeast strain, it can activate the reporter genes without binding

partner (Galletta and Rusan .,2015). This is known as Autoactivation or self-activation of reporter genes.

To check the autoactivation activity, PSTOL1 WT and PSTOL1$^{2K/R}$ gene were subcloned into pDEST 32 vector. Empty vector pDEST 32, pDEST 32 PSTOL1 WT and pDEST 32 PSTOL1$^{2K/R}$ were transformed into PJ69-4α yeast strain. Besides transforming empty vector, the control plasmid KrevI from ProQuest^{TM} Two Hybrid System was also transformed into PJ69-4α yeast strain. KrevI plasmid will be control plasmid for checking autoactivation activity.

We had checked the reporter activity of lacz gene. The cultures were plated on SD/-L and SD/-L+X-α-Gal and incubated for 2 days. The color of cultures was observed. The culture will turn blue if the bait or empty vector is autoactivating the reporter gene. In the absence of autoactivation of reporter gene, the culture would appear white.

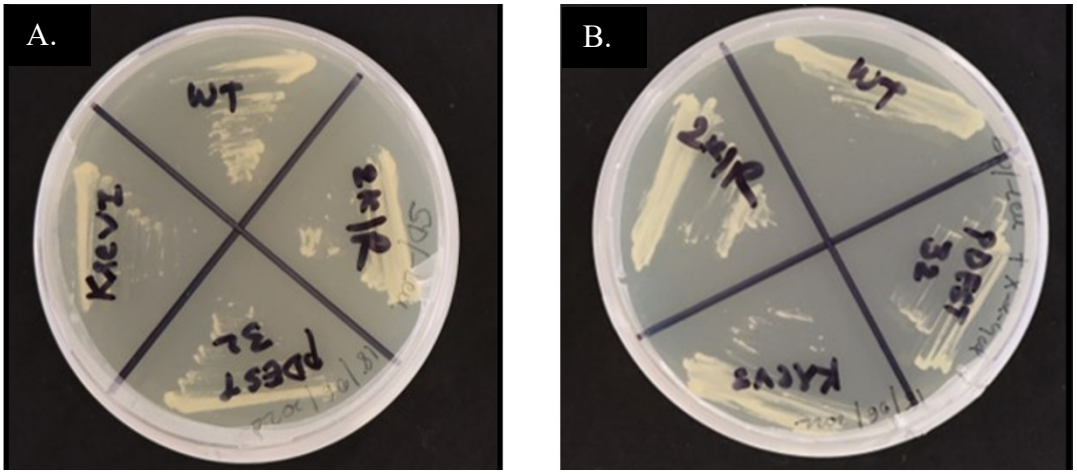

Figure 3.15: Autoactivation test for target proteins.

PSTOL1 WT and PSTOL1$^{2K/R}$ gene was subcloned into pDEST 32 vector and transformed into PJ69-4α yeast strain along with empty vector. (A.) Negative control was included to check the autoactivation activity of bait plasmid. Cultures plated on SD/-L plates and after 2 days of incubation, the color of cultures was observed. (B.) Detection of self-activation of bait plasmid on SD/-L+X-α-Gal plates.

Figure 3.15 A and **B** shows that the color of cultures was same in both negative control (SD/-L) and SD/-L+X-α-Gal plates. This experiment confirmed that empty vector, PSTOL1 WT and PSTOL1$^{2K/R}$ do not autoactivate the reporter gene transcription in absence of activation domain.

3.8.1c Validating the controls for positive interactions in Yeast -two hybrid assays

The next step is to set up a mating experiment with positive controls. Positive controls were used to assay the interaction in a two-hybrid system. As a result, activation of specific reporter gene will confirm that fusion protein is properly folded and directed to nucleus. However, PSTOL1 does not have any known interactor yet, therefore, to assay the interaction, we decided to use the controls plasmids suggested by ProQuest™ Two Hybrid System. These controls are built on the interaction between RalGDS and KrevI. Mutations in RalGDS (m1 and m2) affect the interaction with KrevI. Mating between RalGDS WT and KrevI was strongest while the interaction between KrevI and RalGDS (m1) weakened and further weakened when KrevI was mated with RalGDS (m2). Along with positive controls, yeast strains harboring empty vectors were also mated as negative controls for experimental system. Negative control is required to standardize the suppression of background growth, but it is important to consider that suppression of background should be enough to distinguish the weak interaction with background growth.

Control plasmid	Backbone	Insert	Mutant	Role	Interaction with pEXP™32/Krev1
pEXP™32/ Krev1	pDEST™32	full-length rat Krev1	*wt*	Bait	not applicable
pEXP™22/ RalGDS-*wt*	pDEST™22	ras association domain of RalGDS, *wt*	*wt*	Prey	strong
pEXP™22/ RalGDS-m1	pDEST™22	ras association domain of RalGDS, m1	I77T[1]	Prey	weak
pEXP™22/ RalGDS-m2	pDEST™22	ras association domain of RalGDS, m2	L65P[1]	Prey	not detectable

Figure 3.16: The interaction controls recommended following transformation.

Adapted from ProQuest™ Two Hybrid System manual.

pDEST 32 KrevI was transformed into PJ69-4α yeast strain, and the other three control plasmids were transformed into another yeast strain -YM4271. Mated cultures were spotted on the SD/-LWH (Synthetic Defined (SD) base media without leucine, tryptophan, and histidine) plates and incubated at 30˚C for 2-3days.

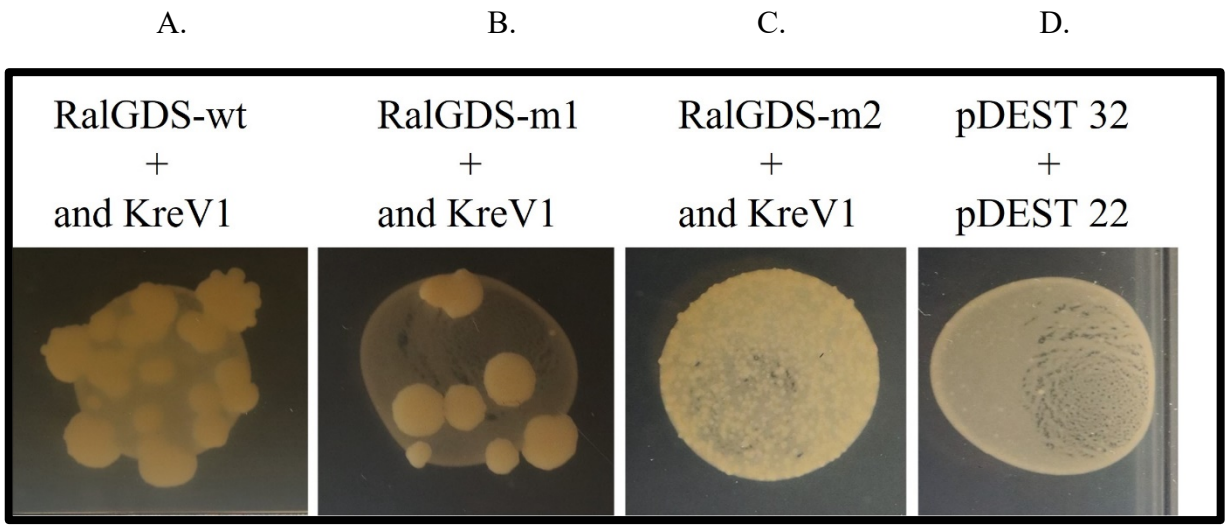

Figure 3.17: Interaction between controls plasmids recommended by ProQuest™ Two Hybrid System.

Controls plasmids were transformed into yeast strains and interaction between control plasmids were systematically examined. Standard mating protocol was used for this experimental setup. (A.) shows strong interaction between RalGDS-wt and KrevI. (B.) shows intermediate interaction between RalGDS-m1 and KrevI. (C.) shows weak interaction between RalGDS-m2 and KrevI. (D.) shows interaction between empty vectors - pDEST32 and pDEST22.

With this experiment, we were able observe a strong, intermediate, and weak interaction. While strong and intermediate interactions (**Figure 3.17 A** and **B**) will be easily visible and distinguished, it can be difficult to distinguish weak interaction (**Figure 3.17 C**) with background growth. From **Figure 3.17 C** and **D**, it was important to distinguish the weak

interaction from non-specific background interactions. This is a relevant reference while screening potential interactors of OsPSTOL1 using arrayed yeast library. A common limitation of yeast two hybrid screening is that sometimes bait, or prey constructs produce extensive background growth which generates a substantial number of false positives as shown in **Figure 3.17 D**. There are two different types of false positives: Firstly, comprise of "biological" false positives which can only be eliminated by comprehensive knowledge of protein of interest. Second type of false positives developed as result of technical issues (Vidalain et al., 2004). This creates a problem when detecting a positive interaction. To overcome this issue, yeast strains harboring empty vectors (pDEST 32 and pDEST22) were also mated which will act as suitable negative two-hybrid controls for non-specific interactions.

Before starting the yeast two hybrid screening, we had determined the autoactivation activity of PSTOL1 WT independent of the activation domain (AD). Also, positive and negative controls were included in the experimental set up of yeast two hybrid screening.

3.8.1d *Arabidopsis* TF library for Yeast two hybrid

To investigate the targets of PSTOL1, we used an arrayed yeast library generated by Castrillo and Turck., 2010 et al added to previously known library of *A.thaliana* transcription factors (Regia project). This library consists of 1200 *A.thaliana* transcription factors (TFs) (Regia Project) and 288 (Regulators) hereafter known as REGIA+REGULATORS; RR library. The protocol for yeast two hybrid screening was followed as described by Castrillo and Turck., 2010. . The RR library was purchased from Nottingham *Arabidopsis* Stock Centre (NASC). The library was sent as glycerol stocks of the TFs in yeast (YM4271) on 15 separate 96 well plates. Since PSTOL1 is in plant nuclei – it may have nuclear substrates, such as TFs.

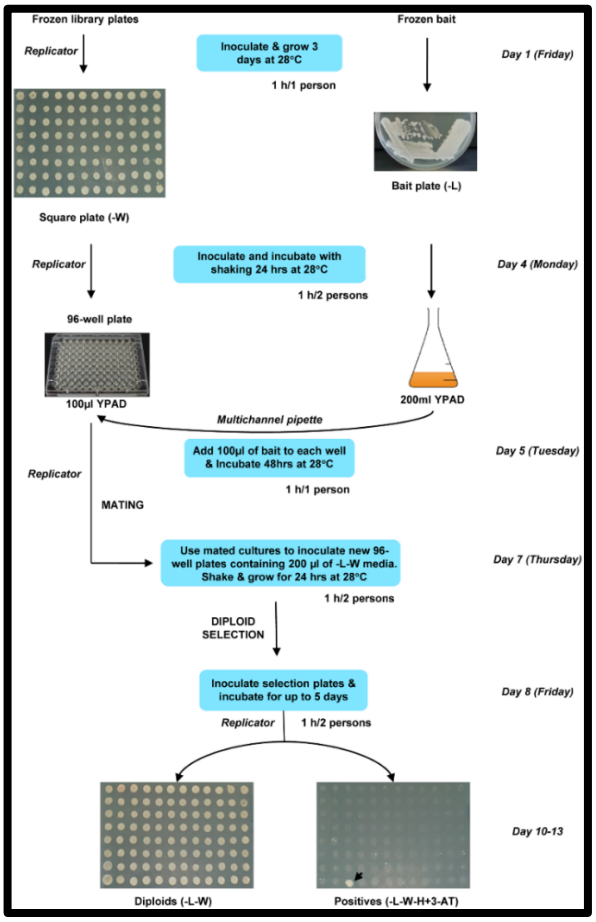

Figure 3.18: Schematic representation to screen RR library.

Adapted from Castrillo et al., 2011.

To investigate the transcription factors interacting with PSTOL1 WT, the gene was cloned into pDEST32 (bait). The clone was confirmed by PCR and transformed into PJ69-4α yeast strain. A single colony after transformation was inoculated in YPDA media and simultaneously TF yeast library (prey) was inoculated in 96-well plate with YPDA. Both bait and prey were allowed to grow at 28˚C overnight with shaking at 180rpm. The next step was to mate the two yeast strains. The 100µl bait was inoculated to 100µl prey in 96-well plates. The plates were allowed to incubate for 2days at 28˚C with shaking with 180rpm. Mated culture was used to inoculate to selective medium SD/-LW to score diploids and SD/-LWH for checking the positive interactions. The pictures of the plates were taken after 3 days to check for positive interactions (**Figure 3.18**).

Next step was to investigate the identity of AD insert which showed interaction with PSTOL1 WT. The colonies were inoculated in SD/-LWH media and allowed to grow overnight at 30°C with shaking 220rpm. The DNA was isolated from all colonies. pDEST 22 vector specific primers were designed and these primers were used to amplify the CDS of interacting partner. PCR product was run on 1% agarose gel and using gel extraction kit the corresponding bands were eluted and sent for sequencing (**Figure 3.19**). Table 1 shows the probable transcription factors as interactors of PSTOL1.

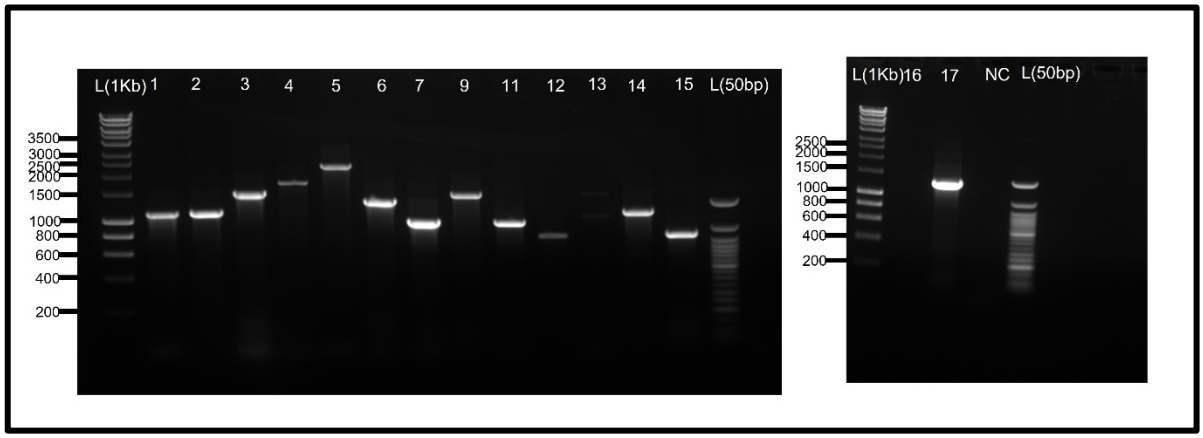

Figure 3.19: Image of DNA gel showing amplification of PCR product of AD.

Vector specific primers were used to amplify from yeast colonies grown on SD/-LWH media and run on 1% agarose gel. The agarose gel was cut using sharp scalpel and DNA purified using a Gel extraction kit. The samples were eluted in 12µl in sterile water and send it for sequencing.

Table 3.1 : Potential positive interactors of PSTOL1 identified through arrayed yeast library of transcription factors from *Arabidopsis thaliana* and their homologs in rice

S.No	Clone Number	Gene ID	Gene Description	Homolog in Rice genome (Japonica)
1.	2	AT5G53420	CCT motif family protein	Uncharacterized protein
2.	11	AT5G56840	myb-like transcription factor family protein	Transcription factor MYBS3-like
3.	3	AT4G11680	Zinc finger, C3HC4 type (RING finger) family protein	E3 ubquitin-protein ligase
4.	14	AT1G25470	Cytokinin Response Factor 12	Ethylene response factor ERF117
5.	6	AT2G37260	WRKY 44	Hypothetical protein DAI22
6.	15	AT1G29160	COGWHEEL1	Dof-type zinc finger protein 02
7.	7	AT2G31230	Ethylene responsive element binding factor 15	Putative DNA binding protein
8.	17	AT5G54070	Heat shock transcription factor A9	Heat stress transcription factor A-2e
9.	5	AT1G17770	SDG17, SET DOMAIN PROTEIN 17, SU(VAR)3-9 HOMOLOG 7, SUVH7	Histone-lysine N-methyltransferase, H3 lysine-9 specific SUVH1
10.	4	AT4G08250	GRAS family transcription factor	Nodulation-signalling pathway 2 protein
11.	9	AT1G55960	Polyketide cyclase/dehydrase and lipid transport superfamily protein	stAR-related lipid transfer protein 7, mitochondrial isoform X2 and X1
12.	8	AT1G48150	MADS-box transcription factor family protein (AGAMOUS-Like 74)	Agamous-like MADS-box protein AGL61
13.	10	AT2G22850	basic leucine-zipper 6	bZIP transcription factor 44

The next step was to test the strength of interaction between the PSTOL1 WT and TFs that grew in Y2H library screening. 13 TFs were shortlisted for checking the strength of interaction from screening based on the growth of the yeast on selections media. Here we checked the activity of Histidine reporter gene. Background growth can be reduced by adding a small amount of 3-Amino-1,2,4-trizole (3-AT) in SD/-LWH media. 3-AT is a competitive inhibitor of the HIS3 enzyme, so increasing concentration of 3-AT will reduce the background growth. 3-AT is also used to fine-tune the stringency of the assay. Strength of positive interactions are

usually determined by increasing concentration of 3-AT. The colonies from SD/-LWH were dissolved into 10µl water and pipetted onto the plates containing SD/-LWH without 3-AT, SD/-LWH+ 0.5mM, SD/-LWH+ 5mM and SD/-LWH+ 10mM. **Figure 3.20** shows the representative growth and strength of interaction of PSTOL1 WT with 13 TFs.

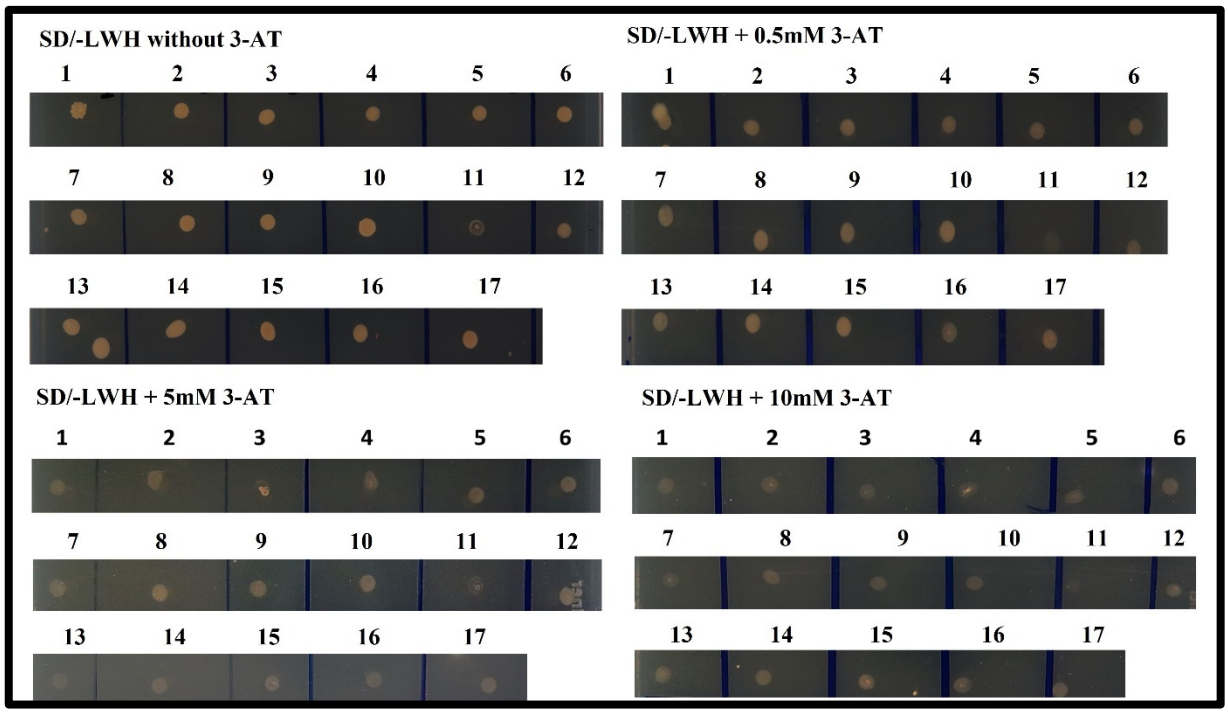

Figure 3.20: A representation of 13 transcription factors interacting with PSTOL1 through a yeast two hybrid experiment.

Positive interactions were confirmed on high stringency 3-AT plates. After mating process, the positive colonies were dissolved in 10µl sterile water and pipetted out on plates with and without 3-AT. In this experiment, three different 3-AT concentrations- 0.5mM, 5mM and 10mM were used.

Table 3.2 : Putative strong interactors of PSTOL1 confirmed on high stringency media

S.No	Gene ID	Gene description	Homolog in rice genome (Japonica)
1.	ATIG48150	MADS-box transcription factor family protein (AGAMOUS-Like 74)	Agamous-like MADS-box protein AGL61
2.	AT1G25470	Cytokinin response factor 12	Ethylene response factor ERF117
3.	AT1G29160	COGWHEEL1	Dof-type zinc finger protein 02
4.	AT5G54070	Heat shock transcription factor A9	Heat stress transcription factor A-2e

The **Figure 3.20** shows the representative growth on increasing levels of 3-AT concentration. We found that clones 8,14,15 and 17 showed stronger interaction than other clones at 10mM 3-AT concentration (**Table 3.2**). The increasing 3-AT concentration suppressed the interaction. The probable reason could be that 5mM and 10mM 3-AT concentrations were very high to suppress the growth of weak interaction. Therefore, we decided that the next experiment will be performed with 0.5mM, 1mM and 2mM 3-AT concentration for final observation of strength of interaction. However, it is important to confirm the yeast two hybrid screening results using *in vivo*- technique because any positive result demonstrating that two proteins interacting or have ability to interact does not certainly prove that these proteins will interact *in vivo* in plant cells (Wong and Naumovski et al., 1997).

3.8.2 Complex-Immunoprecipitation (Co-IP)

Another key technique used to study protein-protein interactions is Coimmunoprecipitation which provides very necessary information whether the proteins in study interact in vivo. To determine the targets of PSTOL1 protein, we used co-immunoprecipitation technique.

SUMOylation is a reversible process and SUMO proteases are necessary to deSUMOylate target proteins. From the **Figure 3.8 A** and **3.11 B**, it was confirmed that PSTOL1 WT is SUMOylated, we hypothesized that identifying a SUMO protease which deSUMOylates PSTOL1 will unravel any new role for the SUMO system machinery in regulating phosphate homeostasis in plants. We have synthesized a few rice SUMO proteases in fusion with YFP as a tag for subcellular localization of SUMO proteases. As **Figure 3.13** showed PSTOL1 WT and PSTOL1$^{2K/R}$ localized in both cell membrane and nucleus, we checked the localization of ULPs (Ubiquitin Like Proteases) using confocal microscopy and based on the localization of ULPs, we decided to select ULPs which localize in both nucleus and cell membrane for investigating their interaction with PSTOL1.

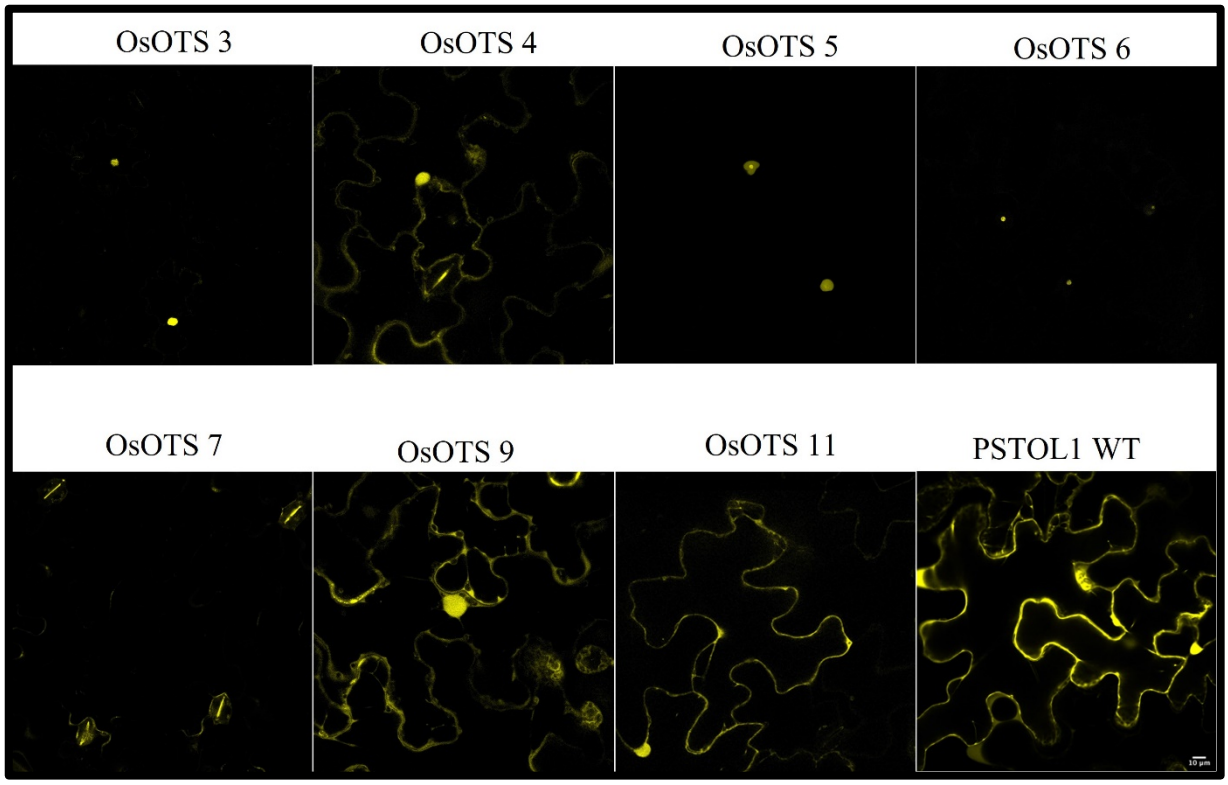

Figure 3.21: Localization of YFP-tagged ULPs in *Nicotiana benthamiana* leaves.

A.tumefaciens expressing P19 and YFP-tagged ULPs were diluted in 10mM $MgCl_2$ to O.D. 600 of 0.3 each. The infiltrated plants were allowed to grow for 3 days.The localization was analysed by Zeiss LSM 880 confocal laser scanning microscope using a 60 × 1.4NA lens using laser excitation at 514 nm and emission filters 524-580 nm.

OsOTS11 and OsOTS9 localized both in nuclei and cell membrane in *N.benthamiana* leaves like PSTOL1 WT (**Figure 3.21**). Firstly, we selected OsOTS11 to check its interaction with PSTOL1 WT. To investigate the interaction between OsOTS11 and PSTOL1 WT, both the genes were cloned with different tags in Gateway destination vector. OsOTS11 was cloned in destination vector pEG100 (this vector is without a fluorescent protein tag) since OsOTS11 was already tagged with YFP in the Entry vector. Whereas PSTOL1 was cloned in the destination vector pEG201 consisting of an N-terminal HA tag.

The transient expression data shows that HA-PSTOL1 and YFP-OsOTS11 in input lanes when immunoblotted with αHA and αGFP respectively. The single band was observed in the IP sample showed that OTS11 was expressed in all lanes and successfully immunoprecipitated (**Figure 3.22 A** and **B**) while CO-IP data showed that there is no interaction between OsOTS11 and PSTOL1. However, further validation is required to confirm this result. Reverse pull down is another way to further validate the result. Due to time constraints, interaction of PSTOL1 with other ULPs was not investigated.

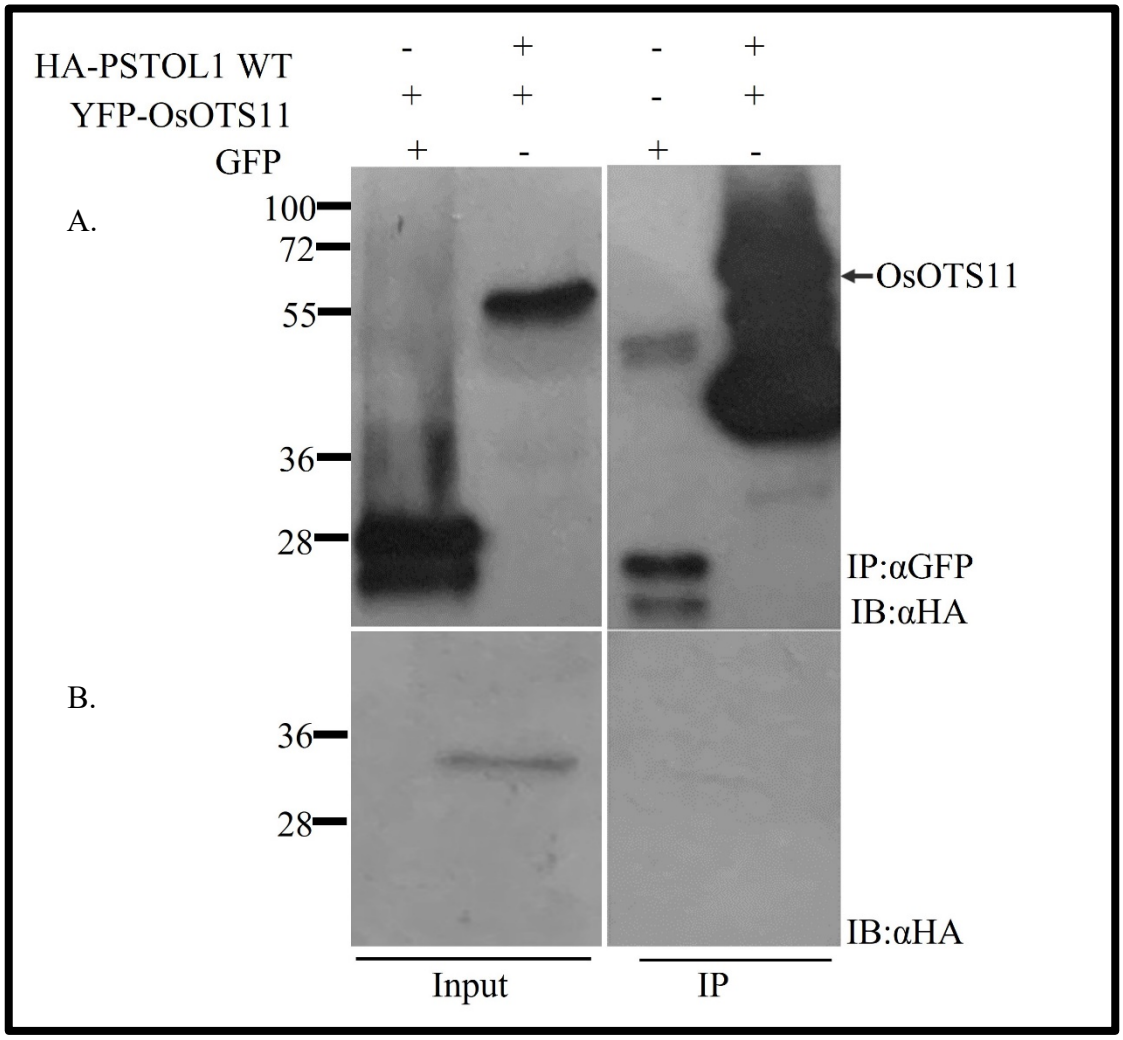

Figure 3.22: Investigating the interaction between YFP-tagged OsOTS11 and HA-tagged PSTOL1.

Western blotting shows α-GFP IP (immunoprecipitated with GFP beads) and α-HA IB of recombinant OsOTS11 and PSTOL1 WT protein to identify protein-protein interaction between these two proteins. Band corresponding to OsOTS11 and PSTOL1 can be seen in input lanes. OsOTS11 was successfully immunoprecipitated with GFP beads (A.) and probed with αGFP. The corresponding immunoblot of

αHA does not show any band corresponding to PSTOL1 **(B.)**. 10µl of IP and 50µl of total protein extract was loaded on gel.

3.9 Discussion

Proteins are subjected to various Post-Translational Modification (PTMs) which significantly increase the functionality and diversity of the proteome, improving the ability of plants to respond to abiotic or biotic stresses. As a result, plants can fine-tune responses, and studying these responses is an important aspect of crop improvement efforts (Zhang and Zeng., 2020).

In recent years, it is well established that cross talk between different Post-Translational Modifications will regulate protein activity and its fate (Khan et al., 2014). Sadanandom et al., 2015 showed binding of phytochrome B to Phytochrome Interacting Factors (PIFs) transcriptional regulators is intervene by conjugation of SUMO to phytochrome B whereas Medzihradszky et al., 2013 demonstrated that phosphorylation of phytochrome B negatively regulates the light signalling. Thus, both SUMOylation and phosphorylation regulate the light induced signalling via different mechanisms. Similarly, SUMOylation of WRKY33 is necessary to interact with Mitogen-Activated Protein Kinases (MAPKs) which results in phosphorylation of WRKY33 and thus activation (Verma et al., 2020). Thus, emerging evidence like above verify the concept that cross talk between different PTMs allow additional layers of regulation and thus fine-tuning the responses to environmental cues (Zhang, Y and Zeng, L., 2020). In this chapter, we investigated crosstalk between SUMOylation and phosphorylation. In the current chapter, we demonstrated that SUMO sites (K20 and K225) in PSTOL1 plays a vital role in regulating autophosphorylation and probably trans-phosphorylation in vitro (**Figure 3.9** and **3.10**). The data likely suggests that SUMOylation is the PTM regulating basal-level PSTOL1 kinase activity and, SUMOylation may plays a regulatory role for selectivity of substrate by PSTOL1 kinase during normal growth conditions

and stress conditions. Therefore, an interplay between phosphorylation and SUMOylation can be associated with activation or repression of PSTOL1 kinase activity. A similar immunokinase assay was set up using immunoprecipitated protein from *N.benthamiana* leaves. However, phosphorylated and dephosphorylated forms of PSTOL1 WT protein were not seen when the protein was subjected to Phos-tag analysis. In the future, determining the biological conditions and optimizing the conditions under which PSTOL1 will autophosphorylate is important to establish SUMO's role in PSTOL1 autophosphorylation activity.

This thesis showed for the first time that PSTOL1 protein localized in both nucleus and cell membrane in *N.benthamiana* leaves. Use of appropriate cellular compartment markers would allow full verification of the localization of PSTOL1. Nevertheless, we observed that there is no difference in localization of PSTOL1 WT and PSTOL1$^{2K/R}$ protein. Thus, the data showed that SUMOylation of PSTOL1 does not affect the localization of the protein in *N. benthamiana.*

Parallelly, we investigated the potential targets for PSTOL1 kinase since there are no known targets of PSTOL1 till this date. Exploring the targets of PSTOL1 is important because we speculate that selectivity of substrate by this kinase might be affected by SUMOylation status of PSTOL1. Therefore, we decided two approaches to ascertain the targets for PSTOL1- Firstly, by screening yeast library for potential transcription factors. We have found 13 transcription factors potentially interacting with PSTOL1. Surprisingly, we found that many of these transcription factors and their homologs in rice are not well characterized yet. Secondly, we used Co-immunoprecipitation as a method to investigate the interaction between PSTOL1 and SUMO proteases. This work was started with *N. benthamiana Agrobacterium* transient assays to ascertain a protein-protein interaction between PSTOL1 and OsOTS 11. It was established that these two proteins do not interact. Unfortunately, due to lack of time, the interaction of PSTOL1 with other SUMO proteases could not be further explored.

In conclusion, the work done in this chapter suggests that mutating SUMO sites in PSTOL1 can abolish its SUMOylation and its autophosphorylation activity (in-vitro phosphorylation assay). However, not much is known about how these two post-translational modifications

interplay to regulate the PSTOL1 mechanism as no such targets are known of PSTOL1 yet till now. Whilst there is still much work required to determine the targets of PSTOL1, the initial experiment of yeast two hybrid screening described in this thesis has identified potential targets of PSTOL1. The next step will be to verify the interactions *in-planta*. The plasmid of potential interactors of PSTOL1 will be isolated from yeast clones and subsequently subcloned into the plant expression vector system to confirm the interaction by co-immunoprecipitation. Parallelly, the interaction can also be verified by Bimolecular fluorescence complementation (BiFC).

Chapter 4

Characterization of Os*PSTOL1* gene in *Arabidopsis* using a transgenic approach

4.1 Introduction:

Inorganic phosphate (Pi) is a macroelement indispensable for plant growth and development as it is an important element for nucleic acids, photosynthesis and respiration, ATP, phosphorylated and dephosphorylated intermediates in various reactions and phospholipids (Wang et al., 2021, Crombez et al., 2019). The plant can only take up phosphate from the soil as inorganic phosphate, but it is usually complexed with metal ions such as iron or aluminium or converted by microbial activity or form a water-insoluble compound or taken up by soil matrices which makes it difficult for plants to absorb it (Wang et al., 2021, Crombez et al., 2019). As a result, Pi fertilizers are also very ineffective because only 10%-25% of Pi from fertilizers is taken up by plants and the rest of the phosphate is bound to iron or aluminium in the soil. The high sorption tendency of phosphate to particles in the soil causes poor distribution and low mobility of phosphate available to plants (Peret et al., 2014). The limitation of phosphate greatly affects the crop yield in over 60% of the world's fertile land. Therefore, a profound grasp of the regulatory mechanisms of P signalling and sensing in plants is the first

step for improving crop P use efficiency but there many information gaps in studying crops exist even now. Hence, it is crucial to study molecular responses under Pi deficiency in *Arabidopsis* because of its shorter generation time and limited requirement of growth facilities. The knowledge acquired from studying molecular mechanisms in *Arabidopsis* can help in resolving and explaining several research problems in economically important crops such as rice.

Adaptive strategies of *Arabidopsis thaliana* to cope with Pi deficiency are well-documented in the literature. The strategies can be roughly classified into three main categories: 1) Developmental responses such as modulating primary root length, length/density of root hair and lateral roots and crown root angle (in the case of crops). This adaptation of root system architecture promotes a shallower root system which helps plants forage topsoil where phosphate tends to be present in the soil. 2) Physiological responses include activation of Pi transporters responsible for remobilization and translocation of Pi uptake, relocation of Pi from source to sink and recovering Pi from phospholipids. 3) Biochemical responses involve higher secretion of RNases, phosphatases, and organic acids (Gutiérrez-Alanís et al., 2018).

The above responses to low Pi are attributed to two separate signalling pathways in response to Pi starvation. These pathways are known as local and systemic responses to Pi starvation. Change in the external level of Pi initiates local responses in plants such as changes in the Root System Architecture (RSA). Modulation of RSA involves inhibition of primary root length, enhancement in the number and length of root hairs and lateral root density. If internal Pi levels are low, then responses include the activation of a large set of genes involved in increased Pi uptake and improved P use efficiency. These responses are known as systemic responses (Gutiérrez-Alanís et al., 2018). Understanding fundamental molecular mechanisms underpinning Pi starvation responses using fast-cycling *Arabidopsis thaliana* as a model plant, will allow rapid translation of new findings in crop plants (Krämer et al., 2015)

4.1.1 Local responses: Adaptations of RSA under low Pi

Low Pi inhibits primary root (PR) growth in *Arabidopsis*. This is because of reduced cell elongation and cessation of cell division activity which ultimately results in the exhaustion of root meristematic activity (Gutiérrez-Alanís et al., 2018, Péret, et al., 2014). *Low Phosphate root 1/2* (LPR1/2) protein co-localizes with *Phosphate Deficiency Response 2* (PDR2) in the endoplasmic reticulum (ER) of root tips to establish an inhibitory effect on primary root under low Pi. Auxin signalling also plays a key role in the regulation of primary root growth in Pi starvation (Péret et al., 2014 and Fang et al., 2009). Parallelly with PR growth retardation, low Pi stimulates LR initiation through increased auxin sensitivity by enhancing the expression of auxin receptor TIR1 in the pericycle cells (Ham Kook et al., 2018) which results in more lateral root emergence and initiation (Péret et al., 2014). Moreover, it had been studied well that root hair growth is influenced due to local changes in phosphorus regardless of the Pi status of the plant. In response to low phosphorus concentration, root hair length and density are increased logarithmically (Bates and Lynch et al., 1996). Previous reports showed that auxin and ethylene signalling affects root hair development, however, some contradictory reports also exist. According to Muday et al., 2012 and Rahman et al., 2002 auxin is required for root hair elongation but there is also an indirect effect of ethylene on root hair elongation. Auxin response mutants- *axr2*, *axr 3* and *aux1* displayed reduced initiation of root hair. On the other hand, ethylene response mutant *ein2-1* mutant does not show any significant reduction in root hair initiation. But double mutant *aux1 ein2* shows a considerable decrease in root hair initiation when compared to either single mutant. However, Masucci and Schiefelbein, 1996 showed that neither the ethylene response mutant nor the auxin response mutant shows any effect on root hair initiation.

4.1.2 Systemic responses: Adaptation through phosphate utilization and mobilization

Hydrolases such as ribonucleases and acid phosphatases release inorganic phosphate (Pi) from organic sources. *Arabidopsis* has 29 Purple acid phosphatases (PAPs) and releases Pi from organic material either from internal reserves or into the soil, depending upon their localization (Kavka et al., 2021). Under Pi starvation conditions, ribonucleases (RNases) also play an important role in mobilizing Pi from RNA. For example, AtRNS1 and AtRNS2 are RNases that are involved in the mobilization of Pi from intracellular or extracellular RNA sources under low Pi, senescence or wounding conditions (Fang et al., 2009). Another adaption to low Pi is

the release of organic acid (OAs) such as citric acid act as chelators species (Al^{+3}, Ca^{+2} and Fe^{+2}) which are bound to Pi and facilitates its release into roots (Panchal et al., 2021).

4.1.3 Systemic responses: Adaptation through phosphate transport

Another approach by which plants improve performance in Pi starvation conditions is by increasing the expression of high-affinity transporters (HATs). *Arabidopsis* encodes 19 PHT genes and the genome of rice encodes 16 PHT genes which include HATs, low-affinity transporters (LATs) and constitutively expressed transporters. PHTs are classified into five different classes – PHT1, PHT2, PHT3, PHT4 and PHT5. In *Arabidopsis*, PHT1 is active under low Pi, whereas the other four are active at high Pi concentrations (Prathap et al., 2022).

4.1.4 Regulators of phosphate signalling are under tight regulation by post-translational modification

Emerging studies on Phosphate starvation responses (PSR) showed the importance of PTMs such as SUMOylation in regulating PSR. Miura et al., 2005 demonstrated that SUMO E3 ligase (AtSIZ1) modulates root architecture under low Pi where *siz1* displayed exaggerated Pi starvation responses such as inhibition of length of the primary root, increase in lateral root and root hair number, greater root/shoot ratio and increased anthocyanin accumulation although intrinsic Pi level in WT and *siz1* plants were similar. Various proteins involved in phosphate starvation responses are SUMOylated by AtSIZ1 and this is the only SUMO ligase in *Arabidopsis* involved in phosphate stress responses. AtPHR1, a master regulator to maintain nutrient homeostasis in *Arabidopsis* plants, is a target of AtSIZ1 (Miura et al., 2005 and Sega et al., 2019). Other targets of AtSIZ1 are AtLPR1 and AtLPR2 respectively which control responses in root when external Pi changes. Miura et al., 2010 also showed the upregulation of auxin-induced genes in the *siz1* mutant. This could suggest a link between SUMO E3 ligase and the auxin pathway. In 2018, Orosa et al. established that ARF7 is rapidly SUMOylated and PHR1 is a target of both ARF7 and ARF19. *PHR1* expression decreased in mutants of ARF7 and ARF19 which was further validated by the phenotypic data of mutants. *arf7*, *arf19* and *arf7arf19* showed hyperaccumulation of anthocyanin in shoots and defective Pi uptake in roots

(Huang et al., 2018). These studies showed the emerging role of SUMOylation in phosphate signalling in *Arabidopsis* and perhaps in the future this knowledge can readily be transferred to different crops.

We previously established that OsPSTOL1 is SUMOylated in rice (**Figure 5.8, Chapter 5**) and this is important for root development. Given the importance of PSTOL1 in rice we wanted to ascertain its role in the model plant *Arabidopsis* and identify any conserved molecular mechanisms, however, PSTOL1 is not present in the genome of *Arabidopsis thaliana*. The objective of this chapter is to investigate whether PSTOL1 can confer low Pi tolerance in *Arabidopsis* like in rice. In this study, I overexpressed under the constitutive CaMV 35S promoter both PSTOL1 and non-SUMOylatable version of PSTOL1 protein in *Arabidopsis* to get more in-depth knowledge on the effect of PSTOL1 in Pi-induced root system architecture changes. This study may lead to more rapid identification of PSTOL1 substrates which can pave the way to generating stress-resilient crops. To determine the role of SUMOylation of PSTOL1 in *Arabidopsis*, plant expression constructs of PSTOL1 WT and PSTOL1$^{2K/R}$ were made and transform in *Arabidopsis* Col-0 plants. These transgenic lines were then analysed for Pi responses in high and low Pi.

4.2 Creation of *Arabidopsis* stable transformation constructs

In *Arabidopsis*, the gene or protein will be referred as *PSTOL1 WT* /*PSTOL1$^{2K/R}$* and PSTOL1WT/PSTOL1$^{2K/R}$ in this chapter. The full-length *PSTOL1 WT/ PSTOL1$^{2K/R}$* gene was amplified using NEB Q5 polymerase. It was already cloned into the pDTOPO entry clone and sequenced to confirm the sequence of PSTOL1 WT and SUMO site mutations in PSTOL1$^{2K/R}$. The gene constructs (*PSTOL1 WT* and *PSTOL1$^{2K/R}$*) were sub-cloned upstream of YFP in the gateway destination vector pEARLYGATE 104 using Gateway LR clonase. The vector has an enhanced CaMV 35S promoter to drive gene expression with an N-terminal YFP tag. These

constructs were transformed into *Agrobacterium* strain *GV3101* and positive colonies were checked by two sets of primers - gene-specific (**Figure 4.1 A**) and vector-specific-gene-specific fusion primers (**Figure 4.1 B**).

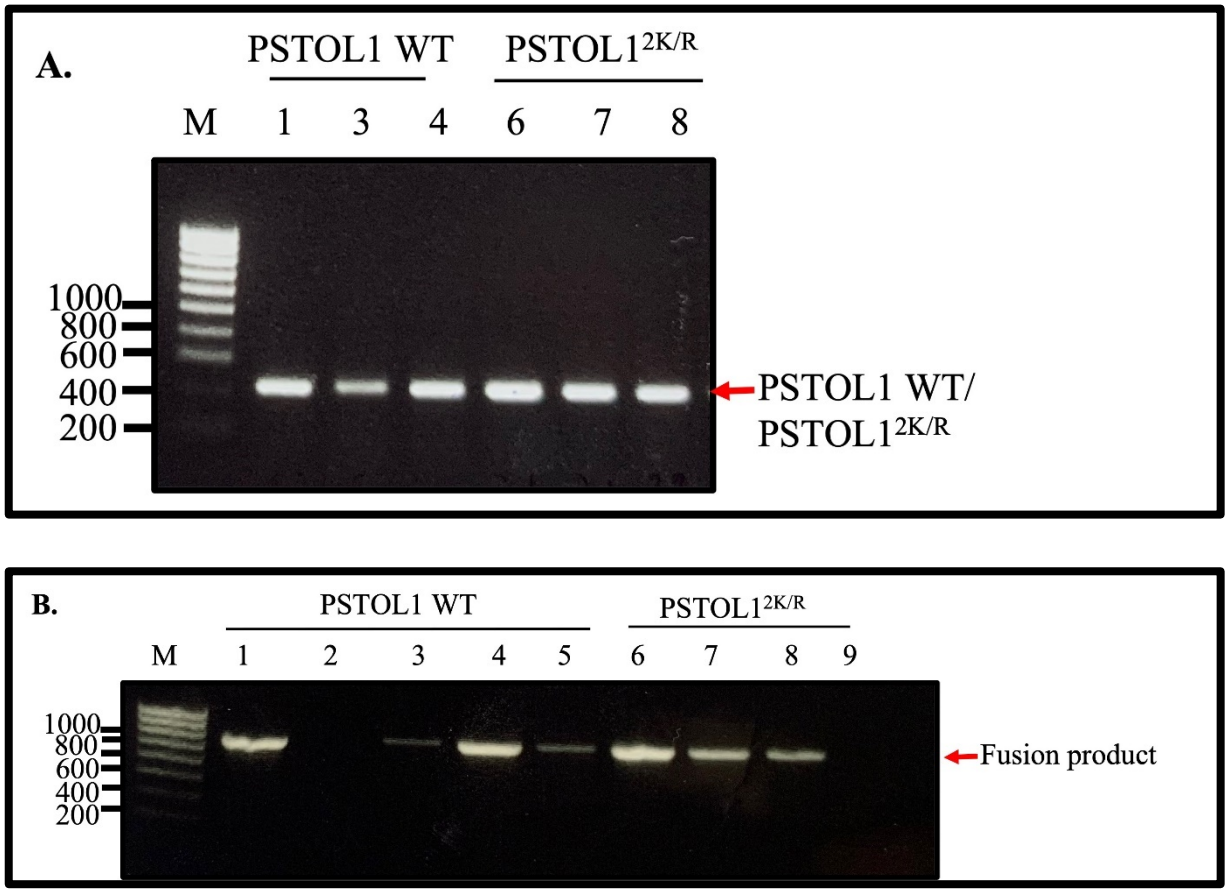

Figure 4.1: pEG104 *PSTOL1 WT* and *PSTOL1 2K/R* constructs transformed into *Agrobacterium* strain *GV3101*.

Image of DNA gel showing amplification of positive colonies from *Agrobacterium*. Two different sets of primers were used to test positive colonies. (A.), shows PCR amplification of product size at 400bp using gene-specific primers. (B.), The figure shows the amplification of products at 875bp using gene-vector specific primers.

The *Agrobacterium* construct was transformed into *Arabidopsis* plants using the floral dip method (Clough and Bent 1998). Transformed plants (T1) were selected on soil with Glufosinate (BASTA) treatment. *Col-0* seeds were used on BASTA selection as a negative control. The selected plants (**Figure 4.2**) were carefully picked out of the soil and transferred into fresh soil with no selection and grown under long-day conditions. Around 60 transgenic lines from *PSTOL1 WT* construct and 20 transgenic lines from *PSTOL12K/R* were obtained after BASTA selection. Alongside these two constructs, the YFP vector alone was also dipped which will act as a negative control for experimentation. The seeds were collected from each individual plant separately.

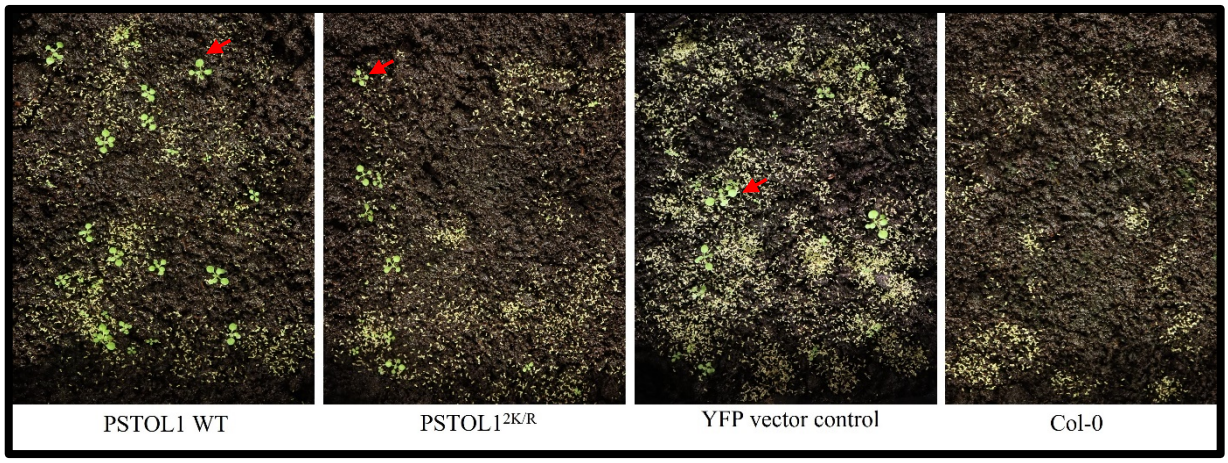

Figure 4.2: Identification of transformed *Arabidopsis* lines generated using floral dip protocol.

Seeds were harvested from a mother plant after floral dipping of each genotype and were put on soil supplemented with BASTA and stratified at 4°C for 3 days. The seeds were then transferred to the growth room after 3 days. Seeds of *Col-0* were used as negative controls for selection. The BASTA solution was replaced after 2-3 days to keep the soil moist. The figure shows the growth of plants after 20 days on BASTA selection. After 20 days, the seedlings were carefully transferred to the soil without selection and were allowed to set seed.

T2 generation seeds were again selected on ½ MS plate supplemented with BASTA (20mg/ml) to identify lines showing a Mendelian ratio of 3:1 or single copy insertions. Individual seedlings were transferred to soil and seeds were collected from each individual plant for determining homozygosity. The seeds were again selected on ½ MS plates with BASTA selection and lines

showing 100% survival were used for further experiments. The presence of the transgene was confirmed by PCR. Further, the primary selection of independent lines for checking transgene expression and protein levels was based on their similar phenotype on BASTA plates at T2 generation. The next step was to confirm the expression levels of a minimum of 3 independent transgenic lines – PSTOL1 WT 2-1, PSTOL1 6-8, PSTOL1 16-2, PSTOL1$^{2K/R}$ 4-1, PSTOL1$^{2K/R}$ 7-8 and PSTOL1$^{2K/R}$ 8-1 by real-time qPCR. Total RNA was extracted from 10-day old seedlings grown on ½ MS agar media and cDNA was synthesised. At least two transgenic lines showing a similar level of expression per construct were further analysed (**Figure 4.3**).

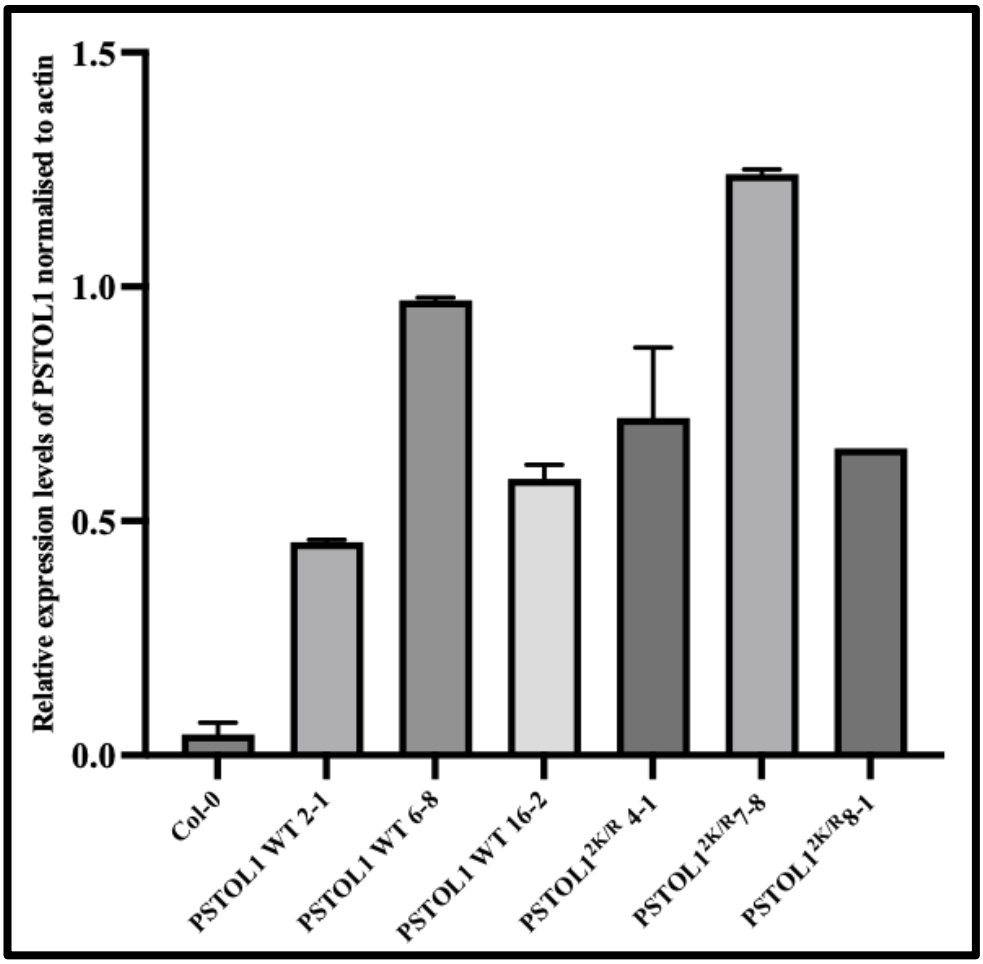

Figure 4.3: Analysis of *PSTOL1 WT* and *PSTOL1$^{2K/R}$* gene expression in homozygous independent *Arabidopsis* transgenic lines analysed by Real-time PCR.

PSTOL1 WT/PSTOL1$^{2K/R}$ expression was analysed in 10 days old seedlings relative to actin as a housekeeping gene. Total RNA was isolated from 10-day-old seedlings of all independent lines from each genotype and cDNA was prepared from the RNA by reverse transcription. The cDNA was diluted

in a 1:5 ratio and resulted in cDNA being used as a template for qRT-PCR Error bars representing SEM of expression except PSTOL1$^{2K/R}$ 8-1 because technical replicate values were close to each other.

Expression analysis from **Figure 4.3** revealed that transgene expression in PSTOL1 16-2 and PSTOL1$^{2K/R}$ 4-1 were comparable. Similarly, mRNA levels in the other two transgenic lines - PSTOL1 WT 6-8 and PSTOL1$^{2K/R}$ 7-8 were similar. However, low level of non-specific expression was seen in *Col-0*, which probably due to the low - specificity of primers or high cDNA concentration in the sample.

Parallelly, to ensure the phenotype observed in the transgenic lines was due to the expression of PSTOL1 protein, the levels of proteins were analysed by western blotting (**Figure 4.4**). PSTOL1 WT 6-8 and PSTOL1 WT 16-2 lines show a similar level of protein which can also be confirmed by loading controls as shown in **Figure 4.4**. PSTOL1$^{2K/R}$ 7-8 and PSTOL12$^{K/R}$ 4-1 show much weaker protein expression than other transgenic lines even though the loading control is similar. However, this may be due to the extraction technique. Total Protein was also extracted from *Col-0* seedlings as negative controls and YFP protein from isolated from YFP transgenic lines seedlings was a positive control for immunoblot analysis by αGFP antibodies.

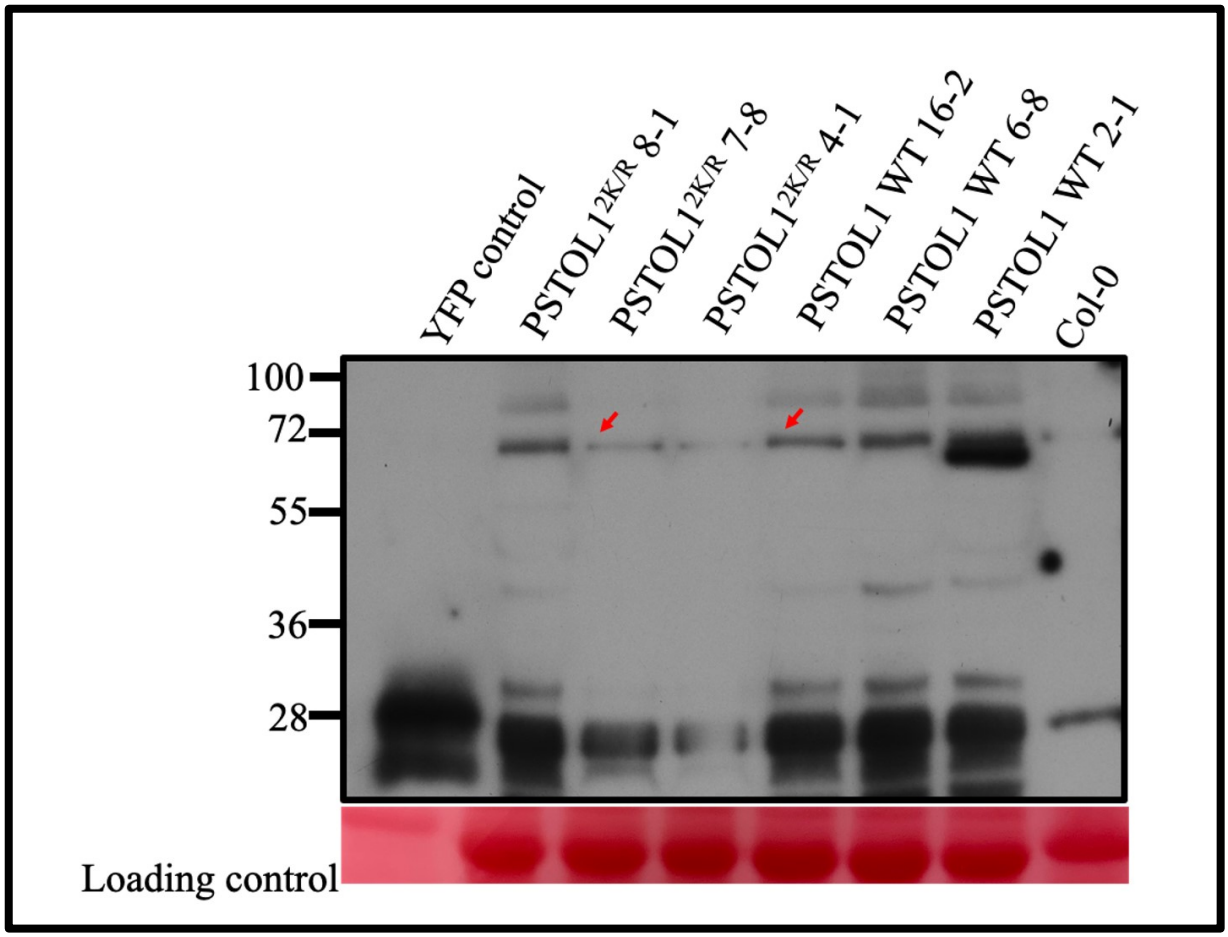

Figure 4.4: Analysing the PSTOL1 WT and PSTOL1$^{2K/R}$ protein levels in overexpressing PSTOL1 WT and PSTOL1$^{2K/R}$ transgenic lines.

Western blot analysis showing the protein levels in each independent line of 35S::PSTOL1 WT and 35:: PSTOL1$^{2K/R}$. 10 days old *Arabidopsis* seedlings were used to extract total protein using 1x laemmli sample buffer in 1:1 ratio and subjected to SDS-PAGE analysis. The proteins were transferred to the PVDF membrane and immunoblotted using αGFP antibodies. The protein band of PSTOL1 kinase was seen in both PSTOL1 WT and PSTOL1$^{2K/R}$ independent lines (shown by red arrow) but the band corresponding to PSTOL1 kinase in absent from Col-0 and YFP control. *Col-0 Arabidopsis* seedlings without PSTOL1 insertion (empty vector) were utilised as a negative control. 30µl of total protein was loaded on SDS-PAGE.

Data from **Figures 4.3** and **4.4** demonstrated that PSTOL1 WT 6-8, PSTOL1 WT 16-2, PSTOL1$^{2K/R}$ 4-1 and PSTOL1$^{2K/R}$ 7-8 were chosen for further phenotypic analysis. The result also suggests that mRNA levels will not always correlate with protein levels because overall

protein levels in PSTOL1$^{2K/R}$ 4-1 and PSTOL1$^{2K/R}$ 7-8 transgenic lines are reduced. There could be two plausible reasons: First, levels of protein in PSTOL1$^{2K/R}$ 4-1 and PSTOL1$^{2K/R}$ 7-8 transgenic lines are low probably because of the extraction technique. Secondly, changes in protein abundance could be due to post-translational regulation which cannot be seen at the mRNA levels.

4.2 Localisation of N-terminal YFP tagged PSTOL1 WT and PSTOL1$^{2K/R}$ in *Arabidopsis* seedling roots

Additionally, subcellular localisation of PSTOL1 was determined to ascertain whether SUMO site mutation altered the localisation of PSTOL1 in *Arabidopsis* seedlings both in roots and leaves. The localisation was observed using a fluorescence microscope Zeiss 880. 7-day-old seedlings were grown on ½ MS media and root samples were carefully placed on a microscope slide for imaging. Perfluoroperhydrophenanthrene (PP11) solution was used for mounting the root sample on a microscope slide to improve the resolution of images. Expression of PSTOL1 WT 16-2, PSTOL1$^{2K/R}$ 7-8 and YFP were analysed in root tip, apical meristem and elongation zone of transgenic lines.

A. PSTOL1 WT 16-2

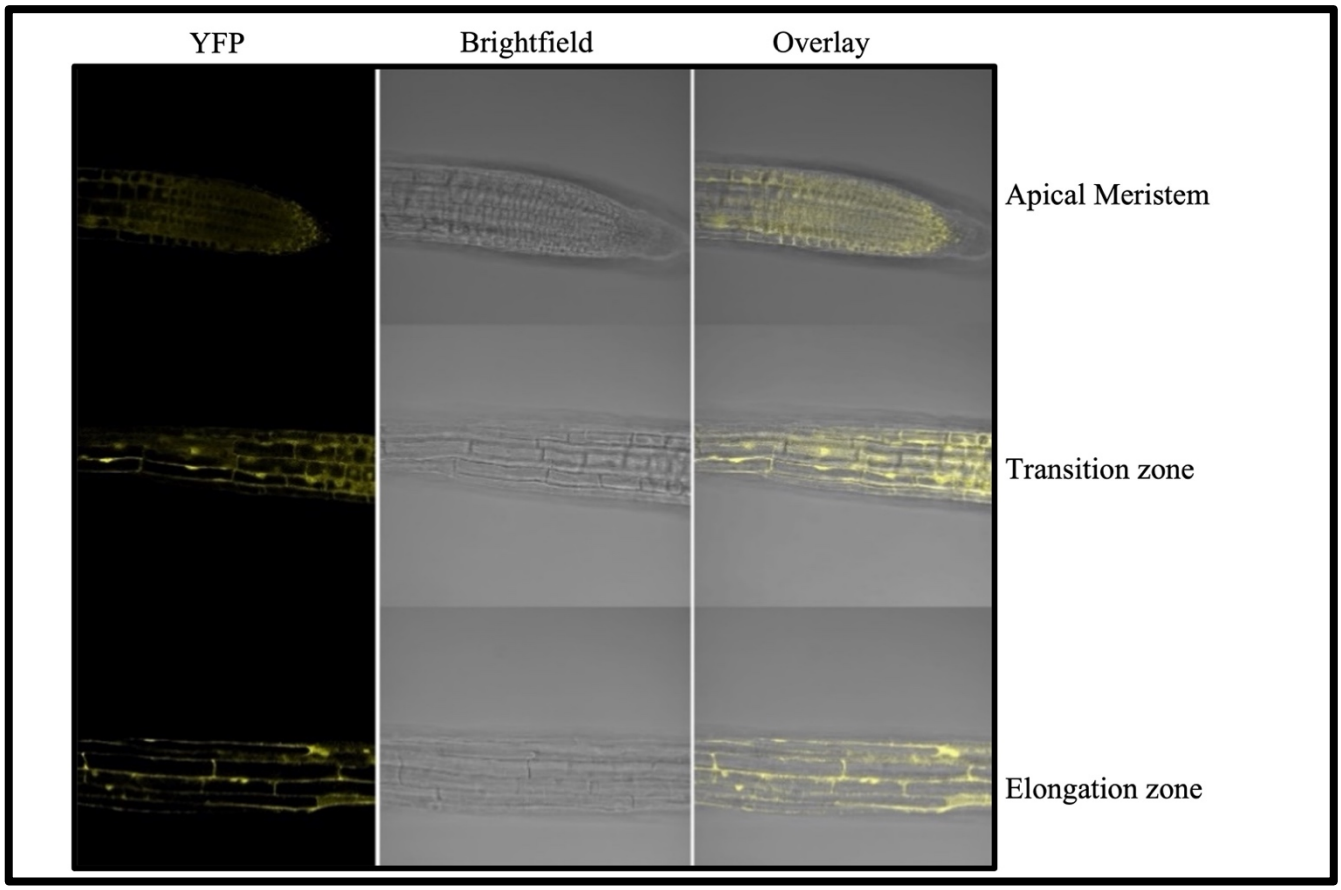

B. PSTOL1$^{2K/R}$ 7-8

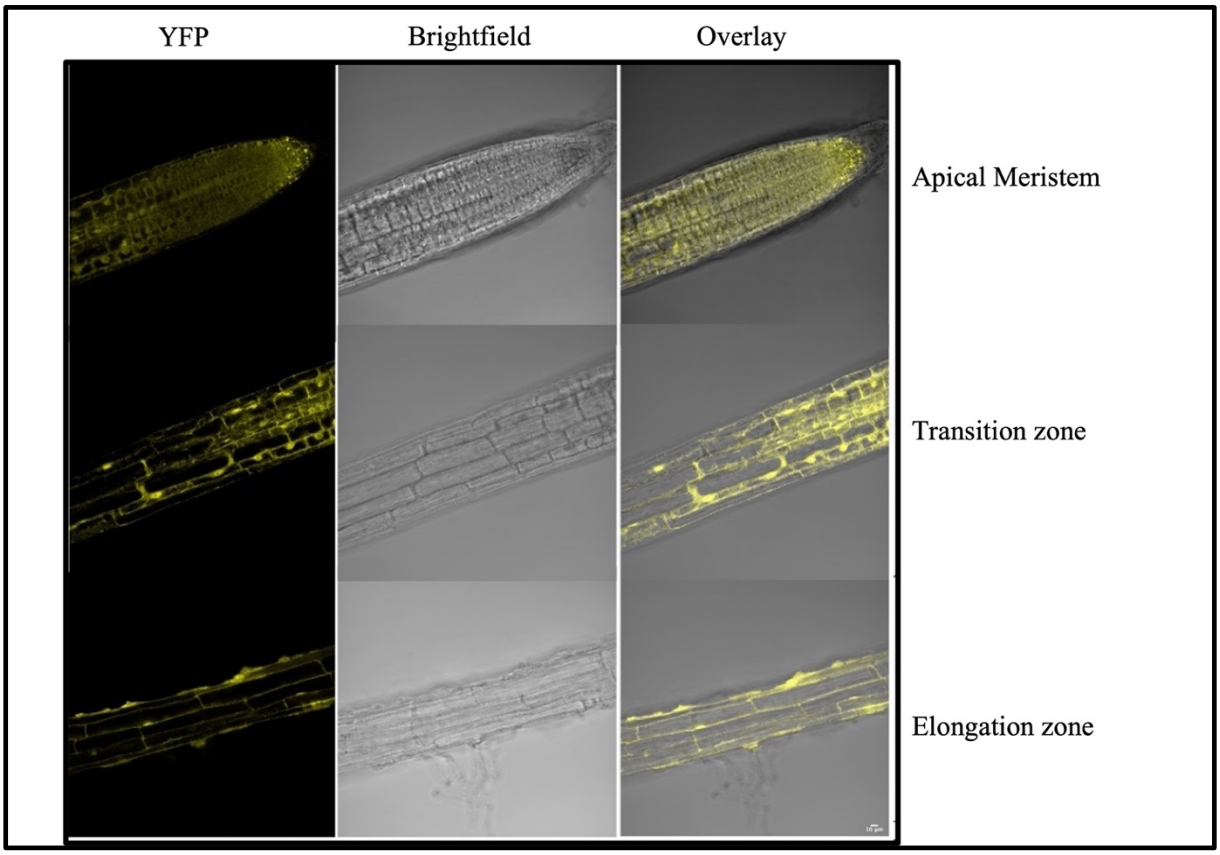

C. YFP vector only

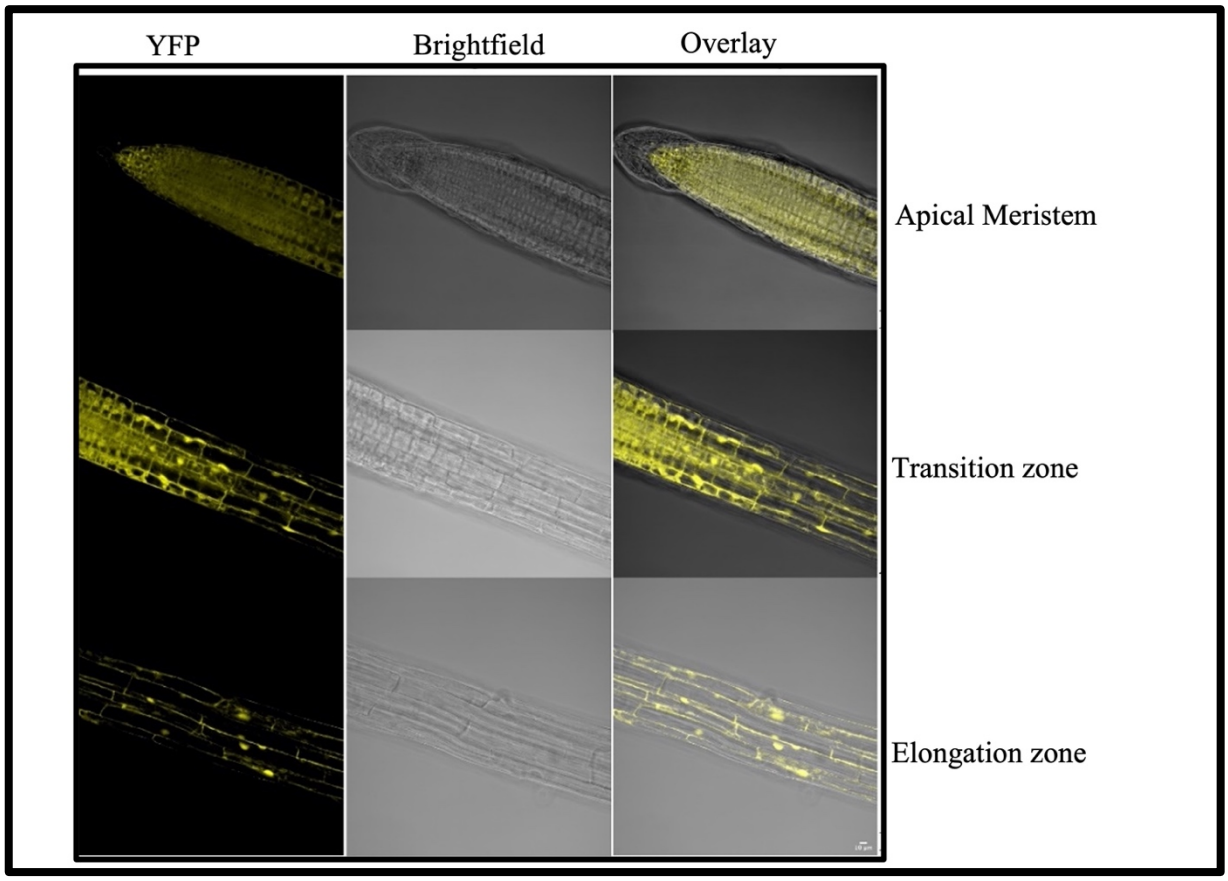

Figure 4.5: Confocal images of 7-day-old transgenic 35S::YFP-PSTOL1 WT 16-2, 35S::YFP- PSTOL1$^{2K/R}$ 7-8 and YFP vector.

N-terminal YFP tagged PSTOL1 WT 16-2, PSTOL1$^{2K/R}$ 7-8 and YFP vector control localised in the nucleus and cell membrane when stably expressed in roots of *Arabidopsis* seedlings. The localization was analysed by Zeiss LSM 880 confocal laser scanning microscope using a 60 × 1.4NA lens and using laser excitation at 514 nm and emission filters 524-580 nm. **A**. PSTOL1 WT 16-2 **B**. PSTOL1$^{2K/R}$ 7-8 **C**. YFP vector control. 7-day old seedlings were mounted on microscope slides using PP11. Scale bar = 10µm.

Localization of PSTOL1 WT 16-2, PSTOL1$^{2K/R}$ 7-8 and YFP vector in the root tip and apical meristem can be seen in both the nucleus and cell membrane or cytoplasm. However, we observed a difference in the pattern of localization of PSTOL1 WT 16-2 and PSTOL1$^{2K/R}$ 7-8 when compared to YFP vector control in the elongation zone. YFP alone can be seen in both

the nucleus and cell membrane in cells of the elongation zone but there is a decrease in nuclear localization of PSTOL1 WT and PSTOL1$^{2K/R}$. However, a ratiometric quantification of fluorescence in the nuclear/cytoplasm or cell membrane will confirm this finding. Moreover, change in cellular localization of PSTOL1 WT and PSTOL1$^{2K/R}$ was checked in leaves of lines overexpressing PSTOL1 WT/ PSTOL1$^{2K/R}$ transgenic lines.

4.3 Localisation of N-terminal YFP tagged PSTOL1 WT 16-2 and PSTOL1$^{2K/R}$ 7-8 in *Arabidopsis* seedling leaves

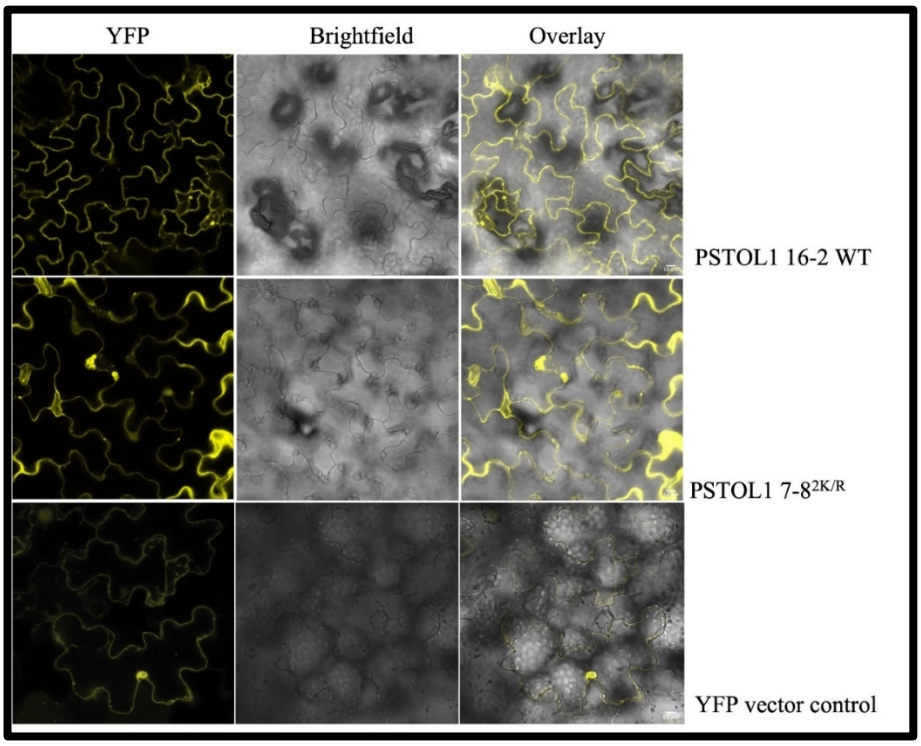

Figure 4.6: N-terminal YFP tagged PSTOL1 WT, PSTOL1$^{2K/R}$ and YFP vector control localised in the nucleus of cells and cell membrane/cytoplasm when stably expressed in leaves of *Arabidopsis* seedlings.

7-day old seedlings were mounted on microscope slides. Strong expression of both PSTOL1 WT and PSTOL1$^{2K/R}$ can be seen in the nucleus and cell membrane of the cells. The localization was analysed by Zeiss LSM 880 confocal laser scanning microscope using a 60 × 1.4NA lens and using laser excitation at 514 nm and emission filters 524-580 nm. Scale bar = 10µm.

Figure 4.6 showed no difference in the localisation of PSTOL1 WT and PSTOL1$^{2K/R}$ in *Arabidopsis* leaves. The expression of PSTOL1 WT and PSTOL1$^{2K/R}$ was like vector control. The reason there was no difference observed with vector control in expression of both PSTOL1 WT and PSTOL1$^{2K/R}$ in leaves and roots probably because PSTOL1 WT/PSTOL1$^{2K/R}$ transgene expression is constitutively driven under CaMV 35S promoter. To exclude the possibility that observed YFP-tagged PSTOL1 WT/PSTOL1$^{2K/R}$ localization pattern is not because of YFP vector only, the protein from respective lines (PSTOL1 WT 16-2/ PSTOL1$^{2K/R}$ 7-8) was immunoprecipitated and was checked using western blotting (**Figure 4.7**). Immunoprecipitation assay confirmed YFP-tagged PSTOL1 WT/ PSTOL1$^{2K/R}$ protein expression and therefore we can correlate those confocal images of PSTOL1 WT/ PSTOL1$^{2K/R}$. Although YFP-tagged PSTOL1 WT/ PSTOL1$^{2K/R}$ shows similar localization like YFP vector control, however, western blot shows the band of YFP tagged PSTOL1 WT/PSTOL1$^{2K/R}$ and YFP vector alone at expected size which indirectly indicates that confocal images of YFP alone and YFP-tagged PSTOL1 WT/ PSTOL1$^{2K/R}$ can be seen because respective proteins (**Figure 4.5** and **4.6)**.

Parallelly we also analysed the SUMOylation status of YFP-PSTOL1 WT and YFP-PSTOL1$^{2K/R}$ in *Arabidopsis* transgenics lines. To begin with, the expression of immunoprecipitated YFP-PSTOL1 WT and YFP- PSTOL1$^{2K/R}$ was analysed on SDS-PAGE (**Figure 4.7**). The bands corresponding to YFP-PSTOL1 WT and YFP- PSTOL1$^{2K/R}$ was seen at 64.4kDa size. Micro column used for immunoprecipitating YFP protein was unfortunately clogged and due to high back pressure for elution there was not binding between protein and αGFP beads and therefore expression of YFP only cannot be observed.

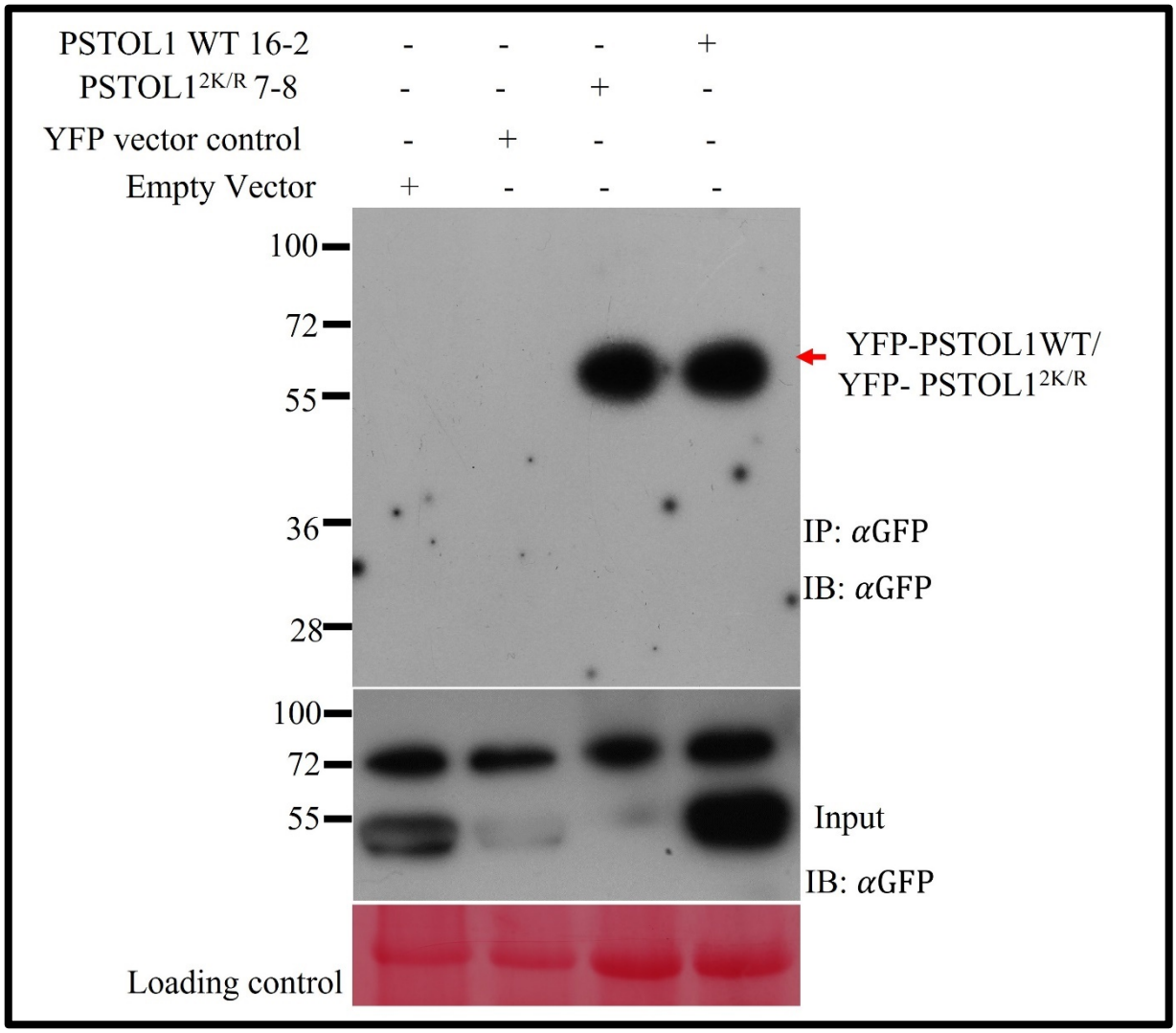

Figure 4.7: Immunoblot analysis showed the protein expression of YFP-PSTOL1 WT and YFP- PSTOL1$^{2K/R}$ in *Arabidopsis* transgenic lines.

Immunoblot analysis of immunoprecipitation experiments of PSTOL1 WT, PSTOL1$^{2K/R}$, YFP vector control and Col-0 (negative control) was carried out with αGFP beads. 10-days old seedlings were grown on ½ MS media and tissue was weighted and flash frozen in liquid N_2. Protein extract was subjected to immunoprecipitation (IP: αGFP) with αGFP immunoaffinity beads followed by immunoblot analysis anti-GFP antibody (IB: αGFP) to confirm the expression of PSTOL1 WT/PSTOL1$^{2K/R}$. RuBisCO was used as loading control.

Finally, we wanted to analyse the SUMOylation status of YFP-PSTOL1 WT and YFP-PSTOL1$^{2K/R}$ in *Arabidopsis* seedlings overexpressing PSTOL1 WT and PSTOL1$^{2K/R}$ protein

respectively. **Figure 4.8** shows SUMO conjugated YFP-PSTOL1 WT around 64.4kDa (indicated by red arrow) while SUMO conjugated YFP- PSTOL1$^{2K/R}$ was significantly reduced. Since, the protein expression of YFP tagged PSTOL1 WT and PSTOL1$^{2K/R}$ was the same when probed with anti-GFP antibodies in IP lane (**Figure 4.7**), we can confirm that mutation of lysine to arginine significantly reduced the level of SUMOylation of PSTOL1$^{2K/R}$ in *Arabidopsis* seedlings. However, SUMOylation status was not tested in other PSTOL1 WT and PSTOL1$^{2K/R}$ transgenic lines.

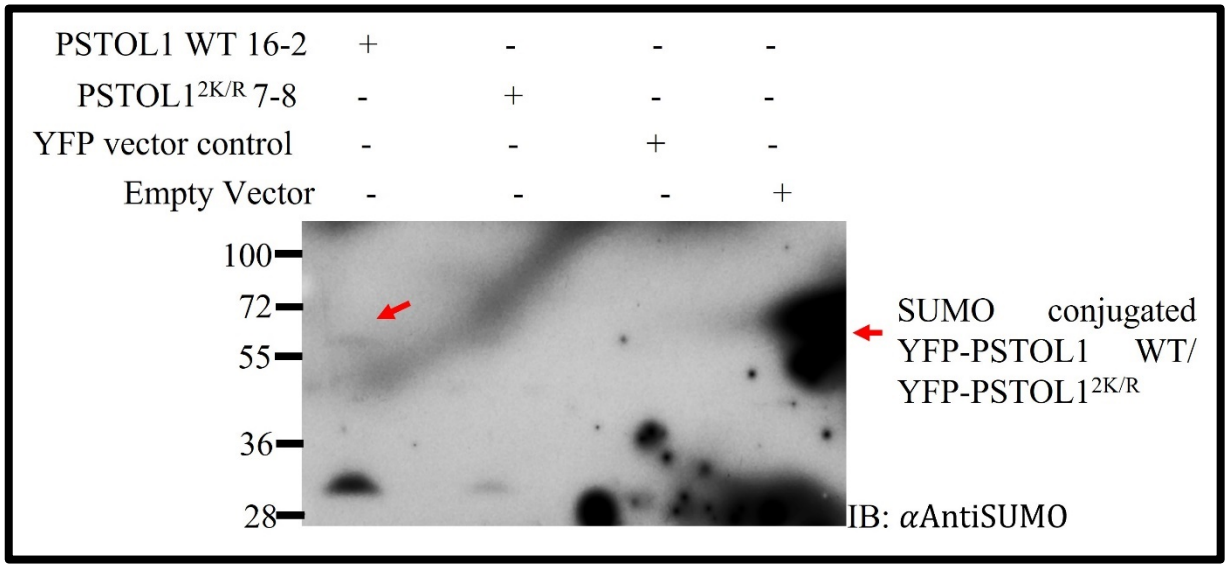

Figure 4.8: Immunoblot analysis showed mutation of the two Lysines to Arginines in PSTOL1$^{2K/R}$ reduces SUMOylation in Arabidopsis seedlings.

Immunoblot analysis of immunoprecipitation experiments of PSTOL1 WT, PSTOL1$^{2K/R}$, YFP and Col-0 (negative control) was carried out with αGFP beads. AntiSUMO1 antibody was used to detect SUMO conjugated protein (IB: αAntiSUMO). SUMO-conjugated PSTOL1 WT can be seen in the IP lane of PSTOL1 WT while the reduced/abolished SUMOylation can be seen in the IP lane of PSTOL1$^{2K/R}$. The red arrow indicates the SUMO conjugated YFP-PSTOL1 WT at an expected size of 64.4kDa.

4.4 Standardizing the Phosphate treatment condition on Col-0 plants

Once the SUMOylation status of PSTOL1 was confirmed in *Arabidopsis* seedlings, our next step was to analyse the phenotype of plants expressing PSTOL1 WT and PSTOL1$^{2K/R}$ under different phosphate concentrations. From previous studies, it is apparent that primary root growth is inhibited in low Pi. We chose primary root length as a major parameter for standardizing the phenotyping of Arabidopsis plant responses to different concentrations of phosphate. We performed a pilot experiment to examine the impact on *Arabidopsis* root growth at high and low phosphate concentrations, which we can use as a basis to analyse PSTOL1 *Arabidopsis* transgenics.

The strategy was to employ different phosphate concentrations as shown by Huang et al., 2018, Bhosale et al., 2018, Miura et al., 2005 and Dong et al., 2017. A few studies also showed the various strength of MS medium for their studies. For instance, Huang et al., 2018 studied the phenotype of *Arabidopsis* root growth on full-strength MS while Dong et al., 2017 did the phenotypic analysis on ½ MS media. Therefore, we decided to choose 2mM, 1.25mM, 0.625mM, 312µM, 12.5µM, 10µM, 3µM and no phosphate conditions to study the primary root length on both ½ MS and full-strength MS medium.

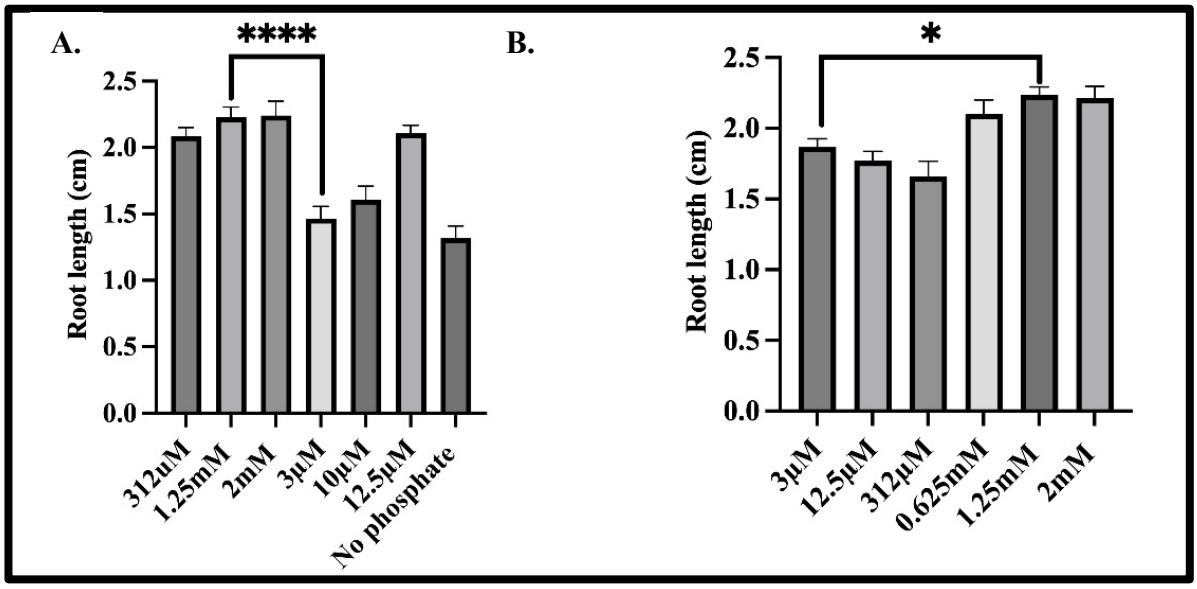

Figure 4.9: Quantification of root growth inhibition in Col-0 seedlings on various phosphate concentrations (A.) With Full Strength (B.) With half strength.

Four-day-old seedlings of Col-0 were transferred to full strength MS and half strength MS and were grown for additional 11 days before root lengths were measured. Data are averages $\pm$ SEM (n = 21 each). One way ANOVA determined a statistical significance between Col-0 seedlings on 1.25mM and 3µM phosphate concentration. * Indicates a statistically significant difference ($P \leq 0.05$-0.0001)

From this experiment, it was determined that 1.25mM as high phosphate concentration and 3µM as low phosphate concentration based on root growth inhibition. These concentrations were then used to analyse the difference between Col-0, PSTOL1 WT and PSTOL1$^{2K/R}$ *Arabidopsis* transgenics lines on full strength MS.

4.5 Analysis of transgenic *Arabidopsis* plants overexpressing PSTOL1 WT and PSTOL1$^{2K/R}$

4.5.1 Characterization of PSTOL1 in *Arabidopsis* plants response to phosphate starvation

As described above, 1.25mM and 3µM were used as high and low phosphate concentration respectively for analysing the impact of PSTOL1 WT and PSTOL1$^{2K/R}$ function in *Arabidopsis*. Two independent lines of the PSTOL1 WT and PSTOL1$^{2K/R}$ with similar transcript (**Figure 4.3**) and protein levels (**Figure 4.4**) were analysed and chose for further experimentation. Col-0, PSTOL1 WT 6-8, PSTOL1 WT 16-2, PSTOL1$^{2K/R}$ 4-1, PSTOL1$^{2K/R}$ 7-8, and YFP only controls were germinated on ½ MS plates and grown under long day conditions for 4 days. After 4 days of germination, the seedlings were transferred to MS plates with high (1.25mM) and low (3µM) phosphate concentration respectively and were grown under long day light conditions for 11 days (**Figure 4.11**). Under differing phosphate treatments, primary root length, lateral root density, lateral root per plant and biomass of seedlings were measured.

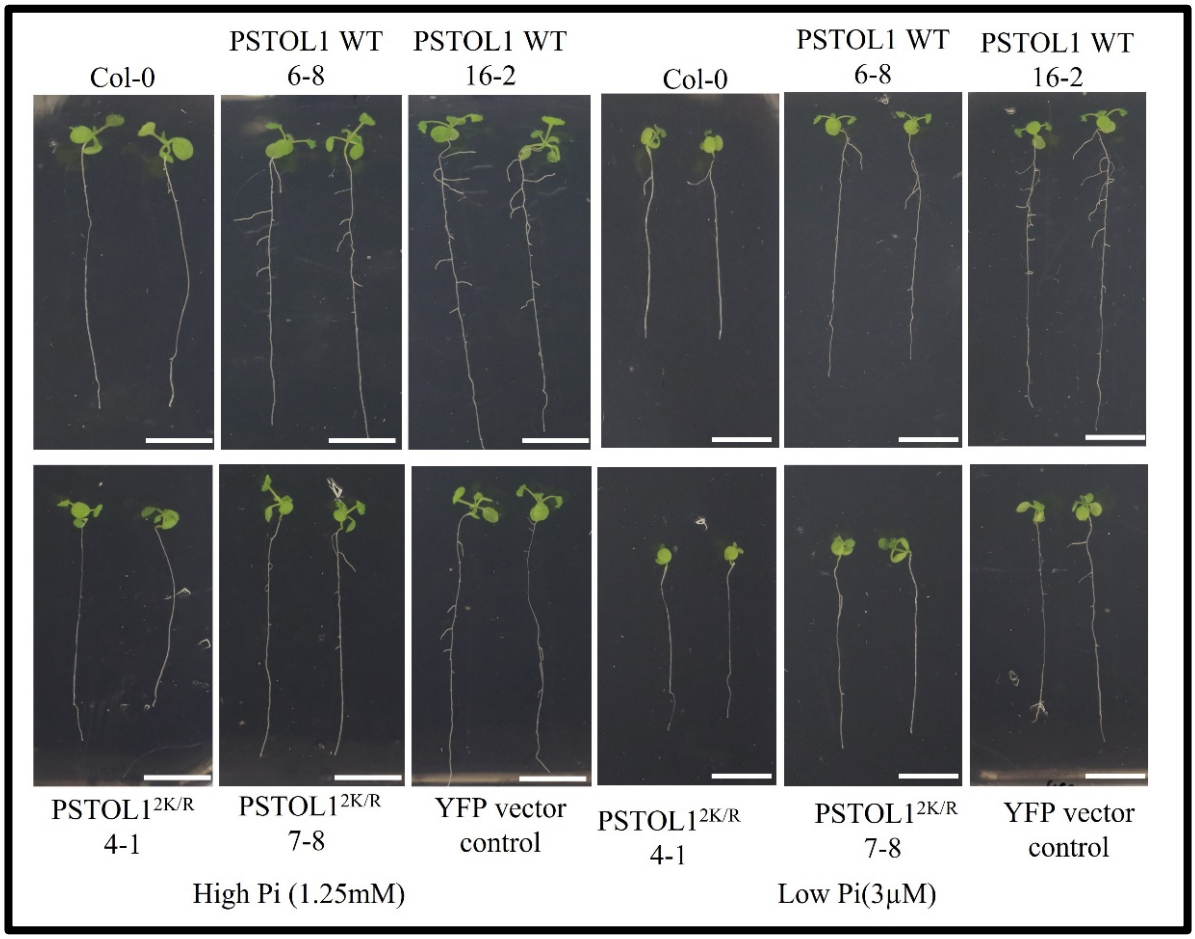

Figure 4.10: Analysis of the morphology of wild-type and PSTOL1 transgenic lines under high Pi (1.25mM) and low Pi (3µM).

Representative images of 11-day-old seedlings grown on high Pi (A.) and low Pi (B.) on vertically oriented MS agar plates. Approximately 40-50 seedlings were transferred to MS media supplemented with different phosphate concentration, 1.25mM (high phosphate) and 3µM (low phosphate) from ½ MS media after 4 days. Photographs were taken after 11 days to analyse the different parameters – primary root length, lateral root density, lateral root per plant and fresh weight biomass. *Col-0* and YFP vector control were taken as negative controls. Scale bar = 1cm.

To understand the effect of low Pi conditions, we examined primary root length, lateral root density, lateral root per plant and fresh weight biomass of seedlings (**Figure 4.11**). The data suggest that overexpression of PSTOL1 WT in *Arabidopsis* results in reduced sensitivity to Pi deficiency by improving root growth compared to wild-type, *Col-0* and PSTOL1$^{2K/R}$ seedlings (**Figure 4.10**).

A. Primary root length

All transgenic lines showed a significant increase in primary root length when compared to *Col-0* seedlings in high phosphate concentration media (**Figure 4.11 A**). Under low Pi conditions, we observed that Col-0 seedlings exhibited inhibition of primary root length which is well-documented in the literature (Miura et al., 2005). This represents here that the experimental setup works well. PSTOL1 WT expression improves primary root length irrespective of Pi status, while we observed that more reduction in PSTOL1$^{2K/R}$ overexpressing transgenic lines under low Pi where the same pattern can be observed in *Col-0*. The percentage of primary root growth inhibition was 21.2% observed in *Col-0* seedlings under low Pi when compared to high Pi whereas primary root growth reduction in PSTOL1$^{2K/R}$ seedlings was seen between 22.7% - 29%. However, inhibition of primary root length under low Pi was not observed compared to high Pi in overexpressing PSTOL1 WT transgenic lines and in fact these transgenic lines displayed a 2.1% - 5.3% increase in primary root length in low Pi than high Pi.

B. Lateral root density and lateral root per plant

The lateral root density was calculated by dividing the lateral root number by the length of the primary root length. This is an important step to consider while calculating because it is necessary to normalize the treatment effect on the length of the primary root. The result (**Figure 4.11 B** and **4.12**) showed that low Pi availability accelerated the formation of lateral roots in PSTOL1 WT *Arabidopsis* transgenic lines. PSTOL1 WT probably acts partially irrespective of Pi supply because we observed that there is no reduction in lateral root density. Conversely, overexpressing PSTOL1$^{2K/R}$ seedlings exhibited a higher density of LR when compared to *Col-0* under high Pi but showed a decrease in lateral root density under low Pi as same trend was observed in the wild-type *Col-0* seedlings. The percentage decrease in lateral root density is 10-22% in PSTOL1$^{2K/R}$ seedlings while in *Col-0* only a 3.5% decrease was observed (**Figure 4.11 B**).

On the other hand, lateral roots per plant were calculated and we observed an 8-9% decrease in lateral root number in PSTOL1 WT transgenic lines whereas *Col-0* seedlings exhibited a 22% reduction under low Pi. Interestingly, overexpressing PSTOL1$^{2K/R}$ transgenic lines showed considerable reduction ranging in lateral roots per plant from 12% to 35% under Pi-starved conditions (**Figure 4.11 C**).

C. Fresh weight biomass

We observed Pi starvation also affects the overall growth of the plant. The result indicates that the fresh weight of PSTOL1 WT transgenic lines was slightly decreased ranging from 4% - 4.8%, whereas PSTOL1$^{2K/R}$ exhibited a reduction between 19.1% - 26.2% under Pi-starved conditions. Meanwhile, the marked decrease (37.9%) in the overall growth of plants was seen in *Col-0* under -Pi conditions (**Figure 4.11 D**).

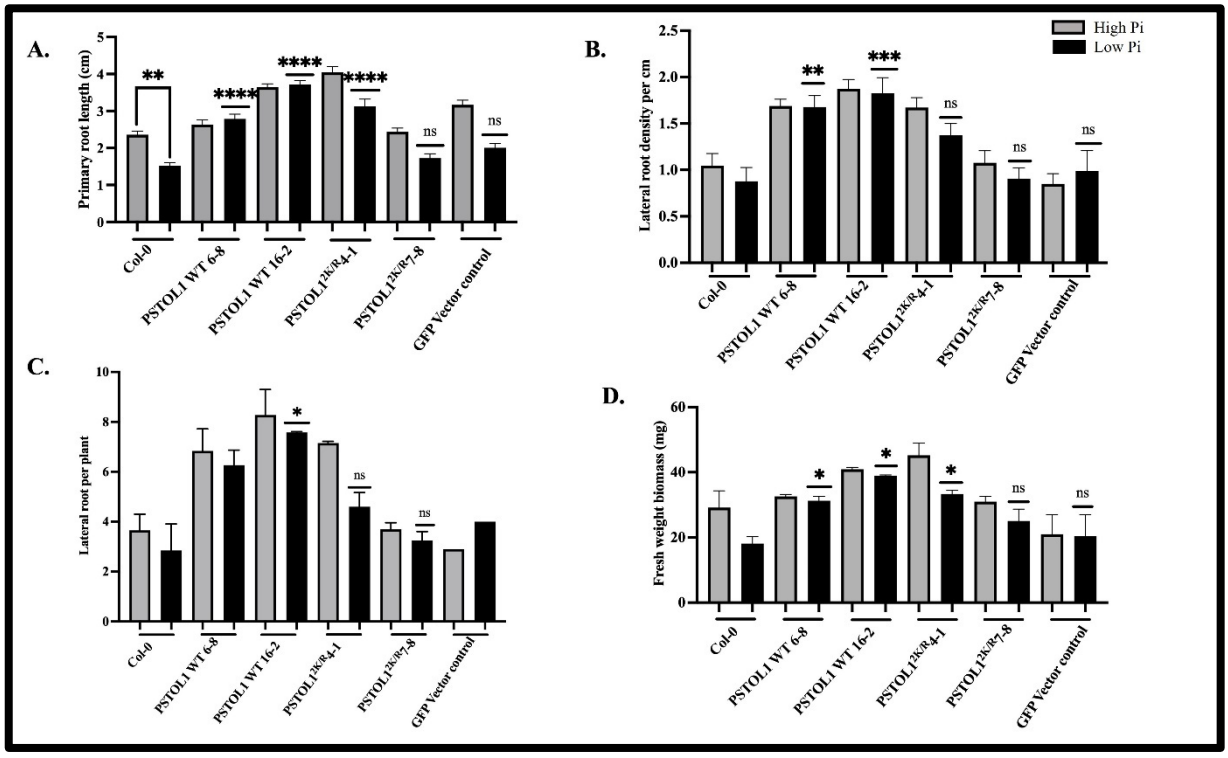

Figure 4.11: Quantification of root length, lateral root density, lateral root per plant and fresh weight biomass of *Col-0*, PSTOL1 16-2, PSTOL1$^{2K/R}$ 4-1, PSTOL1$^{2K/R}$ 7-8, YFP vector control on high (1.25mM) and low phosphate (3µM).

Four-day-old seedlings of different genotypes were transferred to MS with high (1.25mM) and low phosphate (3µM) and grown for additional 11 days until primary root length, lateral root density, lateral root per plant and fresh weight biomass were measured. (A.) Primary root length was measured after 11 days on MS media. (B.) and (C.) 11 days old seedlings were used to measure lateral root density and lateral root per plant. (D.) The fresh biomass of 11 seedlings was measured after being grown on MS media. Data was analysed relative to the growth of *Col-0* on high and low phosphate. Data are averaged $\pm$ SEM (n = 40-50). One-way ANOVA determined a statistical significance between the groups for analysing primary root length and lateral root density. * Indicates a statistically significant difference compared with wild-type subjected to low Pi treatment (Col-0) ($P \leq 0.05$-0.0001). Student t-test was used to determine statistical significance between transgenic lines with *Col-0* seedlings subjected to low phosphate treatment. * Indicates a statistically significant difference ($P = 0.01$).

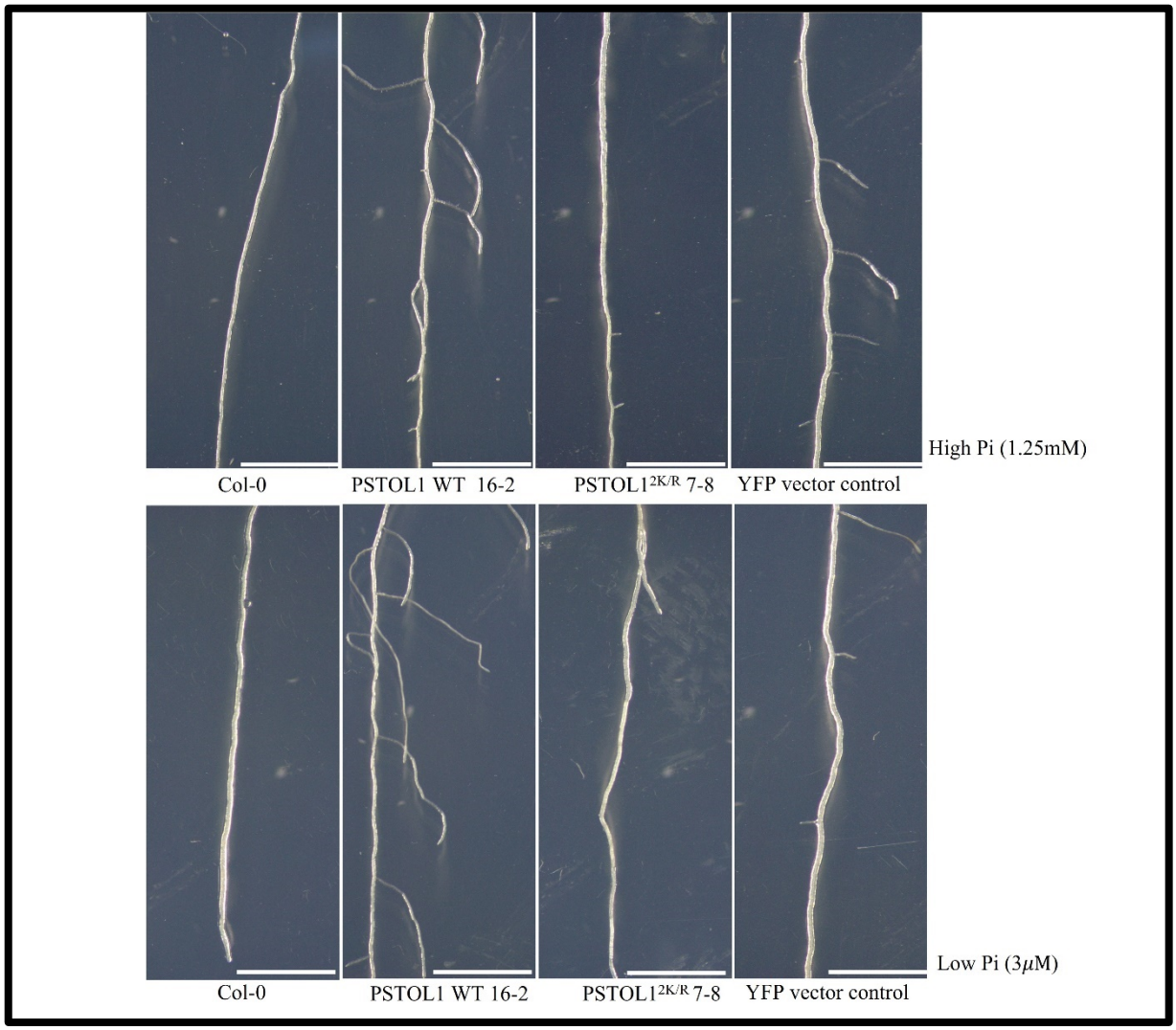

Figure 4.12: A representative white light images of all the genotypes grown under high and low Pi.

A representative white light image of 11-day-old seedlings of different genotyped root grown high and low Pi MS agar plates indicating lateral root development of *Col-0*, PSTOL1 WT, PSTOL1$^{2K/R}$ and YFP vector control when grown on high (1.25mM) and low Pi (3µM). The white light images were taken on a stereomicroscope with an integrated HD camera. Scale = 1cm.

4.5.2 Analysis of root gravitropism in overexpressing PSTOL1 WT and PSTOL1$^{2K/R}$ *Arabidopsis* seedlings

The limitation of phosphorus in soil is known to induce alterations in root system architecture. Changes in RSA maximize nutrient uptake and therefore, this is an important parameter to

study. Recently, studies on root growth angle (RGA) or root gravitropism showed that it is a necessary parameter of RSA because shallower roots (larger RGAs) are known to improve phosphate uptake from the topsoil (topsoil foraging). Root gravitropism is the orientation of root growth towards gravity (Wang et a., 2018). Seeing the importance of root gravitropism in low Pi conditions, we chose to analyse PSTOL1 WT and PSTOL1$^{2K/R}$ *Arabidopsis* transgenic lines on ½ MS for a gravitropic response on high and low Pi. The *Col-0*, PSTOL1 WT 6-8, PSTOL1 WT 16-2, PSTOL1$^{2K/R}$ 4-1, PSTOL1$^{2K/R}$ 7-8, YFP only vector control seeds were sterilized and using a sterile scalpel the seeds were transferred to ½ MS media with 1% sucrose. The seeds were placed in a row and vernalized in the dark at 4°C for 3 days (Muller et al., 2018). After vernalization, the plates were transferred to 22°C and plates were placed vertically. Seedlings were grown vertically for 5-7 days on ½ MS plates and then turned at an angle of 90° for 24 hours. The photographs were taken after 24 hours to record the change in the angle of root tips. The images were analysed to measure root bending by ImageJ software. The root bending angle was measured as shown in **Figure 4.13** for every seedling.

Figure 4.13: Quantification of root gravitropic curvature using Image J software.

Figure 4.14 and **4.15** shows that after 24 hr of gravistimulation, 44.7% of Col-0 showed bending between 90°-120° while PSTOL1 transgenic lines revealed a different pattern. 70% PSTOL1 WT seedlings shows bending angle between 90°-120° while 81.25% PSTOL1$^{2K/R}$ seedlings displayed faster response to gravity stimulus. We also observed that 10% of Col-0 seedlings showed a bending angle between 60°-90° while this pattern was also seen in PSTOL1$^{2K/R}$ seedlings (4%-11%). Interestingly, quantification in **Figure 4.15** revealed that this pattern was not seen in PSTOL1 WT transgenic seedlings. Further analysis also revealed that there is a gradual decrease in the frequency of seedlings of PSTOL1$^{2K/R}$ (8% - 13%) while PSTOL1 WT (27% - 31%) and Col-0 (44.7%) showing a root angle between 120°-150°.

Unfortunately, due to the fewer number of seeds available for YFP vector control, the result obtained may not be conclusive. Therefore, the experiment has to be repeated again with the same number of seeds for all genotypes.

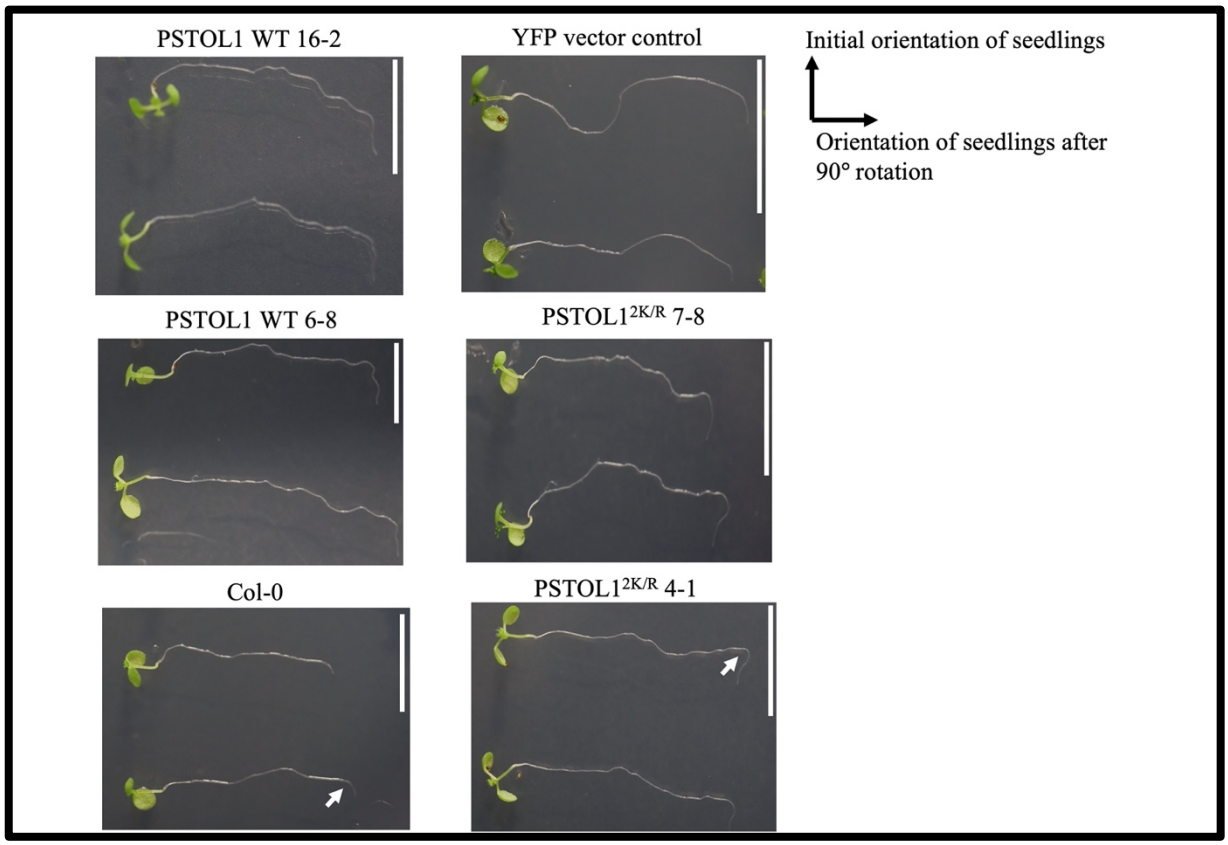

Figure 4.14: Representative image of comparison of root gravitropic response of 7-day-old seedlings of *Col-0*, PSTOL1 WT, PSTOL1$^{2K/R}$ seedlings and YFP vector control.

Comparison of root gravitropic response of 7-day-old seedlings of Col-0, PSTOL1 WT PSTOL1$^{2K/R}$ and YFP vector control seedlings. Sterilised seeds were transferred by a sterile scalpel to ½ MS plates + 1% sucrose. The seeds were stratified at 4°C in dark for 3 days and subsequently, plates were transferred to light where seedlings were allowed to grow for 5-7 days before gravity stimulus. Plates were turned by 90° and kept in the dark for 24hr. Root bending is shown here at 24hr rotation of vertically grown seedlings. Scale bare = 1cm.

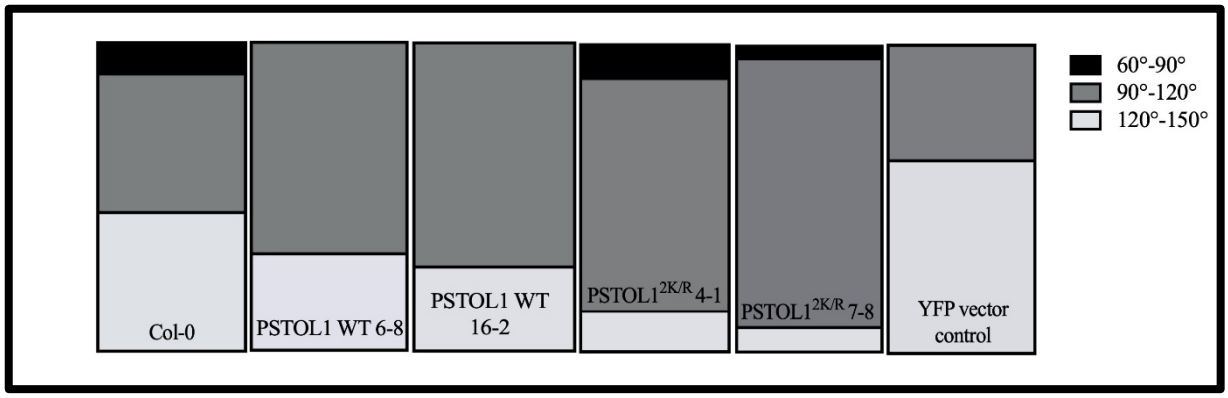

Figure 4.15: Quantification of root gravitropic curvature of *Col-0*, PSTOL1 WT 6-8, PSTOL1 WT 16-2, PSTOL1$^{2K/R}$ 4-1 and PSTOL1$^{2K/R}$ 7-8.

Seeds were sterilised and transferred to ½ MS with a 1% sucrose plate. The seedlings were allowed to grow for 5-7 days after vernalization and turned 90° for 24 hours. Root curvature was measured using FIJI software.

4.6 Discussion

Plant fitness is improved through a change in RSA under Pi depletion. As a result, the plant reduces root depth growth by cessation of primary root length in *Arabidopsis*(Crombez et al., 2019). On the other hand, modulation in RSA also involves root branching such as increased lateral root and root hairs densities which impacts the spatial configuration of the root system to acquire low mobility Pi from the topsoil, a strategy referred to as 'topsoil foraging' (Miura et al., 2011). More lateral roots results in an increased number of root tips. Despite the smaller surface of root tips, they account for approximately 20% of the total Pi uptake.

Here, in this chapter, the functional characterization of PSTOL1 WT and PSTOL1$^{2K/R}$ was further investigated by expressing the proteins in a heterologous system, *Arabidopsis thaliana*. Transgenic lines overexpressing PSTOL1 WT, PSTOL1$^{2K/R}$ and YFP only vector control was generated, and these lines were analysed for their response under high and low Pi. To begin with, real-time analysis of *PSTOL1 WT* and *PSTOL1$^{2K/R}$* gene expression was tested in atleast 3 independent transgenic lines and furthermore, PSTOL1 WT and PSTOL1$^{2K/R}$ protein

expression was also analysed on western blot. The results from **Figures 4.3** and **4.4** suggest that PSTOL1 WT 6-8 and PSTOL1 WT 16-2 has similar protein levels when compared to PSTOL1 WT 2-1. Further detailed analysis also showed that PSTOL1 WT 6-8 has more protein then PSTOL1 WT 16-2 which shows a reasonable correlation with mRNA levels in **Figure 4.3**. Analysis of transgene expression also revealed that PSTOL1$^{2K/R}$ 4-1 and PSTOL1$^{2K/R}$ 8-1 have comparable transcript levels but based on western blot analysis in **Figure 4.4**, the protein levels are not the same. So, PSTOL1$^{2K/R}$ 4-1 and PSTOL1$^{2K/R}$ 7-8 independent lines were chosen based on western blot results for further experimental analysis. The next step was to ascertain the SUMOylation status of PSTOL1 WT and the non-SUMOylated version of PSTOL1 (**Figures 4.7** and **4.8**). GFP antibody detection showed YFP-PSTOL1 WT and YFP-PSTOL1$^{2K/R}$ levels were similar in immunoprecipitated lanes (**Figure 4.7**). Further, *Arabidopsis SUMO1*-specific antibodies displayed SUMO conjugation to YFP-PSTOL1 WT whereas SUMO conjugation was reduced in YFP- PSTOL1$^{2K/R}$ (**Figure 4.8**). A similar pattern of SUMOylation of YFP-PSTOL1 WT and YFP- PSTOL1$^{2K/R}$ was observed in *N.benthamiana* (Chapter 3, **Figure 3.11**). Therefore, the data from *N.benthamiana* substantiated our data in *Arabidopsis*. Due to time constraints, the phosphate-dependent SUMOylation status of PSTOL1 WT and PSTOL1$^{2K/R}$ in *Arabidopsis* seedlings was not explored. Following the analysis of SUMOylation status in transgenic lines, Col-0 seedlings were grown in different phosphate concentrations and different strengths of MS media to standardize experimental conditions for analysing the PSTOL1 transgenic lines impact on plant growth in low Pi. We compared primary root growth, lateral root density, lateral root number per plant and fresh weight biomass of Col-0, PSTOL1 WT, PSTOL1$^{2K/R}$ and YFP vector control transgenic lines in high Pi and low Pi conditions. This Pi concentration-dependent analysis indicated that PSTOL1 WT positively impacts overall plant growth under high and low Pi. We observed that PSTOL1 WT transgenic lines under the 35S constitutive promoter displayed improved performance than wild-type Col-0 plants in all four parameters we analysed in response to high and low Pi. Overexpression of PSTOL1 in *Arabidopsis* showed enhanced root growth, more lateral root density, lateral root number and fresh weight biomass than Col-0 plants which provides strong evidence of PSTOL1 acting irrespective of Pi supply which has been substantiated by earlier reports in rice and wheat (Gamuyao et al., 2012 and Kettenburg et al., 2022). However, our research aim was to decipher the role of SUMOylation in the mediating response under low Pi by PSTOL1. The data (**Figure 4.11**) indicates that primary root length was reduced in PSTOL1$^{2K/R}$ transgenic lines nearly to 22.7% - 29% and the percentage of reduction was more than Col-0 and PSTOL1 WT lines suggesting that P starvation does limit

plant growth considerably in PSTOL1$^{2K/R}$ transgenic lines. This phenotype observed in PSTOL1$^{2K/R}$ lines could probably be because of two reasons: either the formation of new cells is reduced in root apical meristem or a significant reduction of cell expansion in the elongation zone or a combination of both. Fresh weight biomass data also showed that there is an increase in biomass of PSTOL1 WT transgenic lines compared to wild-type Col-0 plants under low Pi which suggest that probably there could be increased cell division. But these phenomena might be altered in PSTOL1$^{2K/R}$ transgenic lines (Sánchez-Calderón et al., 2005), thereby suggesting that SUMO might play a critical role in phosphorus deficiency. Another important parameter we analysed was lateral root density and lateral root number per plant. **Figure 4.11 B** and **C** indicate that there is no significant difference in lateral root density of PSTOL1 WT transgenic lines grown under high and low Pi however PSTOL1$^{2K/R}$ transgenic lines showed a reduction in lateral root formation (lateral root density and lateral root number) under low Pi. Previous reports showed *ARF7* and *ARF19* are important genes for lateral root initiation under Pi starvation both in *Arabidopsis*. Cho et al., 2013 showed that phosphorylation of *ARF7* and *ARF19* mediated by BIN2 (BRASSINOSTEROID INSENSITIVE 2) is an essential step to initiate the lateral root organogenesis by increasing the transcription activity of *LATERAL ORGAN BOUNDARIES-DOMAIN16 (LBD16)* and *LATERAL ORGAN BOUNDARIES-DOMAIN29 (LBD29)*. We hypothesize that PSTOL1 being a kinase might be promoting auxin signalling through phosphorylation of *ARF7* and *ARF19*, thereby activating downstream targets involved in lateral root organogenesis. Further, our yeast two-hybrid (**Table 3.1**, chapter 3) data suggest that cytokinin response factors and ethylene response factors can be possible targets of PSTOL1. It is well documented in rice that ARFs regulate Pi starvation responses by regulating cytokinin response factors (Shen et al., 2014). Therefore, another possible hypothesis can be that PSTOL1 phosphorylates the ARFs and phosphorylated ARFs could mediate responses to Pi starvation through cytokinin or ethylene signalling because Y2H screening showed CRF12 and ERF15 as potential targets of PSTOL1. Our previous data from **Figure 3.9** (chapter 3) showed *in-vitro* that mutating SUMO sites would result in the loss of both autophosphorylation and trans-phosphorylation activity of PSTOL$^{2K/R}$. Therefore, PSTOL$^{2K/R}$ is probably not able to phosphorylate downstream targets important for mounting a response under low Pi. Hence, SUMO sites may be important for selectively interacting with substrates which are critical for phosphate starvation responses.

Another important aspect we decided to explore was to determine the role of PSTOL1 in the modulation of root angle. Data from Bai et al., 2013 confirmed that low Pi influence gravitropic

root curvature. Wild-type Col-0 showed a reduction in gravitropic angle in response to low Pi. They also showed altered lateral root angle in *pgm-1* and *pin3-1* mutants in response to high and low Pi. **Figures 4.11** and **4.12** showed that high expression of PSTOL1 WT in *Arabidopsis* enhances overall root growth independent of Pi supply and change in RSA is an important factor to improve Pi uptake. Therefore, we analysed the role of PSTOL1 WT and PSTOL1$^{2K/R}$ growth angle of the primary root under normal conditions. Our data suggest that (**Figures 4.11 and 4.12**), PSTOL1$^{2K/R}$ has reduced overall gravitropic curvature compared to PSTOL1 WT under normal conditions. Further analysis also revealed that a greater proportion of roots of PSTOL1 WT adopted an angle between 120° - 150° than PSTOL1$^{2K/R}$. This data indicates that PSTOL1 WT probably favors a shallow root system which is an important factor for Pi uptake from topsoil (Lynch and brown., 2001). On the other hand, some roots of PSTOL1$^{2K/R}$ and Col-0 adopt an angle between 60° - 90° and none of the PSTOL1 WT roots showed an angle in this range. However, *Arabidopsis* has a tap root system so it is difficult to conclude how these findings will play a role under P starvation. Therefore, the next step will be to analyse the lateral root orientations under different phosphate statuses in *Arabidopsis* and rice.

Taken together, the data in this chapter indicates that SUMOylation of PSTOL1 is essential for regulating phosphate starvation responses by altering root architecture.

Chapter 5

Molecular Characterization of Phosphate tolerance of rice plants expressing modified PSTOL1 gene.

5.1 Introduction

Rice has always been an important staple crop and responsible for one-fifth of the calorie supply globally. Therefore, rice is of great relevance to socioeconomic stability and global food security (Pandey et al., 2010 and Zeigler and Barclay ., 2008). Environmental stresses such as changes in temperature, alterations in water quality, contamination of soil by heavy metals, or nutrient deficiency limit crop productivity. One of the critical issues to address here is the phosphorus nutrition in the soil. Soil contains various forms of phosphate, including organic phosphate and inorganic phosphate (Pi), while plants can only uptake inorganic phosphate (Pi), but its absorption by plants is difficult because of easy chelation of Pi with cations- Ca, Fe and Al, or form organic molecules (Zhang et al., 2014, Hu and Chu ., 2011 and Wang et al., 2018). The application of fertilizers is another way for sustaining crop productivity; however, it also has limitations due to slow diffusion of Pi and its high chemical fixation. Moreover, the increasing cost of fertilizers is a critical issue for poor farmers having limited resources to survive. To overcome Pi limitation, plants have evolved adaptive responses such as remobilization, acquisition and recycling of Pi to maintain homeostasis (Wu et al., 2013, Zhang et al., 2014, Pariasca-Tanaka et al., 2014). Therefore, it is important to study and investigate

the mechanisms for these adaptive responses and the application of this knowledge will help to develop crops to improve P uptake and P use efficiency.

An important QTL was mapped known as *Phosphate uptake 1 (Pup1)* on chromosome 12 from Kasalath, an aus-type rice variety. *Pup1* near-isogenic lines (NILs) were shown to improve phosphorus uptake efficiency more than Nipponbare (Kumari et al., 2017). The *Pup1* locus in Kasalath was sequenced and it showed the presence of a nearly 90-kb transposon-rich insertion-deletion (INDEL) region. When the sequence was aligned with the Nipponbare genome, the entire region was absent from the genome of Nipponbare (Heuer et al., 2009). To understand the function of *Pup1*, candidate genes from this locus were short-listed and the associated transcript levels analysed under low Pi conditions. Further analysis of the qRT-PCR data indicated a novel protein kinase was identified and was named *phosphorus-starvation tolerance 1* (*PSTOL1*). Expression of *PSTOL1* boosted grain yield by 60% under Pi-deficient soil because overexpression of PSTOL1 in rice plants has a bigger root system to improve uptake of Pi from the soil. Specifically, expression of PSTOL1 was confirmed in specific tissue regions from where crown roots begin to emerge (Gamuayo et al., 2012). Nonetheless, the knowledge of the mechanism regulating root architecture in low Pi by PSTOL1 is still very limited in rice. Investigation of changes in root architecture in crops can potentially improve nutrient uptake and nutrient use efficiency. The manipulation of root architecture is termed the "Second Green Revolution" because plants have evolved with a sophisticated mechanism to explore resources from soil (Huang et al., 2018).

5.2 Physiological changes in roots in response to low Pi

Alteration of root architecture is one of the most important adaptions to low Pi by plants because root architecture is extremely plastic in response to differences in phosphate conditions. In rice, to improve Pi uptake and topsoil foraging, plants tend to make shallow root systems, elongate primary root and increase root hair length and density (Pandey et al., 2021).

5.2.1 PR response in rice under low Pi

Unlike *Arabidopsis*, in rice there is a less pronounced effect on PR in low Pi, probably because their seeds have ample amounts of phosphate reserves. In Japonica varieties, PR growth is increased in low Pi, though, data from some reports are contradictory because the difference in experimental conditions and crop cultivators may attribute to differences in results. Not many genes regulating PR development are identified to date. OsPHR2 (homolog of AtPHR1) is an important transcription factor in the Pi starvation mechanism in rice. Overexpression of OsPHR2 stimulates the increased number of roots and enhances root hair proliferation (Hu and Chu., 2011). Another important gene, the *OsMYB4P* gene encoding an R2R3-type MYELOBLASTOSIS (MYB) protein is induced in low Pi and overexpression of this gene will enable plants to increase the length of PR. A closely related MYB transcription factor gene, *OsMYB2P-1* expression is induced in roots when seedlings were grown in Pi deficient media. PR length was longer in overexpressing *OsMYB2P-1* transgenic lines than in the wild-type. Forward genetics has also identified a mutant, *leaf tip necrosis (ltn1)* which showed increased Pi uptake and longer PR when plants are grown in a Pi-deficient medium. Another gene in rice is known as *NUTRITION AND ROOT GROWTH* (*NRR*) and the knockdown of this gene results in improved root growth in rice under low Pi (Huang and Zhang., 2020).

5.2.2 Effect of Pi on crown root formation and angle

Rice developed the strategy for topsoil foraging by enhancing crown root growth and increasing angle to cope with Pi deficient conditions. Crown roots can branch by making more lateral roots and increasing the proliferation of root hairs, thereby, increasing root surface area and root number which is an important strategy for exploring topsoil to increase Pi uptake. Rice MORPHOLOGY DETERMINANT (RMD) expression was negatively correlated with phosphate availability. Expression of RMD is a crucial step for switching between shallow and deep root systems under low- and high-phosphate conditions respectively. In high Pi or normal conditions, *RMD* gene expression was downregulated resulting in the swift movement of statoliths and enhancing the process of gravity-sensing, subsequently causing deep root systems. On the other hand, *RMD* expression is induced in low Pi conditions, resulting in a slow rate of sedimentation of statoliths and a gravity-sensing process, finally forming a shallow root system (Huang and Zhang., 2020). Another well-known gene, *DEEPER ROOTING 1*

(*DRO1*) reduced drought stress to increase grain yield by making more vertical roots. Vertical root distribution will improve water uptake in drought stress, while the *dro1* was associated with shallower rooting, thereby, plants are more susceptible to drought stress (Kitomi et al., 2020). Studies on *RMD* and *DRO1* showed that root gravitropic responses are adapted by abiotic stress conditions. Previous reports on *DEFECTIVE IN OUTER CELL LAYER SPECIFICATION* 1 (*DOCS1*) and *LARGE ROOT ANGLE 1* encoding *OsPIN2* are also regulators for controlling gravitropic responses (Wang et al., 2018 and Bettembourg et al., 2017).

5.2.3 Effect of Pi deficiency on lateral roots formation

Phosphate starvation in rice induces the formation of more lateral roots. *OsIPS1* and *OsIPS2* are two genes that play a crucial role in the initiation and development of lateral roots under low Pi. Under Pi deficiency conditions, expression of these genes is strongly induced in roots, thereby modulating RSA to increase the uptake of Pi (Pandey et al., 2014).

While manipulation of genes involved in the Pi starvation pathway may suggest a solution to improve Pi acquisition and utilization, tracking and identifying genetic variation is also an effective strategy for future crop improvement like *Pup1*.

5.3 Role of post-translational modification in regulating phosphate signalling in rice

Over the last 15 years, the study of PTMs has developed to identify the proteins in plants involved in regulating in responses during abiotic or biotic stresses. In recent years, SUMOylation is considered a versatile process involved in many abiotic and biotic stress responses (Srivastava, et al., 2021). SUMOylation is dynamic in nature and plays a key role in protein stability, localization and activity thereby, making it an important PTMs to investigate its potential application in crop improvement (Prathap et al., 2022 and Clark et al., 2022).

OsSIZ1, an E3 ligase in the SUMOylation pathway, responds to Pi deficiency by modifying the protein that functions downstream of it. Wang et al., 2015 demonstrated that expression of OsSIZ1 was seen in the root system, as well as in root tips, lateral roots and lateral root primordia and regulate the root development. Moreover, the expression of OsSIZ1 regulates the expression of PTs such as *OsPT1*, *OsPT2*, *OsPT3*, *OsPT4*, *OsPT6* and *OsPT8* in both positive and negative, which probably result in an increase in total P and Pi in both roots and shoots when *OsSIZ1* is mutated. Consistent with the findings about AtSIZ1 mediating SUMOylation of AtPHR1 in *Arabidopsis*, two SUMOylation sites were found in *OsPHR2* and mRNA levels of *OsPHR2* is changed when *OsSIZ1* was mutated under high Pi conditions. The data suggest that OsPHR2 acts downstream of OsSIZ1, however, further validation is required. Taken together, there is clear evidence of the key role of SUMOylation in controlling Pi starvation responses in rice.

As mentioned earlier, overexpression of *PSTOL1* in phosphate intolerant modern varieties remarkably increases grain yield in phosphorus-deficient soil. We want to determine if SUMOylation plays a role in regulating the function of PSTOL1 in Pi homeostasis in rice. Our in-silico studies show that *PSTOL1* has two SUMO sites. The lysine residues at the 20^{th} and 225^{th} positions were identified as potential SUMO sites in PSTOL1. We hypothesize that SUMO plays a role in regulating PSTOL1-dependent Pi response mechanisms and hence regulates phosphorus starvation tolerance. We aim to mutate the two predicted SUMO sites in rice *PSTOL1* (**Figure 5.1 A** and **B**) and investigate its effect on phosphorus starvation tolerance in rice.

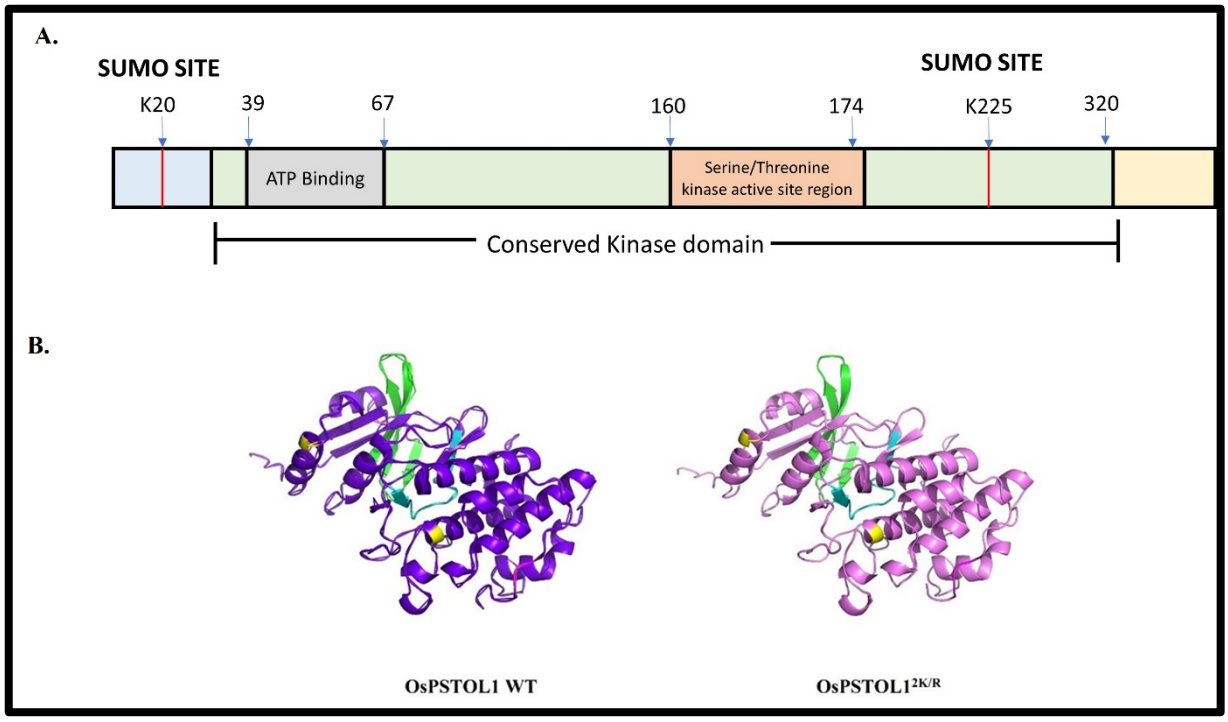

Figure 5.1: Predicted SUMO sites were identified in PSTOL1 using in-silico analysis.

(A). The conserved kinase domain is highlighted in green. The serine/threonine kinase domain is depicted in orange. The grey colour shows the ATP-binding domain and two SUMO sites are highlighted in red. **(B.)** 3D structure of OsPSTOL1 WT and OsPSTOL1$^{2K/R}$ depicting the location of SUMO sites predicted with AlphaFold (Kindly donated by Kawinnat Sue-Ob). The conserved kinase domain is highlighted in purple and pink respectively. The serine/threonine kinase domain is depicted in blue. The green colour shows the ATP-binding domain, and two SUMO sites are highlighted in yellow.

5.4 Generation of ProUBI::OsPSTOL1 WT and ProUBI:: OsPSTOL1$^{2K/R}$ rice transformants (Kindly done by Dr. Cunjin Zhang)

The Coding Sequence (CDS) of OsPSTOL1 WT and SUMO sites mutated version, OsPSTOL1$^{2K/R}$ (generated using a site-directed mutagenesis approach) tagged with C-terminal YFP was subcloned into the binary vector pIPKb002 under the maize ubiquitin promoter-driven. The ubiquitin promoter managed to drive higher transgene expression in monocots than the CaMV 35S promoter, which is known to be active in dicots plant tissues, however, its activity is much lower in monocots (Cornejo et al., 1993 and Wilmink et al., 1995). Both constructs were transformed in *Agrobacterium tumefaciens* strains EHA105 and then

transformed into *O.sativa* cv Nipponbare (NB). T_0 plants were screened for single-copy insertion and 3:1 segregation ratio.

5.5 Screening of ProUBI::OsPSTOL1 transformants

5.5.1 Analysis of the copy number in transgenic rice using real-time PCR

After transformation, analysis of transgenic plants is a crucial step for planning subsequent experiments. Here, we have analysed the single-copy transformants by investigating the genomic insertion of the transgene, also known as copy number. Copy number analysis refers to analyses of the number of transgenes inserted per haploid genome (described in section 2.4.2 of material and methods) (Bubner and Baldwin., 2004). T_0 transgenic plants are usually hemizygous or heterozygous for transgene after transformation. **Figures 5.2 A** and **B** show 30 T_1 plants of each genotype analysed for transgene copy number. Transgenic plants must be characterized properly since multiple transgene insertions (copy number) lead to complex events. Here we analysed copy number of transgenic lines by qPCR using the relative quantification method that determines copy number of a transgene by comparing the transcript level of a transgene (in this case hygromycin) to that of an endogenous reference gene (in this case *Sucrose-Phosphate synthase*, *SPS*) with a determined copy number (Shepherd, C.T et al., 2009, Xiujie, Z et al., 2019). The qRT-PCR analysis confirmed eight and nine independent lines of UBI::ProPSTOL1 WT and UBI::ProPSTOL1$^{2K/R}$ transformants respectively (**Figure 5.2**). The independent lines were allowed to grow and set seeds in a 16/8 hours photoperiod with approximately 70% relative humidity at 28°C.

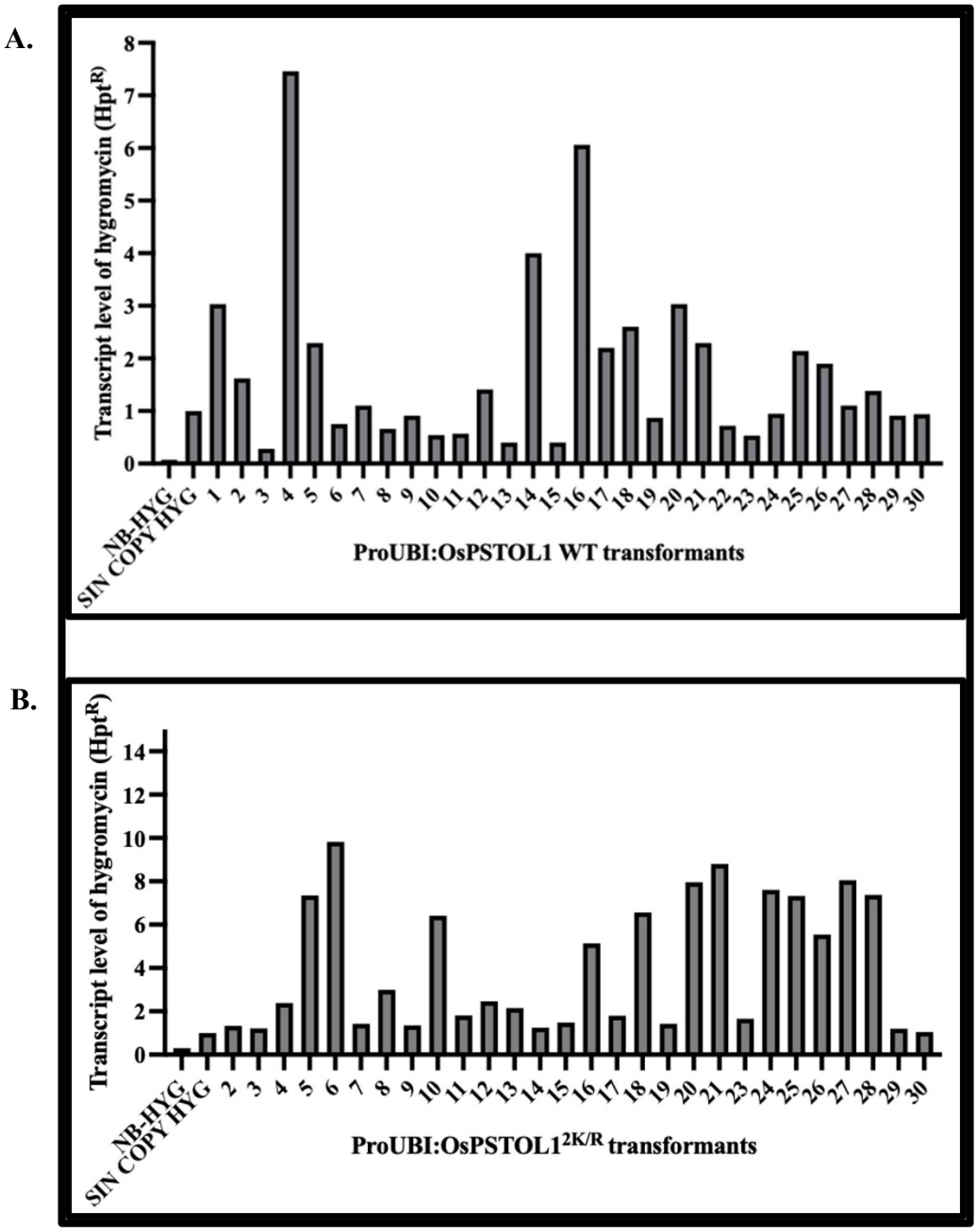

Figure 5.2: Copy number analysis of ProUBI::OsPSTOL1 transformants.

Pure genomic DNA was isolated from rice seedlings. Primers were designed to amplify the Hygromycin gene (Hpt^R) and *Sucrose Phosphate Synthase* (*SPS*) gene to determine the copy number. SIN COPY HYG is a positive control of hygromycin resistance transgenic rice plants with single-copy gene insertion. Nipponbare (NB-HYG) was taken as a negative control without the insertion of the transgene. Transcript analysis was examined by qPCR. (A.) Analysis of ProUBI::PSTOL1 WT transformants. (B.) Analysis of ProUBI::$PSTOL1^{2K/R}$ transformants.

The integration of transgene at a particular locus in the genome is considerably variable among independent transformants and therefore, this factor has a profound effect on the stability and level of transgene expression (Kohli, A et al., 2003 and Sanagala, R et al., 2017). Therefore, we checked RNA expression using qPCR, protein expression level by western blotting and seeds set to select independent lines for further analysis.

5.5.2 Quantitative determination of transgene expression by real-time PCR

Transcript levels of 7-8 independent lines from each genotype were confirmed by qRT-PCR. Total RNA was isolated from 10-day-old rice seedlings grown on ½ MS plates supplemented with hygromycin. A minimum of two independent lines showing similar expression levels and seed sets from each genotype were further analysed (**Figure 5.3**).

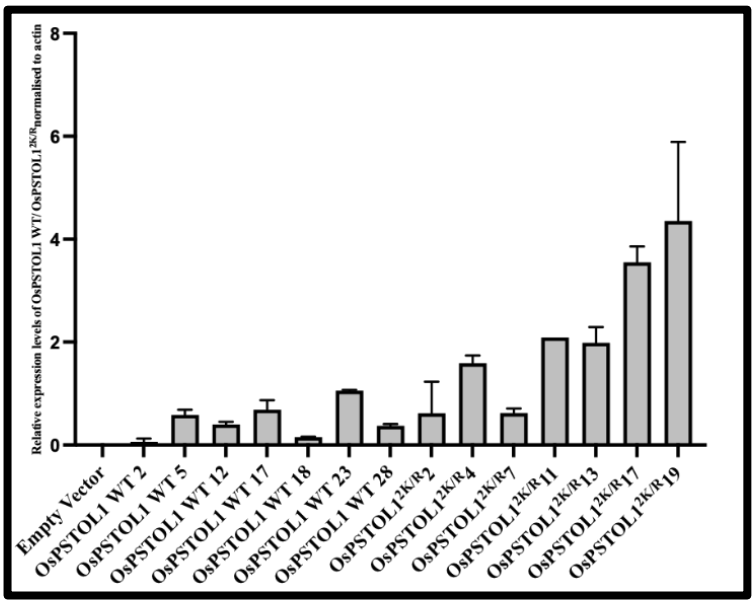

Figure 5.3: Analysis of *OsPSTOL1* transcript levels in YFP-OsPSTOL1 WT and YFP-OsPSTOL1$^{2K/R}$ rice transgenic lines.

Transcript analysis of *OsPSTOL1* in empty vector (Nipponbare seedlings), OsPSTOL1 WT and OsPSTOL1$^{2K/R}$ rice transgenic lines. Total RNA was isolated from 10-day-old seedlings of all independent lines from each genotype and cDNA was prepared from the RNA by reverse transcription. The cDNA was diluted in a 1:5 ratio and resulted in cDNA being used as a template for qRT-PCR and the expression was normalised by actin which was used as an internal control. Error bars represent SEM.

5.5.3 Determining the homozygosity of OsPSTOL1 rice transgenic lines

Independent transgenic lines from each genotype were screened to identify homozygous lines. 25-35 seeds were placed on ½ MS media supplemented with hygromycin for demonstrating homozygous gene insertion (**Figure 5.4**). The survival ratio between 92-100% confirmed at least two homozygous independent single-copy lines of OsPSTOL1 WT and OsPSTOL1$^{2K/R}$ for further analysis .

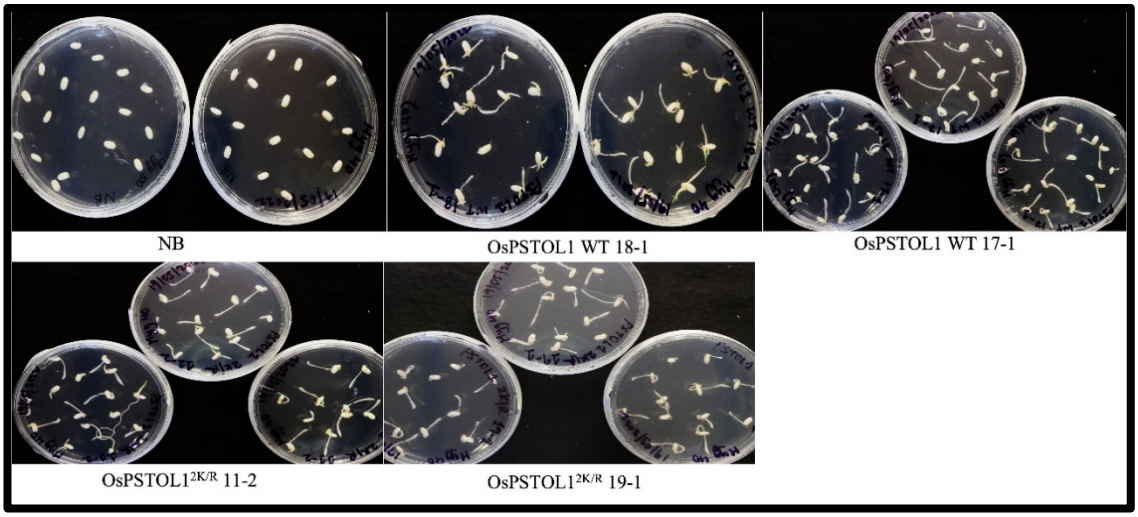

Figure 5.4: Using antibiotic selection to determine seedling zygosity.

25-35 sterilized seeds were placed on ½ MS media supplemented with 40µg/ml hygromycin. Seeds were allowed to germinate in darkness at 28°C for 3 days. After 3 days, the seeds were transferred to 24 hours light at 28°C. The germination rate was observed after 5 days to determine a homozygous transgenic line.

5.5.4 Analysis of YFP-OsPSTOL1 WT and YFP-OsPSTOL1$^{2K/R}$ protein levels in YFP-tagged OsPSTOL1 rice transgenic lines

Furthermore, to ensure equal expression of protein levels in the selected transgenic lines, total protein was extracted using 1x Laemmli sample buffer. **Figure 5.5** shows the band corresponding to YFP-OsPSTOL1 WT (line 17 and 18) and YFP-OsPSTOL1$^{2K/R}$ (line 11 and 19) (shown by red arrow). The protein level in the total protein extract is similar in all the independent lines. But the breakdown of YFP-OsPSTOL1 was observed which may be due to the extraction technique.

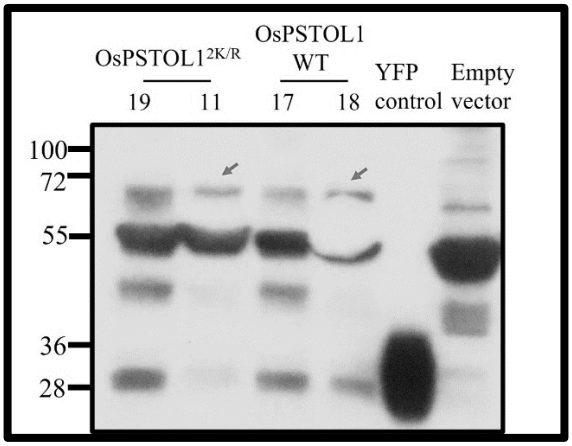

Figure 5.5: Protein levels of YFP-OsPSTOL1 and YFP-OsPSTOL1$^{2K/R}$ in overexpressing YFP-tagged OsPSTOL1/OsPSTOL1$^{2K/R}$ independent rice transgenic lines.

Western blot analysis showing the protein levels in each independent line of UBI::OsPSTOL1 WT (line 17 and 18) and UBI::OsPSTOL1$^{2K/R}$ (line 19 and 11) rice transgenic lines. 14 days old rice seedlings were used to extract total protein using 1x Laemmli sample buffer in a 1:1 ratio and subjected to SDS-PAGE analysis. The proteins were transferred to the PVDF membrane and immunoblot using αGFP antibodies. The protein band of PSTOL1 kinase was seen in both OsPSTOL1 WT and OsPSTOL1$^{2K/R}$ independent lines (shown by grey arrow) but the band corresponding to PSTOL1 kinase is absent from empty vector and YFP control. Nipponbare rice plant without PSTOL1 insertion (empty vector) was taken as a negative control. 30µl of total protein was loaded on SDS-PAGE.

5.5.5 Genotyping of UBI::OsPSTOL1 WT and UBI::OsPSTOL1$^{2K/R}$ transformants

Before characterizing the transgenic lines in phosphate treatment, it is important to determine the genotype of the independent transgenic lines using Cleaved Amplified Polymorphic Sequences (CAPS) marker. CAPS is based on the very simple principle of 3 subsequent steps:

1. Specific primers are used for PCR to amplify gene of interest.
2. The amplified product is digested by restriction enzymes.
3. The digested product is separated on an agarose gel.

CAPS marker can show any mutation in gene sequence by digestion patterns of PCR because of nucleotide polymorphism within each sample (Shavrukov, Y.N., 2016). Introducing mutation of lysine to arginine give rise to the recognition site of the BglII enzyme at the 675th nucleotide position in the *OsPSTOL1* gene sequence. Thereby, the recognition site for the BglII enzyme is absent from the *OsPSTOL1 WT* gene sequence while it is present in the

OsPSTOL1$^{2K/R}$ sequence. Using gene-specific primers, the target region of DNA was amplified, and the PCR product was gel purified. The purified product was digested with BglII enzyme, and the separation of the digested product was analysed on an agarose gel. Digestion of amplicon/ plasmid with BglII enzyme will result in a single band of size 247bp (shown by red arrow) indicating the genotype of the plant as PSTOL1 WT. In contrast, the presence of the exact recognition site for BglII in amplicon will result in two fragments after digestion corresponding to sizes 193bp (depicted by the blue arrow) and 54bp (shown by the white arrow). Two fragments after digestion directed that PSTOL1$^{2K/R}$ was the genotype of the plant (**Figure 5.6**).

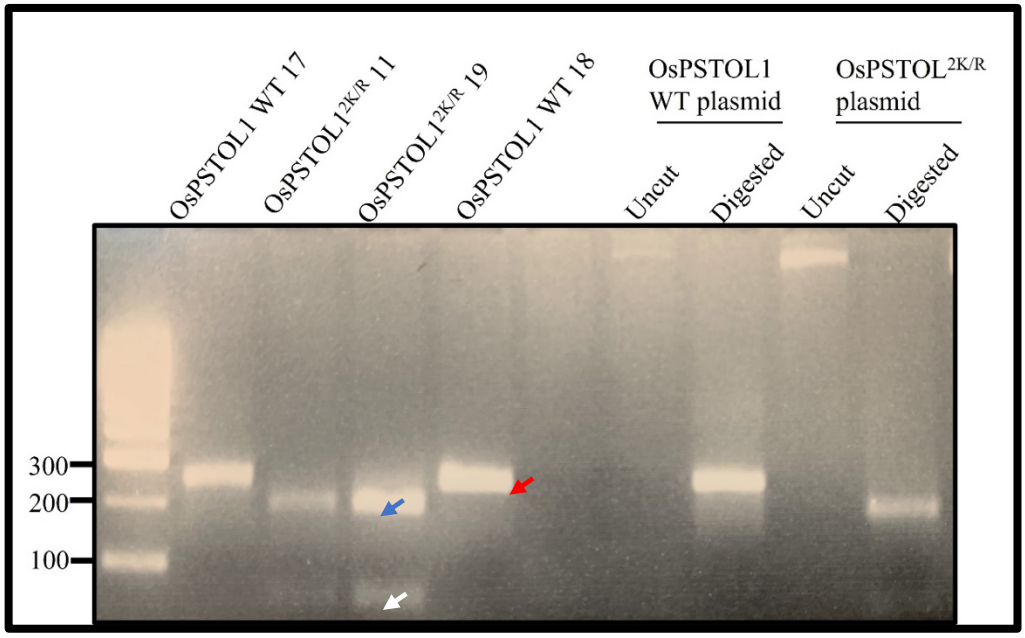

Figure 5.6: Genotyping of UBI::YFP-OsPSTOL1 WT and UBI::YFP-OsPSTOL1$^{2K/R}$ transformants.

Gene-specific primers were designed to amplify the target region in DNA (675th nucleotide position in gene sequence) by PCR and the subsequent PCR product was gel purified. The gel-purified PCR product was digested with BglII enzyme at 37°C overnight. The digested product was run on 1.5% agarose gel for further analysis. The resulting fragment after digestion of PCR product amplified from OsPSTOL1 WT plants will run as a single band (showed by red arrow) as it does not have a recognition site for BglII enzyme while digestion of PCR product amplified from OsPSTOL1$^{2K/R}$ plants will result in two fragments of 193bp and 54bp (depicted by blue and white arrow respectively).

5.6 To confirm the SUMOylation status of YFP-OsPSTOL1 WT and YFP-OsPSTOL1$^{2K/R}$ in rice transgenic lines

We wanted to investigate the SUMOylation status in rice transgenic lines overexpressing YFP-OsPSTOL1 WT and YFP-OsPSTOL1$^{2K/R}$. 10-12 seeds were put on ½ MS media and were germinated in 28°C for 3days. After 3 days, the seeds were transferred to 24 hours light at 28°C and tissue was harvested after 10 days. Samples were ground up to fine powder in a pestle and mortar with SUMO extraction buffer optimized for extracting protein from rice (described in the material and method section 2.1.9). **Figure 5.7** shows the result of the immunoblot (IB:αGFP) where OsPSTOL1 WT and OsPSTOL1$^{2K/R}$ tagged with YFP can be detected (expected size of protein is 64.4kDa). YFP breakdown was observed from both YFP-OsPSTOL1 WT and YFP-OsPSTOL1$^{2K/R}$ protein in IP lanes, which can be due to extraction issues. Moreover, YFP-OsPSTOL1 WT and YFP-OsPSTOL1$^{2K/R}$ protein was observed in input lanes. YFP control transgenic lines were used as a positive control for immunoblot analysis with αGFP monoclonal antibodies, whereas an empty vector (Nipponbare seedlings) was used as a negative control for the experiment.

We detected no significant difference in protein expression levels of YFP-OsPSTOL1 WT and YFP-OsPSTOL1$^{2K/R}$. Interestingly, we observed SUMO conjugated to YFP-OsPSTOL1 WT in the OsPSTOL1 IP lane in immunoblot with anti-GFP antibody (shown by an asterisk in **Figure 5.7**). This conjugation was significantly reduced in YFP-OsPSTOL1$^{2K/R}$. However, it is important to confirm this SUMO conjugation using an antiSUMO antibody which is discussed below in detail.

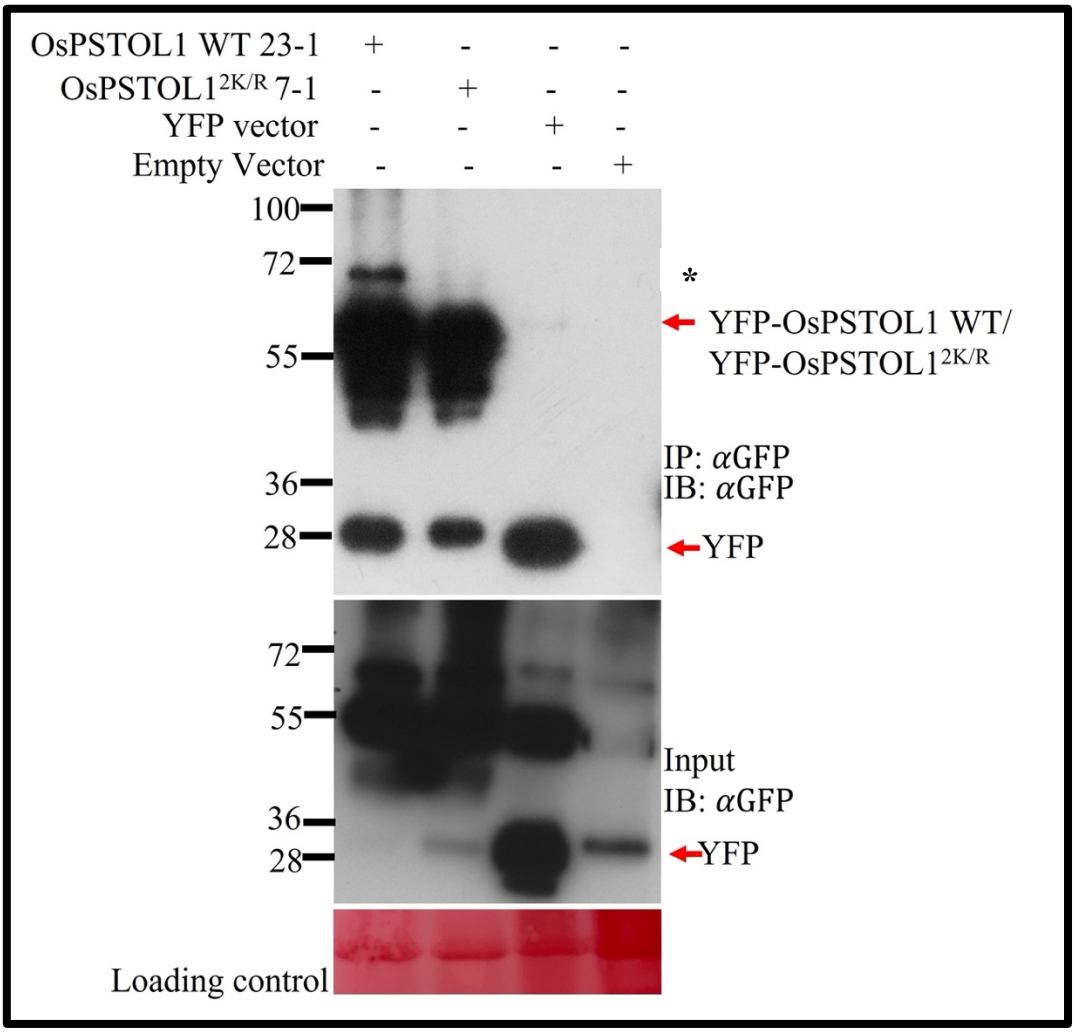

Figure 5.7: Immunoprecipitation of YFP tagged OsPSTOL1 WT and OsPSTOL1$^{2K/R}$ protein from young rice transgenic seedlings overexpressing YFP-OsPSTOL1 WT and YFP-PSTOL1$^{2K/R}$.

Immunoblot analysis of immunoprecipitation experiment of OsPSTOL1 WT, OsPSTOL1$^{2K/R}$, YFP and empty vector was carried out with αGFP beads. Seeds of overexpressing transgenic lines of YFP-OsPSTOL1 WT, YFP-OsPSTOL1$^{2K/R}$, YFP and Nipponbare were put on ½ MS and were allowed to germinate in dark at 28°C for 3 days. After 3 days, seeds were transferred to 24 hour light and tissue was harvested after 10 days. Using SUMO extraction buffer, the supernatant obtained was incubated with beads to immunoprecipitate (IP) the YFP-tagged proteins. The eluted protein was run on SDS-PAGE and probed. Size (64.4kDa) corresponding to YFP-OsPSTOL1 WT, YFP-OsPSTOL1$^{2K/R}$ and YFP (27kDa) was observed after immunoblot analysis with αGFP monoclonal antibodies. No bands were observed in the empty vector lane. 15µl of IP sample was loaded on the SDS-PAGE. Ponceau stained RuBisCO is shown as a loading control for the experiment.

Immunoblot analysis in **Figure 5.8** with αAntiSUMO antibodies confirmed that the band of SUMO-tagged YFP-OsPSTOL1 WT (monoSUMOylation) whereas the band corresponding to SUMO conjugated to YFP-OsPSTOL1$^{2K/R}$ is absent from its lane which substantiate our result

from **Figure 5.7**. Also, previous results from vivo and in-planta experiments (**Figures 3.8** and **3.11** from Chapter 3, **Figure 4.8** from Chapter 4) also validate these results. Non-specific background from the antibody can be seen in the blot (shown by asterisks). These non-specific bands are also present in YFP vector control therefore, these bands do not correspond to either SUMO conjugates or PSTOL1 protein. However, SUMOylation status was not tested in other YFP-OsPSTOL1 WT and YFP-OsPSTOL1$^{2K/R}$ transgenic lines.

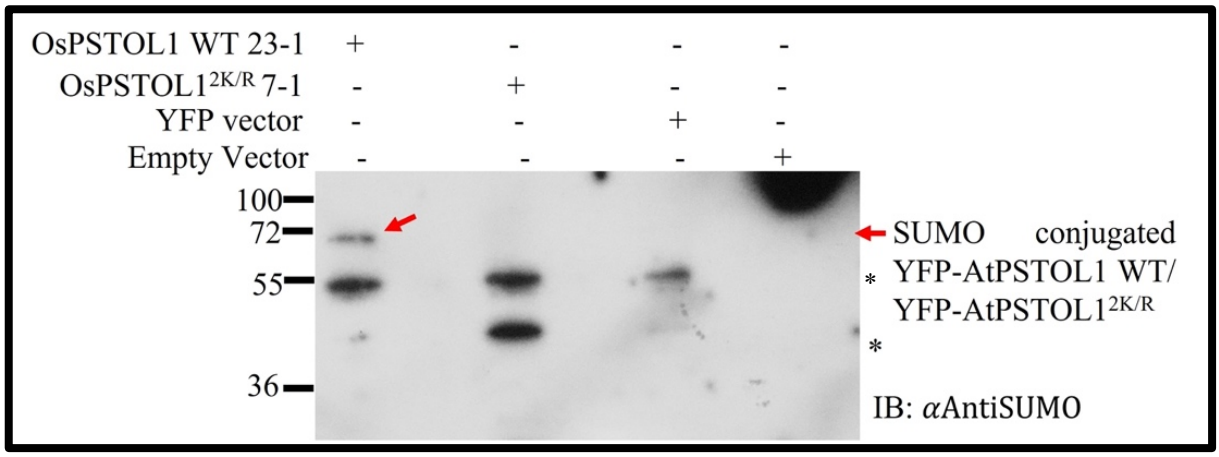

Figure 5.8: YFP-OsPSTOL1$^{2K/R}$ is probably not SUMOylated in overexpressing YFP-OsPSTOL1$^{2K/R}$ rice transgenic seedlings.

Western blot showing immunoblot analysis with αAntiSUMO antibodies of YFP-OsPSTOL1 WT, YFP-OsPSTOL1$^{2K/R}$, YFP and Nipponbare seedlings. A band corresponding to YFP-OsPSTOL1 WT can be seen in its IP lane, indicating SUMOylation of YFP-OsPSTOL1 WT. No corresponding band can be seen in the IP lane of OsPSTOL1$^{2K/R}$, indicating the successful removal of the SUMO sites. The band at 55kDa can be in the lane of YFP-OsPSTOL1 WT, YFP-OsPSTOL1$^{2K/R}$ and YFP which may be due to cross-reactivity or background. No bands were seen in the lane of the empty vector. 80 µl of IP sample was loaded on SDS-PAGE. The red arrow indicates the band corresponding to SUMOylated form of YFP-OsPSTOL1 WT.

5.7 Subcellular localization of YFP-OsPSTOL1 WT and YFP-OsPSTOL12K/R in roots of rice transgenic lines

The next aim was to test the in-planta function and ascertain if lysine to arginine mutation affects the cellular localization of YFP-OsPSTOL1 WT and YFP-OsPSTOL1$^{2K/R}$. The localization was investigated in the 5-7-day-old seedling roots of rice (**Figure 5.9**).

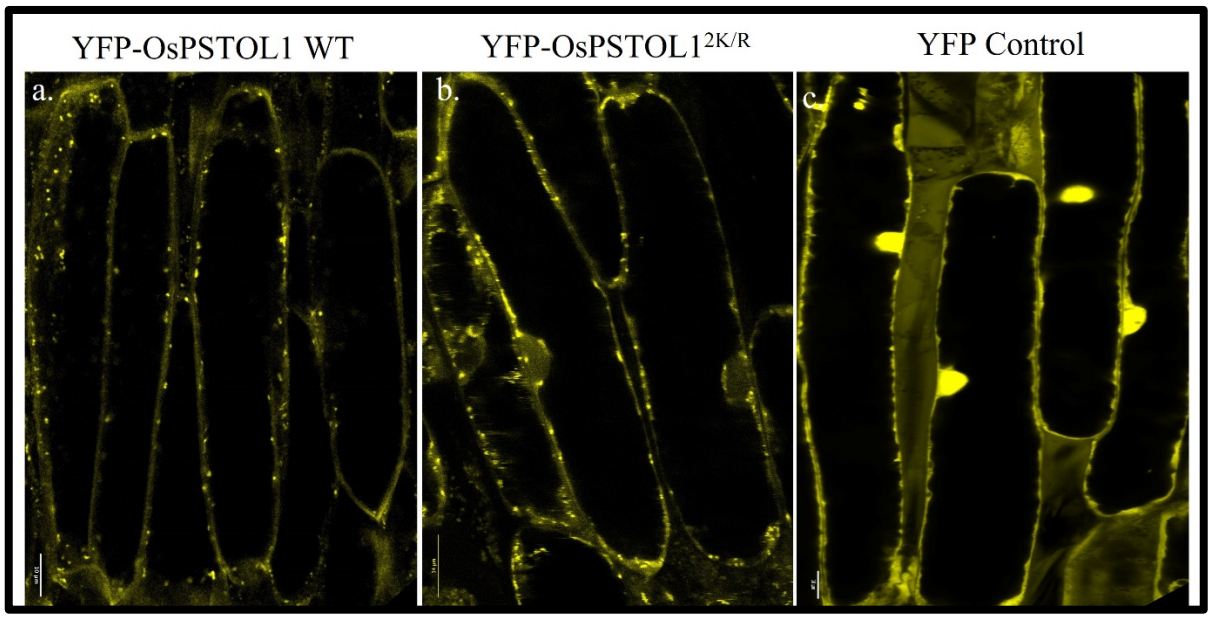

Figure 5.9: Subcellular localization of YFP tagged OsPSTOL1 WT and OsPSTOL1$^{2K/R}$ in roots of rice transgenic lines.

Representative images of YFP-tagged OsPSTOL1 WT and OsPSTOL1$^{2K/R}$ roots cells. Images were obtained using a confocal laser scanning microscope with YFP excitation (514nm) and emission filters (524-560nm). (a.) YFP-OsPSTOL1 WT (b.) YFP-OsPSTOL1$^{2K/R}$ (c.) YFP control. Scale bar = 10µm

Both YFP-OsPSTOL1 WT and YFP-OsPSTOL1$^{2K/R}$ have been implicated for the first time to localize to the nucleus and cell membrane/cytoplasm in roots of rice, but some difference was observed between the localization of YFP-OsPSTOL1 WT and YFP-OsPSTOL1$^{2K/R}$. Number of cells corresponds to YFP-OsPSTOL1 WT localization in nucleus were fewer when compared to YFP-OsPSTOL1$^{2K/R}$. The next step is to conduct a ratiometric quantification of fluorescence in the nuclear/cell membrane or cytoplasm will further confirm these findings. However, the use of cellular compartment markers will further validate the localisation of PSTOL1 and its non-SUMOylatable version.

5.8 Characterization of YPF tagged UBI::OsPSTOL1 WT and UBI::OsPSTOL1$^{2K/R}$ transgenic lines in high and low phosphate media

5.8.1 Standardization of experimental protocol

Deficiency symptoms of phosphorus in rice plants can be easily observable because plants are stunted, have spindly and thin stems, and leaves are very erect, short, narrow and have a pale green colour. Some reports also suggest that low Pi promotes PR growth, especially in Japonica varieties, but the overall growth of the root is decreased, therefore only longer PR can be seen (Péret et al., 2014). In low phosphate conditions, the uptake of +Fe is considerably promoted which sometimes results in bronzing of the roots of rice plants (Yamauchi ., 1988).

Initial experiments were set up to evaluate the phenotype of Nipponbare under phosphate-deficient and sufficient conditions. 100µM, 31µM and 3µM concentration of phosphate were used as high (100µM or 31µM) and low phosphate concentration (3µM) respectively for experimental set up. Nipponbare seeds were surface sterilized and transferred to ½ MS plates without antibiotics. The seeds were germinated in dark for 3 days at 28°C and the seeds were transferred to 24 hours of light for 1 day. Equal or similar germinated seeds were transferred to Yoshida media with modified phosphate concentration (described in material and methods table 2.9). The plants were raised in a 16/8 hour photoperiod with approximately 70% relative humidity. The phenotype of Nipponbare plants was evaluated after 28 days.

Figure 5.10 and **5.11** (**A** and **B**) demonstrates the visible phosphorus deficiency in both roots and shoots of Nipponbare plants when grown in P-deficient media for 28 days. **Figure 5.10 (C)** shows the quantification of root and shoot length which confirms that the change in root and shoot length is significant. This proves that the experimental setup is working and can be used in further experiments to analyse OsPSTOL1 transgenic lines.

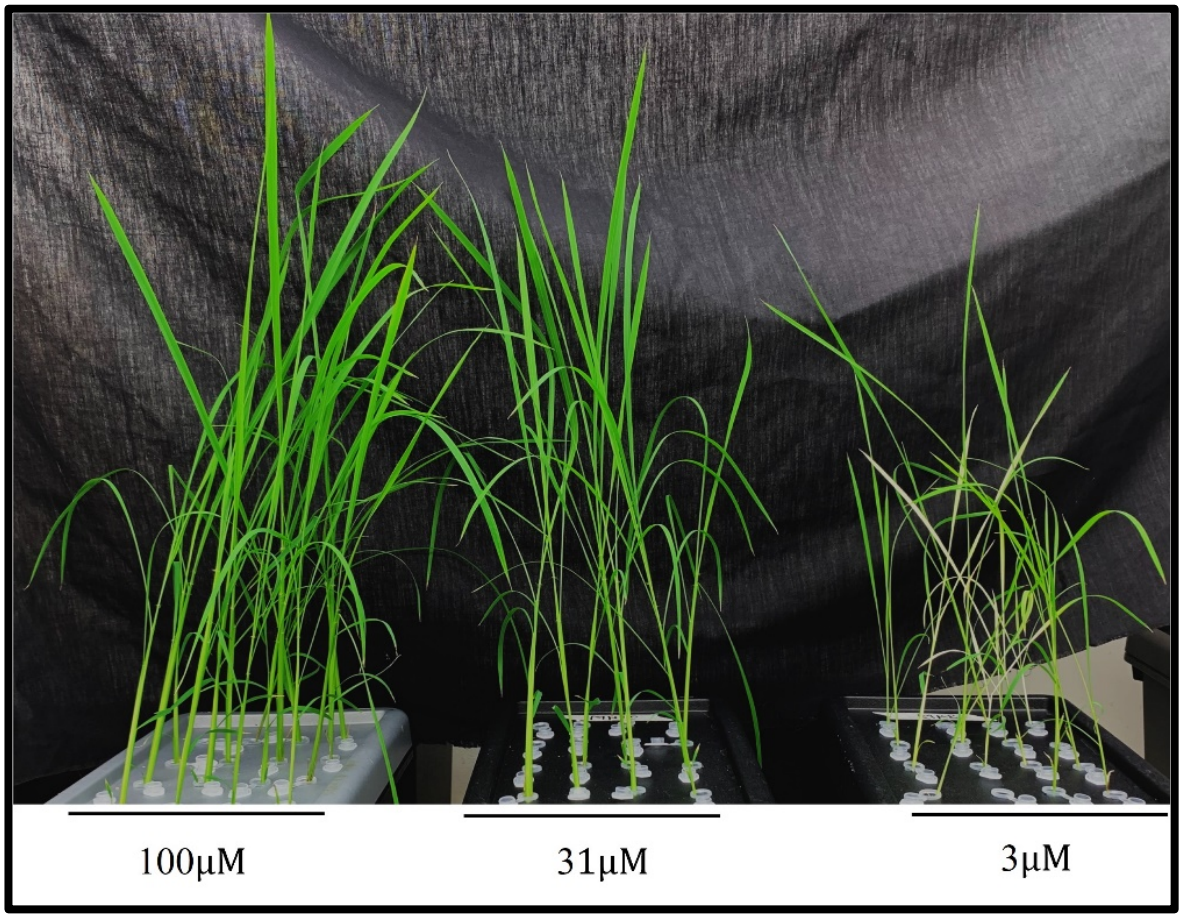

Figure 5.10: Overall growth analysis of Nipponbare plants grown under different phosphorus concentrations (100µM, 31µM and 3µM).

Nipponbare plants grown in P-deficient conditions showed visible symptoms such as stunted growth of the plant, thin stems and pale green leaves of phosphorus deficiency. 3 biological replicates were set up for final observation.

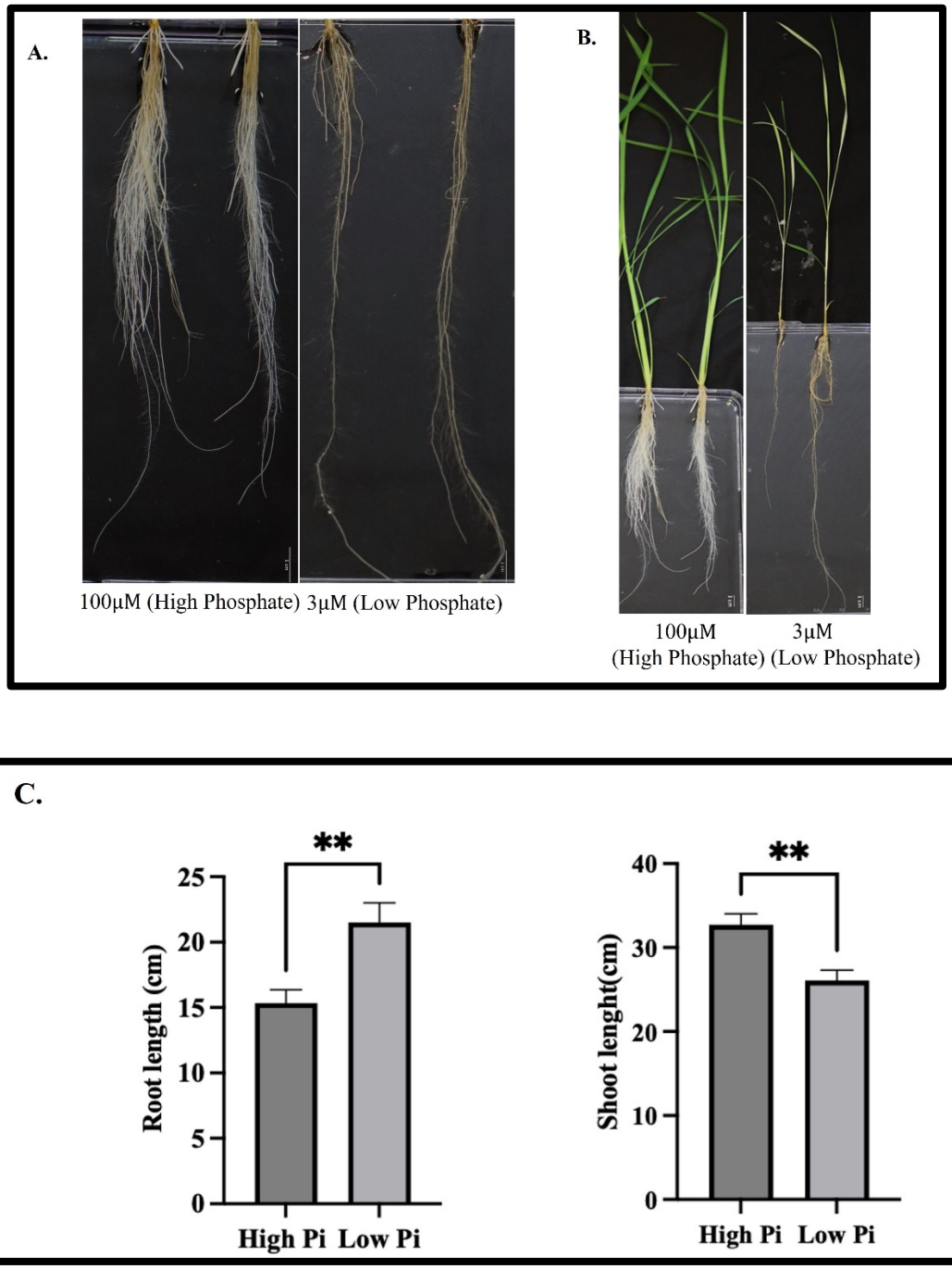

Figure 5.11: Nipponbare growth behaviour in high and low Pi conditions.

The phenotype of 28-day-old hydroponically grown Nipponbare plants under different concentrations of phosphate was recorded (NaH_2PO_4). Nipponbare seeds were surface sterilised and put on ½ MS without antibiotics. The seeds were germinated in dark for 3 days at 28°C and the seeds were transferred to 24 hours light for 1 day. Seeds with similar germination rates were transferred to Yoshida media modified for phosphate concentration - P-sufficient (100µM) and P-deficient (3µM). The phenotype was observed after 28 days of treatment. (A.) Developmental response of root of Nipponbare in high Pi and low Pi. (B.) Overall growth performance of Nipponbare plants under high and low Pi conditions. (C.) Average of root length and shoot length where error bars represent $\pm$ SEM of 3 biological replicates. p value determined by t-test where "**" = $p \leq 0.05$. Scale bar = 1cm.

5.8.2 Characterization of YFP-OsPSTOL1 WT and YFP-OsPSTOL1$^{2K/R}$ rice transgenic lines in high Pi (100µM) and low Pi (3µM)

Gamuyao et al., 2012 demonstrated that overexpression of PSTOL1 will enhance root growth and development when plants are grown in low-phosphorus soil, thereby improving the plant's ability to 'mine' phosphorus from soil. However, it is still unknown the molecular mechanism of PSTOL1 to regulate root growth. In this chapter, we investigated the role SUMOylation PSTOL1 may play in regulating its function . Initially, two independent lines of each genotype – OsPSTOL1 WT 17, OsPSTOL1 18, OsPSTOL1$^{2K/R}$ 11 and OsPSTOL1$^{2K/R}$ 19 along with controls- empty vector (Nipponbare and YFP only) plants were analysed under high Pi (100µM) and low Pi (3µM). These transgenic lines were chosen according to the availability of seeds. We studied root and shoot dry weight, root and shoot length, total root surface area, mean diameter of roots and total root length of plants grown in hydroponic media for 28 days.

In **Figure 5.12**, we demonstrated the overall effect of overexpression of OsPSTOL1 WT/OsPSTOL1$^{2K/R}$ in roots of Nipponbare plants when subjected to hydroponic culture supplemented with 100µM and 3µM. Under high Pi, no visible difference was observed in roots between empty vector (Nipponbare plants) and OsPSTOL1 overexpressing transgenic lines (**Figure 5.12 A**). Under low Pi, a relative increase in root biomass was seen in OsPSTOL1 WT/OsPSTOL1$^{2K/R}$ transgenic lines when compared to plants lacking the protein kinase (empty vector and YFP control) (**Figure 5.12 B**). This change in root phenotype was confirmed by quantification of root biomass and other root traits which is described below in detail.

A.

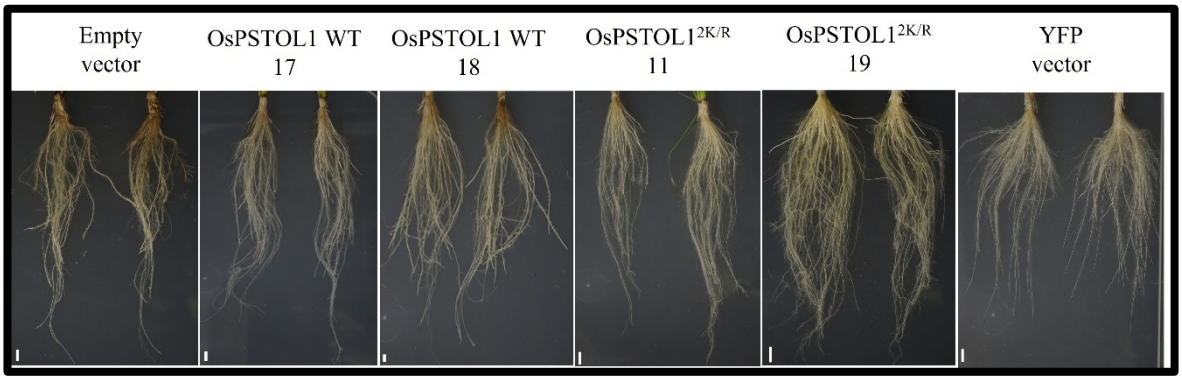

B.

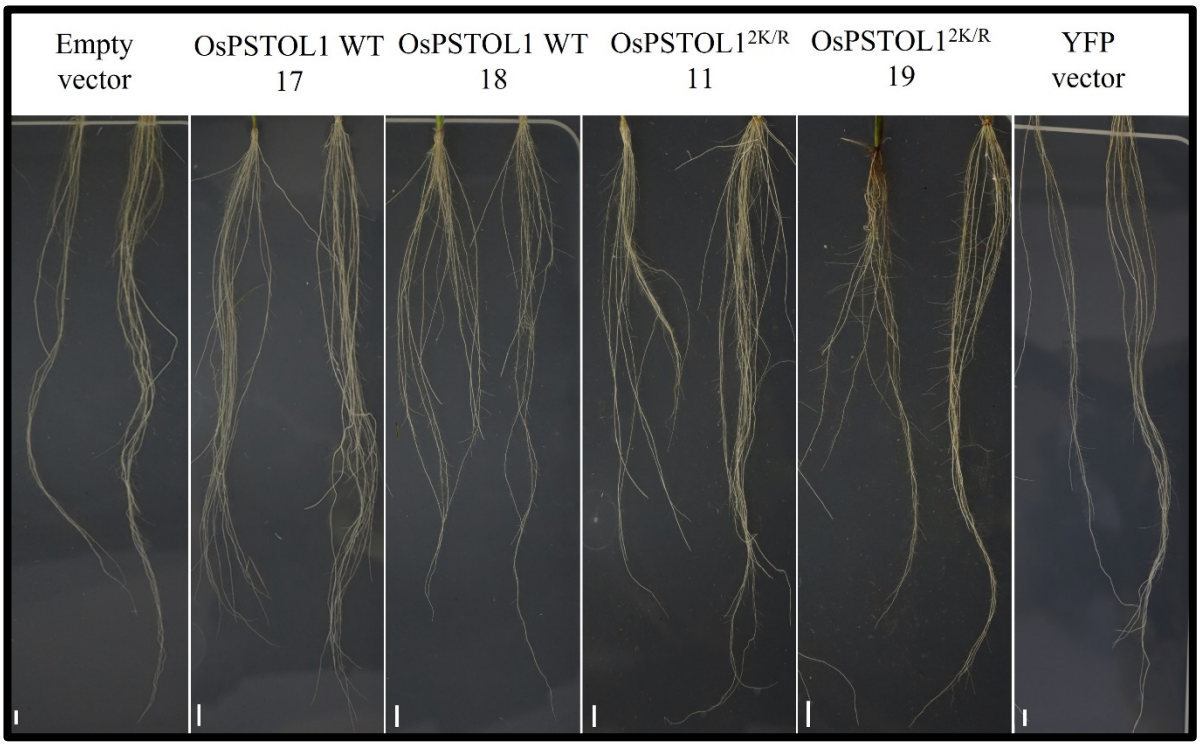

Figure 5.12: Effects of overexpression of OsPSTOL1 WT and OsPSTOL1$^{2K/R}$ on tolerance to Pi deficiency.

Seeds of empty vector, OsPSTOL1 WT, OsPSTOL1$^{2K/R}$ and YFP control were grown in modified Yoshida media. Root Phenotype of 1-month-old rice plants grown under (A.) high Pi (100µM) and (B.) low Pi (3µM). Two representative plants from each genotype were used for imaging. Scale bar = 1cm.

a. Root and shoot dry weight

Our data indicate that OsPSTOL1 WT/ OsPSTOL1$^{2K/R}$ transgenic lines exhibited higher root biomass irrespective of Pi regimes when compared to empty vector (Nipponbare) and YFP control transgenic lines. Thereby, our data substantiate the previous result from Gamuyao et al., 2012. However, we cannot observe any obvious difference in root biomass between OsPSTOL1 WT and OsPSTOL1$^{2K/R}$ transgenic lines (**Figure 5.13 B**).

In contrast to root dry weight, we did not observe any significant difference in shoot dry weight between OsPSTOL1 WT/ OsPSTOL1$^{2K/R}$ transgenic lines and Nipponbare in high or low Pi. (**Figure 5.13 A**). The root and shoot dry weight were collectively calculated for 5 seedlings and therefore, there are no error bars for assessing this parameter.

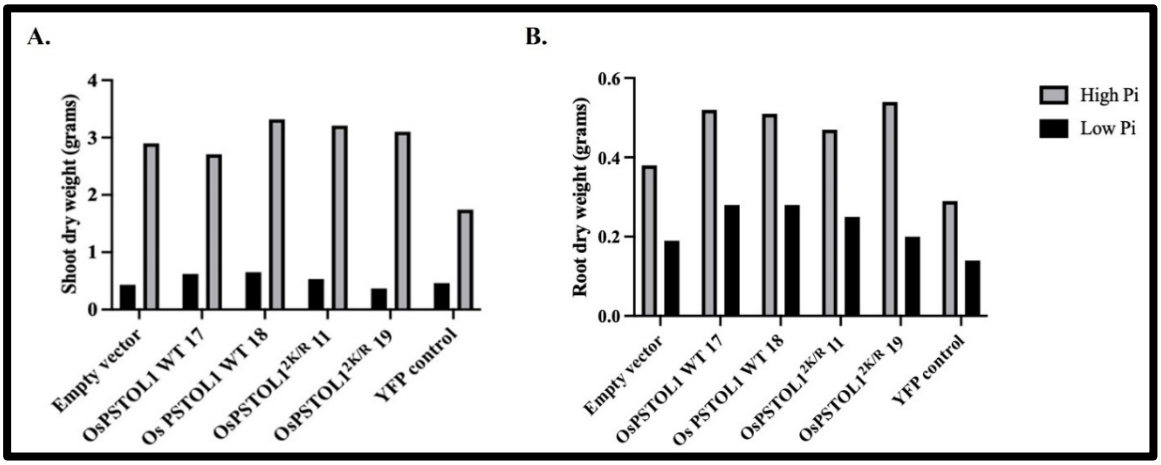

Figure 5.13: Shoot and root dry weight of overexpressing UBI::YFP-OsPSTOL1 WT, UBI::YFP-OsPSTOL1$^{2K/R}$, YFP control transgenic lines with corresponding empty vector (Nipponbare) under high Pi (100µM) and low Pi (3µM).

Seeds from each genotype were grown in Yoshida media with modified phosphorus concentrations, +P (100µM) and -P (3µM) for 28 days. Data represents (A.) Shoot dry weight (B.) Root dry weight. Statistical analysis was not conducted as this experiment was conducted once because of time constraints. Error bars are not present because shoot and root dry weights were calculated collectively for 5 seedlings per genotype.

b. Shoot length and root length

Next, we analysed the root and shoot length using FIJI software. The data shown in **Figure 5.14 (A)** indicates that there is the least significant difference in shoot length irrespective of Pi concentrations between genotypes. Data on shoot length directly coincides with shoot biomass which exhibited no change in length and therefore no change in biomass. OsPSTOL1 WT/OsPSTOL1$^{2K/R}$ might not significantly influence the developmental responses in shoots compared to Nipponbare.

Primary root elongation is a major adaptive response in rice when grown in low Pi to forage more Pi from the soil. Therefore, the primary root of the plant will be longer in low Pi when compared to high Pi conditions. In **Figure 5.14 (B)** it is evident that the empty vector has longer PR growth in low Pi, whereas OsPSTOL1 WT 17, OsPSTOL1$^{2K/R}$11, OsPSTOL1$^{2K/R}$ 19 transgenic lines exhibited shorter or similar PR growth in low Pi compared to high Pi. We reason that overexpressing OsPSTOL1 WT/ OsPSTOL1$^{2K/R}$ protein controls root architecture probably by enhancing more root number by either producing more lateral roots or root hairs and eventually inhibiting the primary root growth. Data analysis from root length does validate our previous result from root dry weight (**Figure 5.14 B**). However, we observed a discrepancy between two independent lines of the OsPSTOL1 WT genotype. This difference can be overcome by using other OsPSTOL1 WT independent lines.

Our main aim is to detect any phenotypic difference between OsPSTOL1 WT and OsPSTOL1$^{2K/R}$ transgenic lines, but from our data, we cannot observe notable differences among both genotypes when subjected to phosphate treatment with respect to root and shoot lengths.

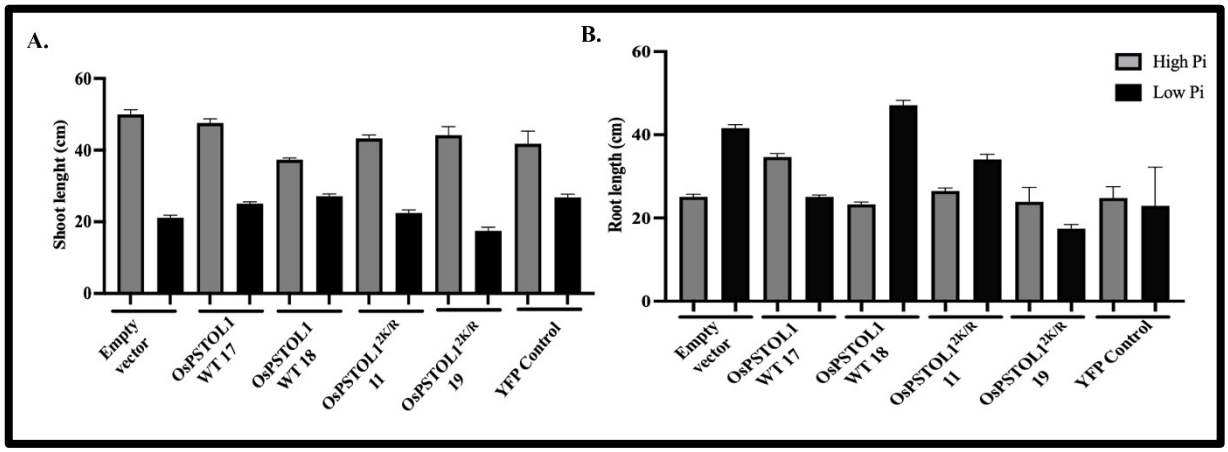

Figure 5.14: Shoot and root length of overexpressing UBI::YFP-OsPSTOL1 WT, UBI::YFP-OsPSTOL1$^{2K/R}$, YFP control transgenic lines with corresponding empty vector (Nipponbare) under high Pi (100µM) and low Pi (3µM).

Seeds from each genotype were grown in Yoshida media with modified phosphorus concentrations, +P (100µM) and -P (3µM) for 28 days. Data represents (A.) Shoot length (B.) Root length. Error bars represent ± SEM of technical replicates. Statistical analysis was not conducted as this experiment was conducted once because of time constraints. Number of plants in the study = 16

c. Total root length, Total root surface area and Mean diameter of roots

Enhanced total root length and total root surface area are adaptive responses of plants to improve phosphorus exploration in topsoil. Therefore, quantification of plant root parameters such as total root length, total root surface area, mean diameter and root length density are important to understand plant physiology if a foreign DNA is introduced. Over the years, algorithms have been developed to measure root parameters of crops. In our analysis, we used open-source software, IJ_rhizo for measuring root parameters (**Figure 5.15**). Gamuyao et al., 2012 investigated total root surface area and total root length using WinRhizo. They showed that both parameters were higher in overexpressing PSTOL1 transgenic lines under low Pi.

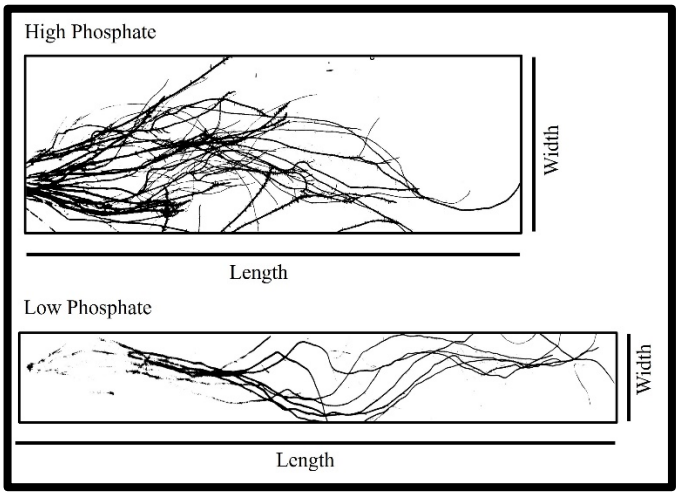

Figure 5.15: Working of IJ_Rhizo.

IJ_Rhizo is based on the Kimura approach for calculating root parameters. The Kimura method is built on differentiating each pixel of the medial axis of the transformed image of the root according to orthogonal and diagonal numbers.

Root images were scanned using IJ_rhizo for three parameters- total surface area, total root length and mean root diameter. Under low Pi conditions, PR growth in an empty vector (Nipponbare) is longer (**Figure 5.14 B**), as a result, the surface area occupied by the root is higher than in high Pi conditions. Unlike empty vector, transgenic lines showed a lower surface area under low Pi indicating cessation of primary root length (**Figure 5.16 A**). Further analysis of the total root length showed no change in the empty vector. Unlike empty vector, change in total root length in overexpressing OsPSTOL1 transgenic lines is evident (**Figure 5.16 B**). **Figure 5.16 C** showed that the mean diameter of roots in OsPSTOL1 WT transgenic lines is the same in both high Pi and low Pi, signifying the function of OsPSTOL1 whereas SUMO mutant version showed an overall less mean diameter of roots under low Pi. Figure A, B and C demonstrated that a change in root architecture may promote the proliferation of lateral roots and root hairs to increase nutrient assimilation.

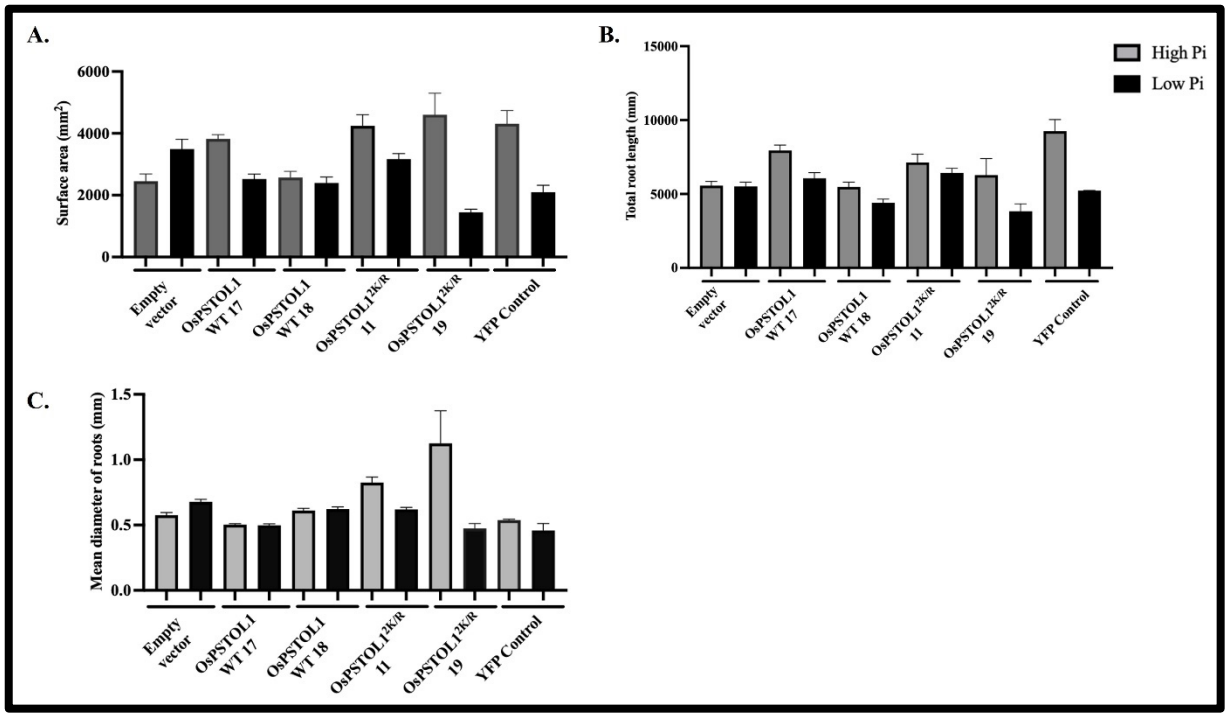

Figure 5.16: Analysis of surface area, total root length and mean diameter of roots of overexpressing UBI::YFP-OsPSTOL1 WT, UBI::YFP-OsPSTOL1$^{2K/R}$, YFP control transgenic lines with corresponding empty vector (Nipponbare) under high Pi (100µM) and low Pi (3µM).

Seeds from each genotype were grown in Yoshida media with modified phosphorus concentrations, +P (100µM) and -P (3µM) for 28 days. Data represents (A.) Surface area (B.) Total root length (C.) The mean diameter of roots. Error bars represent ± SEM of technical replicates. Statistical analysis was not conducted as this experiment was conducted once because of time constraints. Number of plants in the study = 16

Although this experiment provided some preliminary data on the phenotype of YFP-OsPSTOL1 WT/ YFP-OsPSTOL1$^{2K/R}$ transgenic lines, in conclusion, we must conduct this experiment more times for statistical robustness.

5.8.3 Characterization of YFP-OsPSTOL1 WT and YFP-OsPSTOL1$^{2K/R}$ rice transgenic lines in response to gravitropism stimuli

Modulation of root architecture to increase nutrient uptake efficiency is an important factor. To explore more phosphate from the soil, root growth orientation is changed to form a shallower root system. This root growth orientation is dynamically sustained with respect to

gravity (Huang et al., 2018). We proposed that the expression of OsPSTOL1 might fine-tune the root angle to form a shallower root system under low Pi.

Seeds were surface sterilised and germinated on the ½ MS media plates. The plates were kept at 110° to ensure that roots remain in contact with the plate. For gravitropic stimulation, 5-day-old seedlings were rotated at 90° and continued to grow for 24 hours. The curved angle was measured using FIJI software (described in Figure 4.13 in chapter 4).

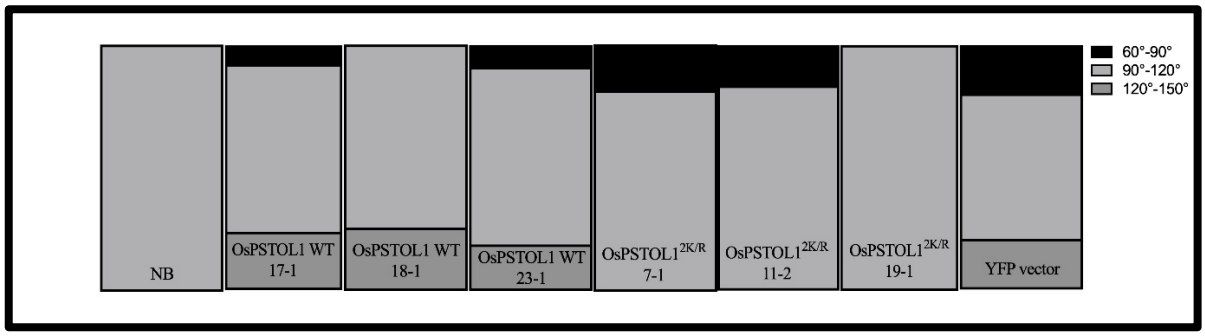

Figure 5.17: Quantification of root gravitropic curvature of empty vector, YFP-OsPSTOL1 WT, YFP-OsPSTOL1$^{2K/R}$ and YFP control.

Seeds from each genotype were grown on ½ MS media and germinated. 5-day-old seedlings were rotated on a horizontal axis for 24 hours. For evaluation of the root gravitropic responses under normal conditions, root curvature was measured using FIJI software. The number of seeds used in this study (n) = 25.

Quantification in **Figure 5.17** revealed that all the Nipponbare seedlings showed bending angles between 90°-120°. But YFP-OsPSTOL1 transgenic lines do reveal a different pattern. About 16.6%-18.75% of YFP-OsPSTOL1$^{2K/R}$ transgenic lines showed a steeper root angle between 60°-90° and while only 7.6%-9% of OsPSTOL1 WT seedlings showed a root bending angle between 60°-90°. Detailed analysis also revealed that root bending between 90°-120° is shown more by YFP-OsPSTOL1$^{2K/R}$ (81%-83%) than YFP-OsPSTOL1 WT (69%-72%). On the other hand, the root angle of YFP-OsPSTOL1 WT (18%-23%) exhibited a shallower angle between 120°-150°. Interestingly, YFP-OsPSTOL1$^{2K/R}$ seedlings do not display root angle between 120°-150°.

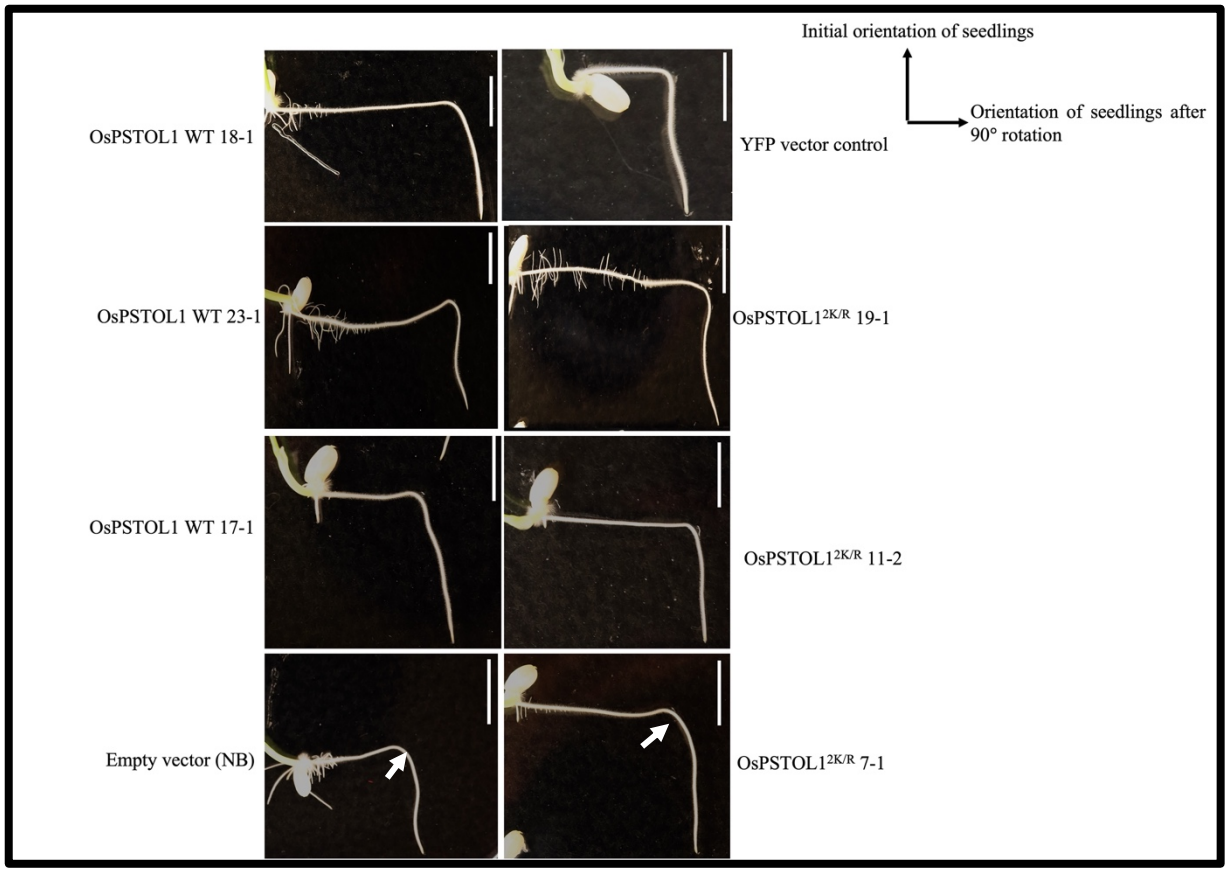

Figure 5.18: Representative image of comparison of root gravitropic response of 5-day-old seedlings of empty vector, YFP-OsPSTOL1 WT, YFP-OsPSTOL1$^{2K/R}$ and YFP control.

Seeds from each genotype were surface sterilised and put on ½ MS without antibiotics. The seeds were germinated in dark for 3 days at 28°C and seeds were transferred to 24 hours of light for 1 day before plates were turned by 90°. Root bending is shown here at the 24-hour rotation of vertically grown seedlings. The number of seeds (n) = 15-25. Scale bar = 1cm

The OsPSTOL1$^{2K/R}$ responded more sharply to gravitropic stimuli than OsPSTOL1 WT (**Figures 5.17** and **5.18**) and Nipponbare. We hypothesise that OsPSTOL1 WT protein might help in making a shallower whole root system in normal conditions. But the experiment must be repeated with an equal number of seeds from each genotype for conclusive results and statistical difference. Moreover, it will be interesting to investigate the phenotype of OsPSTOL1 WT and OsPSTOL1$^{2K/R}$ under phosphorus-deficient media.

As described in section 5.8B, two independent lines of both PSTOL1 genotypes were showing differences in the trend of parameters in the study. Therefore, for investigating the gravitropic

response in OsPSTOL1 rice transgenic lines, I decided to choose another independent line based on the availability of seeds along with the transgenic lines already used in the experimental setup in section 5.8B. Two independent lines (OsPSTOL1 WT 17-1, OsPSTOL1 23-1, OsPSTOL1$^{2K/R}$ 7-1 and OsPSTOL1$^{2K/R}$ 11-2) which show a similar trend to gravitropic response will be used in further experiments. These transgenic lines will be further tested and subjected to phosphate treatment for a better understanding of the important role played by SUMO in conferring tolerance under low Pi.

5.9 Discussion

Little is known of the mechanism to enhance root growth under low Pi mediated by PSTOL1 kinase. In this chapter, we investigated the role of a small ubiquitin-like modifier (SUMO), a posttranslational modification system, in fine-tuning root growth parameters regulated by OsPSTOL1 protein kinase. YFP-OsPSTOL1 WT and YFP-OsPSTOL1$^{2K/R}$ independent rice transgenic lines under maize ubiquitin promoter (UBI::YFP-OsPSTOL1 and UBI::YFP-OsPSTOL1$^{2K/R}$) were generated (kindly done by Dr. Cunjin Zhang). qRT-PCR analysis was done to confirm the single-copy insertion of transgene and subsequently, checked the transcript level of the transgene to select two independent lines from each genotype for further analysis. We also observed that transcript levels of *OsPSTOL1 WT* are consistently low across all independent lines. The possible reason can be epigenetic regulation of *OsPSTOL1 WT* expression because its insertion might have occurred in a repressive chromatin environment.

The next important step is to confirm the SUMOylation of YFP-OsPSTOL1 WT and YFP-OsPSTOL1$^{2K/R}$ in rice transgenic lines. It was confirmed that OsPSTOL1 WT is SUMOylated when protein was isolated from overexpressing OsPSTOL1 WT rice transgenic seedlings in normal conditions while we observed that OsPSTOL1$^{2K/R}$ protein was not SUMOylated (**Figure 5.7 and 5.8**). To confirm the SUMOylation status of OsPSTOL1$^{2K/R}$, other transgenic lines of YFP-OsPSTOL1$^{2K/R}$ will be tested in the future.

OsPSTOL1 showed to three-fold increase in phosphate uptake by enhancing root surface area when grown in low Pi soil. Orthologs of OsPSTOL1 identified in wheat, sorghum and maize

also showed a strong association with total root length, root surface area and root biomass which results in enhanced performance of plants under low Pi (Gamuyao et al., 2012, Abbas et al., 2022, Hufnagel et al., 2014, Azevedo et al., 2015). Although, PSTOL1 function is well established, the molecular mechanism mediating changes in root distribution by PSTOL1 is still unknown. We have observed that overexpression of OsPSTOL1 WT/ OsPSTOL1$^{2K/R}$ showed higher root dry weight than Nipponbare plants when grown under low Pi. These results validated by previous reports from Gamuayo et al., 2012 where they showed the superior performance of IR64 plants overexpressing PSTOL1 transgenic lines under low Pi was due to increase root dry weight. In rice, primary root length is increased under Pi deficiency, but overexpressing OsPSTOL1 WT/ OsPSTOL1$^{2K/R}$ transgenic lines (except OsPSTOL1 WT 18) showed some inhibition to primary root length (**Figure 5.15 B**). This indicates that PSTOL1 protein probably is investing energy in the proliferation of lateral root and root hairs for maximum top-soil exploration for Pi under stress conditions. The result was further substantiated by surface area, total root length and mean diameter. In phosphorus starvation conditions, an increased number of roots and shallower root distribution are crucial adaptive responses. The surface area of empty vector under low Pi is increased but overexpressing OsPSTOL1 WT/ OsPSTOL1$^{2K/R}$ transgenic lines showed the opposite effect which indicates that OsPSTOL1 WT/ OsPSTOL1$^{2K/R}$ protein kinase are functional. Total root length in empty vector did not change under both P treatments unlike showed by Gamuyao et al., 2012 because root or shoot traits can be different due to the genetic variation of rice plants used in the study. The author demonstrated the superior performance of OsPSTOL1 in IR64 (Indica), while we are characterizing the OsPSTOL1 in Nipponbare plants (Japonica). However, we observed that total root length in transgenic lines was decreased which agrees with previous reports on the response of rice roots in low Pi (Vejchasarn et al., 2016) where they showed a decreased length of large lateral roots but increase root hair length and density in phosphate starvation conditions. We demonstrated that total root length decreased in transgenic lines which can be validated by a report from Vejchasarn et al., 2016. Further, we also calculated the mean diameter of roots using IJ_rhizo software. We see the difference in mean diameter between controls and transgenic lines. Overexpressing OsPSTOL1 WT transgenic lines displayed similar mean diameters irrespective of Pi regimes, but overexpressing OsPSTOL1$^{2K/R}$ transgenic lines showed a decrease in mean diameter under low Pi. Further investigation reveals that root diameter is generally reduced in response to low Pi, a process known as "root etiolation" to minimize the metabolic cost and improve soil exploration. While OsPSTOL1$^{2K/R}$ does show root etiolation, OsPSTOL1 WT exhibited no such difference in mean diameter.

Overall, OsPSTOL1 WT will act better independent of Pi status as showed by Gamuyao et al., 2012 without exhibiting root etiolation thereby conserving metabolic cost. Further, there was no substantial difference observed in shoot dry weight and shoot length of transgenic lines regardless of Pi regimes. Nevertheless, the experiment must be repeated because we realized that both independent transgenics of OsPSTOL1 WT lines showed a difference in root length of primary root and OsPSTOL1$^{2K/R}$ 19 response to low Pi is like YFP control while analysing surface area, root length and total root length. This difference can be observed due to the position of integration of gene in the genome being a random event. Therefore, we planned to use another independent line from each genotype based on similar transcript levels and the availability of seeds. The overall trend within three transgenic lines from each genotype will be analysed to determine conclusive results.

We observed a gravitropic response difference between OsPSTOL1 WT and Non-SUMO versions of OsPSTOL1. A shallower root system ensures more uptake of Pi from topsoil. Therefore, the redistribution of roots is linked to a change in root angle (Fang et al., 2009). We analysed the root angle of curvature of OsPSTOL1 WT/ OsPSTOL1$^{2K/R}$ transgenic lines along with controls (**Figure 5.18**). Phenotypic analysis of young seedlings of OsPSTOL1$^{2K/R}$ responded sharply to gravity stimuli than OsPSTOL1 WT signifying a stronger gravitropic response which is very similar to the response observed in *rmd* mutants under normal conditions. According to Huang et al., 2018, *rmd* mutants have a strong gravitropic response but no significant difference was observed in the angle of roots under high and low Pi when compared to control. Therefore, hypothesis can be that OsPSTOL1 WT will have a less gravitropic response, hence making a shallower root system. However, future work would be required to determine phosphate-dependent changes in the root angle of OsPSTOL1 WT/ OsPSTOL1$^{2K/R}$ transgenic lines.

The findings in this chapter might have opened a new direction to elucidate the mechanism and downstream targets of PSTOL1. The knowledge of these findings can be beneficial to improve phosphate uptake efficiency in rice crops.

Chapter 6

Final discussion

6.1 Summary

The main objective of the thesis was to underline the importance of SUMOylation in phosphate starvation signalling. Previous reports had inferred a connection between the role of SUMOylation and phosphate starvation signalling (Datta et al., 2018). Here, the results presented in all three chapters will give an overview of the role of a protein kinase, PSTOL1 under phosphorus deficiency and further how the non-SUMOylatable version of PSTOL1 will affect overall phosphate signalling in plants. Thereby, establishing the necessity of understanding SUMOylation when studying nutrient deficiency.

6.2 Investigating the function of PSTOL1 kinase using a biochemical assay

To begin with, the PSTOL1 protein sequence was searched for possible SUMO binding sites using our in-house bioinformatic tool, HyperSUMO (Neils, PhD thesis 2014). We found two likely SUMO sites and we aimed to mutate these sites. The SUMOylated version of PSTOL1 and non-SUMOylatable version of PSTOL1 respectively (PSTOL1 WT and PSTOL1$^{2K/R}$) proteins were tested for their SUMOylation status in *E.coli*. The gene sequence of PSTOL1 WT and PSTOL1$^{2K/R}$ were cloned in a pMAL vector (c5X) with N-terminal MBP tag and proteins were expressed and purified. *in-vitro* reconstituted SUMOylation assay system showed conjugation on SUMO moieties to PSTOL1 WT while conjugation was not seen in PSTOL1$^{2K/R}$ (**Figure 3.8**). However, the MBP tag also showed SUMO conjugation in *in-vitro* reconstituted SUMOylation assays, therefore, the next step was to investigate PSTOL1 SUMOylation status *in-planta.* PSTOL1 WT and PSTOL1$^{2K/R}$ were subcloned in the plant expression vector with N-terminal YFP tag and transiently expressed in *N.benthamiana*. Immunoprecipitation of YFP-PSTOL1 WT and YFP-PSTOL1$^{2K/R}$ showed a significant reduction in the conjugation of SUMO to YFP-PSTOL1$^{2K/R}$ when compared to YFP-PSTOL1 WT (**Figure 3.11**).

The role of SUMOylation was further explored by investigating the cross-talk of SUMOylation with other PTMs. Previous research from Sadanandom et al., 2015, Khan et al., 2014, Medzihradszky et al., 2013 and Verma et al., 2020 has led us to hypothesize that SUMO may provide a new facet to regulating phosphorylation activity. PSTOL1 being a protein kinase was subjected to two different PTMs - SUMOylation and phosphorylation. **Figures 3.9** and **3.10** showed that PSTOL1 WT was autophosphorylated and can also cross-phosphorylate a test substrate while mutation of SUMO sites in PSTOL eliminated autophosphorylation and cross-phosphorylation activity. Hence, SUMO is appeared to be essential for the full phosphorylation activity of PSTOL1. We hypothesize that the interplay between SUMOylation and phosphorylation may play important role in substrate selectivity by PSTOL1 during normal and stress conditions. Therefore, this interaction may be linked with the repression or activation of the genes regulated by PSTOL1 under phosphate starvation signalling. A similar immunokinase assay was set up using proteins (YFP-PSTOL1 WT and YFP-PSTOL1$^{2K/R}$)

isolated from *N.benthamiana* where autophosphorylated activity was again investigated, however, we could not observe the same trend (**Figure 3.12**). Optimizing the conditions such as establishing the biological conditions or standardizing the buffer conditions for protein isolation for Phos-tag analysis were not tested because of time constraints. Based on this data, we confirmed that PSTOL1 is SUMOylated and that mutation of lysine to arginine produces a significant decrease in SUMO conjugation *in planta* and *in vitro*. Further, SUMOylation also has a fundamental role in regulating the phosphorylation activity of PSTOL1, therefore highlighting the importance of SUMOylation in prioritizing molecular mechanisms.

This chapter also aims to identify potential targets because there are no established targets of PSTOL1 till this study. We chose two techniques – yeast two-hybrid and complex immunoprecipitation (CO-IP). PSTOL1 localizes to the plasma membrane and nucleus in all three systems – *N.benthamiana* leaves, roots and leaves of PSTOL1 *Arabidopsis* transgenic lines and roots of OsPSTOL1 rice transgenic lines. Therefore, PSTOL1 kinase may regulate gene expression by targeting transcription factors to maintain nutrient homeostasis. Y2H screening of the RR library (collection of 1200 *Arabidopsis* thaliana TFs) is a powerful approach to detecting the interaction between two proteins. 13 TFs were identified as the potential targets of PSTOL1 by Y2H screening, however, these transcription factors have to be characterized for their function under phosphate homeostasis. Future work will include real-time PCR analysis of these transcription factors in PSTOL1 *Arabidopsis* transgenic subjected to phosphate treatment. Expression change of these transcription factors under phosphate treatment will be analyzed and based on this data, probable candidate genes will be tested to confirm the interactions *in planta* by CO-IP or BiFC. Interestingly, Y2H screening also identified CRF12 and ERF15 which can be regulated by ARFs to initiate lateral root organogenesis by activating the transcription activity of *LBD16* and *LBD29*. The next step is to phenotype *crf12* and *erf15* mutants under phosphate starvation conditions thereby establishing the role of the hormonal pathway regulated by PSTOL1 under stress conditions.

6.3 Functional characterization of PSTOL1 in a heterologous system, *Arabidopsis*

6.3.1 Studying the role of SUMOylation in regulating PSTOL1 function under phosphate starvation in *Arabidopsis* transgenic lines

The result from the transient expression of PSTOL1 WT/ PSTOL1$^{2K/R}$ in *Nicotiana benthamiana* and in-vivo reconstituted SUMOylation assay has shown that PSTOL1 WT undergoes modification by SUMO (**Figure 3.8 and 3.11**). Following these experiments, SUMOylation of PSTOL1 WT/PSTOL1$^{2K/R}$ was also investigated in *Arabidopsis* transgenic lines. The data from **Figure 4.8** demonstrated that PSTOL1 WT is SUMOylated and that mutation of lysine to arginine considerably abolishes the SUMOylation in PSTOL1$^{2K/R}$. Next, to confirm that PSTOL1 kinase is indeed the subject of SUMOylation, *Arabidopsis* transgenic plants expressing rice protein, PSTOL1 WT and PSTOL1$^{2K/R}$ tagged with N-terminal YFP under constitutive promoter, CaMV 35S - were subjected to high (1.25mM) and low (3µM) Pi treatment. The growth of seedlings was monitored on high and low Pi for 11 days and responses were noted. The Pi-dependent analysis revealed that *Arabidopsis* transgenic plants expressing 35S::PSTOL1 WT-YFP showed significant improvement in overall plant growth while *Arabidopsis* transgenic plants expressing 35S::PSTOL1$^{2K/R}$-YFP showed the phenotype of decrease in the number of lateral roots per cm (lateral root density) and lateral root per plant, inhibition of primary root length and reduced fresh weight biomass. The data indicate that, under low Pi conditions, root growth parameters are impaired in 35S::PSTOL1$^{2K/R}$-YFP *Arabidopsis* transgenic plants and therefore, PSTOL1 kinase positively regulates root growth conferred by SUMOylation. Additionally, the content of free Pi will be analysed in roots and shoots under high and low Pi to further validate PSTOL1 kinase function in phosphate starvation conditions (Huang et al., 2018).

Furthermore, an analysis of PSTOL1's role in regulating root angle will also highlight the mechanism for how the expression of PSTOL1 kinase improves root growth under low Pi in *Arabidopsis* transgenic plants. Previous literature showed that nutrient limitation can induce

changes to RSA. Our data also revealed that the non-SUMOylatable version of PSTOL1 shows a faster alignment of the primary root after gravity stimulation whereas PSTOL1 WT exhibited a defective gravity response which suggests that PSTOL1 WT might make a shallower root system in normal conditions. The next step will include an analysis of the response to gravity stimulation of PSTOL1 WT and PSTOL1$^{2K/R}$ transgenic seedlings on high and low Pi medium.

Wang et al., 2015 showed *PIN3* and *PIN7* are involved in root gravitropism. Real-time analysis of these genes will further indicate that auxin transport might contribute to the gravitropic response in PSTOL1 *Arabidopsis* transgenic plants. Interestingly, *PIN3* is regulated by ARF7. So, PSTOL1 kinase probably phosphorylates ARF7 and in cooperation with auxin transporters (PIN2, PIN3, PIN4 and PIN7) regulates responses to both phosphate starvation and gravity stimulus. However, *Arabidopsis* being a dicot plant has a tap root system therefore it is also important to understand the response of lateral root to gravitropic stimulus.

6.4 SUMO sites in PSTOL1 are critical for regulatory influences on responses in phosphate starvation

6.4.1 Mutation in lysine to arginine affects the SUMOylation status of OsPSTOL1$^{2K/R}$ in rice transgenic lines.

Chapter 5 detailed examination of the role of SUMOylation in regulating PSTOL1 function under low external phosphate conditions in rice. To begin with, transgene expression analysis by real-time PCR revealed that mRNA levels of *OsPSTOL1 WT* in all over-expressing OsPSTOL1 WT rice transgenic lines were low when compared to *OsPSTOL1*$^{2K/R}$ gene expression (**Figure 5.3**). The integration of genes in the genome is a random event, therefore, epigenetic regulation might play an important role in regulating the expression of *PSTOL1*.

The next step was to ascertain the SUMOylation status of YFP-OsPSTOL1 WT and YFP-OsPSTOL1$^{2K/R}$ in rice transgenic lines. We observed from **Figure 5.7** that YFP-OsPSTOL1$^{2K/R}$ and YFP-PSTOL1 WT protein expression levels are same, interestingly, we also observed SUMO conjugated YFP-OsPSTOL1 WT on western blot probed with anti-GFP antibody. Immunoblot analysis in **Figure 5.8** with antiSUMO antibody confirmed the SUMO conjugation of YFP-OsPSTOL1 WT while SUMO conjugation to YFP-OsPSTOL1$^{2K/R}$ was considerably reduced in rice transgenic lines. Due to time constraints, phosphate-dependent SUMOylation of YFP-OsPSTOL1 WT and YFP- OsPSTOL1$^{2K/R}$ was not tested. Moreover, the localization of YFP-OsPSTOL1 WT and YFP- OsPSTOL1$^{2K/R}$ was observed first time in the root of rice transgenic lines. Unlike the localization of PSTOL1 and PSTOL1$^{2K/R}$ in *N. benthamiana* and Arabidopsis, we observed that both YFP-OsPSTOL1 WT and YFP-OsPSTOL1$^{2K/R}$ localized in the nucleus/cytoplasm or cell membrane. Cells showing nuclear localization of YFP-OsPSTOL1 WT decreased and significant number of cells showed the cytoplasm/cell membrane localization of YFP-OsPSTOL1 WT. On the other hand, we did not observe a clear effect on ratio of nuclear/cytoplasm or cell membrane localization of YFP-OsPSTOL1$^{2K/R.}$ Srivastava et al., 2020 showed that on Brassinolide treatment localized BZR1-WT transcription factor in the nucleus more than cytoplasm while there was no difference observed for localization of the non-SUMOylatable version of BZR1. Therefore, ratiometric quantification of nuclear/cytoplasm or cell membrane localization of YFP-OsPSTOL1 WT and YFP- OsPSTOL1$^{2K/R}$ in rice roots under normal conditions will confirm these findings.

6.4.2 Phenotypic analysis of overexpressing YFP-OsPSTOL1 WT and YFP-OsPSTOL1$^{2K/R}$ rice transgenic lines under high and low Pi

Gamuayo et al., 2012 showed that overexpression of PSTOL1 in IR64 (indica) rice plants tends to have more P content due to higher root dry weight compared to null segregants. In rice, usually, the adaptive responses under low Pi are enhanced primary root elongation, increase root hair length and density and shallower root system (Pandey et al., 2021). Overexpression of OsPSTOL1 WT/ OsPSTOL1$^{2K/R}$ in Nipponbare showed primary root length inhibition which indirectly indicates that PSTOL1 kinase might be involved in the proliferation of lateral root and root hairs to make shallower root system to increase top-soil foraging for Pi.

Furthermore, analysis of the surface area, total root length and mean diameter were conducted using IJ-rhizo software. Data analysis of the surface area of roots showed OsPSTOL1 WT/ OsPSTOL1$^{2K/R}$ transgenic lines and Nipponbare (empty vector) showed contrasting phenotypes which indicate that both OsPSTOL1 WT and OsPSTOL1$^{2K/R}$ kinases are functional. On the other hand, there was no significant difference observed in total root length in empty vector seedlings under high and low Pi unlike shown by Gamuyao et al., 2012 which is probably either due to genetic variation between Indica and Japonica rice varieties or technical issues because of software. But we observed that total root length decreased in transgenic lines under Pi-deficient conditions. We speculate that overall root length including the length of lateral root and root hairs is decreased to maximize the surface area for enhanced Pi acquisition. The mean diameter of roots analysis showed that OsPSTOL1$^{2K/R}$ transgenic lines displayed root etiolation in low Pi while OsPSTOL1 WT transgenic lines have the same mean diameter in both conditions. The next important experiment to set up is to measure the total P and Pi content in plants subjected to high and low Pi treatment. Analysis of Pi content in transgenic plants and controls will conclusively indicate that SUMO is a key component of P homeostasis. However, we observed contradictory results between two independent lines of the same genotype while analysing the root parameters. The experiment will have to be repeated with another independent line from each genotype.

Furthermore, based on the gravitropic response of PSTOL1 *Arabidopsis* transgenic lines analysed, we set up the same experiment to evaluate the gravitropic response of OsPSTOL1 rice transgenic lines. OsPSTOL1 WT transgenic lines showed a similar response to PSTOL1 WT *Arabidopsis* transgenic lines when a gravity stimulus is given while the same trend of response was observed between OsPSTOL1$^{2K/R}$ and OsPSTOL1$^{2K/R}$ transgenic lines. The data suggest that there can be a conserved mechanism between monocots and dicots in response to gravity stimulus. Nonetheless, work must be done to validate these preliminary results obtained from evaluating PSTOL1 and OsPSTOL1 transgenic lines. The real-time analysis of genes such as auxin transporters *PIN* and using DR5-based auxin reporter to measure auxin accumulation will further substantiate our phenotype data observed in **Figures 4.14** and **5.19** (Bhosale et al., 2018 and Wang et al., 2015).

From Table 3.2 in Chapter 3, CRF12 was identified as a potential target of PSTOL1. So, we checked its homolog in rice. We found that the homolog of *Arabidopsis* CRF12 is ERF117 in rice. Huang et al., 2022 showed that ethylene is a key hormone that inhibits the elongation of

the primary root and promotes radial expansion usually during soil compaction. We speculate that ERF117 might promote radial expansion which would validate our result of the increase in mean diameter shown in Figure **5.17 C** and primary root elongation was inhibited as shown in **5.15 B**. Buer et al., 2006 showed that in *Arabidopsis* inhibition of root elongation and gravitropic curvature was reduced upon treatment with the ethylene precursor 1-aminocyclopropane carboxylic acid. We hypothesize that difference in gravitropic curvature observed in both *Arabidopsis* and rice as shown in **Figures 4.15** and **5.17** can be due to regulation by ethylene.

Taken together, the same series of experiments conducted with PSTOL1 and OsPSTOL1 transgenic lines and eventually phenotypic analysis indicated a conserved regulatory network, nevertheless, components of this network are yet to be identified.

6.5 Concluding remarks

Taken together, to study the role of SUMO in the phosphate signalling pathway, the project started using a bioinformatic approach (Nelis, PhD thesis 2014) to identify two potential SUMO sites in the *PSTOL1* gene sequence. The research was conducted to unravel the involvement of SUMOylation in regulating PSTOL1 function in phosphate homeostasis in rice and the model plant, *Arabidopsis thaliana* using biochemical assay and phenotypic analysis. The thesis also aims to provide additional experiments that are required to validate the experimental results further. Moreover, integrative global approaches such as the whole transcriptome and proteasome studies will help in deciphering the integration of other PTMs along with SUMOylation in many signalling pathways as shown in this thesis. Given the implications of SUMOylation shown in *Arabidopsis* and rice on plant growth under stress conditions, further research in this area will be an important step to improve crop yield especially economically important crops that are grown in less than perfect growing conditions.

Appendix

Table A.1 Primer sequence used for cloning PSTOL1 WT and PSTOL1$^{2K/R}$ in c5X vector and colony PCR.

The cloning primers used for cloning PSTOL1 WT and PSTOL1$^{2K/R}$ in c5X vector where the forward sequence has extra nucleotides flanking the restriction site, SalI restriction site and start sequence of the gene while reverse primer has end sequence of the gene, PstI restriction site and extra nucleotide flanking the restriction site. pMAL vector-specific primers include forward primer from MBP tag and reverse primer was homologous to rrnB T1 terminator.

Gene Name	Forward sequence	Reverse sequence	Expected size (bp)
PSTOL1	ACG CGT CGA CAT GGA TTA CAA GGA TGA CGA C	AAA CTG CAG TCA AAG CCC TTT TGG TGG	975
pMAL Vector specific primer	GGT CGT CAG ACT GTC GAT GAA GCC	TGT CCT ACT CAG GAG AGC GTT CAC	260

Table A.2 Primers used for qPCR analysis of gene expression.

qPCR primers were used to check the PSTOL1 WT and PSTOL1$^{2K/R}$ in both rice and *Arabidopsis* transgenic lines. Actin primers were used to check actin expression to normalize for changes in specific gene expression. Each primer contains a sequence homologous to a portion of the gene, which was checked against the rice and *Arabidopsis* genome, to ensure it would not bind to other nonspecific sequences of the genome. The primers were first tested on standard PCR and analysed on an agarose gel by electrophoresis to ensure the amplification product is of the expected size by designed primers.

Gene Name	Forward sequence	Reverse sequence	Expected size (bp)
OsPSTOL1	CTG AGC TGGGAT AGA CTG TT	GGT GTTCCTCTTAGTCCGTT	216
PSTOL1	TTT ATA AAG GTA GCC TGC C	GGG TGT TAT CTC CTT GG	246
OsActin	GACCCAGATCATGTTTGAGA CCT	CAGTGTGGCTGACACCAT CAC	130
AtActin	CTTGCACCAAGCAGCATGA A	CCGATCCAGACACTGTAC T TCCTT	68

Table A.3 List of primers for genotyping the transgenic lines and colony PCR.

Genotyping primers are homologous to a portion binding either to fluorescent tag or SUMO sites in a gene. Each primer was checked against rice or *Arabidopsis* to ensure there is no non-specific binding within the genome. The colony PCR primer set includes one vector-specific primer and one gene-specific primer. The forward primer is from the YFP tag, and the reverse primer includes the gene sequence.

Gene Name	Forward primer	Reverse primer	Expected size (bp)
pEarlyGate 104 YFP FP	ACTTCAAGATCCGCCACAAC		
pEarlyGate 201 HA FP	CCACTGACGTAAGGGATGA CGC		
OsOTS 1	GTGGTTCCAACGTGAAGAG G	GGC TCG GTT GAC AAG ACT TC	209
OsOTS 2	ACCATGGCCCGTTTCTTCTA	ACTCTCAGTTTGTGCCCA GA	175
OsOTS 3	TTTCATCCAAAGCAGCAGGG	CCCTTGTGCCAGAAACC TTC	151
OsOTS 4	TTTCATGGAAGCAGGAGGGT	TTGGCAGTCCTCTTCCGA AA	188
OsOTS 5	CTCGACGATTCCCACTTCCA	TCGTCGTGCCTAGGTTTA CC	167
OsOTS 6	TAAAGGAGAGGGCGCAAAG A	TCTCACACTCAACAAGC CCA	198
OsOTS 7	ACACTGGTACCTAGCCGTTC	TGTGGGTGCTGATTCTCT GT	160
OsOTS 8	AGCGGGAAGAGAATGAGCA A	GCTGGCTGAAATCTTCTC CC	188
OsOTS 9	ATGGACAGGCTGAGGATTC A	CATCAGCTCGCTTTGGA CAA	176
OsOTS 10	CTGATGCTGAGATGCCACAC	CCGCCATCATCTTTCTGC AA	219
OsOTS 11	CTCCATCCCCTACCTCCTCT	CGTTGGAGTTGTCGAGG A	176
OsOTS 12	AGTGTGCGTTCAGGGGATAA	CCAGAACATGTATGGCG CAA	221

PSTOL1 CYFP	AGTTTTGTTGCCCCACGGGC	AGGGTCAGCTTGCCGTAGG	322
PSTOL1 K225R	CTGGCTACATTGCACCTGAA	CCAACGACAACCATCTTCCT	247
PSTOL1 K20R	AAGGGCATCAAAGAATGCAC	ATGAATTCCTCCCCATCACC	225
BAR	GAA GTC CAG CTG CCA GAAAC	AGT CGA CCG TGT ACG TCT CC	243
SPS	AGAGATCGACGAAAA	TTTTCGGGATGATCCGAGCC	
Hygromycin	ACTGTCGGGCGTACA	GGTTTCCACTATCGG	85

A.4 Plasmid maps

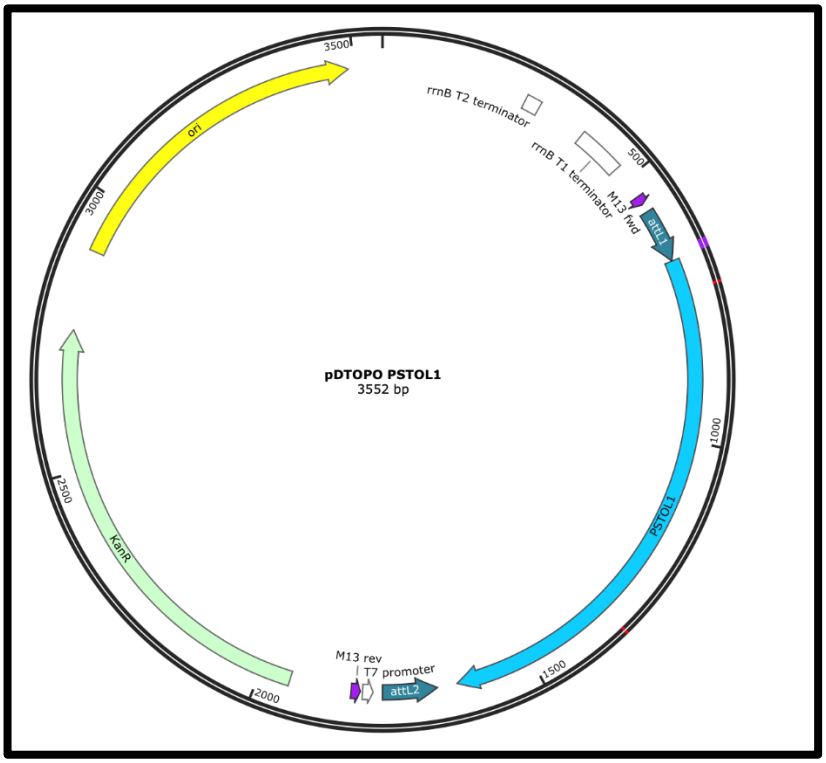

A.4.1 Plasmid map of entry vector pDTOPO PSTOL1

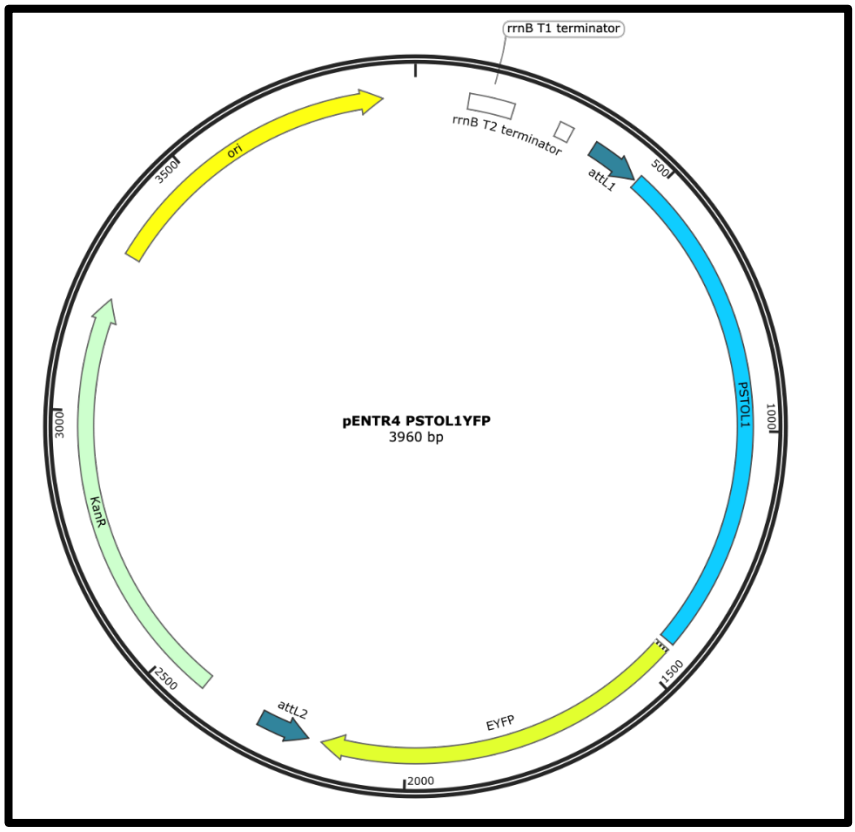

A.4.2 Plasmid map of entry vector pENTR4 PSTOL1 with C-terminal YFP tag

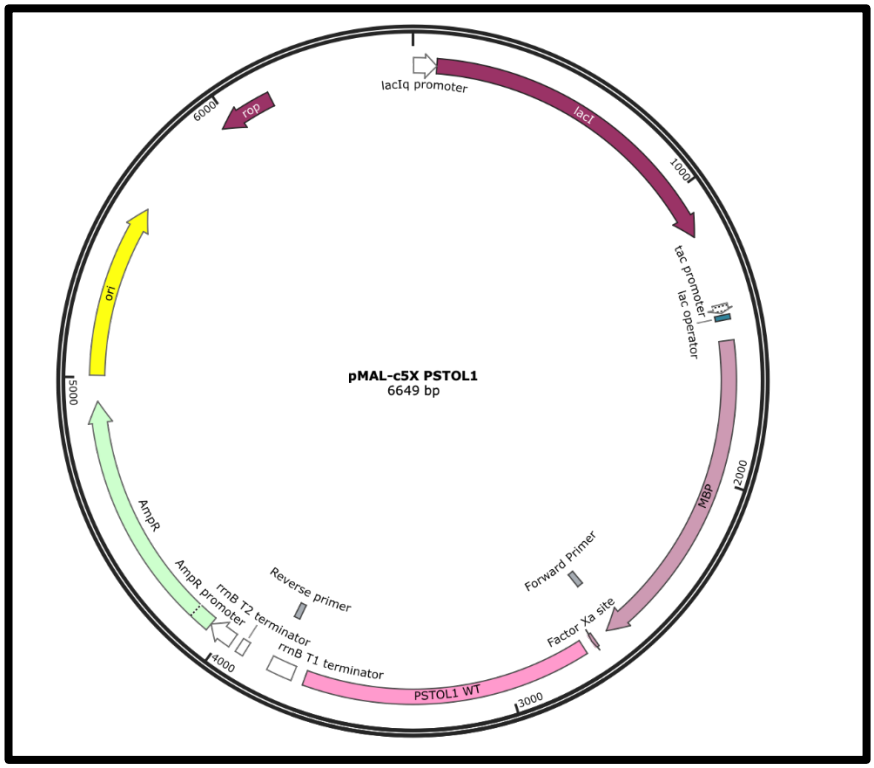

A.4.3 Plasmid map of pMAL-c5X PSTOL1

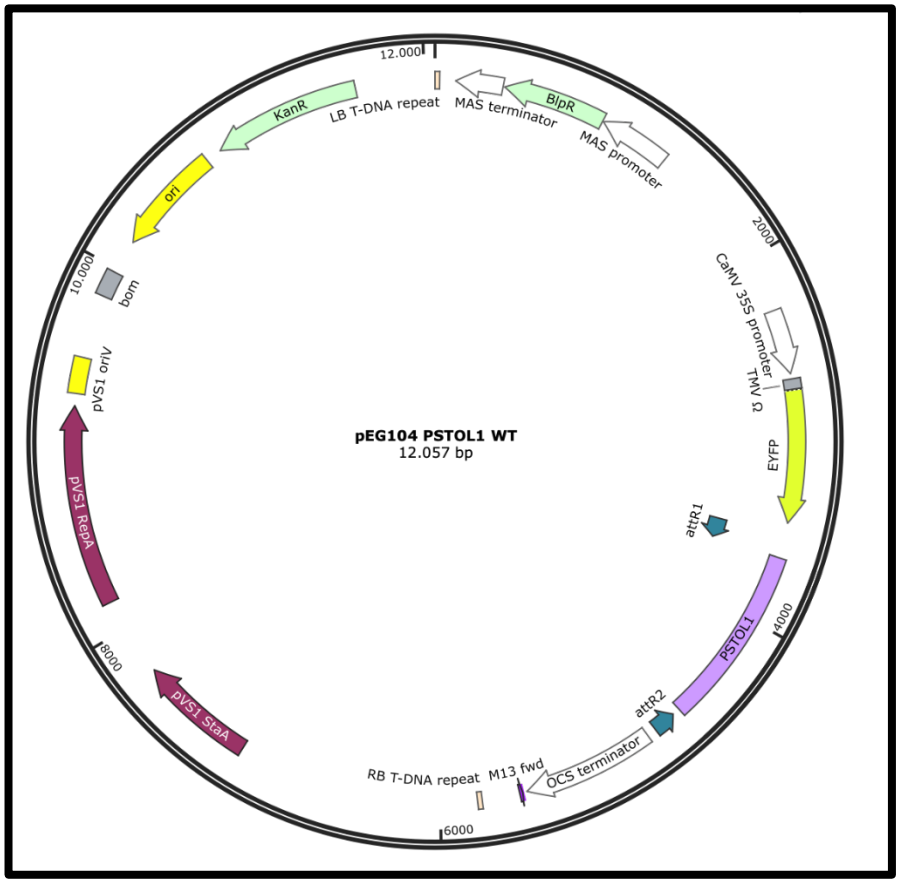

A.4.4 Plasmid map of plant expression vector pEG104 PSTOL1

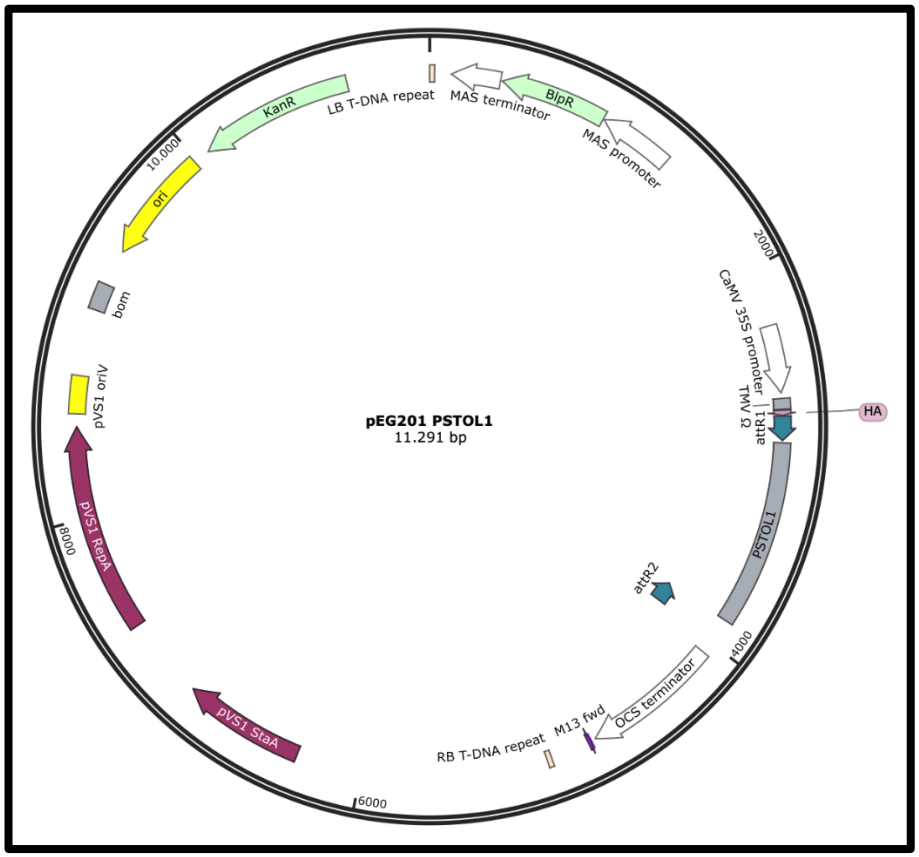

A.4.5 Plasmid map of plant expression vector pEG201 PSTOL1

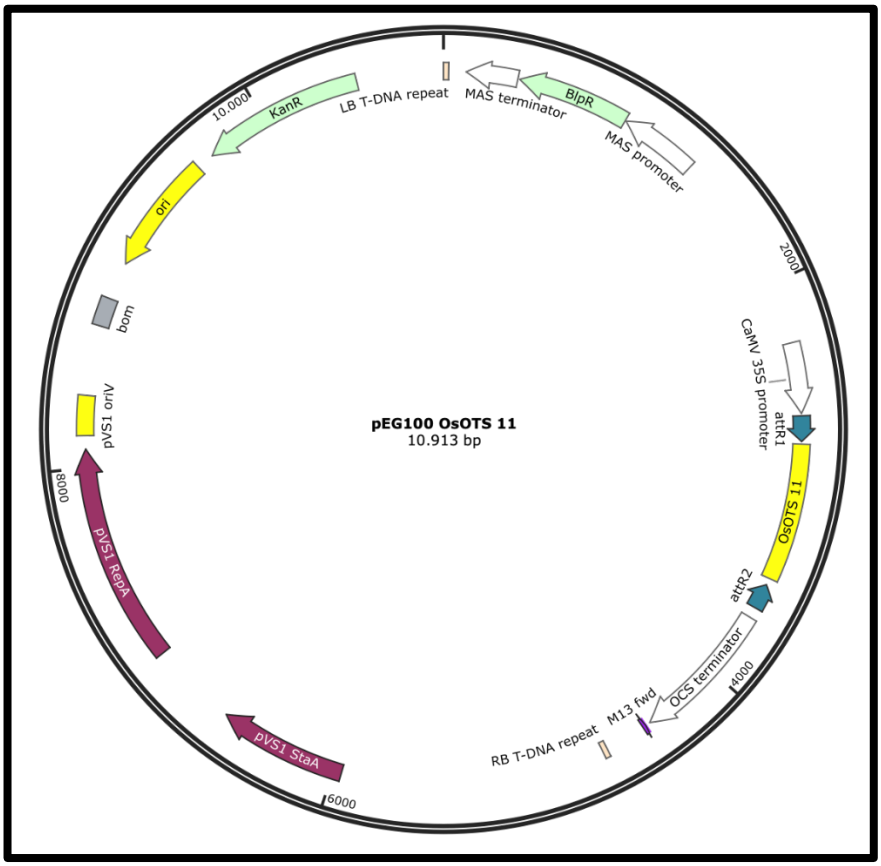

A.4.6 Plasmid map of plant expression vector pEG100 OsOTS 11

References

1. Alewell, C., Ringeval, B., Ballabio, C., Robinson, D.A., Panagos, P. and Borrelli, P., 2020. Global phosphorus shortage will be aggravated by soil erosion. Nature communications, 11(1), pp.1-12.
2. Azevedo, G.C., Cheavegatti-Gianotto, A., Negri, B.F., Hufnagel, B., Magalhaes, J.V., Garcia, A.A.F., Lana, U.G., de Sousa, S.M. and Guimaraes, C.T., 2015. Multiple interval QTL mapping and searching for PSTOL1 homologs associated with root morphology, biomass accumulation and phosphorus content in maize seedlings under low-P. BMC plant biology, 15(1), pp.1-17.
3. Bailey, M., Srivastava, A., Conti, L., Nelis, S., Zhang, C., Florance, H., Love, A., Milner, J., Napier, R., Grant, M. and Sadanandom, A., 2016. Stability of small ubiquitin-like modifier (SUMO) proteases OVERLY TOLERANT TO SALT1 and-2 modulates salicylic acid signalling and SUMO1/2 conjugation in Arabidopsis thaliana. Journal of Experimental Botany, 67(1), pp.353-363.
4. Bari, R., Pant, B.D., Stitt, M. and Scheible, W.R., 2006. PHO2, microRNA399, and PHR1 define a phosphate-signaling pathway in plants. Plant physiology, 141(3), pp.988-999.
5. Bates, T.R. and Lynch, J.P., 1996. Stimulation of root hair elongation in Arabidopsis thaliana by low phosphorus availability. Plant, cell & environment, 19(5), pp.529-538.
6. Beenstock, J., Mooshayef, N. and Engelberg, D., 2016. How do protein kinases take a selfie (autophosphorylate)?. Trends in biochemical sciences, 41(11), pp.938-953

7. Bellini, C., Pacurar, D.I. and Perrone, I., 2014. Adventitious roots and lateral roots: similarities and differences. Annual review of plant biology, 65, pp.639-666.
8. Bernardino, K.C., Pastina, M.M., Menezes, C.B., de Sousa, S.M., Maciel, L.S., Jr, G.C., Guimarães, C.T., Barros, B.A., da Costa e Silva, L., Carneiro, P.C. and Schaffert, R.E., 2019. The genetic architecture of phosphorus efficiency in sorghum involves pleiotropic QTL for root morphology and grain yield under low phosphorus availability in the soil. BMC plant biology, 19, pp.1-15.
9. Bettembourg, M., Dal-Soglio, M., Bureau, C., Vernet, A., Dardoux, A., Portefaix, M., Bes, M., Meynard, D., Mieulet, D., Cayrol, B. and Périn, C., 2017. Root cone angle is enlarged in docs1 LRR-RLK mutants in rice. Rice, 10(1), pp.1-8.
10. Bhosale, R., Giri, J., Pandey, B.K., Giehl, R.F., Hartmann, A., Traini, R., Truskina, J., Leftley, N., Hanlon, M., Swarup, K. and Rashed, A., 2018. A mechanistic framework for auxin dependent Arabidopsis root hair elongation to low external phosphate. Nature communications, 9(1), pp.1-9.
11. Bhutia, K.L., Nongbri, E.L., Gympad, E., Rai, M. and Tyagi, W., 2020. In silico characterization, and expression analysis of rice golden 2-like (OsGLK) members in response to low phosphorous. Molecular Biology Reports, pp.1-21.
12. Bubner, B. and Baldwin, I.T., 2004. Use of real-time PCR for determining copy number and zygosity in transgenic plants. Plant cell reports, 23(5), pp.263-271.
13. Bustos, R., Castrillo, G., Linhares, F., Puga, M.I., Rubio, V., Pérez-Pérez, J., Solano, R., Leyva, A. and Paz-Ares, J., 2010. A central regulatory system largely controls transcriptional activation and repression responses to phosphate starvation in Arabidopsis. PLoS genetics, 6(9).
14. Cao, Y., Yan, Y., Zhang, F., Wang, H.D., Gu, M., Wu, X.N., Sun, S.B. and Xu, G.H., 2014. Fine characterization of OsPHO2 knockout mutants reveals its key role in Pi utilization in rice. Journal of plant physiology, 171(3-4), pp.340-348.
15. Castrillo G, Turck F, Leveugle M, Lecharny A, Carbonero P, Coupland G, Paz-Ares J, Oñate-Sánchez L. Speeding cis-trans regulation discovery by phylogenomic analyses coupled with screenings of an arrayed library of Arabidopsis transcription factors. PLoS One. 2011;6(6):e21524. doi: 10.1371/journal.pone.0021524. Epub 2011 Jun 27. PMID: 21738689; PMCID: PMC3124521.
16. Castrillo, G., Teixeira, P.J.P.L., Paredes, S.H., Law, T.F., de Lorenzo, L., Feltcher, M.E., Finkel, O.M., Breakfield, N.W., Mieczkowski, P., Jones, C.D. and Paz-Ares, J.,

2017. Root microbiota drive direct integration of phosphate stress and immunity. Nature, 543(7646), pp.513-518

17. Catala, R., Ouyang, J., Abreu, I.A., Hu, Y., Seo, H., Zhang, X. and Chua, N.H., 2007. The Arabidopsis E3 SUMO ligase SIZ1 regulates plant growth and drought responses. The Plant Cell, 19(9), pp.2952-2966.
18. Causier, B. and Davies, B., 2002. Analysing protein-protein interactions with the yeast two-hybrid system. Plant molecular biology, 50(6), pp.855-870.
19. Chien, P.S., Chiang, C.P., Leong, S.J. and Chiou, T.J., 2018. Sensing and signaling of phosphate starvation: from local to long distance. Plant and Cell Physiology, 59(9), pp.1714-1722.
20. Chiou, T.J. and Lin, S.I., 2011. Signaling network in sensing phosphate availability in plants. Annual review of plant biology, 62, pp.185-206.
21. Cho, H., Ryu, H., Rho, S., Hill, K., Smith, S., Audenaert, D., Park, J., Han, S., Beeckman, T., Bennett, M.J. and Hwang, D., 2014. A secreted peptide acts on BIN2-mediated phosphorylation of ARFs to potentiate auxin response during lateral root development. Nature cell biology, 16(1), pp.66-76.
22. Clark, L., Sue-Ob, K., Mukkawar, V., Jones, A.R. and Sadanandom, A., 2022. Understanding SUMO-mediated adaptive responses in plants to improve crop productivity. Essays in biochemistry, 66(2), pp.155-168
23. Clough, S.J. and Bent, A.F., 1998. Floral dip: a simplified method for Agrobacterium-mediated transformation of Arabidopsis thaliana. The plant journal, 16(6), pp.735-743.
24. Cong, W.F., Suriyagoda, L.D. and Lambers, H., 2020. Tightening the Phosphorus Cycle through Phosphorus-Efficient Crop Genotypes. Trends in Plant Science.
25. Conti, L., Nelis, S., Zhang, C., Woodcock, A., Swarup, R., Galbiati, M., Tonelli, C., Napier, R., Hedden, P., Bennett, M. and Sadanandom, A., 2014. Small ubiquitin-like modifier protein SUMO enables plants to control growth independently of the phytohormone gibberellin. Developmental cell, 28(1), pp.102-110.
26. Cordell, D. and White, S., 2011. Peak phosphorus: clarifying the key issues of a vigorous debate about long-term phosphorus security. Sustainability, 3(10), pp.2027-2049
27. Cordell, D., Drangert, J.O. and White, S., 2009. The story of phosphorus: global food security and food for thought. Global environmental change, 19(2), pp.292-305.

28. Cornejo, M.J., Luth, D., Blankenship, K.M., Anderson, O.D. and Blechl, A.E., 1993. Activity of a maize ubiquitin promoter in transgenic rice. Plant molecular biology, 23, pp.567-581.
29. Crombez, H., Motte, H. and Beeckman, T., 2019. Tackling plant phosphate starvation by the roots. Developmental cell, 48(5), pp.599-615.
30. Dai Vu, L., Gevaert, K. and De Smet, I., 2018. Protein language: post-translational modifications talking to each other. Trends in plant science, 23(12), pp.1068-1080.
31. Dai, X., Wang, Y., Yang, A. and Zhang, W.H., 2012. OsMYB2P-1, an R2R3 MYB transcription factor, is involved in the regulation of phosphate-starvation responses and root architecture in rice. Plant physiology, 159(1), pp.169-183.
32. Dardick, C., Chen, J., Richter, T., Ouyang, S. and Ronald, P., 2007. The rice kinase database. A phylogenomic database for the rice kinome. Plant physiology, 143(2), pp.579-586.
33. Datta, M., Kaushik, S., Jyoti, A., Mathur, N., Kothari, S.L. and Jain, A., 2018, February. SIZ1-mediated SUMOylation during phosphate homeostasis in plants: Looking beyond the tip of the iceberg. In Seminars in cell & developmental biology (Vol. 74, pp. 123-132). Academic Press.
34. de Bruijne, G., Caldwell, I. and Rosemarin, A., 2009. Peak phosphorus–The next inconvenient truth.
35. De Vega, D., Newton, A.C. and Sadanandom, A., 2018. Posttranslational modifications in priming the plant immune system: ripe for exploitation? FEBS letters, 592(12), pp.1929-1936.
36. Ding, J., Jia, J., Yang, L., Wen, H., Zhang, C., Liu, W. and Zhang, D., 2004. Validation of a rice specific gene, sucrose phosphate synthase, used as the endogenous reference gene for qualitative and real-time quantitative PCR detection of transgenes. Journal of agricultural and food chemistry, 52(11), pp.3372-3377.
37. Doni, F., Suhaimi, N.S.M., Mispan, M.S., Fathurrahman, F., Marzuki, B.M., Kusmoro, J. and Uphoff, N., 2022. Microbial contributions for rice production: From conventional crop management to the use of 'omics' technologies. International Journal of Molecular Sciences, 23(2), p.737.
38. Dubouzet, J.G., Sakuma, Y., Ito, Y., Kasuga, M., Dubouzet, E.G., Miura, S., Seki, M., Shinozaki, K. and Yamaguchi-Shinozaki, K., 2003. OsDREB genes in rice, Oryza

sativa L., encode transcription activators that function in drought, high salt and cold responsive gene

39. Fang, Z., Shao, C., Meng, Y., Wu, P. and Chen, M., 2009. Phosphate signaling in Arabidopsis and Oryza sativa. Plant Science, 176(2), pp.170-180
40. Ferro, E. and Trabalzini, L., 2013. The yeast two-hybrid and related methods as powerful tools to study plant cell signalling. Plant molecular biology, 83(4), pp.287-301.
41. Fixen, P.E. and Johnston, A.M., 2012. World fertilizer nutrient reserves: a view to the future. Journal of the Science of Food and Agriculture, 92(5), pp.1001-1005.
42. Flotho, A. and Melchior, F., 2013. Sumoylation: a regulatory protein modification in health and disease. Annual review of biochemistry, 82.
43. Fujii, H., Chiou, T.J., Lin, S.I., Aung, K. and Zhu, J.K., 2005. A miRNA involved in phosphate-starvation response in Arabidopsis. Current Biology, 15(22), pp.2038-2043.
44. Galletta, B.J. and Rusan, N.M., 2015. A yeast two-hybrid approach for probing protein–protein interactions at the centrosome. In Methods in cell biology (Vol. 129, pp. 251-277). Academic Press.
45. Gamuyao, R., Chin, J.H., Pariasca-Tanaka, J., Pesaresi, P., Catausan, S., Dalid, C., Slamet-Loedin, I., Tecson-Mendoza, E.M., Wissuwa, M. and Heuer, S., 2012. The protein kinase Pstol1 from traditional rice confers tolerance of phosphorus deficiency. Nature, 488(7412), p.535.
46. Gao, W., Lu, L., Qiu, W., Wang, C. and Shou, H., 2017. OsPAP26 encodes a major purple acid phosphatase and regulates phosphate remobilization in rice. Plant and Cell Physiology, 58(5), pp.885-892.
47. Garris, A.J., Tai, T.H., Coburn, J., Kresovich, S. and McCouch, S., 2005. Genetic structure and diversity in Oryza sativa L. Genetics, 169(3), pp.1631-1638
48. Geer, L.Y., Marchler-Bauer, A., Geer, R.C., Han, L., He, J., He, S., Liu, C., Shi, W. and Bryant, S.H., 2010. The NCBI biosystems database. Nucleic acids research, 38(suppl_1), pp.D492-D496.
49. George Seaton, Chris S. Haley, Sara A. Knott, Mike Kearsey, Peter M. Visscher, QTL Express: mapping quantitative trait loci in simple and complex pedigrees , Bioinformatics, Volume 18, Issue 2, February 2002, Pages 339–340
50. Giri, J., Bhosale, R., Huang, G., Pandey, B.K., Parker, H., Zappala, S., Yang, J., Dievart, A., Bureau, C., Ljung, K. and Price, A., 2018. Rice auxin influx carrier

OsAUX1 facilitates root hair elongation in response to low external phosphate. Nature communications, 9(1), p.1408.

51. González, E., Solano, R., Rubio, V., Leyva, A. and Paz-Ares, J., 2005. PHOSPHATE TRANSPORTER TRAFFIC FACILITATOR1 is a plant-specific SEC12-related protein that enables the endoplasmic reticulum exit of a high-affinity phosphate transporter in Arabidopsis. The Plant Cell, 17(12), pp.3500-3512.
52. Guo, M., Ruan, W., Li, C., Huang, F., Zeng, M., Liu, Y., Yu, Y., Ding, X., Wu, Y., Wu, Z. and Mao, C., 2015. Integrative comparison of the role of the PHOSPHATE RESPONSE1 subfamily in phosphate signaling and homeostasis in rice. Plant Physiology, 168(4), pp.1762-1776.
53. Gutiérrez-Alanís, D., Ojeda-Rivera, J.O., Yong-Villalobos, L., Cárdenas-Torres, L. and Herrera-Estrella, L., 2018. Adaptation to phosphate scarcity: tips from Arabidopsis roots. Trends in plant science, 23(8), pp.721-730.
54. Ham, B.K., Chen, J., Yan, Y. and Lucas, W.J., 2018. Insights into plant phosphate sensing and signaling. Current opinion in biotechnology, 49, pp.1-9.
55. Hammond, J.P., Bennett, M.J., Bowen, H.C., Broadley, M.R., Eastwood, D.C., May, S.T., Rahn, C., Swarup, R., Woolaway, K.E. and White, P.J., 2003. Changes in gene expression in Arabidopsis shoots during phosphate starvation and the potential for developing smart plants. Plant Physiology, 132(2), pp.578-596
56. Hasanuzzaman, M. ed., 2020. Agronomic Crops: Volume 3: Stress Responses and Tolerance. Springer Nature.
57. Heuer, S., Lu, X., Chin, J.H., Tanaka, J.P., Kanamori, H., Matsumoto, T., De Leon, T., Ulat, V.J., Ismail, A.M., Yano, M. and Wissuwa, M., 2009. Comparative sequence analyses of the major quantitative trait locus phosphorus uptake 1 (Pup1) reveal a complex genetic structure. Plant Biotechnology Journal, 7(5), pp.456-471.
58. HORIZONTE, B., 2019. Caracterização funcional de genes PSTOL1 na modulação do sistema radicular em milho e sorgo (Doctoral dissertation, UNIVERSIDADE FEDERAL DE MINAS GERAIS)
59. Hu, B., Jiang, Z., Wang, W., Qiu, Y., Zhang, Z., Liu, Y., Li, A., Gao, X., Liu, L., Qian, Y. and Huang, X., 2019. Nitrate–NRT1. 1B–SPX4 cascade integrates nitrogen and phosphorus signalling networks in plants. Nature plants, 5(4), p.401.

60. Hu, B., Zhu, C., Li, F., Tang, J., Wang, Y., Lin, A., Liu, L., Che, R. and Chu, C., 2011. LEAF TIP NECROSIS1 plays a pivotal role in the regulation of multiple phosphate starvation responses in rice. Plant Physiology, 156(3), pp.1101-1115.
61. Hu, B. and Chu, C., 2011. Phosphate starvation signaling in rice. Plant signaling & behavior, 6(7), pp.927-929.
62. Huang, G., Kilic, A., Karady, M., Zhang, J., Mehra, P., Song, X., Sturrock, C.J., Zhu, W., Qin, H., Hartman, S. and Schneider, H.M., 2022. Ethylene inhibits rice root elongation in compacted soil via ABA-and auxin-mediated mechanisms. *Proceedings of the National Academy of Sciences*, *119*(30), p.e2201072119.
63. Huang, G. and Zhang, D., 2020. The plasticity of root systems in response to external phosphate. International Journal of Molecular Sciences, 21(17), p.5955.
64. Huang, G., Liang, W., Sturrock, C.J., Pandey, B.K., Giri, J., Mairhofer, S., Wang, D., Muller, L., Tan, H., York, L.M. and Yang, J., 2018. Rice actin binding protein RMD controls crown root angle in response to external phosphate. Nature communications, 9(1), p.2346.
65. Huang, K.L., Ma, G.J., Zhang, M.L., Xiong, H., Wu, H., Zhao, C.Z., Liu, C.S., Jia, H.X., Chen, L., Kjorven, J.O. and Li, X.B., 2018. The ARF7 and ARF19 transcription factors positively regulate PHOSPHATE STARVATION RESPONSE1 in Arabidopsis roots. Plant physiology, 178(1), pp.413-427.
66. Hufnagel, B., de Sousa, S.M., Assis, L., Guimaraes, C.T., Leiser, W., Azevedo, G.C., Negri, B., Larson, B.G., Shaff, J.E., Pastina, M.M. and Barros, B.A., 2014. Duplicate and conquer: multiple homologs of PHOSPHORUS-STARVATION TOLERANCE1 enhance phosphorus acquisition and sorghum performance on low-phosphorus soils. Plant physiology, 166(2), pp.659-677.
67. Ibrahim, E.I., Attia, K.A., Ghazy, A.I., Itoh, K., Almajhdi, F.N. and Al-Doss, A.A., 2022. Molecular Characterization and Functional Localization of a Novel SUMOylation Gene in Oryza sativa. Biology, 11(1), p.53.
68. Ingham, D.J., Beer, S., Money, S. and Hansen, G., 2001. Quantitative real-time PCR assay for determining transgene copy number in transformed plants. Biotechniques, 31(1), pp.132-140.
69. Inukai, Y., Sakamoto, T., Ueguchi-Tanaka, M., Shibata, Y., Gomi, K., Umemura, I., Hasegawa, Y., Ashikari, M., Kitano, H. and Matsuoka, M., 2005. Crown rootless1,

which is essential for crown root formation in rice, is a target of an AUXIN RESPONSE FACTOR in auxin signaling. The Plant Cell, 17(5), pp.1387-1396.

70. Jiang, J., Xie, Y., Du, J., Yang, C. and Lai, J., 2021. A SUMO ligase OsMMS21 regulates rice development and auxin response. Journal of Plant Physiology, 263, p.153447.
71. Johnston, A.E., Poulton, P.R., Fixen, P.E. and Curtin, D., 2014. Phosphorus: its efficient use in agriculture. In Advances in agronomy (Vol. 123, pp. 177-228). Academic Press.
72. Kavka, M., Majcherczyk, A., Kües, U. and Polle, A., 2021. Phylogeny, tissue-specific expression, and activities of root-secreted purple acid phosphatases for P uptake from ATP in P starved poplar. Plant Science, 307, p.110906.
73. Keskin, O., Gursoy, A., Ma, B. and Nussinov, R., 2008. Principles of protein− protein interactions: what are the preferred ways for proteins to interact?. Chemical reviews, 108(4), pp.1225-1244.
74. Kettenburg, A.T., Lopez, M.A., Yogendra, K., Prior, M.J., Rose, T., Bimson, S., Heuer, S., Roy, S.J. and Bailey-Serres, J., 2022. OsPSTOL1 is prevalent in upland rice and its expression in wheat enhances root growth and hastens low phosphate signaling. bioRxiv, pp.2022-11.
75. Khan, M., Rozhon, W., Unterholzner, S.J., Chen, T., Eremina, M., Wurzinger, B., Bachmair, A., Teige, M., Sieberer, T., Isono, E. and Poppenberger, B., 2014. Interplay between phosphorylation and SUMOylation events determines CESTA protein fate in brassinosteroid signalling. Nature communications, 5(1), pp.1-10.
76. Kinoshita, E., Kinoshita-Kikuta, E. and Koike, T., 2017. Zn (II)–Phos-Tag SDS-PAGE for Separation and Detection of a DNA Damage-Related Signaling Large Phosphoprotein. In ATM Kinase (pp. 113-126). Humana Press, New York, NY.
77. Kinoshita, E., Kinoshita-Kikuta, E. and Koike, T., 2015. Advances in Phos-tag-based methodologies for separation and detection of the phosphoproteome. Biochimica et Biophysica Acta (BBA)-Proteins and Proteomics, 1854(6), pp.601-608.
78. Kinoshita, E., Kinoshita-Kikuta, E. and Koike, T., 2022. History of Phos-tag technology for phosphoproteomics. Journal of Proteomics, 252, p.104432.
79. Kinoshita, E., Kinoshita-Kikuta, E., Takiyama, K. and Koike, T., 2006. Phosphate-binding tag, a new tool to visualize phosphorylated proteins. Molecular & cellular proteomics, 5(4), pp.749-757.

80. Kitomi, Y., Hanzawa, E., Kuya, N., Inoue, H., Hara, N., Kawai, S., Kanno, N., Endo, M., Sugimoto, K., Yamazaki, T. and Sakamoto, S., 2020. Root angle modifications by the DRO1 homolog improve rice yields in saline paddy fields. Proceedings of the National Academy of Sciences, 117(35), pp.21242-21250.
81. Kitomi, Y., Ito, H., Hobo, T., Aya, K., Kitano, H. and Inukai, Y., 2011. The auxin responsive AP2/ERF transcription factor CROWN ROOTLESS5 is involved in crown root initiation in rice through the induction of OsRR1, a type-A response regulator of cytokinin signaling. The Plant Journal, 67(3), pp.472-484.
82. Kohli, A., Twyman, R.M., Abranches, R., Wegel, E., Stoger, E. and Christou, P., 2003. Transgene integration, organization and interaction in plants. Plant molecular biology, 52(2), pp.247-258.
83. Krämer, U., 2015. Planting molecular functions in an ecological context with Arabidopsis thaliana. Elife, 4.
84. Kumar, S., Stecher, G., Li, M., Knyaz, C. and Tamura, K., 2018. MEGA X: molecular evolutionary genetics analysis across computing platforms. Molecular biology and evolution, 35(6), p.1547.
85. Kumar, S., Chugh, C., Seem, K., Kumar, S., Vinod, K.K. and Mohapatra, T., 2021. Characterization of contrasting rice (Oryza sativa L.) genotypes reveals the Pi-efficient schema for phosphate starvation tolerance. BMC Plant Biology, 21(1), pp.1-26.
86. Labrou, N.E., 2013. Clostripain. In Handbook of Proteolytic Enzymes (pp. 2323-2327). Academic Press.
87. Lan, P., Li, W. and Schmidt, W., 2012. Complementary proteome and transcriptome profiling in phosphate-deficient Arabidopsis roots reveals multiple levels of gene regulation. Molecular & Cellular Proteomics, 11(11), pp.1156-1166.
88. Larkin, M.A., Blackshields, G., Brown, N.P., Chenna, R., McGettigan, P.A., McWilliam, H., Valentin, F., Wallace, I.M., Wilm, A., Lopez, R. and Thompson, J.D., 2007. Clustal W and Clustal X version 2.0. bioinformatics, 23(21), pp.2947-2948.
89. Li, J.Y., Wang, J. and Zeigler, R.S., 2014. The 3,000 rice genomes project: new opportunities and challenges for future rice research. Gigascience, 3(1), pp.2047-217X.
90. Li, Z., Hu, Q., Zhou, M., Vandenbrink, J., Li, D., Menchyk, N., Reighard, S., Norris, A., Liu, H., Sun, D. and Luo, H., 2013. Heterologous expression of Os SIZ 1, a rice SUMO E 3 ligase, enhances broad abiotic stress tolerance in transgenic creeping bentgrass. Plant Biotechnology Journal, 11(4), pp.432-445.

91. Liao, Z., Yu, H., Duan, J., Yuan, K., Yu, C., Meng, X., Kou, L., Chen, M., Jing, Y., Liu, G. and Smith, S.M., 2019. SLR1 inhibits MOC1 degradation to coordinate tiller number and plant height in rice. Nature communications, 10(1), p.2738.
92. Lin, S.I., Santi, C., Jobet, E., Lacut, E., El Kholti, N., Karlowski, W.M., Verdeil, J.L., Breitler, J.C., Périn, C., Ko, S.S. and Guiderdoni, E., 2010. Complex regulation of two target genes encoding SPX-MFS proteins by rice miR827 in response to phosphate starvation. Plant and Cell Physiology, 51(12), pp.2119-2131
93. Londo, J.P., Chiang, Y.C., Hung, K.H., Chiang, T.Y. and Schaal, B.A., 2006. Phylogeography of Asian wild rice, Oryza rufipogon, reveals multiple independent domestications of cultivated rice, Oryza sativa. Proceedings of the National Academy of Sciences, 103(25), pp.9578-9583.
94. Lott, J.N., Kolasa, J., Batten, G.D. and Campbell, L.C., 2011. The critical role of phosphorus in world production of cereal grains and legume seeds. Food Security, 3(4), pp.451-462.
95. Lu, H., Wang, F., Wang, Y., Lin, R., Wang, Z. and Mao, C., 2022. Molecular mechanisms and genetic improvement of low-phosphorus tolerance in rice. Plant, Cell & Environment.
96. Mao, C., He, J., Liu, L., Deng, Q., Yao, X., Liu, C., Qiao, Y., Li, P. and Ming, F., 2020. OsNAC2 integrates auxin and cytokinin pathways to modulate rice root development. Plant biotechnology journal, 18(2), pp.429-442.
97. Medzihradszky, M., Bindics, J., Ádám, É., Viczián, A., Klement, É., Lorrain, S., Gyula, P., Mérai, Z., Fankhauser, C., Medzihradszky, K.F. and Kunkel, T., 2013. Phosphorylation of phytochrome B inhibits light-induced signaling via accelerated dark reversion in Arabidopsis. The Plant Cell, 25(2), pp.535-544.
98. Matsumoto, T., Wu, J., Itoh, T., Numa, H., Antonio, B. and Sasaki, T., 2016. The Nipponbare genome and the next-generation of rice genomics research in Japan. Rice, 9(1), p.33.
99. Meng, F., Xiang, D., Zhu, J., Li, Y. and Mao, C., 2019. Molecular mechanisms of root development in rice. Rice, 12(1), pp.1-10.
100. Mickelbart, M.V., Hasegawa, P.M. and Bailey-Serres, J., 2015. Genetic mechanisms of abiotic stress tolerance that translate to crop yield stability. Nature Reviews Genetics, 16(4), pp.237-251.

101. Mieog, J.C., Howitt, C.A. and Ral, J.P., 2013. Fast-tracking development of homozygous transgenic cereal lines using a simple and highly flexible real-time PCR assay. BMC Plant Biology, 13(1), pp.1-9.

102. Mishra, N., Srivastava, A.P., Esmaeili, N., Hu, W. and Shen, G., 2018. Overexpression of the rice gene OsSIZ1 in Arabidopsis improves drought-, heat-, and salt-tolerance simultaneously. PLoS One, 13(8), p.e0201716.

103. Miura, K., Sato, A., Ohta, M. and Furukawa, J., 2011. Increased tolerance to salt stress in the phosphate-accumulating Arabidopsis mutants siz1 and pho2. Planta, 234, pp.1191-1199.

104. Miura, K. and Hasegawa, P.M., 2010. Sumoylation and other ubiquitin-like post-translational modifications in plants. Trends in cell biology, 20(4), pp.223-232.

105. Miura, K., Jin, J.B., Lee, J., Yoo, C.Y., Stirm, V., Miura, T., Ashworth, E.N., Bressan, R.A., Yun, D.J. and Hasegawa, P.M., 2007. SIZ1-mediated sumoylation of ICE1 controls CBF3/DREB1A expression and freezing tolerance in Arabidopsis. The Plant Cell, 19(4), pp.1403-1414.

106. Miura, K., Lee, J., Gong, Q., Ma, S., Jin, J.B., Yoo, C.Y., Miura, T., Sato, A., Bohnert, H.J. and Hasegawa, P.M., 2011. SIZ1 regulation of phosphate starvation-induced root architecture remodeling involves the control of auxin accumulation. Plant physiology, 155(2), pp.1000-1012.

107. Miura, K., Rus, A., Sharkhuu, A., Yokoi, S., Karthikeyan, A.S., Raghothama, K.G., Baek, D., Koo, Y.D., Jin, J.B., Bressan, R.A. and Yun, D.J., 2005. The Arabidopsis SUMO E3 ligase SIZ1 controls phosphate deficiency responses. Proceedings of the National Academy of Sciences, 102(21), pp.7760-7765.

108. Mukatira, U.T., Liu, C., Varadarajan, D.K. and Raghothama, K.G., 2001. Negative regulation of phosphate starvation-induced genes. Plant Physiology, 127(4), pp.1854-1862.

109. Mukherjee, A., Sarkar, S., Chakraborty, A.S., Yelne, R., Kavishetty, V., Biswas, T., Mandal, N. and Bhattacharyya, S., 2014. Phosphate acquisition efficiency and phosphate starvation tolerance locus (PSTOL1) in rice. Journal of genetics, 93, pp.683-688.

110. Muday, G.K., Rahman, A. and Binder, B.M., 2012. Auxin and ethylene: collaborators or competitors?. Trends in plant science, 17(4), pp.181-195.

111. Nedelciu, C.E., Ragnarsdottir, K.V., Schlyter, P. and Stjernquist, I., 2020. Global phosphorus supply chain dynamics: Assessing regional impact to 2050. Global food security, 26, p.100426.

112. Negi, M., Sanagala, R., Rai, V. and Jain, A., 2016. Deciphering phosphate deficiency-mediated temporal effects on different root traits in rice grown in a modified hydroponic system. Frontiers in plant science, 7, p.550.

113. Nemoto, K., Seto, T., Takahashi, H., Nozawa, A., Seki, M., Shinozaki, K., Endo, Y. and Sawasaki, T., 2011. Autophosphorylation profiling of Arabidopsis protein kinases using the cell-free system. Phytochemistry, 72(10), pp.1136-1144.

114. Neogy, A., Garg, T., Kumar, A., Dwivedi, A.K., Singh, H., Singh, U., Singh, Z., Prasad, K., Jain, M. and Yadav, S.R., 2019. Genome-Wide Transcript Profiling Reveals an Auxin-Responsive Transcription Factor, OsAP2/ERF-40, Promoting Rice Adventitious Root Development. Plant and Cell Physiology, 60(10), pp.2343-2355.

115. Ni, J.J., Wu, P., Senadhira, D. and Huang, N., 1998. Mapping QTLs for phosphorus deficiency tolerance in rice (Oryza sativa L.). Theoretical and Applied Genetics, 97(8), pp.1361-1369.

116. Nigam, N., Singh, A., Sahi, C., Chandramouli, A. and Grover, A., 2008. SUMO-conjugating enzyme (Sce) and FK506-binding protein (FKBP) encoding rice (Oryza sativa L.) genes: genome-wide analysis, expression studies and evidence for their involvement in abiotic stress response. Molecular Genetics and Genomics, 279, pp.371-383.

117. Nirubana, V., Vanniarajan, C., Aananthi, N. and Ramalingam, J., 2020. Screening tolerance to phosphorus starvation and haplotype analysis using phosphorus uptake 1 (Pup1) QTL linked markers in rice genotypes. Physiology and Molecular Biology of Plants, pp.1-15.

118. Nishioka, K., Kato, Y., Ozawa, S.I., Takahashi, Y. and Sakamoto, W., 2021. Phos-tag-based approach to study protein phosphorylation in the thylakoid membrane. Photosynthesis research, 147(1), pp.107-124.

119. Nurdiani, D., Widyajayantie, D. and Nugroho, S., 2018. OsSCE1 encoding SUMO E2-conjugating enzyme involves in drought stress response of Oryza sativa. Rice Science, 25(2), pp.73-81.

120. O'Donoghue, L. and Smolenski, A., 2022. Analysis of protein phosphorylation using Phos-tag gels. Journal of Proteomics, 259, p.104558

121. O'Donoghue, L. and Smolenski, A., 2022. Analysis of protein phosphorylation using Phos-tag gels. Journal of Proteomics, 259, p.104558

122. Okada, S., Nagabuchi, M., Takamura, Y., Nakagawa, T., Shinmyozu, K., Nakayama, J.I. and Tanaka, K., 2009. Reconstitution of Arabidopsis thaliana SUMO pathways in E. coli: functional evaluation of SUMO machinery proteins and mapping of SUMOylation sites by mass spectrometry. Plant and cell physiology, 50(6), pp.1049-1061.

123. Pan, W., Wu, Y. and Xie, Q., 2019. Regulation of ubiquitination is central to the phosphate starvation response. Trends in plant science, 24(8), pp.755-769.

124. Panchal, P., Miller, A.J. and Giri, J., 2021. Organic acids: versatile stress-response roles in plants. Journal of Experimental Botany, 72(11), pp.4038-4052.

125. Pandey, B.K., Verma, L., Prusty, A., Singh, A.P., Bennett, M.J., Tyagi, A.K., Giri, J. and Mehra, P., 2021. OsJAZ11 regulates phosphate starvation responses in rice. Planta, 254(1), pp.1-16.

126. Pandey, S., Byerlee, D., Dawe, D., Dobermann, A., Mohanty, S., Rozelle, S. and Hardy, B., 2010. Rice in the global economy. Los Banos, Phillipines: International Rice Research Institute.

127. Pariasca-Tanaka, J., Chin, J.H., Dramé, K.N., Dalid, C., Heuer, S. and Wissuwa, M., 2014. A novel allele of the P-starvation tolerance gene OsPSTOL1 from African rice (Oryza glaberrima Steud) and its distribution in the genus Oryza. Theoretical and applied genetics, 127(6), pp.1387-1398.

128. Pariasca-Tanaka, J., Satoh, K., Rose, T., Mauleon, R. and Wissuwa, M., 2009. Stress response versus stress tolerance: a transcriptome analysis of two rice lines contrasting in tolerance to phosphorus deficiency. Rice, 2(4), pp.167-185.

129. Pei, W., Jain, A., Zhao, G., Feng, B., Xu, D. and Wang, X., 2020. Knockdown of OsSAE1a affects the growth and development and phosphate homeostasis in rice. Journal of Plant Physiology, 255, p.153275

130. Pei, W., Jain, A., Sun, Y., Zhang, Z., Ai, H., Liu, X., Wang, H., Feng, B., Sun, R., Zhou, H. and Xu, G., 2017. OsSIZ 2 exerts regulatory influences on the developmental responses and phosphate homeostasis in rice. Scientific Reports, 7(1), p.12280.

131. Péret, B., Clément, M., Nussaume, L. and Desnos, T., 2011. Root developmental adaptation to phosphate starvation: better safe than sorry. Trend in plant science, 16(8), pp.442-450

132. Péret, B., Desnos, T., Jost, R., Kanno, S., Berkowitz, O. and Nussaume, L., 2014. Root architecture responses: in search of phosphate. Plant physiology, 166(4), pp.1713-1723.

133. Pierret, A., Gonkhamdee, S., Jourdan, C. and Maeght, J.L., IJ-Rhizo: an open-source software to measure scanned images of root samples (2013) Plant Soil.

134. Prathap, V., Kumar, A., Maheshwari, C. and Tyagi, A., 2022. Phosphorus homeostasis: acquisition, sensing, and long-distance signaling in plants. Molecular Biology Reports, pp.1-16.

135. Pitts, R.J., Cernac, A. and Estelle, M., 1998. Auxin and ethylene promote root hair elongation in Arabidopsis. The Plant Journal, 16(5), pp.553-560

136. Puga, M.I., Mateos, I., Charukesi, R., Wang, Z., Franco-Zorrilla, J.M., de Lorenzo, L., Irigoyen, M.L., Masiero, S., Bustos, R., Rodríguez, J. and Leyva, A., 2014. SPX1 is a phosphate-dependent inhibitor of Phosphate Starvation Response 1 in Arabidopsis. Proceedings of the National Academy of Sciences, 111(41), pp.14947-14952.

137. Raghothama, K.G. and Karthikeyan, A.S., 2005. Phosphate acquisition. Plant and Soil, 274(1-2), p.37.

138. Ramazi, S. and Zahiri, J., 2021. Post-translational modifications in proteins: resources, tools and prediction methods. Database, 2021.

139. Ray, J.D., Yu, L., McCouch, S.R., Champoux, M.C., Wang, G. and Nguyen, H.T., 1996. Mapping quantitative trait loci associated with root penetration ability in rice (Oryza sativa L.). Theoretical and Applied Genetics, 92(6), pp.627-636.

140. Rosa, M.T., Almeida, D.M., Pires, I.S., da Rosa Farias, D., Martins, A.G., da Maia, L.C., de Oliveira, A.C., Saibo, N.J., Oliveira, M.M. and Abreu, I.A., 2018. Insights into the transcriptional and post-transcriptional regulation of the rice SUMOylation machinery and into the role of two rice SUMO proteases. *BMC plant biology*, *18*(1), pp.1-18.

141. Roy, D. and Sadanandom, A., 2021. SUMO mediated regulation of transcription factors as a mechanism for transducing environmental cues into cellular signaling in plants. Cellular and Molecular Life Sciences, 78, pp.2641-2664.

142. Rubio, V., Linhares, F., Solano, R., Martín, A.C., Iglesias, J., Leyva, A. and Paz-Ares, J., 2001. A conserved MYB transcription factor involved in phosphate starvation signaling both in vascular plants and in unicellular algae. Genes & development, 15(16), pp.2122-2133.

143. Sadanandom, A., Ádám, É., Orosa, B., Viczián, A., Klose, C., Zhang, C., Josse, E.M., Kozma-Bognár, L. and Nagy, F., 2015. SUMOylation of phytochrome-B negatively regulates light-induced signaling in Arabidopsis thaliana. Proceedings of the National Academy of Sciences, 112(35), pp.11108-11113.

144. Sanagala, R., Moola, A.K. and Diana, R.K.B., 2017. A review on advanced methods in plant gene targeting. Journal of Genetic Engineering and Biotechnology, 15(2), pp.317-321.

145. Sánchez-Calderón, L., López-Bucio, J., Chacón-López, A., Cruz-Ramírez, A., Nieto-Jacobo, F., Dubrovsky, J.G. and Herrera-Estrella, L., 2005. Phosphate starvation induces a determinate developmental program in the roots of Arabidopsis thaliana. Plant and Cell Physiology, 46(1), pp.174-184.

146. Satheesh, V., Tahir, A., Li, J. and Lei, M., 2022. Plant phosphate nutrition: sensing the stress. Stress Biology, pp.1-14.

147. Schönberg, A., Rödiger, A., Mehwald, W., Galonska, J., Christ, G., Helm, S., Thieme, D., Majovsky, P., Hoehenwarter, W. and Baginsky, S., 2017. Identification of STN7/STN8 kinase targets reveals connections between electron transport, metabolism and gene expression. The Plant Journal, 90(6), pp.1176-1186.

148. Sega, P. and Pacak, A., 2019. Plant PHR transcription factors: put on a map. Genes, 10(12), p.1018.

149. Shao, Y., Zhou, H.Z., Wu, Y., Zhang, H., Lin, J., Jiang, X., He, Q., Zhu, J., Li, Y., Yu, H. and Mao, C., 2019. OsSPL3, an SBP-domain protein, regulates crown root development in rice. The Plant Cell, 31(6), pp.1257-1275.

150. Sharma, S., Borah, P., Meena, M.K., Bindraban, P. and Pandey, R., 2018. Evaluation of genotypic variation for growth of rice seedlings under optimized hydroponics medium. Indian J. Genet, 78(3), pp.292-301.

151. Shavrukov, Y.N., 2016. CAPS markers in plant biology. Russian Journal of Genetics: Applied Research, 6(3), pp.279-287

152. Shen, C., Wang, S., Zhang, S., Xu, Y., Qian, Q., Qi, Y. and Jiang, D.A., 2013. OsARF16, a transcription factor, is required for auxin and phosphate starvation response in rice (Oryza sativa L.). Plant, cell & environment, 36(3), pp.607-620.

153. Shepherd, C.T., Lauter, A.N.M. and Scott, M.P., 2009. Determination of transgene copy number by real-time quantitative PCR. In Transgenic Maize (pp. 129-134). Humana Press, Totowa, NJ.

154. Shin, H., Shin, H.S., Dewbre, G.R. and Harrison, M.J., 2004. Phosphate transport in Arabidopsis: Pht1; 1 and Pht1; 4 play a major role in phosphate acquisition from both low-and high-phosphate environments. The Plant Journal, 39(4), pp.629-642.

155. Singh, P. and Sinha, A.K., 2016. A positive feedback loop governed by SUB1A1 interaction with MITOGEN-ACTIVATED PROTEIN KINASE3 imparts submergence tolerance in rice. The Plant Cell, 28(5), pp.1127-1143.

156. Srivastava, M., Sadanandom, A. and Srivastava, A.K., 2021. Towards understanding the multifaceted role of SUMOylation in plant growth and development. Physiologia plantarum, 171(1), pp.77-85.

157. Srivastava, A.K., Zhang, C., Caine, R.S., Gray, J. and Sadanandom, A., 2017. Rice SUMO protease Overly Tolerant to Salt 1 targets the transcription factor, Osb ZIP 23 to promote drought tolerance in rice. The Plant Journal, 92(6), pp.1031-1043.

158. Srivastava, A.K., Zhang, C., Yates, G., Bailey, M., Brown, A. and Sadanandom, A., 2016. SUMO is a critical regulator of salt stress responses in rice. Plant Physiology, 170(4), pp.2378-2391

159. Strock, C.F., De La Riva, L.M. and Lynch, J.P., 2018. Reduction in root secondary growth as a strategy for phosphorus acquisition. Plant physiology, 176(1), pp.691-703.

160. Sugiyama, Y. and Uezato, Y., 2022. Analysis of protein kinases by Phos-tag SDS-PAGE. Journal of Proteomics, p.104485.

161. Teramura, H., Yamada, K., Ito, K., Kasahara, K., Kikuchi, T., Kioka, N., Fukuda, M., Kusano, H., Tanaka, K. and Shimada, H., 2021. Characterization of novel SUMO family genes in the rice genome. Genes & Genetic Systems, 96(1), pp.25-32.

162. Tran, H.T., Hurley, B.A. and Plaxton, W.C., 2010. Feeding hungry plants: the role of purple acid phosphatases in phosphate nutrition. Plant Science, 179(1-2), pp.14-27

163. Ueda, Y., Kiba, T. and Yanagisawa, S., 2020. Nitrate-inducible NIGT1 proteins modulate phosphate uptake and starvation signalling via transcriptional regulation of SPX genes. The Plant Journal, 102(3), pp.448-466.

164. Ueda, Y., Sakuraba, Y. and Yanagisawa, S., 2021. Environmental control of phosphorus acquisition: a piece of the molecular framework underlying nutritional homeostasis. Plant and Cell Physiology

165. Vaccari, D.A., 2009. Phosphorus: a looming crisis. Scientific American, 300(6), pp.54-5

166. Verma, V., Srivastava, A.K., Gough, C., Campanaro, A., Srivastava, M., Morrell, R., Joyce, J., Bailey, M., Zhang, C., Krysan, P.J. and Sadanandom, A., 2021. SUMO enables substrate selectivity by mitogen-activated protein kinases to regulate immunity in plants. Proceedings of the National Academy of Sciences, 118(10), p.e2021351118.

167. Verma, V., Croley, F. and Sadanandom, A., 2018. Fifty shades of SUMO: its role in immunity and at the fulcrum of the growth–defence balance. Molecular plant pathology, 19(6), pp.1537-1544.

168. Vidalain, P.O., Boxem, M., Ge, H., Li, S. and Vidal, M., 2004. Increasing specificity in high-throughput yeast two-hybrid experiments. Methods, 32(4), pp.363-370

169. Vigueira, C.C., Small, L.L. and Olsen, K.M., 2016. Long-term balancing selection at the Phosphorus Starvation Tolerance 1 (PSTOL1) locus in wild, domesticated and weedy rice (Oryza). BMC Plant Biology, 16, pp.1-10

170. Wissuwa, M. and Ae, N., 2001. Genotypic variation for tolerance to phosphorus deficiency in rice and the potential for its exploitation in rice improvement. Plant Breeding, 120(1), pp.43-48

171. Wissuwa, M., Yano, M. and Ae, N., 1998. Mapping of QTLs for phosphorus-deficiency tolerance in rice (Oryza sativa L.). Theoretical and Applied Genetics, 97(5-6), pp.777-783.

172. Wissuwa, M., 2005. Combining a modelling with a genetic approach in establishing associations between genetic and physiological effects in relation to phosphorus uptake. Plant and Soil, 269(1-2), pp.57-68.

173. Walan, P., Phosphate: All hopes rest on Morocco with 75% of remaining reserves.

174. Wang, F., Deng, M., Xu, J., Zhu, X. and Mao, C., 2018, February. Molecular mechanisms of phosphate transport and signaling in higher plants. In Seminars in cell & developmental biology (Vol. 74, pp. 114-122). Academic Press.

175. Abbas, H., Naeem, M.K., Rubab, M., Widemann, E., Uzair, M., Zahra, N., Saleem, B., Rahim, A.A., Inam, S., Imran, M. and Hafeez, F., 2022. Role of Wheat Phosphorus Starvation Tolerance 1 Genes in Phosphorus Acquisition and Root Architecture. Genes, 13(3), p.487.

176. Lynch, J.P., 2011. Root phenes for enhanced soil exploration and phosphorus acquisition: tools for future crops. Plant physiology, 156(3), pp.1041-1049

177. Wang, H., Sun, R., Cao, Y., Pei, W., Sun, Y., Zhou, H., Wu, X., Zhang, F., Luo, L., Shen, Q. and Xu, G., 2015. OsSIZ1, a SUMO E3 ligase gene, is involved in the regulation of the responses to phosphate and nitrogen in rice. Plant and Cell Physiology, 56(12), pp.2381-2395.

178. Wang, H.Z., Yang, K.Z., Zou, J.J., Zhu, L.L., Xie, Z.D., Morita, M.T., Tasaka, M., Friml, J., Grotewold, E., Beeckman, T. and Vanneste, S., 2015. Transcriptional regulation of PIN genes by FOUR LIPS and MYB88 during Arabidopsis root gravitropism. Nature Communications, 6(1), p.8822.

179. Wang, L., Guo, M., Li, Y., Ruan, W., Mo, X., Wu, Z., Sturrock, C.J., Yu, H., Lu, C., Peng, J. and Mao, C., 2018. LARGE ROOT ANGLE1, encoding OsPIN2, is involved in root system architecture in rice. Journal of Experimental Botany, 69(3), pp.385-397.

180. Wang, L., Li, Z., Qian, W., Guo, W., Gao, X., Huang, L., Wang, H., Zhu, H., Wu, J.W., Wang, D. and Liu, D., 2011. The Arabidopsis purple acid phosphatase AtPAP10 is predominantly associated with the root surface and plays an important role in plant tolerance to phosphate limitation. Plant Physiology, 157(3), pp.1283-1299

181. Wang, S., Zhang, S., Sun, C., Xu, Y., Chen, Y., Yu, C., Qian, Q., Jiang, D.A. and Qi, Y., 2014. Auxin response factor (Os ARF 12), a novel regulator for phosphate homeostasis in rice (Oryza sativa). New Phytologist, 201(1), pp.91-103

182. Wang, X., Zafian, P., Choudhary, M. and Lawton, M., 1996. The PR5K receptor protein kinase from Arabidopsis thaliana is structurally related to a family of plant defense proteins. Proceedings of the National Academy of Sciences, 93(6), pp.2598-2602.

183. Wang, Y., Wang, F., Lu, H., Liu, Y. and Mao, C., 2021. Phosphate uptake and transport in plants: an elaborate regulatory system. Plant and Cell Physiology.

184. Wang, Z., Ruan, W., Shi, J., Zhang, L., Xiang, D., Yang, C., Li, C., Wu, Z., Liu, Y., Yu, Y. and Shou, H., 2014. Rice SPX1 and SPX2 inhibit phosphate starvation responses through interacting with PHR2 in a phosphate-dependent manner. Proceedings of the National Academy of Sciences, 111(41), pp.14953-14958.

185. Wilmink, A., Van de Ven, B.C.E. and Dons, J.J.M., 1995. Activity of constitutive promoters in various species from the Liliaceae. Plant molecular biology, 28, pp.949-955.

186. Wong, C. and Naumovski, L., 1997. Method to screen for relevant yeast two-hybrid-derived clones by coimmunoprecipitation and colocalization of epitope-tagged fragments—application to Bcl-xL. Analytical biochemistry, 252(1), pp.33-39.

187. Wong, J.H., Alfatah, M., Sin, M.F., Sim, H.M., Verma, C.S., Lane, D.P. and Arumugam, P., 2017. A yeast two-hybrid system for the screening and characterization of small-molecule inhibitors of protein–protein interactions identifies a novel putative Mdm2-binding site in p53. BMC biology, 15(1), pp.1-17.

188. Wu, P. and Wang, X.M., 2008. Role of OsPHR2 on phosphorus homoestasis and root hairs development in rice (Oryza sativa L.). Plant signaling & behavior, 3(9), pp.674-675.

189. Wu, P., Shou, H., Xu, G. and Lian, X., 2013. Improvement of phosphorus efficiency in rice on the basis of understanding phosphate signaling and homeostasis. Current opinion in plant biology, 16(2), pp.205-212

190. Xiujie, Z., Wujun, J., Wentao, X., Xiaying, L., Ying, S., Sha, L. and Hongsheng, O., 2019. Comparison of five endogenous reference genes for specific PCR detection and quantification of rice. Rice Science, 26(4), pp.248-256.

191. Yang, L., Ding, J., Zhang, C., Jia, J., Weng, H., Liu, W. and Zhang, D., 2005. Estimating the copy number of transgenes in transformed rice by real-time quantitative PCR. Plant cell reports, 23(10-11), pp.759-763.

192. Yang, X.J. and Finnegan, P.M., 2010. Regulation of phosphate starvation responses in higher plants. Annals of Botany, 105(4), pp.513-526.

193. Yang, Y.Y., Ren, Y.R., Zheng, P.F., Qu, F.J., Song, L.Q., You, C.X., Wang, X.F. and Hao, Y.J., 2020. Functional identification of apple MdMYB2 gene in phosphate-starvation response. Journal of Plant Physiology, 244, p.153089.

194. Yates, G., Srivastava, A.K. and Sadanandom, A., 2016. SUMO proteases: uncovering the roles of deSUMOylation in plants. Journal of Experimental Botany, 67(9), pp.2541-2548.

195. Yangueez, E., Castro-Sanz, A.B., Fernandez-Bautista, N., Oliveros, J.C. and Castellano, M.M., 2013. Analysis of genome-wide changes in the translatome of Arabidopsis seedlings subjected to heat stress. PloS one, 8(8), p.e71425.

196. Yoo, C.Y., Miura, K., Jin, J.B., Lee, J., Park, H.C., Salt, D.E., Yun, D.J., Bressan, R.A. and Hasegawa, P.M., 2006. SIZ1 small ubiquitin-like modifier E3 ligase

facilitates basal thermotolerance in Arabidopsis independent of salicylic acid. Plant Physiology, 142(4), pp.1548-1558.

197. Zeigler, R.S. and Barclay, A., 2008. The relevance of rice. Rice, 1(1), pp.3-10

198. Zhang, Y. and Zeng, L., 2020. Crosstalk between ubiquitination and other post-translational protein modifications in plant immunity. Plant communications, 1(4), p.100041.

199. Zhang, Z., Liao, H. and Lucas, W.J., 2014. Molecular mechanisms underlying phosphate sensing, signaling, and adaptation in plants. Journal of integrative plant biology, 56(3), pp.192-220.

200. Zhou, J., Jiao, F., Wu, Z., Li, Y., Wang, X., He, X., Zhong, W. and Wu, P., 2008. OsPHR2 is involved in phosphate-starvation signaling and excessive phosphate accumulation in shoots of plants. Plant Physiology, 146(4), pp.1673-1686.